THE UNIVERSITY
of EDINBURGH

College of Medicine & Veterinary Medicine

DORSAL ANTERIOR CINGULATE CORTEX GLUTAMATE CONCENTRATIONS AND THEIR RELATIONSHIPS IN ADULTS WITH AUTISM SPECTRUM DISORDER

Jennifer Eileen Siegel-Ramsay

Doctor of Philosophy

University of Edinburgh

2018

This thesis is dedicated to my mother and friend, Peggy Lynn Harbeck.

You taught me that love is the most important thing that we leave behind.

I declare that this thesis was my own work. At the early stages of the study, I contributed to the study data collection protocol by adding the resting-state functional magnetic resonance imaging (fMRI) sequence and the Attentional Network Test (ANT). I recruited participants and administered consent for all but three individuals participating in this study. I coordinated and administered the clinical and psychometric assessments, including the Wechsler Abbreviated Scale of Intelligence (WASI) and the ANT. I attended and oversaw all but two magnetic resonance imaging (MRI) participant scans, which included preparing the participant for the scan and confirming that the radiographer selected the correct voxel location during the hydrogen proton magnetic resonance spectroscopy (1H-MRS) sequence. I collected and organised all study data. I established the study hypothesise and objectives. Finally, I completed the data analysis and wrote this thesis. None of this work has been submitted for any other degree or professional qualification.

Although I completed most of the work for this project, this thesis would not have been successful without assistance from other people at various stages. Prior to my arrival as a doctoral student, most of the ethics approval and study protocol was completed by Dr M Dauvermann with the assistance of Prof S M Lawrie and Prof A Stanfield. Dr M Dauvermann trained me on study recruitment and data collection procedures. Prof A Stanfield and Dr S Campbell completed the Autism Diagnostic Observation Interview because I was not qualified to administer this assessment. I also received some

Signed: _____

Dated: 31/10/2017

Acknowledgements

was a pleasure working with you. Thank you to all the participants who took the time out of their day to help out with this research.

Abstract:

Previous studies have reported altered glutamate (Glu) concentrations in the blood and brain of individuals with autism spectrum disorder (ASD) compared to neurotypical controls (NC), but the direction (increased or decreased) of metabolite differences is still unclear. Moreover, the relationship between Glu and both brain function and clinical manifestations of the disorder require further investigation. Within this study, we investigated metabolite concentrations within the dorsal anterior cingulate cortex (dACC), a brain region functionally associated with inhibitory executive control tasks and also part of the salience network.

There were 19 participants with ASD and 20 NCs between the ages of 23 and 58 years who participated in this study. A study clinician administered the Autism Diagnostic Observation Schedule (ADOS) to individuals with ASD to further confirm their diagnosis. In addition, all participants in this study completed assessments of general intelligence and attention, which included an inhibitory executive control task. Researchers also acquired *in vivo* single-voxel proton magnetic resonance spectroscopy (^{1}H-MRS) in the dACC to quantify both Glu and combined Glu and glutamine (Glx) concentrations. We hypothesised that these metabolite concentrations would be altered (decreased or increased) in adult participants with ASD compared to NCs and would correlate with inhibitory performance and ASD severity in individuals with ASD. Participants also underwent a resting-state functional magnetic resonance imaging (fMRI) scan to assess the relationship between

functional connectivity and Glu and Glx concentrations. We also hypothesised that there would be an altered relationship between local Glu and Glx concentrations and seed-based functional connectivity in adults with ASD compared to NCs.

There were no significant group differences in Glu or Glx concentrations between individuals with ASD and NCs. Furthermore, we did not find any relationship between metabolite concentrations and either inhibitory performance or clinical symptoms of the disorder. This evidence suggests that increased or decreased Glu and Glx concentrations were not a core marker of altered brain function in the dACC in this group of adult individuals with ASD. When individuals taking psychotropic medications were excluded from the analysis, there was a significant interaction between age and group for Glx concentrations. This evidence weakly suggests disease-specific variations in Glx concentrations over the lifespan of an individual with ASD. Nevertheless, this result did not survive correction for multiple comparisons and requires further replication.

In our final experiment, we reported that Glu concentrations were negatively correlated with right and left dACC seed-based resting-state functional connectivity to the left medial temporal lobe only in individuals with ASD. We also reported an interaction between groups in the association between Glx concentrations and both left and right dACC functional connectivity to other salience network regions including the insular cortex. This evidence suggests that local Glu and Glx concentrations were incongruent with long-distance

functional connectivity in individuals with ASD. This analysis was largely exploratory, but further investigation and replication of these relationships may further explain the pathophysiology of the disorder as well as provide a useful marker for therapeutic intervention.

Lay Summary

Glutamate (Glu) is the primary chemical messenger used by brain cells (neurones) to stimulate or excite other neurones. Glutamate is necessary for normal brain functions, such as learning and memory, but must also be tightly controlled in the brain, because too much or too little can harm brain cells. Following release from a neurone, Glu not immediately taken up by neurones is converted to glutamine (Gln) to prevent overstimulation of brain cells and later converted back into Glu in the neurone for further chemical signalling.

Autism spectrum disorder (ASD) is a developmental brain disorder associated with social-communication difficulties and repetitive and restricted behaviours or interests. The severity and clinical presentation of symptoms vary widely among individuals diagnosed with the disorder. The cause of the disorder is still unclear. Researchers have reported altered Glu and combined Glu and Gln (Glx) concentrations in the brains of people with ASD, but this research is at an early stage.

We compared Glu and Glx concentrations in adults with ASD to healthy control (HC) participants. Furthermore, to better understand how Glu was associated with the disorder, we also investigated the relationships between Glu and Glx and both behaviour and brain function in individuals with ASD compared with HCs.

All participants completed tests of intelligence and attention. Individuals with ASD were also assessed for core symptoms of the disorder. Finally, all persons in our study participated in brain scans which were used to measure Glu and Glx concentrations and functional connectivity, thought to reflect patterns of synchronisation or communication across the brain.

We did not find group differences in Glu or Glx concentrations in adults with ASD compared to HCs. Also, we did not find any association between Glu or Glx concentrations and symptoms of the disorder or behaviour, suggesting that increased or decreased Glu concentrations were not a clear marker of individuals with ASD compared to HCs.

For participants free of antidepressant and anticonvulsant medications, we reported a greater reduction in Glx concentrations with age in individuals with ASD compared to NCs. This evidence weakly suggested that Glx concentrations differ depending on the age of the adult with ASD. Nevertheless, this result requires further replication in a larger sample of participants with ASD.

We also reported that increased local Glx concentrations were associated with reduced functional connectivity in individuals with ASD but increased functional connectivity in HCs, suggesting an inconsistency between local function and long-distance brain synchronisation in individuals with ASD.

In conclusion, we did not report group differences in Glx or Glu concentrations. Nevertheless, this research suggested that Glx

concentrations might vary across the lifespan and have an altered relationship to functional connectivity in individuals with ASD compared to HCs. Future research into these relationships may assist in developing tailored interventions in a heterogeneous disorder.

Table of Abbreviations

ACC	Anterior cingulate cortex
ADI-R	Autism Diagnostic Interview-Revised
ADOS	Autism Diagnostic Observation Schedule-Generic Module 4
ADOS-G	Combined social and communication scores on ADOS
AMPA	α-amino-3-hydroxy-5-methyl-4-isoxazolepropionic acid
ANT	Attentional Network Test
ANCOVA	Analysis of covariance
APA	American Psychiatric Association
ART	Artefact Detection Toolbox
ASD	Autism spectrum disorder
BA	Brodmann area
BOLD	Blood oxygen level dependent
CBF	Cerebral blood flow
Cho	Choline containing compounds
cm^3	Cubic centimetre
Cre	Creatine plus phosphocreatine
CRIC	Clinical Research Imaging Centre
CRLB	Cramér-Rao lower bounds
CSF	Cerebral spinal fluid
dACC	Dorsal anterior cingulate cortex
DLPFC	Dorsolateral prefrontal cortex
DSM-IV	Diagnostic and Statistical Manual of Mental Disorders 4th Edition
DSM-V	Diagnostic and Statistical Manual of Mental Disorders 5th Edition
EPI	Echo-planner imaging
ER	Error Rate
FDR	False discovery rate
fMRI	Functional magnetic resonance imaging
FXS	Fragile X syndrome
GABA	Gamma-Aminobutyric acid
GGC	Glutamate to glutamine cycle
Gln	Glutamine
Glu	Glutamate
Glu/Cre	Glu concentrations relative to creatine plus phosphocreatine concentrations
Glx	Glutamate and glutamine
GM	Grey matter
HC	Healthy control
HR	Hemodynamic response
IQ	Intelligence quotient
LCModel	Linear Combination Model
LOC	Lateral occipital cortex
LTD	Long-term depression
LTP	Long-term potentiation

M	Mean
MATLAB	Matrix laboratory
mI	Myo-inositol
Mm	Millimoles per litre of brain tissue
MNI	Montreal Neurological Institute coordinates
MPFC	Medial prefrontal cortex
MP-RAGE	Three-dimension magnetization prepared rapid gradient-echo
MRI	Magnetic resonance imaging
ms	milliseconds
^{1}H-MRS	Hydrogen proton magnetic resonance spectroscopy
MRS	Magnetic resonance spectroscopy
MRUI	Magnetic resonance user interface
NAA	N-acetyl-aspartate
NAAG	N-acetyl-aspartyl-glutamate
NC	Neurotypical control
NMDA	N-methyl-D-aspartate
PEPSI	Proton echo-planar spectroscopic imaging
PET	Positron emission tomography
PMF	Psychotropic medication free
ppm	parts per million
pACC	Pregenual anterior cingulate cortex
PRESS	Point resolved spectroscopy sequence
RF	Radio frequency
ROI	Region of interest
RT	Response time
SD	Standard deviation
SNR	Signal to noise ratio
SPECT	Single-photon emission computed tomography
STEAM	Stimulated echo acquisition mode
SPM	Statistical Parametric Mapping
T	Tesla
tDCS	Transcranial direct current stimulation
TE	Echo time
VLPFC	Ventrolateral prefrontal cortex
VOI	Volume of interest
WASI	Wechsler Abbreviated Scale of Intelligence
WM	White matter

1   GLUTAMATE, BEHAVIOUR AND BRAIN FUNCTION

1.1 INTRODUCTION

Autism spectrum disorder (ASD) is a lifelong neurodevelopmental disorder. Symptoms include both social communication deficits and repetitive and stereotyped behaviours [1]. In 2014, researchers estimated that ASD costs more than £32 billion in treatment, support services and productivity loss in the United Kingdom. This disorder also comes with a huge emotional burden for both individuals with ASD and their caregivers [2,3]. Therefore, there is a great need to investigate and understand the pathophysiology of this disorder to develop improved treatment and support for individuals diagnosed with ASD.

The overall objective of this research was to investigate glutamate (Glu) and its relationship to behaviour and brain function in individuals with ASD. In this chapter, we lay the foundation for later analyses. We firstly discuss the clinical characteristics of ASD (chapter 1.2). We then briefly present the theory of executive dysfunction in ASD and introduce inhibitory behaviour, a focus within this thesis (chapter 1.2.2). We conclude this section by discussing the prevalence, aetiology and current treatment for ASD (chapter 1.2.3, 1.2.4 and 1.2.5 respectively). Next, the role of both Glu and glutamine (Gln) in the brain is discussed (chapter 1.3). Following this, a summary of the evidence of altered Glu and Glx concentrations in individuals with ASD compared with neurotypical controls (NC) is presented (chapter 1.4). Next, evidence that Glu and Glx have a relationship to behaviour (chapter 1.5) and brain function is further discussed (chapter 1.6). The final section of this

chapter discusses the primary brain region investigated, the dorsal anterior cingulate cortex (dACC) in NCs (chapter 1.7) and individuals with ASD (1.8).

1.2 AUTISM SPECTRUM DISORDER

1.2.1 Clinical Diagnostic Criteria

Autism spectrum disorder is considered a lifelong neurodevelopmental disorder [4,5]. Clinicians base diagnosis of the disorder on the presence of social communication deficits and stereotyped or repetitive behaviours or interests which result in substantial impairment in social, professional or other critical areas of life. A diagnosis of ASD can only be given when behavioural symptoms are not better explained by other intellectual or developmental disabilities [1,6]. The early behavioural symptoms of this disorder are typically observed in the first three years of life. Nevertheless, a definite diagnosis in early development can be challenging as social or communicative deficits may not be fully evident until greater social demands are placed upon an individual in adolescence and adulthood. Additionally, some individuals learn strategies to mask ASD behaviours [6].

The current American Psychiatric Association's (APA) Diagnostic and Statistical Manual of Mental Disorders, Fifth Edition (DSM-V) combines the Diagnostic and Statistical Manual of Mental Disorders 4th, Fourth Edition (DSM-IV) diagnostic categories of autistic disorder, Asperger syndrome and pervasive developmental disorder into one category of ASD. In the DSM-V, a diagnosis of ASD is given in accordance with the level of severity to indicate the amount of support an individual requires [1,6]. For greater clarity, we

present the exact DSM-V diagnostic criteria below which lists typical behaviours and symptoms of the disorder [6]:

A. Persistent deficits in social communication and social interaction across multiple contexts, as manifested by the following, currently or by history (examples are illustrative, not exhaustive; see text):

1. Deficits in social-emotional reciprocity, ranging, for example, from abnormal social approach and failure of normal back-and-forth conversation; to reduced sharing of interests, emotions, or affect; to failure to initiate or respond to social interactions.

2. Deficits in nonverbal communicative behaviors used for social interaction, ranging, for example, from poorly integrated verbal and nonverbal communication; to abnormalities in eye contact and body language or deficits in understanding and use of gestures; to a total lack of facial expressions and nonverbal communication.

3. Deficits in developing, maintaining, and understand relationships, ranging, for example, from difficulties adjusting behavior to suit various social contexts; to difficulties in sharing imaginative play or in making friends; to absence of interest in peers.

   Specify current severity:

   Severity is based on social communication impairments and restricted, repetitive patterns of behavior.

B. Restricted, repetitive patterns of behavior, interests, or activities, as manifested by at least two of the following, currently or by history (examples are illustrative, not exhaustive; see text):

1. Stereotyped or repetitive motor movements, use of objects, or speech (e.g., simple motor stereotypes, lining up toys or flipping objects, echolalia, idiosyncratic phrases).

2. Insistence on sameness, inflexible adherence to routines, or ritualized patterns of verbal or nonverbal behavior (e.g., extreme distress at small changes, difficulties with transitions, rigid thinking patterns, greeting rituals, need to take same route or eat same food every day).

3. Highly restricted, fixated interests that are abnormal in intensity or focus (e.g., strong attachment to or preoccupation with unusual objects, excessively circumscribed or perseverative interests).

4

4. Hyper- or hyporeactivity to sensory input or unusual interest in sensory aspects of the environment (e.g. apparent indifference to pain/temperature, adverse response to specific sounds or textures, excessive smelling or touching of objects, visual fascination with lights or movement).

Specify current severity:

Severity is based on social communication impairments and restricted, repetitive patterns of behavior.

C. Symptoms must be present in the early developmental period (but may not become fully manifest until social demands exceed limited capacities, or may be masked by learned strategies in later life).

D. Symptoms cause clinically significant impairment in social, occupational, or other important areas of current functioning.

E. These disturbances are not better explained by intellectual disability (intellectual developmental disorder) or global developmental delay. Intellectual disability and autism spectrum disorder frequently co-occur; to make comorbid diagnoses of autism spectrum disorder and intellectual disability, social communication should be below that expected for general developmental level

Note: Individuals with a well-established DSM-IV diagnosis of autistic disorder, Asperger's disorder, or pervasive developmental disorder not otherwise specified should be given the diagnosis of autism spectrum disorder. Individuals who have marked deficits in social communication, but whose symptoms do not otherwise meet criteria for autism spectrum disorder, should be evaluated for social (pragmatic) communication disorder.

1.2.2 Executive Control and Inhibition

Executive control, often used interchangeably with executive function or cognitive control [7], is defined as the adaptive influence of cognitive processes to coordinate external sensory stimuli, environmental conditions, prior learning and internal state, to influence behaviour and achieve an internally desired goal. Executive control is critical to human adaptability during unfamiliar, multi-dimensional tasks [8–12]. Typically, tasks which initiate executive control require greater initiation of an effortful cognitive response

[7,13]. Executive control is a broad construct which includes inhibition, behaviour regulation, working memory and mental planning. Executive control performance has been associated with academic achievement [14,15], improved health [16–18], life satisfaction [19] and long-term accomplishments in NCs [20], suggesting that it is important for both success and happiness in life.

Many research groups have reported that participants with ASD have reduced performance on executive controls tasks [21–35] including flexibility [21,36,37], inhibition [26,38,39] and planning tasks [22]. Executive control has also been linked with severity of other autistic symptoms. For example, response inhibition and cognitive flexibility were associated with the severity of repetitive movements in ASD [40–42]. In addition, executive control skills were also correlated with social performance [41] and even independence in adulthood in individuals with ASD [43].

This evidence has led to the executive dysfunction theory, a hypothesis that individuals with ASD have core executive control deficits compared to NCs [31,44,45]. Nevertheless, one problem with this theory is that executive control is an incredibly broad concept and associated with a diverse range of tasks and underlying brain regions [9]. Several groups have reported a lack of performance differences on various executive control tasks in individuals with ASD compared to NCs [27,41,46,47], suggesting that executive control deficit may not be pervasive within the disorder.

Although we present the executive dysfunction theory of ASD for further context, a full investigation of executive control tasks in individuals with ASD

is well beyond the scope of this thesis. Instead, we focus on a specific inhibitory executive control task. Inhibition is defined as the control of automatic behaviour, with a more goal appropriate response to achieve an objective. Inhibition permits us to change our habits and learn new ways to react to our environment [7].

Even within the domain of inhibition, ASD performance deficit varies depending on the type of inhibition task. There is little evidence that individuals with ASD have reduced performance on the Stroop task, a task which the participants must inhibit a prepotent response [27,41,46–49]. In contrast, there has been evidence that individuals with ASD exhibit performance deficit when required to inhibit attention to irrelevant non-target stimuli during the flanker conflict effect task [26,27,50–55], a task in which a participant must indicate the direction of a target while inhibiting both attention and motor response to competing non-target stimuli [56]. We discuss the flanker conflict task in much more detail within chapter 1.7.2 and 1.7.3.

1.2.3 Prevalence

In the 1960's, the prevalencen of autism disorder was thought to be less than .05% [57]. Over time, more research, heightened awareness and improved diagnostic tools have likely contributed to an increased diagnosis of ASD in the population [58–63]. More recent studies suggest that around one in 100 adults [64] and school-age children have a diagnosis of ASD in the United Kingdom [65] and estimates in the United States reported a similar prevalence [66]. Currently, four in five individuals with ASD are male [60,67,68]. It is unclear if

being female offers some protection against the disorder [69–71] or if females are overlooked for diagnosis [71].

1.2.4 Aetiology

The precise cause of ASD is still unclear, but evidence suggests that an interplay between various genetic and environmental factors contribute to the disorder [72].

1.2.4.1 Genetics

Twin studies suggest a genetic influence in the disorder and have reported a higher concordance rate for a diagnosis of ASD between monozygotic twins (44 - 90%) compared to dizygotic twins (10 - 36%) [73–76]. Nevertheless, only 10% of all individuals with a diagnosis of ASD have a known monogenetic cause [66,68,77].

One monogenetic disorder with closely overlapping autistic symptoms is fragile X syndrome (FXS) [78,79]. Fragile X is a trinucleotide repeat genetic disorder in which the fragile X mental retardation 1 gene is silenced [78,79], leading to a reduction or complete lack of the fragile X mental retardation protein [80]. Symptoms of the disorder also include physical abnormalities such as large ears, flat feet and an arched palate [81,82]. Individuals with FXS also exhibit some behavioural symptoms which overlap with ASD, such as repetitive and stereotyped movements, heightened sensitivity to sensory stimuli [83] and social deficits [84,85]. Studies have reported that one-third of the children with a diagnosis of FXS also met the criteria for ASD [86,87].

8

Outside of disorders such as FXS, geneticists have been less successful in identifying and replicating singular genetic contributions to the ASD. Typically, researchers have identified genetic contributions linked to only a rare minority of individuals with the disorder or which are also common in NCs [88].

A lack of evidence for strong monogenetic contributors to this disorder has led geneticists to instead proposed that hundreds of genetic loci might interact to increase the risk of ASD [89–93]. Furthermore, these genes might modify a shared biological pathway [92–100], such as genes which modify or interact with glutamatergic signalling [101]. A 2014 genetic literature review reported that more than 50% of all the 249 genes which were known building blocks or moderators of Glu metabolism, transport, receptors and signalling also had at least one genetic linkage or association study linking it to individuals with ASD. Various genetic contributors to Glu signalling pathways may increase the likelihood of the development of ASD, although the separate effect size for each of these genetic contributions was small [101].

1.2.4.2 Environment
Environmental stressors are also likely contributors to ASD. Environmental variables which increase the risk of developing ASD include increased parental age [102], a heightened maternal immune response to infection during pregnancy [103,104], prenatal exposure to anti-epileptic medications [105] and oxygen deprivation at birth [102,106,107]. As with genetic causes, it may be that

environmental stressors which increase risk all differentially impact an underlying biological pathway [101].

1.2.4.3 Neurological Disorder

Finally, although genetics and environmental variables likely initiate the development of ASD, the disorder impacts the brain, and this has been made evident through structural and functional neuroimaging studies [108,109]. For example, structural magnetic resonance imaging (MRI) research has consistently reported early macrocephaly for young children with ASD [110–112] providing further evidence that ASD is a neuro-developmental disorder.

Functional magnetic resonance imaging (fMRI) evaluates relative changes in the BOLD signal in association with an experimental paradigm [113–115] and has been a valuable tool in highlighting focal areas of altered function in the brain of individuals with ASD compared to NCs [116–119]. For example, a metanalysis of non-social fMRI tasks suggests that the dACC might be a core area of hypofunction in individuals with ASD compared to NCs [120,121]. Evidence of altered function is further bolstered by post-mortem studies reporting altered neural architecture in individuals with ASD compared to NC. Within the anterior cingulate cortex (ACC), researchers have reported smaller neuronal size in layers I-III and V-VI of Brodmann area (BA) 24b and reduced cell density in layers V-VI of BA 24c in adults with ASD compared to age-matched NC [122].

1.2.5 Treatment

Given that the cause of ASD is still unknown, it is not surprising that there is no cure. Difficulties in identifying appropriate interventions include heterogeneity in symptoms of the disorder and the many potential genetic and environmental causes [123,124].

Although researchers continue to develop new treatments for ASD [125], current clinical interventions primarily focus on reducing symptom severity and secondary comorbidities. Rigorous behavioural interventions implemented early in development offer some improvements in cognitive ability and adaptive behaviour for individuals with the disorder [126]. Clinicians also typically prescribe antidepressants and antipsychotics to alleviate secondary symptoms such as anxiety, aggression or irritability [127–130]. Nonetheless, greater clarification of the neurobiological origins of the disorder and improved methods to better classify heterogeneity in participants with ASD may assist in the development of better treatment options [123].

1.3 GLUTAMATE FUNCTION IN THE BRAIN

Within this section, the objective is to briefly summarise what Glu does within the brain and highlight potential mechanisms in which altered Glu concentrations can be detrimental. Glutamate has many roles in the brain [131,132], but its primary role is as a neurotransmitter [132] (chapter 1.3.1) which also modulates neuronal plasticity (chapter 1.3.2). Extracellular concentrations of Glu within the brain are removed and regulated via the glutamate to glutamine cycle (GGC) (1.3.3). During development, the brain is

more sensitive to Glu (chapter 1.3.4), although neuronal insult and death can occur throughout life when extracellular Glu concentrations are not tightly controlled (chapter 1.3.5).

1.3.1 Glutamate Receptor Signalling

Glutamate is the primary excitatory neurotransmitter in the brain [133] and necessary for neuronal communication [134]. Glutamate binds to ionotropic Glu receptors [135]. Fast acting Glu ligand-gated ionotropic receptors include N-methyl-D-aspartate (NMDA), α-amino-3-hydroxy-5-methyl-4-isoxazolepropionic acid (AMPA) [131,136] and kainate receptors [134,137]. Ionotropic receptors contain an ion channel which, under the right conditions, open to allow ions entry into the cell leading to an increased likelihood of action potential [134,135]. Signalling pathways association with NMDA receptors also influence the efficacy between the pre and post-neuronal synapse by altering the number of AMPA receptors in the post-synaptic membrane [138]. Researchers have also demonstrated that kainate receptors can moderate excitability and synaptic transmission [137].

Glutamate also binds to metabotropic receptors, which do not contain ion channels, but indirectly modify other receptor ion channels and signalling pathways [139–141]. These receptors can also mediate neural efficacy, signalling and release [142–144].

1.3.2 Neuronal Plasticity

Glutamate receptor signalling can initiate a cascade of proteins which alter the synaptic plasticity or efficacy between two neurones. Long-term

potentiation (LTP) is an increase in responsiveness of the post-synaptic neurone to pre-synaptic signalling [145] and is a prominent biological explanation for learning and memory [146–149]. Animal research of the hippocampus has formed the basis of our understanding of LTP [147], but similar mechanisms have been shown in the ACC [150–152]. One of the most studied mechanisms of LTP is the increase in AMPA receptors in the post-synaptic membrane leading to increased post-synaptic sensitivity to further Glu signalling [151,153–155].

Nevertheless, LTP is associated with many other Glu receptors and signalling pathways. For example, pre-synaptic kainate receptors can moderate the likelihood of pre-synaptic excitation leading to increased Glu release in the pre-synaptic neurone [149,156]. Later stages of LTP also impact gene transcription and protein production in the postsynaptic neurone [157,158]. Changes in morphometry or quantity of dendritic spines [159–161], increased postsynaptic area [157] and intrinsic excitability of ion channels [162] are associated with later stages of LTP.

In contrast, long-term depression (LTD) is associated with reduced efficacy between neurones [157]. Typically, LTD occurs when the Glu signal does not sufficiently depolarise the postsynaptic neurone and is associated with brief or weak stimulation [163,164]. In addition, group I metabotropic Glu receptors can moderate LTD and AMPA receptor endocytosis through complex protein signalling cascades [140,165–168] (figure 1.1).
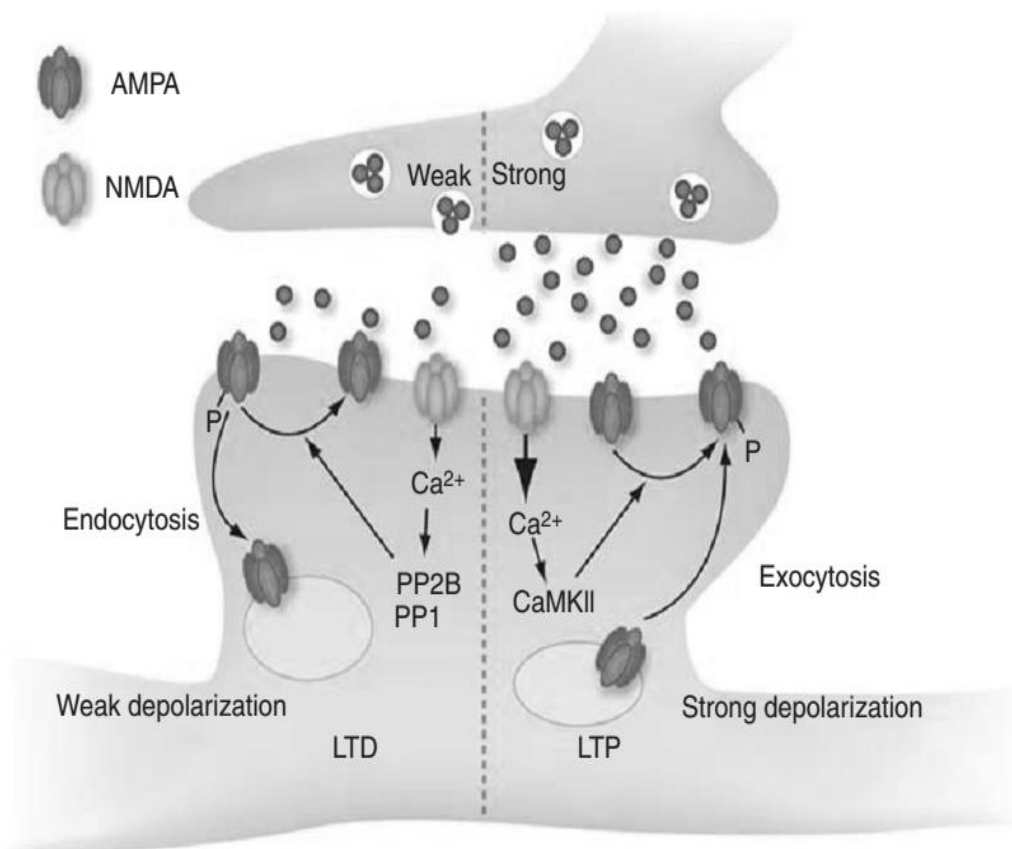
Figure 1.1 Long-term Potentiation and Depression (Reproduced from Lüscher et al. (2014)).

This model highlights the basic mechanisms of neuronal plasticity in association with the AMPA and NMDA receptors. Many other receptors and proteins modulate neuronal plasticity which are not included in this figure. On the left, LTD occurs in association with weak depolarisation of the post-synaptic neurone. A small amount of calcium enters the post-synaptic neurone which further activates phosphates and results in endocytosis of the AMPA receptor. On the right, LTP is shown. Glutamate signalling leads to post-synaptic neurone depolarisation. Calmodulin-dependent kinase II (CaMKII) facilitates AMPA receptor phosphorylation and exocytosis.

1.3.3 Glutamate to Glutamine Cycle

As part of the GGC cycle, Glu transporters collect extracellular Glu that is not immediately taken up by pre-synaptic or post-synaptic neurones. Glutamate transporters shuttle Glu to astrocytes for further synthesis into Gln [169,170] thus limiting hyperexcitation in nearby neurones [171]. Within astrocytes, ammonia is

14

added to Glu to produce Gln. Next, Gln is transferred to the neuron for further processing [170,172,173]. Within a glutamatergic neuron, Gln can be metabolised back into Glu for further release into extracellular space. Ammonia is a bi-product of Gln degradation [173] and must also be regulated within the neuron as it can have a deleterious impact on brain cells including inflammation or seizure [170,174]. The processes associated with the GGC cycle utilise at least 70% of glucose taken up by the brain [175,176].

1.3.4 Development

During development, Glu receptor signalling has been associated with many developmental processes including cell migration [177–179], dendritic growth [180,181], neurogenesis [182] and cell survival [183,184]. In postnatal rats, reducing Glu NMDA receptor expression was associated with increased apoptotic cell death [184], a less severe neurodegenerative process associated with gradual cell shrinkage and containment of cell contents from neighbouring neurones [185]. Researchers also demonstrated that genetic knockout of excitatory amino acid transporter 1 and vesicular Glu transporter 1, known to move Glu from the cytoplasm to the synapse for further release [186], resulted in widespread developmental abnormalities including altered neuronal migration and differentiation in the cortex, hippocampus and olfactory bulb of mice. This evidence suggests that altering Glu transport and likely increasing extracellular Glu concentrations lead to widespread morphological differences in the cortex as demonstrated in these knockout mice [187].

Furthermore, neurones may be more vulnerable to Glu insult during development. Compared to mature mice NMDA receptors in developing mice took in higher quantities of calcium [188] and were less easily blocked by magnesium [189,190], making these receptors more sensitive to Glu signalling. Although increased sensitivity allows for growth and organisation in the developing cortex, atypical alterations in Glu signalling can also result in greater damage to neurones [133,191]. Administration of glutamate agonists caused increased neuronal death during early critical developmental periods, but this vulnerability diminished with age in mice [183,192]. The relationship between cortical development and Glu neuro-signalling may be particularly relevant to ASD as symptoms become evident in early development [193,194].

1.3.5 Excitotoxicity

Excitotoxity is neuronal death and injury caused by excessive neuronal excitation and mitochondrial failure due to calcium build up in the cell [195,196]. Increased extracellular Glu concentrations have been associated with excitotoxity [196–202]. For example, acute ischemic events are associated with high extracellular concentrations of Glu. Excitotoxity results in Glu release from the cell membrane of the dying cell causing further death and inflammation to neighbouring neurones [185,203,204]. Furthermore, blocking both ionotropic and metabotropic Glu receptors had a neuroprotective effect during an ischemic insult in rats [205,206]. In conclusion, although Glu neuronal-signalling is critical for neuronal plasticity and cortical development,

16

extracellular Glu concentrations must be tightly regulated to prevent both altered cortical development and excitotoxicity.

1.4 EVIDENCE OF ALTERED GLUTAMATE CONCENTRATIONS

Altered Glu concentrations may contribute to the pathophysiology of ASD [194,207]. Within this section, we present evidence of altered Glu concentrations in the blood (chapter 1.4.1) and brain (chapter 1.4.2) of individuals with ASD compared to NCs.

1.4.1 Blood

Separate investigations have reported increased Glu concentrations in blood serum and plasma in participants with ASD when compared to NCs [208–217]. For example, Shinohe et al. (2006) reported increased Glu concentrations in serum of adult individuals with ASD compared to age-matched NCs [208]. Investigators also reported a positive correlation between Glu concentrations and the severity of social symptoms as measured by the Autism Diagnostic Interview-Revised (ADI-R). The ADI-R is a diagnosis tool for individuals suspected of having ASD [218]. This evidence suggests that increased Glu concentrations might result in increased severity of social symptoms in the disorder. Finally, another investigation reported that, unlike NCs, children with ASD did not exhibit an age-related decline in blood Glu concentrations [215], further suggesting that Glu alterations might continue into adulthood in individuals with the disorder.

In contrast to these results, other studies report no group differences in Glu

concentrations in the blood of individuals with ASD compared to NCs [219,220]. Nevertheless, a recent metanalysis of all published studies of Glu concentrations in the blood concluded that, overall, there was evidence for increased Glu concentrations in the blood of individuals with ASD compared to NCs [211].

Glutamate transporters can assist in the regulation of extracellular Glu concentrations by transporting Glu across the blood-brain barrier [221,222]. In NCs, Glu concentrations in serum significantly correlated with concentrations in cerebral spinal fluid (CSF) [223,224]. Furthermore, Hassan et al. (2013) reported a positive correlation between plasma and brain Glu concentrations. Glu concentrations were measured by proton magnetic resonance spectroscopy (^{1}H-MRS) in several regions of the brain including the bilateral dACC and left frontal lobe in children with ASD compared to NCs [217]. These studies suggested that Glu concentrations in the blood might be associated with Glu concentrations in the brain of individuals with this disorder. Unfortunately, we were unable to collect blood samples in this study. Future ^{1}H-MRS studies within the brain would strongly benefit from including the measurement of Glu concentrations in the blood for comparison to Glu measurement in the brain.

1.4.2 Brain

Proton magnetic resonance spectroscopy is a neuroimaging technique which researchers have used to quantify Glu or Glutamate and Glutamine (Glx) concentrations in the brain *in vivo*. Many researchers reported altered Glu or

Glx concentrations in the brain of individuals with ASD compared to NCs. Nevertheless, these studies have contradicted each other as some groups reported increased [217,225–232] while others reported decreased [233–238] or no group differences in Glu or Glx concentrations in individuals with ASD compared to NCs [239–246]. We summarise all the published studies investigating Glu or Glx concentrations in adults with ASD in table 1.1. Participant characteristics, brain region investigated and ^{1}H-MRS methodology might contribute to conflicting results between these studies [247].

Table 1.1 Proton Magnetic Resonance Spectroscopy Studies of Glutamate and the Combined Glutamate and Glutamine Concentrations in the Brain of Adults with Autism Spectrum Disorder

Study	Concentration reported	Region Investigated	Cohort Size	Age Mean (SD)	Total IQ Mean (SD)	Outcome	Conclusion for ASD participants compared to NCs	ASD?
Aoki et al. (2012)	Glx	MPFC (including the pACC and paracingulate cortex)	24 ASD, 25 NC	ASD = 29.5 (6.9), NC = 29.4 (6.2)	ASD = 104.2 (11.6), NC = 108 (7.5)	ASD = 7.40 (2.04), NC = 7.46 (1.56), p = .911	No significant difference in Glx in any region	=
Bernardi et al. (2011)	Glx	A. R Thl B. L Thl C. R TPJ D. L TPJ E. R IPS F. L IPS **G. R pACC** H. L pACC	14 ASD, 14 NC	ASD = 29.2 (6.1), NC = 29.7 (8.3)	ASD = 115 (14), NC =111 (16)	**Overall effect = p <.008** A. ASD = 1.57 (0.5), NC = 1.90 (0.9), $p >$ .05 [2] B. ASD = 1.49 (0.3), NC = 1.58 (0.2), $p >$ .05 [2] C. ASD = 1.49 (0.5), NC = 1.67 (1.0), $p >$ .05 [2] D. ASD = 1.23 (0.07), NC = 1.41 (0.7), $p >$ .05 [2] E. ASD= 1.51 (1.0), NC = 1.65 (0.7) , $p >$ .05 [2] F. ASD= 1.12 (0.5),	Overall significant reduction in Glx for all regions Significant reduction in Glx in R pACC No other significant differences for Glx in any other region	↓

					NC = 1.82 (1.3), $p > .05$ [2] **G. ASD= 1.17(0.4), NC = 1.76 (0.5), $p = <.0006$** H. ASD= 1.31 (0.4), NC = 1.41 (0.3)		
Brown et al. (2013)	Glu and Glx	**A. R AC** **B. L AC**	13 ASD, 15 NC	ASD = 36.89 (6.80), NC = 41.08 (6.77)	ASD = 103.55 (16.31), NC = 114.67 (11.82),	**A. Glu p =.008, Glx, $p = .01$** **B. Glu p = .001, Glx, $p = .003$**	Significant increase in Glu and Glx in the L and R auditory cortex	↑
Horder et al. (2013)	Glx	**A. L BG** B. L DLPFC C. L MPL	15 ASD, 13 B_ASD	ASD = ASD: 29 (6.0), NC = 34 (8.8)	ASD = 95 (13), NC = 107 (21)	**A. ASD = 10.12 (1.14), NC = 12.34 (1.45), $p < .001$** B. ASD = 7.49 (1.11), NC = 8.01 (1.42), $p > .05$ [2] C. ASD 10.61 (2.79), NC 11.02 (1.62), all comparisons $p > .05$ [2]	Significant decrease in Glx in the L BG No significant group differences in the L DLPFC or MPL	↓
Libero et al. (2016)	Glx [1]	A dACC B. PCC	19 ASD, 18 NC	ASD = 27.1 (1.38),	ASD = 115.4 (2.88), NC	A. ASD = 9.82 (1.11), NC = 9.83	No significant difference in Glx in any region	=

				NC = 24.6 (1.22)	= 117.5 (2.51)	(1.30), p = .980 B. ASD = 9.46 (.99), NC = 9.48 (1.02), p = .832	
Page et al. (2006)	Glx	**A. R AHR** B. R PC	R AHR: ASD 13, NC 13: PC: ASD 14, NC 19	ASD = 35.9 (11.5), NC = 34.4 (9.3)	ASD = 102 (17), NC = 110 (17)	**A. ASD = 13.6 (2.0), NC = 12.02 (1.01), p = .02** B. ASD = 10.06 (1.18), NC = 9.98 (1.07), p > .05 [2]	Significant increase in Glx in R AHR No difference in the R PC	↑
Robertson et al. (2016)	Glx	A. Visual Cortex B. Motor Cortex	ASD 20, NC 21	ASD = 29.61 (NR), NC = 29.10 (NR)	ASD = 112.15 (NR), NC = 113.95 (NR)	A. ASD = 8.35 (0.35), NC = 8.82 (0.25) p = .27 B. Concentrations NR, p > .32	No significant difference in Glx in individuals with ASD compared to NCs in any region	=
Tebartz Van Elst et al. (2014)	Glu and Glx	**A. pACC Glu** **B. pACC Glx** C. L Cerebellum Glu D. L Cerebellum	29 ASD, 29 NC	ASD = 35.31 (9.1), NC = 35.79 (8.5)	ASD = 125.1 (12.0), NC = 124.97 (13.4)	A. p = .003, ASD = 10.02 (2.10), NC = 11.48 (1.35), p = .003 B. p = .001, ASD = 14.19 (3.05), 16.69, (2.47), p = .001	Decreased Glu and Glx in pACC No significant group difference for cerebellum	↓

		Glx			C. p = NS, ASD = 7.29 (1.13), NC = 7.54 (.94), $p >$ .05 [2] D. ASD = 10.64 (1.55), NC = 11.14 (1.31) $p >$ .05 [2]	

Results and study characteristics (metabolite investigated, brain region investigated, cohort size, cohort age and cohort IQ (Wechsler Abbreviated Scale of Intelligence (WASI)) of ^{1}H-MRS studies investigating Glu and Glx concentrations in individuals with ASD compared to NCs. All studies included investigated adult participants. All significant group differences ($p >$ .05) are highlighted in bold.

[1] Also reported Glx relative to Cre concentrations which was also not significantly different between groups

[2] Actual significance not reported

Abbreviations: AC, Auditory cortex; AHR, amygdala-hippocampal region; B, Bilateral; BG, basal ganglia; DLPFC, dorsolateral prefrontal cortex; dACC, dorsal anterior cingulate cortex; Glu, glutamate concentrations; Glx, glutamate and glutamine concentration; IPS, intraparietal sulcus; MPFC, medial prefrontal cortex; MPL, medial parietal lobe; NR, not reported; pACC, pregenual anterior cingulate cortex; PC, parietal cortex; PCC, posterior cingulate cortex; pACC, pregenual anterior cingulate cortex; R, right; TPJ, Temporal parietal junction; Thl, thalamus.

Glu and Glx concentrations vary throughout the brain. In NCs, researchers reported higher concentrations of Glu and Glx in GM compared to WM [248]. In another study of NCs, investigators report higher Glu concentrations in the pregenual ACC (pACC) (Mean *(M)* = 11.48, Standard Deviation (*SD*) = 1.35 Institutional Units) than in the cerebellum (*M* = 7.54, *SD* = .94 Institutional Units). The same study also reported significant reductions in Glu concentrations in the pACC but not left cerebellum for adults with ASD relative to NCs [237]. Variations in Glu or Glx concentrations in individuals with ASD are likely region specific [247,249,250]. Therefore, we focus on ^{1}H-MRS studies of the ACC because this was one of the most investigated regions for Glu and Glx concentrations in individuals with ASD compared to NCs.

Bejjani and colleagues reported increased Glx concentrations in the pACC in adolescents with ASD compared to neurotypical adolescents [225]. This result was further supported by two studies reporting increased Glu concentrations in the pACC in adolescents with ASD compared to NCs [230,231]. The study by Naaijen and colleagues was particularly interesting as it investigated a large group (NC = 53, ASD = 51) of adolescents [231]. Finally, Hassan and colleagues reported an increase in Glu concentrations in the dACC, left striatum, cerebellum and frontal lobe in children with ASD ages 6 through 14 compared to age-matched NCs [217]. We will discuss the underlying methodology of MRS studies in more detail in chapter two, but the results of Hassan and colleagues require further replication as they reported Glu concentrations in the brain at 1.5 tesla (T). It is incredibly difficult to measure

Glu concentrations with a 1.5 T MRI scanner given the technical constraints of ^{1}H-MRS [232,251].

There were two further studies in children and adolescents which reported no difference between groups in Glu [241] and Glx [240] concentrations in the ACC [240,241]. Brix and colleagues investigated Glx concentrations in a very large voxel overlapping with both the dACC and pACC, while Cochran and colleagues investigated the pACC. Although there is some contradiction between studies, we know of no study reporting reduced Glu or Glx concentrations in children or adolescents with ASD compared to NCs in the ACC.

It has been less clear if Glu ro Glx concentrations are altered in the ACC in adult participants with ASD compared to NCs because there are fewer studies. There have been four studies measuring Glu or Glx concentrations in the ACC in adults with ASD. Researchers have reported reduced Glu [237] and Glx concentrations in the pACC in adults with ASD relative to NCs [233]. In contrast, two other research groups reported no difference in Glx concentrations in the pACC [252] and dACC of individuals with ASD compared to NCs [245].

The conflicting results from these studies warrant further investigation of Glu and Glx in the ACC of adults with ASD. There was some variability in participant characteristics which might have contributed to the variable results of these studies. Furthermore, it is unclear if altered concentrations are associated with altered brain function and behaviour in ASD. Clarifying

metabolite concentrations in adult participants with ASD will have implications for appropriate interventions throughout the lifespan of the disorder.

1.5 GLUTAMATE CONCENTRATIONS AND BEHAVIOR

To further clarify conflicting ^{1}H-MRS results, we investigated the relationship between Glu concentrations and both clinical symptoms of ASD and behaviour. Published evidence that Glu or Glx concentrations are associated with behaviour in individuals with ASD (chapter 1.5.1) and NCs (chapter 1.5.2) is discussed below.

1.5.1 Autism Spectrum Disorder

Again, Tebartz van Elst and colleagues reported a significant reduction in Glu and Glx concentrations in the pACC in individuals with ASD compared to NCs. Investigators also reported that increased Glu concentrations in individuals with ASD correlated with decreased empathy as measured with a self-report questionnaire, the Empathy Quotient [253]. There was no significant relationship between these variables in NCs. The pACC has been associated with emotional tasks [254,255]. Glutamate concentrations in the pACC might be associated with empathy in individuals with ASD within increased concentrations being associated greater deficit [237]. Nevertheless, this was a self-report measure, and these relationships require replication in association with more direct of empathy.

In contrast to this study, Libero et al. (2015) reported no significant correlation between dACC Glx or Glx/Cre concentrations and the Ritvo

Autism Asperger Diagnostic Scale-Revised, an assessment tool to highlight autistic traits and behaviours [256]. This evidence suggests that Glx concentrations in the dACC did not relate to symptoms of the disorder. Another study in adolescents with ASD reported no significant relationship between intelligence or social behaviour and Glu concentrations in the pACC [241]. Unfortunately, most of the studies investigating Glu and Glx concentrations in the ACC did not assess the relationship between clinical symptoms or behaviours [217,225,230,233,239]. Therefore, much more research is needed to investigate the relationship between Glu and Glx concentrations and behaviours or symptoms of individuals with ASD compared to NCs.

1.5.2 Neurotypical Controls

There has been evidence that Glu concentrations, specifically in the dACC, have a relationship to behavioural control in NCs. Studies have reported that increased Glu concentrations in the dACC were associated with increased self-reported impulsivity in both NCs and individuals with borderline personality disorder [257], suggesting that higher Glu concentrations in the dACC might be associated with reduced behavioural inhibition. Another group investigated performance on a delay discounting task in which decreased scores were a measure of increased impulsivity. Researchers reported that increased impulsivity correlated with increased dACC ratio of Glu to creatine plus phosphocreatine concentrations (Glu/Cre) in NCs [258].

 Another study investigated if Glu concentrations would predict what type of information a participant would use when making a cognitive decision. During

this task, the overall objective was to obtain the highest reward with the least effort. When completing this cognitive reward task, participants could either rely on learned feedback information provided over the length of the task or solely utilise the available information on the screen for each trial when completing a cognitive reward task. Investigators reported that increased Glu concentration in the dACC was positively correlated with increased use of previously learned information to guide future behaviour during this task [259].

These studies suggested that Glu concentrations in the dACC were associated with behavioural control in NCs. Given this evidence, we explored the relationship between dACC Glu concentrations and a cognitive inhibition task in both NCs and individuals with ASD. In comparison to broad symptoms of the disorder, we hypothesised that a more finely tuned and regionally specific behavioural performance task might more clearly index the association between Glu and Glx concentrations on behaviour.

1.6 GLUTAMATE CONCENTRATIONS AND FUNCTIONAL CONNECTIVITY

Next, the relationship between both Glu and Glx concentrations and functional connectivity is presented. Firstly, functional connectivity and resting-state functional connectivity is presented (chapter 1.6.1). Evidence that Glu and Glx concentrations have a relationship to functional connectivity in NCs (chapter 1.6.2 and 1.6.3) is then presented. The goal of this section is to present functional connectivity analysis and also provide a theoretical

basis for the investigation of the relationship between metabolite concentrations and functional connectivity.

1.6.1 Introduction to Functional Connectivity

Functional connectivity is a statistical method which measures the correlation or association in time-series between distant brain regions and is typically applied to fMRI data. By definition, functional connectivity analysis methods do not indicate a causal relationship between brain regions. Instead, functional connectivity maps patterns of BOLD activity which are thought to reflect neural activation patterns and organisation of the human brain [116,118,260–263]. Throughout this thesis, we define task-based fMRI as fMRI obtained in association with an externally defined task [264].

In contrast to task-based fMRI, functional connectivity has often been applied to a resting-state fMRI sequence, a fMRI scan which is conducted in the absence of an externally defined paradigm [264]. Resting-state functional connectivity analyses measure the statistical relationships in spontaneous low-frequency BOLD fluctuations, usually between 0.009 and 0.09 Hz [116–118]. Several research groups have demonstrated that regions which were functionally associated with each other during a task-based fMRI analysis continued to exhibit low-frequency BOLD correlations even in the absence of a task [265]. For example, in NCs, researchers have demonstrated that resting-state seed-based functional connectivity from the left motor cortex was associated with sensory-motor brain regions previously associated with a task-based fMRI hand movement experiment [116]. Researchers have also

demonstrated a relationship between altered resting-state fMRI and cognitive performance in neurological disorders such as ASD [266].

1.6.1.1 Advantages of Resting-State Functional Magnetic Resonance Imaging

One advantage of resting-state fMRI is its simplicity. Unlike task-based fMRI, resting-state fMRI is not constrained by a specific experimental paradigm. Given the high cost of MRI and the difficulty of getting a participant to feel comfortable inside an MRI scanner [118], resting-state fMRI data has opened doors for greater innovation in neuroimaging research by allowing more opportunities for data sharing and recycling [108,267]. Nevertheless, not all resting-state MRI scans are the same. Great care should be taken to identify differences which can variably impact the BOLD response, such as variation in instructions (for example eye closed or open).[268–270].

Resting-state fMRI is also more practical for clinical groups because it does not require the participant to attend to a task while being inside an MRI scanner [271]. It may be that symptoms of the disorder rather than reduced neurocognitive ability can confound both task performance and neurocognitive response. For example, there has been some evidence that individuals with ASD are less impacted by social motivation than NCs when completing a cognitive task. Social influences lead to group differences in task performance when there were no actual differences in ability between groups [272]. Therefore, investigating brain function without having account for performance variability during a task can be much less complicated.

1.6.1.2 Disadvantages of Resting-State Functional Connectivity Analysis

Nevertheless, resting-state fMRI has several methodological concerns which need to be considered when interpreting the data. Most critically, resting-state fMRI data is more sensitive to contamination of non-neural artefacts like head movement [271,273] and respiration [274,275]. Movement artefact can lead to signal change resulting in spurious group differences [276–278].

Both during scanning and post-scan processing, we attempted to reduce non-neural artefacts as much as possible. Firstly, evidence suggests that preparing an individual for what to expect during an MRI scan can reduced head movement [276]. Before scanning, we explained the scanning process in detail. Participants also listened to the sound and viewed pictures of an MRI scanner. During scanning, we stressed the importance of staying relaxed but also still.

Prior to our MRI analysis, participants with excessive head movement were excluded from the analysis (greater than 20% of their resting-state fMRI scans being labelled as outliers) [276]. Furthermore, we compared the number of identified outlier scans between groups to determine if motion artefacts might have variably impacted the data of individuals with ASD. Nevertheless, even with these precautions, we concede that movement is a considerable concern in resting-state fMRI data.

1.6.1.3 Functional Connectivity Techniques

Functional connectivity has been a promising method of investigating statistical correlations in time series across the brain, but neuroimaging

researchers have applied many different statistical techniques to map functional connectivity [263] which can impact the outcome of an analysis [118].

A full overview of these methods is beyond the scope of this introduction. Instead, we present the two most common functional connectivity analysis methods: seed-based correlation and independent components functional connectivity analysis. The seed-based correlation analysis method investigates the temporal correlation between a seed and other voxels in a specified region in the brain. This method requires a prior hypothesis in regards to a seed region [263] and is used to identify brain clusters which correlated with the average BOLD time course of that seed [263,279–281]. This technique is not designed to map functional connectivity across the entire brain but in relation to a specific seed region. The primary advantage of seed-based correlation analysis is its simple application and results [262,282]. We applied seed-based functional connectivity analysis because we wanted to investigate functional connectivity in association with the dACC only.

In comparison, independent components analysis is a data-driven method which does not require a prior hypothesis in regards to a seed region. This statistical method is used to segregate and cluster a BOLD dataset into both independent neural networks and signal artefacts which are independent of each other based on temporal-spatial neural associations. Independent components analysis can investigate functional connectivity across the entire brain although the statistical technique is more technically complex compared to the seed-based correlation analysis method [283–285].

1.6.2 Association between Glutamate Concentrations and BOLD Response in Neurotypical Controls

Studies have reported a relationship between Glu or Glx concentrations in a brain region and the BOLD response in closely associated brain regions in NCs [258,286–293], suggesting that Glu concentrations play a role in the strength of functional connectivity between brain regions [294].

For example, one group reported that increased relative ratio of Glu to N-acetyl-aspartate (NAA) concentrations in the medial prefrontal cortex (MPFC), as measured by ^{1}H-MRS, was correlated with increased MPFC resting-state functional connectivity to the nucleus accumbens and dorsomedial thalamus in NCs [286]. Another study reported that Glu concentrations in the dACC predicted the BOLD response in the retrosplenial cortex, basal ganglia, orbitofrontal cortex and inferior parietal lobe during an auditory inhibition task [288]. This evidence suggests that Glu concentrations in the dACC/MPFC may modulate the BOLD response of other closely associated brain regions.

Schmaal and colleagues (2012) reported a positive correlation between the Glu/Cre concentrations and impulsivity [258]. Researchers also reported that increased Glu/Cre concentrations were correlated with increased dACC seed-based resting-state functional connectivity to the substantia nigra, posterior cingulate cortex and ventral tegmental area in NCs. This evidence further suggested that Glu concentrations mediated long-distance functional connectivity to midbrain regions which in turns moderated impulsive behaviour [258].

1.6.3 Manipulation of Glutamate Concentration and Association with Functional Connectivity in Neurotypical Controls

In addition, there is some evidence that manipulating Glu or Glx concentrations with anodal or positively charged transcranial direct-current stimulation is associated with changes in functional connectivity [290,295–297]. Anodal transcranial direct-current stimulation (tDCS) administers low current to the scalp to stimulate the brain [298]. Researchers have reported changes in Glu or Glx concentrations following administration of tDCS to the motor cortex [299,300] and parietal lobe of NCs [290,301].

Hunter and colleagues reported increased Glx concentrations in the right intraparietal sulcus but not the left hemisphere, as measured by ^{1}H-MRS, following administration of tDCS to the right parietal cortex in NCs. At baseline, investigators applied independent components analysis to a resting-state fMRI scan and identified twelve separate brain networks. One of these networks was the salience network, a network of brain regions centred around insular cortex and dACC. As we explain in more detail later in this introduction (chapter 1.7.5.1), the salience network is a group of brain regions associated with integrating external and internal sensory information to guide behaviour [302]. Following tDCS, investigators reported increased functional connectivity across several of the baseline networks including in the salience network [290]. This evidence suggests that changes in Glx concentrations are associated with immediate changes to functional connectivity in NCs. In conclusion, we have presented evidence that Glu or Glx concentrations are associated with both behaviour and functional

connectivity in NCs, but there has been no investigation of these relationships in individuals with ASD.

1.7 DORSAL ANTERIOR CINGULATE CORTEX

The dACC is a central part of executive control tasks in NCs [303,304] and is anatomically and functionally connected with frontal, paralimbic, limbic and motor brain regions [302,305–312]. As the region of investigation with this study, we firstly provide an overview of the anatomical location of the dACC (chapter 1.7.1). We then discuss the dACC's functional relationship to both EC tasks (chapter 1.7.2) and more specifically, the inhibitory flanker conflict task (1.7.3). Finally, we present previous evidence that the dACC is functionally connected with a diverse range of brain regions (chapter 1.7.3).

1.7.1 Location

The dorsal ACC (dACC) is located on the medial surface of the brain and is superior to the corpus callosum. It also overlaps with the cingulate gyrus and sulcus. The dACC is posterior to the genu of the corpus callosum and rostral to the anterior commissure [313,314] in the anterior portion of BA 32 and 24 (figure 1.2) [254,314,315].
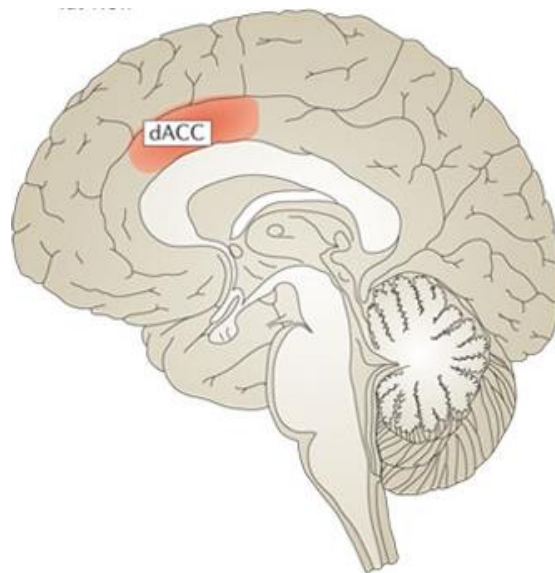
Figure 1.2 Location of the Dorsal Anterior Cingulate Cortex (Reproduced from Eisenberger et al. (2012)).

The dACC is marked in red on the medial surface of the brain just above the corpus callosum.

1.7.2 Function

The dACC has consistently been associated with tasks which require increased executive control [254,255,255,303,313,316–318] and this may explain its association with a range of tasks involving cognition, movement and emotion [314]. For example, researchers have reported an increased functional response in the dACC in association with emotional conflict [319], inhibitory motor control [320], inhibitory resistance to distraction [26,304] and decision making [321,322]; all slightly different tasks which require increased executive control.

Even though the dACC is associated with executive control tasks, researchers still disagree about the precise function of the dACC [313,323]. One prominent theory of dACC function is the conflict theory, which suggests that the dACC may elicit an increased functional response in association with

conflict [8,318,324]. Conflict is defined as an impediment or interaction between separate information processing streams [8,325]. The conflict hypothesis is supported by many neuroimaging studies reporting an increased functional response in the dACC in association with various types of conflict [303,318,325–332].

Nevertheless, the monitoring theory might more completely represent dACC function. According to this theory, the dACC functions in a supervisory role which initiates and adjusts the appropriate type and level of cognitive processing [303,316,329,333–335] to increase performance, reduce future conflict and limit performance error [8,254,325,329,336–340]. According to the monitoring theory, the dACC tends to be most sensitive to conflict when it is new information relevant to an internal goal, rather than because the stimuli are conflicting [341]. In other words, conflict is an indicator of task difficulty and the requirement for increased cognitive effort [313]. The differences between the two theories are minor, but the monitoring theory better explains evidence of an increased dACC functional response to error [342–346] pain [347,348], social exclusion [349,350] or even reward [351–353].

Researchers also postulate that the dACC may be associated with tasks which evaluate the cost versus benefit of initiating greater executive control [313]. Individuals typically engage in executive control processes only when they have sufficient motivation [354,355] and prefer to rely on habitual behaviours as a default [313,356,357]. Given this subjective cost, executive control processes initiate the least effortful response [7,13] to achieve a goal [313,356–358].

Similarly, the dACC may also be associated with motivation to participate in a task. Researchers demonstrated that mice with dACC ablation had reduced motivation to participate in a visuospatial attention task to increase access to sugar [359], presumably because the animal is unable to determine the value of participating in the task. Direct neuronal recording in monkeys found that the dACC encoded values related to probability, payoff and cost manipulations during a task [321]. Furthermore, direct stimulation of the dACC increased task perseverance in human epilepsy patients [360]. Although our understanding of dACC associated function continues to evolve, we suggest that the dACC may function to determine the value of executive control in association with the personal cost, monitor the available information regarding a goal-related task and flexibly adapt executive control processes as appropriate to attain a goal [323].

1.7.3 Conflict Effect Task

We applied the Erikson flanker or conflict effect task, a inhibition to distraction task which measures a participant's efficiency to inhibit attention and motor response to conflicting, non-goal related stimuli [26,338,358,361].

Although there are many variations of this task, we briefly outline the basic design. The goal of the conflict effect is to correctly indicate the direction (left or right) the centre arrow is facing. Flankers are non-target arrows. During congruent conditions of this task, there is little distraction from flankers because flankers face the same direction as the target arrow (←←←←←). During incongruent conditions, contradictory, flankers surround and face the

opposite direction of the target arrow (←←→←←). The conflict effect is calculated by the increase in average response time (RT) and total error rate (ER) during the incongruent conditions minus the congruent conditions. The conflict effect measures the efficiency and accuracy which an individual resists distractions from non-target stimuli [26,304,361–363].

During incongruent conditions, researchers have hypothesised that participants must increase executive control to contend with two competing stimulus information streams [56,364]. Firstly, there is a quick perceptual evaluation which primes a motor response to the dominant visual stimuli. Next, a slower, more deliberate cognitive information stream appraises the target and, in the case of incongruent flankers, inhibits the incorrectly primed motor response. During the incongruent flanker conditions, the competing flankers dominate immediate visual processing and require inhibition of the early incorrect response [361]. Investigators have shown that decreasing the distance between target and distractors [361] or increasing distractor contrast [365] further reduces efficiency in NCs by increasing the dominance of the incongruent visual stimuli and requiring increased inhibition.

Participants with ASD typically perform better than NCs on tasks which benefit from a local rather than global focus properties of visual stimuli [366–368]. For example, compared to NCs, individuals with ASD are faster and have fewer errors on the embedded figures task, in which a participant must find a target concealed within a complex figure [369].

Nevertheless, the propensity for bottom-up visual processing is unlikely to benefit individuals with ASD during the flanker conflict task. There has been evidence that individual with ASD view flankers in a less integrated way [370] and have difficulty filtering irrelevant visual stimuli [371,372]. During variations of the conflict effect task, individuals with ASD have had greater performance impairments with the addition of distracting arrows [26,27,50,52,272,373].

Nevertheless, some studies have not reported performance differences on the conflict effect task in individuals with ASD compared to NCs [35,54,374]. It has been suggested that variability in ASD sample characteristics could contribute to conflicting results between some inhibition to distraction studies [9,358]. Some evidence suggests that comorbidities with attention deficit disorder might underlie reduced executive control performance in ASD groups [375,376]. Additionally, a metanalysis of inhibition to distraction tasks, which included the conflict effect task, reported that varying intelligence quotients (IQ) between groups significantly contributed to performance differences in individuals with ASD compared to NCs [358]. Furthermore, executive control has a prolonged developmental trajectory into late adolescence in NCs [318,377]. Some evidence suggests that group differences in the conflict effect task might be associated with a delayed developmental trajectory rather than a lifelong deficit in inhibition [27,50]. Therefore, within our investigation, we focused only on adult participants with normal IQ to determine if performance differences on the conflict effect task occur in adults individuals without intellectual deficits.

1.7.4 Functional Association with the Conflict Effect Task

Studies have reported an increased BOLD response in the dACC during incongruent flanker conditions compared to congruent flanker conditions (see figure 1.3) in NCs [26,304]. In addition to the dACC, researchers also report an increased BOLD response in other regions such as the thalamus and frontal lobe in association with incongruent flanker conditions [26,304].
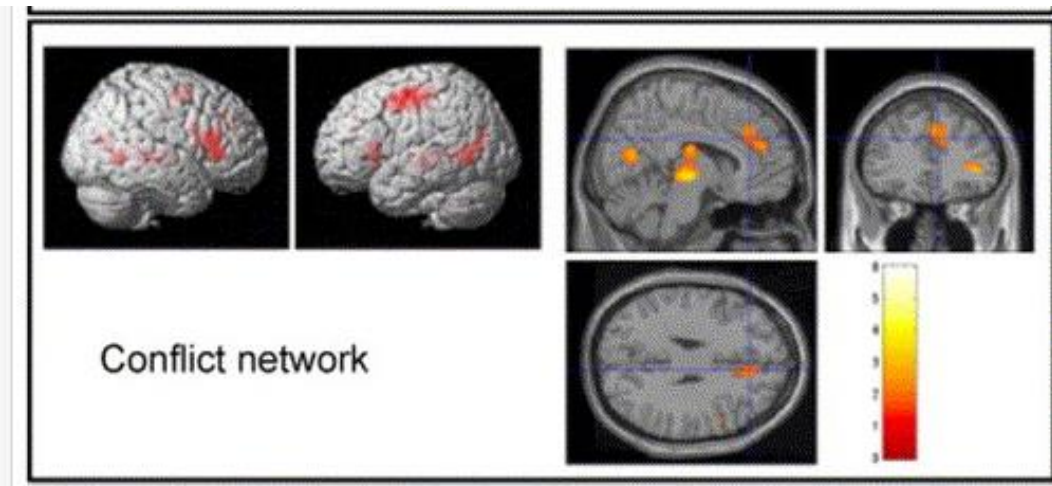
Figure 1.3 Increased Blood Oxygenated Level Dependent Response during Flanker Conflict Task in Neurotypical Controls (Reproduced from Fan et al. (2005)).

The conflict network is a group of brain regions with an increased BOLD response in association with conflicting flanker arrows compared to congruent flanker arrow conditions. as part of the Attentional Network Test (ANT) in NCs. Regions showing increased activation include the dACC, thalamus, left superior frontal gyrus, bilateral inferior frontal gyrus, bilateral fusiform gyrus, cerebellar vermis and right middle frontal gyrus.

1.7.5 Functional Connectivity

Given the integrative role in executive control tasks, it is not surprising that the ACC is a densely connected and influential brain region anatomically and functionally linked with frontal, paralimbic, limbic and sensory-motor areas [302,305–312]. Therefore, a thorough comprehension of neurocognitive function and behaviour, particularly for such an interconnected region, requires

investigation of the interaction between brain regions associated with the dACC.

1.7.5.1 Salience Network

Seeley and colleagues (2007) applied seed-based functional connectivity analysis to a resting-state BOLD dataset [116–118]. In this study, researchers investigated the functional connectivity between a seed region in the right anterior insular cortex and the rest of the brain in a group of NCs. Following analysis, researchers reported a network of brain regions which they referred to as the salience network. These results were further replicated in a second sample of NCs in which investigators applied independent components analysis to regions previously defined in the seed-to-voxel analysis. Both analyses identified a similar network of brain regions, centred around the insular cortex and dACC, but also including other paralimbic regions such as the paracingulate cortex and temporal pole. The paralimbic cortex, which also includes the insular cortex and dACC, rests between limbic and neocortical brain regions [378,379]. Therefore, it was unsurprising that the salience network also included limbic or subcortical regions such as the thalamus, hypothalamus, ventral striatum/ pallidum area, periaqueductal grey and substantia nigra/ ventral tegmental area; and also neocortical regions, such as the superior temporal lobe, frontal pole, operculum cortex, pre-supplementary and supplementary motor areas, ventrolateral and the dorsolateral prefrontal cortex (DLPFC) [302].

In the same year, another research group applied graph theory which defined a set of 39 predefined regions into functional connections using a resting-state BOLD dataset in NCs. Investigators identified a more restricted network which included core salience network regions including the dACC, thalamus, anterior insula, frontal operculum and frontal pole [306].

In yet another resting-state seed-based correlation analysis, researchers investigated functional connectivity between 16 separate seed regions in the ACC and the rest of the brain in NCs. Investigators reported that the left and right dACC (Montreal Neurological Institute coordinates (MNI) ±5, 19, 28) were functionally correlated with para-limbic regions such as the insular cortex; frontal lobe regions such as the ventrolateral prefrontal cortex (VLPFC), DLPFC and supplementary motor cortex; and limbic/subcortical region such as the thalamus [380]. This study further supported the salience network in association with a seed in the dACC rather than in the insular cortex (figure 1.4). In the same study, investigators also reported a negative correlation between the dACC and regions in the parietal and occipital cortex (figure 1.4).

As a first step in the analysis, researchers orthogonolised each of the 16 ACC seed region's time series to the other 15 seed regions in the ACC. The objective of the study was to identify the unique functional connectivity map associated with each seed region independent of the other ACC seed regions. It is possible that this orthogonalisation step undervalued functional connectivity for seed regions such as the dACC by removing shared variation

between seed regions [380]. Nevertheless, this study does agree that the dACC was functionally connected with frontal, paralimbic and limbic/subcortical regions .

.
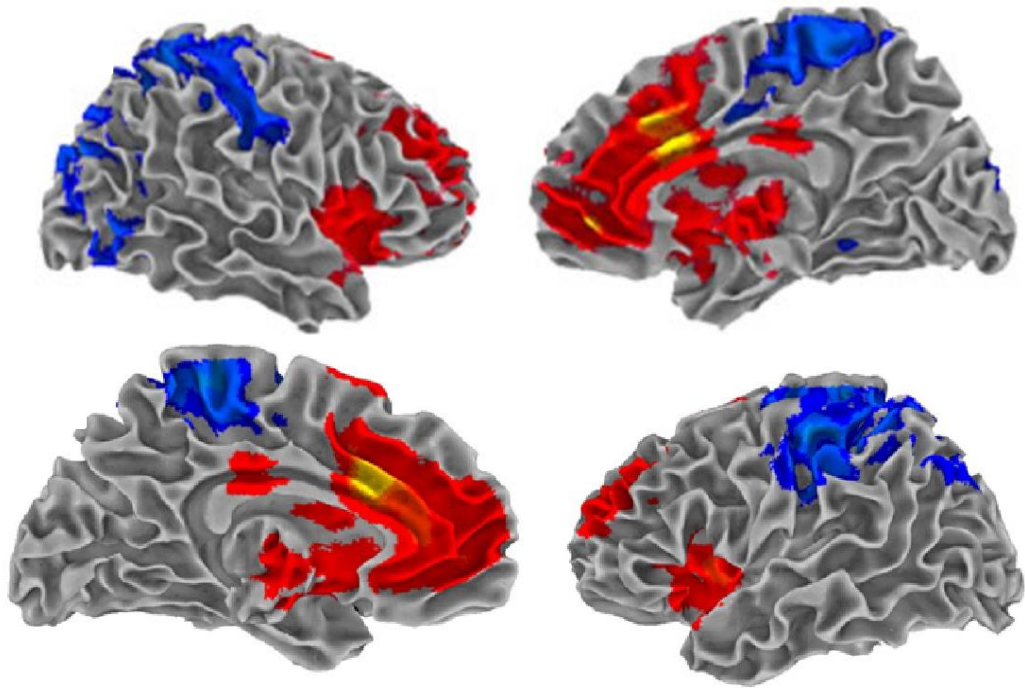
Figure 1.4 Seed-Based Correlation Functional Connectivity Analysis of the Dorsal Anterior Cingulate in Neurotypical Controls (Reproduced from Margulies et al. (2007)).

Seed-to-voxel functional connectivity maps associated with the dACC regions on the right (top images) and left (bottom images) in NCs. The dACC was positively correlated with other ACC, paralimbic, subcortical/limbic and frontal brain regions (red). Investigators reported a negative relationship between the dACC and parietal and occipital brain regions (blue). Seed region located at MNI ± 5, 19, 28.

A further dACC seed-to-voxel analysis was used to compare younger (17 to 25 years of age) and older NCs (51 years of age or greater). Again, researchers reported that the dACC was functionally correlated with the insular cortex, thalamus, superior temporal gyrus, primary motor cortex and superior frontal gyrus. In contrast to Margulies et al. (2007) [380], investigators reported a positive correlation with medial parietal lobe regions such as the inferior parietal lobule, precuneus and supramarginal gyrus (figure 1.5).

44

Researchers also reported that young adults had greater functional connectivity to the temporal parietal junction when compared to older adults [381], suggesting that changes to functional connectivity might vary with age.
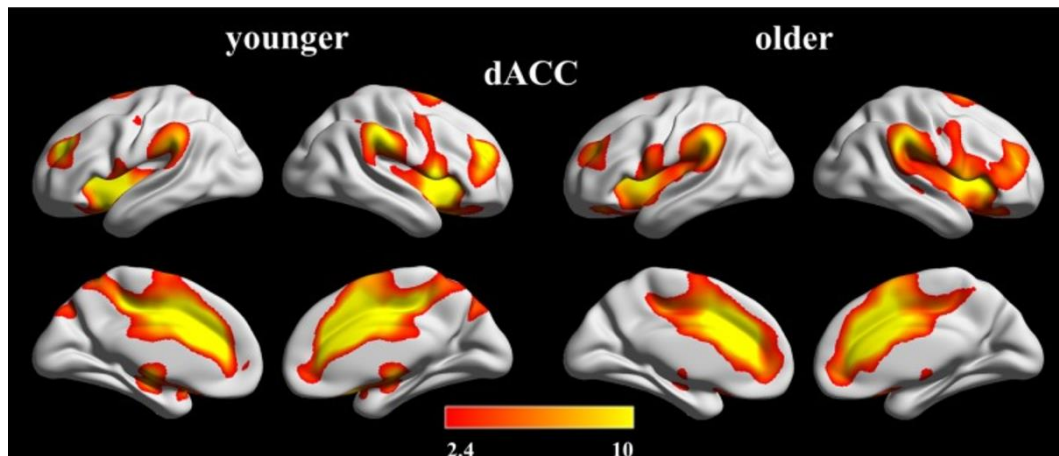
Figure 1.5 Functional Connectivity Analysis of the Dorsal Anterior Cingulate in Younger and Older Neurotypical Controls (Reproduced from Cao et al. (2014)

Functional connectivity maps associated with the dACC seed regions in neurotypical (left) young adults (17 to 25 years) and (right) older participants (51+ years). The dACC was positively correlated with limbic, paralimbic, frontal, temporal and parietal brain regions [381].

Functional Connectivity to Paralimbic and Limbic Brain Regions and Relationship to Internal Experience

Researchers have reported that dACC was functionally connected with other interoceptive, sensory and emotional regions such as the insular cortex, thalamus and amygdala [302,314,381]. Researchers have suggested that these brain regions might represent the value of stimuli to the dACC for further cognitive vetting to determine the most appropriate type of behavioural response [313].

The anterior insula is positioned between frontal, temporal and parietal lobes and functionally associated with tasks requiring interoceptive sensory and

emotional processing [382]. Seeley and colleagues further reported that increased resting-state functional connectivity, as measured by independent components analysis, between the anterior insula and dACC correlated with higher self-reported prescan anxiety in NCs. This evidence suggests that greater functional connectivity between these regions was associated with increased conscious awareness of internal experience [302].

In support of this hypothesis, Critchley et al. (2004) reported an increased BOLD response in salience network regions including the bilateral anterior insula and dACC when participants were asked to attend to their heartbeat. Interoceptive accuracy during this task also correlated with self-reported anxiety, depressive symptoms and negative affect [383]. Moreover, a longitudinal study of individuals with anxiety disorder reported that increased resting-state functional connectivity between the dACC and anterior insula was associated with reductions in anxiety over time. Although this study did not include a control group, it suggested that increased functional connectivity between the dACC and anterior insula might serve to modify a heightened emotional response to stimuli [384]. Tu et al. (2016) also investigated dACC seed-based resting-state functional connectivity. Researchers reported that when dACC functional connectivity increased to the right superior temporal gyrus and decreased to the right putamen and thalamus, there was an increase in social responsiveness scores in NCs [385]. These studies suggest that functional connectivity between the dACC and

paralimbic and subcortical structures are associated with both interoceptive and emotional experience in NCs [302,386].

Dorsal Anterior Cingulate Cortex Association with Cerebral Cortex and Relationship to Cognitive and Motor Response

As we previously mentioned, the dACC is also functionally connected with neocortical regions such as the DLPFC and VLPFC [380,381]. There has been limited evidence that functional connectivity between these regions might impact cognitive performance. Zhao and colleagues investigated participants with brain damage to measure nodal degree, an index of how well brain regions were functional connectivity with each other. Researchers reported that the nodal degree between the ACC and the rest of the brain was significantly associated with performance on general and modality-specific semantic cognitive tasks completed outside of the MRI scanner [312]. In relationship to the conflict effect task, another study reported that functional connectivity between the left dACC and DLPFC was directly associated with conflict effect performance when completed in an MRI scanner in NCs [387].

Finally, the dACC may also initiate a goal appropriate motor response which explains evidence of functional connectivity between the dACC and motor areas including the supplementary pre-motor area, a brain region functionally associated with movement planning [302,314,381]. In support of the association between the dACC and motor cortex, anatomical investigation in non-human primates has identified portions of the anterior cingulate which directly project to motor/ premotor cortex and spinal cord [388–391]. Other fMRI evidence in NCs

suggests that the effective connectivity, which measures the causal direction between brain regions, from the dACC to the supplementary motor area increases during a finger motor task compared to rest [392]. Researchers have reported that lesion to the supplementary motor area and also ACC severely diminished voluntary movements in primates [393]. These studies suggest that the dACC modulates the motor areas when movement is required.

1.8 DORSAL ANTERIOR CINGULATE CORTEX IN AUTISM SPECTRUM DISORDER

An increased functional response in the ACC has been associated with tasks which require greater executive control in NCs [26,334,394–397]. In individuals with ASD, there has been evidence of altered brain function in the dACC (chapter 1.8.1), suggesting that this region may be of interest in the disorder. We also present evidence of both altered function and functional connectivity of the dACC during inhibition tasks (chapter 1.8.2) and more specifically, the conflict effect task (chapter 1.8.3).

1.8.1 Altered Function

Several neuroimaging researchers have reported hypofunction of the dACC in association with individuals with ASD while at rest. Ohnishi and colleagues applied single-photon emission computed tomography (SPECT) to report reduced cerebral blood flow (CBF) in the left ACC in adolescents and young adults with ASD compared to NCs [398]. A further arterial spin labelling study reported reduced CBF in the dACC in adolescents with ASD compared to NCs [399].

In adults, researchers applied positron emission tomography (PET) to report reduced glucose metabolism in the dACC during a verbal learning task in adults with ASD relative to NCs [400]. Within the brain, there has been evidence that glucose metabolism is closely coupled to with Glu cycling [401–403]. A metanalysis of several cognitively-oriented but heterogeneous tasks suggested an overall hypoactivation of the dACC in individuals with ASD compared to NCs [404]. Taken together, this evidence suggests hypofunction of the dACC in individuals with ASD both during cognitive tasks and at rest.

Additionally, altered resting-state functional connectivity in association with the dACC in individuals with ASD may further predict an altered BOLD response when participating in an externally focused experimental task. Delmonte et al. (2013) reported increased resting-state functional connectivity between the dACC and striatum during a region-to-region seed-based correlation analysis in individuals with ASD relative to NCs. Functional connectivity between the dACC and dorsal striatum was associated with hypoactivation of the dorsal striatum during a fMRI social rewards task in adolescents and young adults with ASD but not NCs [405,406].

1.8.2 Altered Function and Functional Connectivity During Inhibition Tasks
There has been evidence of altered function in the dACC during executive control inhibition tasks in individuals with ASD. The Cued Letter Go/No-Go Task is one example of an inhibition task. During this task, individuals are asked to press a button after each letter appears. During the inhibition condition, the participant is asked to inhibit a response to a particular letter.

During inhibition conditions relative to non-inhibition conditions, researchers have reported hypoactivation of the dACC in participants with ASD compared to NCs [407]. Another group also reported hypoactivation in the dACC during a similar letter inhibition task in individuals with ASD relative to NCs [408]. Although neither study reported performance differences during the inhibition task, the neuroimaging evidence suggests altered dACC function in individuals with ASD [407,408].

Researchers also investigated an antisaccade inhibition task in individuals with ASD. During this inhibition task, the participant was asked to move their eyes away from a marker to the left or right of a screen (antisaccade condition) compared to moving their eyes toward the marker (baseline condition). Compared to NCs, adults with ASD had a reduced BOLD response in the dACC and frontal eye field during the antisaccade task compared to the baseline condition [409]. Adults with ASD also made significantly more errors during the antisaccade task than NCs [30,409]. Interestingly, increased antisaccade BOLD response in the dACC predicated improved performance and faster RTs during this inhibitory task in individuals with ASD only. Finally, researchers also reported reduced resting-state functional connectivity in individuals with ASD between both the right and left dACC and the left frontal eye fields [409]. This evidence suggests that reduced BOLD activity in the dACC and further functional connectivity was associated with reduced performance on this antisaccade inhibition task in individuals with ASD.

1.8.3 Altered Function During the Flanker Conflict Task

During the conflict effect task, researchers also reported hypoactivation of the dACC in individuals with ASD compared to NCs. Hypoactivation in the dACC during incongruent trials was positively correlated with ERs on the conflict effect task in adult participants with ASD [26]. This evidence suggests that the altered dACC conflict effect task response was associated with higher ER in individuals with ASD compared to NCs (figure 1.6).
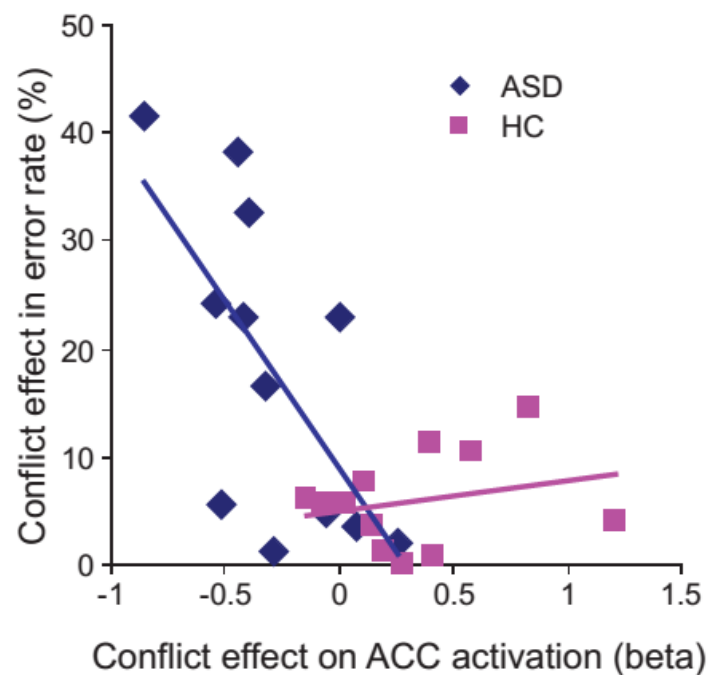
Figure 1.6 Positive correlation between the conflict effect error rate and hypoactivation of the ACC in participants with autism spectrum disorder (Reproduced from Fan et al. (2012))

There was a significant correlation between conflict effect performance and BOLD response in the ACC in participants with ASD. In other words, participants had a reduced flanker conflict effect ER with greater BOLD response in the dACC during incongruent trials when compared to congruent trials. This relationship was not shown in NCs

Another research group reported a similar result during a variation of the conflict effect task in which participants indicated the gaze direction of

people's faces rather than arrow direction. Participants with ASD had reduced activation of the dACC during incongruent conditions compared to congruent gaze conditions. However, in contrast to the previous study, there were no group differences in performance [53]. Both of these studies suggested altered function of the dACC in association with variations of the conflict effect task in individuals with ASD compared to NCs.

We hypothesised that individuals with ASD would continue to have reduced conflict effect performance compared to NCs when completing the ANT outside of an MRI scanner. We were also interested in exploring if Glu and Glx concentrations in the dACC had any relationship to conflict effect performance in both NCs and individuals with ASD.

1.9 GENERAL SUMMARY, HYPOTHESISE AND OVERVIEW

To summarise, Glu is the most prominent excitatory neurotransmitter in the brain [133] and is a critical component of neural communication, plasticity and cortical maturity [225,410]. Pathological alterations in Glu receptor signalling and cycling can be harmful to the brain, particularly during development [196–200]. There has been evidence of altered Glu concentrations in both the brain [247] and blood [211] of individuals with ASD.

Researchers have applied ^{1}H-MRS to report altered *in vivo* concentrations of both Glu and Glx in individuals with ASD, although the results of this research have been inconsistent [247]. Variation in participant characteristics, ^{1}H-MRS methodology and region of interest (ROI) may partially contribute to conflicting results. There is also little understanding of how Glu or Glx

concentrations are associated with behaviour and brain function in individuals with ASD.

In this thesis, we first applied a ^{1}H-MRS sequence optimised to obtain *in vivo* Glu concentrations in the dACC to determine if high functioning adult participants with ASD have altered Glu concentrations compared to NCs. For comparisons both to Glu concentrations with this study and to other ^{1}H-MRS investigations, we also assessed Glx concentrations in the dACC. Based on evidence of altered Glx [225,233,237] and Glu [217,230,231,237] concentrations in the ACC, we hypothesised that our sample of adult participants with ASD would also have altered (reduced or increased) Glu and Glx concentrations in the dACC. We also investigated the relationship between participant characteristics (age, IQ and Autistic Diagnostic Observation-Generic Module 4 (ADOS) scores) and metabolite concentrations to determine if cohort characteristics might have contributed to the conflicting results in previous studies.

Additionally, we investigated if metabolite concentrations might be associated with inhibition to distraction in ASD. Several neuroimaging studies have reported altered function of the dACC both at rest [398,399,411] and during a range of non-social cognitive tasks in individuals with ASD compared to NCs [404], such as the conflict effect task [26]. Hypoactivation of the dACC was also associated with reduced conflict effect performance in individuals with ASD [26]. Given that preliminary studies have reported an association between dACC Glu concentrations and inhibitory performance tasks in NCs [257,258], we

explored the relationship between Glu and Glx concentrations in the dACC and conflict effect performance in individuals with ASD compared to NCs. We hypothesised that altered Glu and Glx concentrations would be associated with reduced inhibitory performance on the conflict effect task in individuals with ASD.

Finally, research has begun to demonstrate that Glu and Glx concentrations in the ACC are associated with functional connectivity to other brain regions in NCs [258,287]. Abnormal excitatory processes in the dACC might impact the development, refinement and synchronization of the dACC with other brain regions. Therefore, we further investigated the relationship between Glu and Glx concentrations and dACC resting-state functional connectivity in participants with ASD compared to NCs. We hypothesised an altered relationship between metabolite concentrations and functional connectivity in individuals with ASD compared to NCs. In addition to highlighting an avenue for future research, the primary objectives of this study was to provide a more meaningful understanding of *in-vivo* Glu and Glx concentrations in participants with ASD and to allow greater context for interpretation of other ^{1}H-MRS studies.

2   GENERAL METHODOLOGY

2.1 INTRODUCTION

In both development and adulthood, maintenance of Glu in the brain is crucial for effective neuronal communication and cerebral health. As we discuss in chapter one, researchers applying ^{1}H-MRS in individuals with ASD have reported altered Glu and Glx concentrations, but the results of these studies are contradictory [247]. Therefore, further investigation of these metabolite concentrations is warranted.

When reviewing ^{1}H-MRS investigations of Glu or Glx concentrations in individuals with ASD, differences in scanning and post-processing methodology can influence the quality of metabolite concentrations [412,413]. On the ^{1}H-MRS spectrum, the Glu metabolic peak closely overlaps with Gln. Therefore, Glu is challenging to measure independently [230,243,414,415]. Within this thesis, we were interested in investigating Glu concentrations in individuals with ASD. Therefore, we applied ^{1}H-MRS parameters optimised to measure Glu concentration. An explanation of scanning parameters and post-processing methods is discussed in relation to this study goal (chapter 2.4.3 and 2.4.4).

Furthermore, to understand Glu concentrations in the brain in more detail, we investigated the relationship between participant demographics, core symptoms of the disorder, resistance to distraction inhibitory performance and functional connectivity in individuals with ASD compared to NCs. We also discuss the methodology behind our behavioural and neuroimaging data collection protocol.

To start, the ANT, which includes an inhibitory performance task, is presented (chapter 2.2). Next, a basic overview of MRI (chapter 2.3) and the various MRI sequences applied in this thesis are presented (chapter 2.4). Next, the metabolite concentrations measured and presented in this thesis are summarised (chapter 2.5). Then the specific methodology applied in this thesis is presented in full detail (chapter 2.6). The final section of this chapter includes demographic and clinical characteristics of participants within this investigation (chapter 2.7). The primary purpose of this chapter is to discuss and present the data collection methods applied in this thesis.

2.2 ATTENTIONAL NETWORK TEST

The ANT is a visuospatial behavioural assessment of attention. Throughout the ANT, the participant is asked to indicate the direction of a centre target arrow. There are three sub-tests to the ANT: the alerting, orienting and conflict effect. We previously presented the conflict effect (chapter 1.7.3), which is associated with decreased efficiency as measured by RT and ER in association with the addition of conflicting, incongruent flanker arrows [361,365,416]. In NCs, several investigations have reported both decreased RT and accuracy in association with incongruent flanker conditions compared to congruent flanker conditions [26,304,363,417]. Successful completion of the incongruent trials of the conflict effect involves increased executive control to inhibit and resist non-target stimuli and motor priming [254,338,361,418,419].

Although not a primary focus, the ANT also includes the alerting and orienting effect. Firstly, the alerting effect is the performance penalty

associated with a lack of a prior cue that a target is about to appear. It is thought to be a measure of internal vigilance to the task [26,363,417]. Therefore, an altered alerting effect in ASD groups could indicate that participants were less vigilant during the task. The orienting effect is defined as the increased RT or error percentage associated with disengaging attention from a cue location and re-engaging attention to the target flanker location [26,363,417,420,421]. The inclusion of these variables in the ANT permitted greater variation in stimuli types as would more typically happen in everyday life. The inclusion of other stimulus sub-conditions (alerting and orienting effect) and the random presentation limited obvious repetition between stimulus types during conflict effect trials.

We included the conflict effect task as our primary behavioural measure mostly because of its functional association with the dACC. Again, several studies have reported an increased BOLD response in the dACC during incongruent flanker conditions compared to congruent conditions in NCs [26,304]. Researchers have also reported a decreased BOLD response in the dACC in adults with ASD. A decreased BOLD response in the dACC was also associated with reduced performance on the conflict effect task in individuals with ASD [26,304]. Based on this research, we felt the task would be a good measure of dACC function in NCs and hypofunction in individuals with ASD.

2.2.1 Advantages

The primary advantage of this assessment was that we could administer the assessment by computer thus reducing social interactions in a clinical group with deficits in social behaviours and skills [422–424]. Previous research has demonstrated that social interaction during various executive control tasks can impact the performance of individuals with ASD differently than NCs [272,424,425]. For example, one research group compared performance on a modified version of the conflict effect task under normal conditions compared to when participants were given the additional social motivation of being told they were competing against other children. Children with ASD had no improvement in performance between conditions while NCs had improvements with greater social motivation [272]. Therefore, the ability to administer the ANT by computer limits social interaction and the potential variable impact of social motivation on performance in both groups.

2.2.2 Disadvantages

The primary disadvantage of the ANT is its monotony. Although it can be administered in less than twenty minutes, the assessment is repetitive and uninteresting. We stressed that each participant complete the test to the best of their abilities, but boredom may have impacted performance or compliance in some cases. In fact, 2 NCs and 2 participants with ASD were excluded because they did not complete incongruent flanker conditions at greater than 60% accuracy. This might have been related to a lack of interest in the assessment.

2.3 MAGNETIC RESONANCE IMAGING

2.3.1 Basic Principles

Magnetic resonance imaging technology obtains information about tissue by exploiting its magnetic properties and is currently one of the most widely utilised tools to investigate the brain. Hydrogen protons inside water and fat are sensitive to magnetic fields and will align with a uniform superconducting magnet, initiating a net tissue magnet vector (B_0). When a radio frequency (RF) pulse at the resonance frequency of hydrogen nuclei is further applied, the net magnetic vector of hydrogen is redirected (B_1). When the RF pulse stops, hydrogen moves back into resting-state and emits a radio wave which is picked up by an RF receiver coil of the scanner [276,426].

During an MRI scan, magnetic gradient coils also subject tissue to three orthogonal gradient magnetic fields, which slightly alter the resonance frequency of hydrogen at different locations. As hydrogen protons are only sensitive to an RF pulse at a specific resonance frequency, slightly altering the magnetic field by location allows MRI to localise signal and target particular sections of tissue during a scan [427,428].

2.3.2 Advantages

Most MRI sequences are non-invasive and *in-vivo*. Researchers can obtain an image of the brain without having to apply radioactive tracers, as is the case with PET [427,429,430].

Magnetic resonance imaging can be utilised to investigate many parameters in the brain [427,429]. The versatility of MRI technology was also an advantage

in this thesis. During a single scanning session, we were able to obtain an anatomic three-dimension magnetisation-prepared rapid gradient-echo (MP-RAGE), resting-state echo planar image (EPI) and ^{1}H-MRS sequence. Our multimodal imaging sequence permitted more detailed investigation of the relationships between measured parameters of the brain including structure, function and metabolite concentrations [431].

2.3.3 Disadvantages

Even with these advantages, MRI is not a perfect technology. Firstly, with current technological constraints, neuroscientists cannot investigate the brain at a microscopic or individual neuronal level. At 3 T, each voxel in an fMRI image is equivalent to about 10,000 neurones. Reduced precision limits the conclusions which can be made about the data [429].

Furthermore, to obtain a quality MRI scan, a participant must lay inside a small cylinder without moving while the scanner makes a great deal of noise. The environment of an MRI scanner is far from natural and can elicit increased anxiety and claustrophobia in individuals, likely impacting brain function during an MRI scan [432,433].

We tried to reduce participant stress associated with an MRI scan by explaining what to expect during the scan, listening to the sound of the machine, practising being in a mock scanner and discussing any of the participant's questions or concerns [434]. These strategies did appear to improve the experience of participating in an MRI scan. Nevertheless, there

were some individuals who were unable to participate in this study due to claustrophobia (NC = 1, ASD =2).

2.4 MAGNETIC RESONANCE IMAGING SEQUENCES

We briefly introduce and highlight the various multimodal MRI techniques that were utilised.

2.4.1 Structural Magnetic Resonance Imaging

Magnetic resonance imaging technology is well suited to measure soft tissue and can differentiate between tissue types in the brain. It is used to generate pictures of brain anatomy. Various tissue types have different concentrations of water and fats and, therefore, different concentrations of hydrogen protons. For example, CSF, having greater proportions of water, has different intensities compared to grey matter (GM) and WM [427,429,430].

2.4.2 Functional Magnetic Resonance Imaging

The BOLD contrast neuroimaging method utilises MRI technology to measure variations in the magnetic qualities of blood oxygenation in the brain [115,435,436]. Blood with reduced concentrations of oxygen has increased magnetic qualities [437] leading to increased MRI signal distortion, faster signal decay and a slightly weaker signal. The percentage signal change is minimal (less than 2%) [429,435,438]. Signal change is too small to be detected visually and requires statistical analysis software to reveal BOLD fluctuations [276,439]. Functional MRI measures localised changes in magnetic properties which are considered an indirect measure of neuronal activity [440].

Fundamentally, fMRI is useful for investigating localised brain function, in which specific brain regions are associated with particular behaviours and cognitions [429]. An fMRI scan measures the hemodynamic response (HR), which occurs in association with increased neuronal activity as evident through changes in the BOLD signal (figure 2.1). The HR is an overcompensation of CBF and oxygenated blood following both neuronal firing and oxygen consumption. The HR typically takes between six and nine seconds to reach a peak.
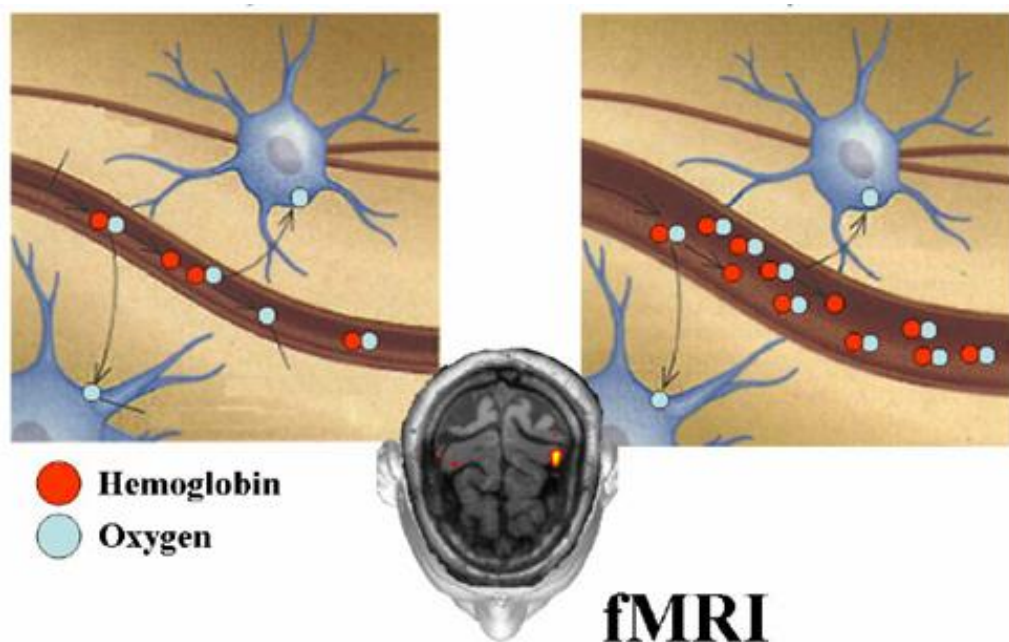
Figure 2.1 The Hemodynamic Response (adapted from Astolfi et al. (2004)).

Biological principles associated with the HR. When a neurone fires, it also consumes an increased amount of oxygen from local CBF (left). Increased energy consumption is following by a compensatory increase in CBF (right) and oxygen levels. The result is an increased proportion of oxygenated blood and a change in the BOLD signal.

2.4.3 Proton Magnetic Resonance Spectroscopy

Proton magnetic resonance spectroscopy harnesses MRI technology to non-invasively quantify different molecular populations in a region of the brain

[412,415,441,442] and is useful in providing *in vivo* biochemical information [412,415].

In this thesis, we applied ^{1}H-MRS as part of a multimodal imaging sequence to investigate Glu and Glx concentrations in the dACC. In the section, we present a brief technical background to ^{1}H-MRS to lay the foundation for our ^{1}H-MRS protocol and analysis.

To start, ^{1}H-MRS indirectly quantifies and measures the concentrations of various molecules containing hydrogen [443]. Electrons can slightly shift or alter the influence of an external magnetic field on hydrogen nuclei, which leads to a minor shift in its resonance frequency. Slight differences in resonance frequency due to the molecular environment of a molecule is known as the chemical shift or signature of a molecule [413]. The various chemical signatures in a sampled brain region are classified and quantified within the ^{1}H-MRS signal and have historically been expressed in parts per million (ppm) to the Larmor frequency of tetramethylsilane [413].

In the brain, ^{1}H-MRS is used to measure biochemical substances that are involved in metabolism and therefore, these substances are called metabolites. Given current technological constraints, ^{1}H-MRS can only detect the chemical shift of metabolites in concentrations greater than .05 millimoles per litre of brain tissue (Mm) [413,444]. At 3 T, ^{1}H-MRS typically measures NAA and N-acetyl-aspartyl-glutamate (NAA+NAAG), creatine plus phosphocreatine (Cre), choline containing compounds (Cho; the combined signal of phosphorylcholine, glycerophosphorylcholine, acetylcholine and free choline), myo-inositol (mI) and Glx in the brain [412,414]. Typically, the ^{1}H-MRS

spectrum within the brain is between 0 and 4.2 ppm while water's chemical signature appears at 4.7 ppm [412,414].

2.4.4 Technical Considerations of Proton Magnetic Resonance Spectroscopy

There is no standardised ^{1}H-MRS scanning sequence or post-processing strategy because experimental criteria vary depending on technological limitations, the metabolite of interest and researcher expertise. Methodological variation needs to be considered when comparing studies and interpreting results [412,413].

Structural or fMRI sequences measure water. In comparison, inhomogeneity in a ^{1}H-MRS experiment is a greater constraint because the metabolites investigated exist in much lower concentrations and thus have a much weaker signal. Therefore, the signal to noise ratio (SNR) is much weaker [251] and any increase in noise is a greater detriment.

This disadvantage becomes even more problematic when measuring Glu concentrations [412,413], which closely overlap with metabolites such as Gln on the ^{1}H-MRS spectrum. The goal of this section is to present data acquisition and post-scan processing methods which were applied in this study to facilitate the independent measurement of Glu concentrations within this ^{1}H-MRS experiment.

2.4.4.1 Software

Software packages which process ^{1}H-MRS data include the linear combination model (LCModel) [445] and the Magnetic Resonance User Interface (MRUI) [446]. Both of the above spectral packages fit the raw spectra to *a priori* metabolite peak models which improve Glu and Gln isolation [414,447]. In the analysis of Glu and Glx concentrations in individuals with ASD previous research has more often applied the LCModel to process raw spectroscopy data [225,226,228–232,236,237,240,241,243,246,443]. Given the wide use of the LCModel and access to the software in our department, we also applied the LCModel to our ^{1}H-MRS data to allow for improved isolation of Glu to Gln.

2.4.4.2 Cramér-Rao low bounds

Cramér-Rao lower bounds (CRLB) scores of variance are a commonly utilised metric of certainty in ^{1}H-MRS experiments. A CRLB score quantifies how closely the measured metabolite fits with *a priori* metabolite peak models taking into account spectral resolution and noise. It is a useful metric to compare the validity of metabolite measurements compared to predicted models both between studies and groups[444,445,448].

The application of improved shimming methods during data collection is one method to improve CRLB scores. Shimming is defined as the addition of hardware or technical methods during scanning which improve homogeneity in the magnetic field. Shimming reduces noise and improves spectral resolution [449]. It can be difficult to compare shimming methods between

studies as they are specific to the scanner model and often unreported. Nevertheless, CRLB scores are an indirect indicator of effective shimming techniques because shimming can greatly improve CRLB scores [450].

A CRLB score below 20% has been suggested as a useful standard for metabolite inclusion [451]. Although some single voxel spectroscopy studies did not report CRLB scores [217,238], most previously reported single voxel spectroscopy studies investigating Glu or Glx concentrations in individuals with ASD were all below or near the 20% CRLB cut-off [225,226,228–231,237,240,241,243,245,246]. Given this precedent, we also elected to include metabolite measurements with a CRLB below 20%.

2.4.4.3 Increased Tesla Strength

Another important moderator of Glu measurement with ^{1}H-MRS is T strength. At 1.5 T, it is nearly impossible to differentiate the Glu chemical signal from Gln, Gamma-Aminobutyric acid (GABA) and glutathione because these metabolites have a similar chemical signature [232,251]. In early ^{1}H-MRS studies, which used 1.5 T scanners, research groups typically reported Glx [225,232,233,235,236,238,242,244,245,452]. Researchers considered Glx a good index of Glu concentrations [247,413,414] based on evidence that Glu accounts for 40-60% of the Glx metabolic peak [414,453].

Of course, this interpretation of Glx has been problematic because it is unclear what proportions of the various metabolite concentrations contribute to the Glx peak. This becomes more problematic when comparing clinical groups to NCs. For example, one post-mortem study reported a reduced ratio

of Glu to Gln in individuals with ASD compared to NCs in the ACC [454] suggesting that the relationship between these metabolites might be altered in this disorder. This highlights the importance of measuring Glu concentrations separately to Gln.

Increasing the external magnetic field increases the magnitude of various chemical shifts leading to an increased chemical spread on a ^{1}H-MRS spectrum and improvement in the SNR. Increasing the external magnetic field allows greater signal differentiation in closely coupled molecules like Glu and Gln [412,455–457]. Tesla strength cannot be increased indefinitely, because increased magnetic strength also introduces greater field inhomogeneity [450,458–460]. Most ^{1}H-MRS studies reporting Glu in individuals with ASD applied a magnetic strength of 3 T [226,237,243] or 4 T [230]. In this experiment, we utilised a 3 T scanner to quantify Glu concentrations separate to Gln.

2.4.4.4 Multi or Single Voxel Spectroscopy

Spectroscopy studies also vary in the number of voxels investigated. Multi-voxel spectroscopy further applies orthogonal magnetic gradients to obtain the chemical shift of several voxels (typically between 20 and 100) at various locations across the brain during the same scanning session [251,412]. One advantage of multivoxel spectroscopy is a spatially diverse representation of metabolite concentrations. On the other hand, multivoxel spectroscopy increases magnetic inhomogeneity across the brain, resulting in reduced metabolite peak definition and variation in water suppression between voxels.

More practically, multivoxel spectroscopy greatly increases acquisition time [413,427] leading to greater difficulties with head movement and participant compliance. For example, Doyle et al. (2014) reported that their multivoxel spectroscopy sequence was completed in 45 minutes. In comparison, our single voxel spectroscopy scanning sequence was completed in less than ten minutes. The researcher needs to consider participant compliance when selecting their ^{1}H-MRS parameters [251].

Single voxel spectroscopy applies ^{1}H-MRS to a single voxel in the brain [412]. Although limited spatially, single voxel spectroscopy is less constrained by magnetic field inhomogeneities and, therefore, typically obtains clearer metabolic peaks [413,427]. Given the increased difficulty in obtaining Glu concentrations, it is little surprise that all other [1]H-MS studies reporting Glu concentrations in individuals with ASD also applied single voxel spectroscopy [217,226,230,237,243]. To limit participant fatigue and also more accurately measure Glu concentrations, we applied single voxel spectroscopy within this study.

2.4.4.5 Increased Voxel Size

Increasing the voxel size investigated in a single voxel spectroscopy sequence can also improve the SNR [445,457,461] because the signal is proportional to the voxel size while noise remains constant [251]. The voxel size in a ^{1}H-MRS experiment is roughly a thousand times larger than a structural MRI voxel [412,462,463]. On the other hand, the voxel size cannot be increased indefinitely because shimming techniques to improve SNR are less efficient over larger brain regions [251].

Most of the voxel sizes for single voxel spectroscopy Glu studies were between 6 and 9 cubic centimetres (cm^3) [217,226,230,237,243]. We elected to investigate a 30 x 20 x 15 mm (9 cm^3) voxel, as this was in the range of most of the previous investigations.

2.4.4.6 Pulse Sequence

The type of pulse sequence also varied between previous ^{1}H-MRS experiments. The two most common pulse sequences were point resolved spectroscopy (PRESS) [464] and stimulated echo acquisition mode (STEAM) [465]. In both sequences, there are three orthogonal slice selective pulses which intersect in three dimensions to select the VOI. The PRESS sequence applies one 90⁰ and then two 180⁰ pulses while steam has three 90⁰ pulses. When comparing the two techniques, the PRESS sequence captures the full ^{1}H-MRS signal and therefore has an increased SNR relative to STEAM [466,467]. Nevertheless, STEAM permits shorter echo times (TE) than PRESS [251]. There has been evidence that the STEAM sequence can be used to obtain Glu concentrations [468]. Nevertheless, as the PRESS sequence has been commonly utilised to measure Glu concentrations in individuals with ASD [217,226,228,230,231,237,241] and has been shown to capture more of the ^{1}H-MRS spectrum [466,467]. Therefore, we elected to apply a PRESS sequence within our study.

2.4.4.7 Relative or Absolute Metabolite Concentrations

Many metabolite concentrations vary depending on GM, WM and CSF tissue type. Therefore, metabolite concentrations must be corrected for tissue

concentrations [412,469]. Presenting metabolite concentrations as relative units is one method of correction. Relative concentrations are a quantified metabolite in proportion to another metabolite thought to be constant in but representative of tissue type. Typically investigators used Cre concentrations as a stable marker of tissue concentrations because previous research has reported that Cre is stable in adult NCs [247,251,413,470,471].

From a practical perspective, relative ratios are a less technically complicated and labour intensive method of correcting for partial volume effects [472] and are therefore a much more common technique [413]. Several single voxel spectroscopy investigations reported the relative ratio of Glx/Cre [238,245] and Glu/Cre [228,229] in the brains of individuals with ASD compared to NCs.

On the other hand, relative ratios are less theoretically sound when comparing groups. Most published ^{1}H-MRS investigations have not reported significant differences in Cre concentrations in individuals with ASD compared to NCs [247], including several ^{1}H-MRS studies of the ACC/MFC [225,233,237,473–475]. Nevertheless, a handful of studies have reported altered Cre concentrations in adults with ASD compared to NCs in the hippocampal and amygdala complex [242,474,476,477] and ACC/MFC [477] suggesting some variations in Cre concentrations in association with the disorder [247]. Therefore it is unclear if group differences in relative ratios were associated with the metabolite of interest or its proportion to the "stable" metabolite [413,478].

In contrast, absolute quantification is a more theoretically sound method but requires increased scan acquisition time and more sophisticated post-

processing techniques [413]. One common strategy for absolute quantification is the acquisition of a ^{1}H-MRS spectrum during data acquisition without water suppression which is applied during post-processing to correct for tissue concentration and possible variations in voxel size. In a single voxel spectroscopy experiment, the inclusion of a non-suppressed ^{1}H-MRS voxel does not increase scanning time significantly [251,413,470]. In our analysis, we acquired 16 averages of the water signal in less than one minute. Also, both a well-placed voxel [470,479] and directly correcting for CSF concentrations in the voxel will also correct for tissue variation between groups [480], and we included all of the above strategies in our analysis in reporting the absolute metabolite concentrations.

2.4.4.8 Echo Time

Furthermore, in the literature, reducing the time between a magnetic pulse and sampling in a ^{1}H-MRS experiment, known as TE reduces T2-decay and therefore increases peak detail for metabolites with shorter relaxation times [481] such as Glu [482–485]. Therefore, the TE applied will vary with the metabolite of interest in a study. A longer TE (> 135 ms) produces a simpler ^{1}H-MRS spectrum with a more defined baseline although it reduces metabolite information of less concentrated metabolites such as Glu [251,413].

Previously reported studies investigating Glu at 3 T in individuals with ASD had a TE less than 35 milliseconds (ms) [217,226,228–231,237,241,243]. Our investigation was the first to report Glu concentrations at a TE of 80 ms in individuals with ASD. Previous studies have suggested that shorter TEs have

been associated with an overestimation of Glu concentrations [482]. Furthermore, previous research in a large number of participants has suggested that a TE of 80 ms was an optimal parameter to separate Glu from Gln in the ACC at 3 T in NCs [484]. Other studies suggested a lower TE of 40 ms was optimal [485,486]. The optimal TE for determining Glu concentrations is still under investigation, but we elected to apply a slightly longer TE of 80 ms.

2.4.4.9 Sedation

Several studies sedated participants to increase compliance and reduce participant head movement [235,242,243]. Moreover, two of these studies disproportionally applied sedation to participants with ASD compared to NCs [235,242]. Researchers investigating rodent brain slices demonstrated that sedatives such as propofol, thiopental and ketamine were associated with reduced Glu release [487]. In humans, propofol administration was also associated with reductions in Glu concentrations as measured by ^{1}H-MRS in the motor cortex, sensory cortex, hippocampus, thalamus and basal ganglia [488]. Given this evidence, ^{1}H-MRS studies that investigated Glu/Glx concentrations in sedated participants are a useful first step in understanding Glu in ASD, but require replication in non-sedated participant populations. Beyond the obvious ethical considerations, this thesis chose not to administer sedatives because of the potential impact on Glu concentrations. We also tried to limit mild stimulants by instructing participants not to intake illegal drugs, nicotine or caffeine at least three hours before their MRI scan [489].

Variations in data collection, post-processing and interpretations greatly impact the value of a ^{1}H-MRS study and must be taken into account in association with the Glu measurement [455]. Magnetic resonance spectroscopy is still an immature MRI analysis method. One must also understanding the underlying principles of spectroscopy, various methods of analysis as well as the current limitations to fully appreciate an experiment [413].

2.5 METABOLITES

We briefly provide an overview of the metabolites investigated.

2.5.1 Glutamate and Combined Glutamate and Glutamine

We provided a detailed overview of Glu and Gln function previously (chapter 1.3). Briefly, Glu is important for development, communication and neural plasticity. Regulation of extracellular Glu concentrations is critical for cerebral health.

As we mentioned previously, the similar chemical structure between Glu and Gln result in a close overlap in the respective signals from these metabolites on the ^{1}H-MRS spectrum, [414]. In NCs, Glu concentrations are quantified at 2.34 ppm [414] and have concentrations between 6.0 and 12.5 Mm in the brain [414]. In contrast, Gln resonates at 2.45 ppm and exists in concentrations between 3 and 6 Mm in the brain [414,490].

2.5.2 N-Acetyl-Aspartate

N-acetyl-aspartate is synthesised in neurons and oligodendrocytes [470,491] and exists in large amounts in the brain [492,493]. Following water and lipid suppression, NAA is the most dominant peak on the ^{1}H-MRS brain spectrum

in healthy brain tissue. N-acetyl-aspartate has concentrations between 7.9 and 16.6 Mm [414], resonates at 2.01 parts per million on the ^{1}H-MRS spectrum [413,441] and has similar concentrations in both GM and WM [248]. Research suggests that NAA's primary location in the mature brain is in the neuron [494–497]. Therefore, NAA is considered a marker of neuronal density and integrity [247,251].

2.5.3 N-acetyl-aspartyl-glutamate

In contrast to NAA, NAAG is a neurotransmitter formed when NAA bonds with Glu [247,498]. N-acetyl-aspartyl-glutamate might assist in communication between neurones and astrocytes [499]. Although, research has also suggested that microglia can synthesise NAAG [500] suggesting some link outside of neurones and astrocytes.

2.5.4 Quantifying N-Acetyl-Aspartate and N-Acetyl-Aspartyl-Glutamate

Given a similar electron environment, NAA and NAAG are separated by .003 ppm on the hydrogen chemical spectrum. It is virtually impossible to distinguish between these metabolites [441,501], although application of increased magnetic fields, faultless shimming or special editing techniques might allow differentiation [501,502]. Given that we have not applied any of these strategies, we report both NAA and NAAG (NAA+NAAG) concentrations as recommended by the LCModel manual [451]. In practice, NAAG only accounts for about 9% of NAA+NAAG concentrations in GM [501,502], although NAAG is more abundant in WM [248]. Nevertheless, as we highlight previously, this limits the conclusions which we can make about our data. There has been

evidence of altered NAA concentrations in individuals with ASD compared to NCs, but this evidence has also been contradictory [247]

2.5.5 Creatine and Phosphocreatine

As with NAA and NAAG, Cre signals overlap and are typically reported together [470]. Cre is associated with additional energy reserves in the brain through adenosine triphosphate metabolism [247,248,470,491,503]. Both neurones and glial cells contain Cre, but synthesis occurs outside of the brain [247,470]. In ^{1}H-MRS, Cre resonates at both 3.03 and 3.93 ppm [247,470]. Creatine and phosphocreatine have higher concentrations in GM than WM [248,442,491] and exist in concentrations around 5 to 10 Mm in the brain of NCs [414].

Historically, Cre has been considered a constant metabolite in adulthood [247,251,470]. Nevertheless, there has been some evidence of altered Cre concentrations in children with ASD [235,242,474] and adult participants with ASD compared to NCs in various regions of the brain [226,232,236,477,504] including the ACC [505], suggesting that this metabolite may be impacted by disease processes of the disorder.

2.5.6 Choline Containing Compounds

Choline containing compounds (Cho) include phosphocholine and glycerophosphocholine. Cho concentrations are also associated with acetylcholine and free choline in the brain [247,470]. Cho is associated with the creation and degradation of phospholipids, which are critical for cell membranes throughout the body [470,503,506]. Changes in Cho concentrations have been interpreted as evidence of changes in phospholipids and

myelination [247,410,477,504,507,508]. In adult participants, increased Cho concentrations have been associated with rapidly multiplying cancer cells in the brain in tumour patients [509,510]. In an ^{1}H-MRS experiment, Cho resonates at 3.2 ppm, and concentrations are typically between .9 and 2.5 Mm in the brain of NCs [247,414]. Choline containing compounds have higher concentrations in WM because of Cho's association with myelination [248,507]. Children also have increased Cho concentrations as myelination within the brain is increased during development [511].

Researchers have suggested that Cho concentrations might provide crucial biochemical information in association with tumour growth in the brain [509,510], but in adults with ASD, there has been little evidence of altered concentrations [247] in frontal [236], parietal [232,233,236,477] temporal [226,233] or the cerebellar lobe compared to NCs [237,504]. Additionally, researchers reported no difference in Cho concentrations in the ACC [233,237,512]. Nevertheless, there have been two adult studies reporting increased Cho concentrations in the hippocampus and amygdala complex [504] and the MPFC in individuals with ASD relative to NCs [477].

2.5.7 Myo-inositol

In the brain, mI is solely expressed in glial cells [503,513,513] and has been associated with water regulation [453,491,503,514]. Some evidence suggests that mI might be associated with glial inflammation [503,515] and it is thought to be a marker of glial density and proliferation [248,470,470,503]. The mI peak is located at

3.56 ppm [248,453,470] and concentrations are typically between 3 to 8 Mm in NCs [414].

Most ^{1}H-MRS studies also have reported no significant difference in mI concentrations in the brains of individuals with ASD [247] including those investigating the ACC/MFC [225,233,237]. Nevertheless, one study in children with ASD reported increased mI concentrations in the ACC/MPFC compared to NCs [475].

2.6 METHODS

2.6.1 Study Population

Participants with ASD were recruited both from psychiatrist referrals at the Royal Edinburgh Hospital and the "Number 6: One Stop Shop" for individuals with ASD, a regional ASD consultancy and psychiatric service in Edinburgh. Recruitment began in January 2013 and was completed in August 2014. Study exclusion criteria included being female, seizure in the previous 12 months, a diagnosis of psychosis, schizophrenia, bipolar disorder or inability to safely participate in an MRI scan. In addition, we included only individuals with a total IQ above 80, because there has been evidence that reduced IQ in individuals with ASD compared to HC contributed to performance differences during inhibition tasks [358] (see chapter 1.7.3). Nevertheless, future studies would benefit from assessing individuals with lower IQ.

Funding restricted our participant sample size and we, therefore, elected to investigate only adult participants. We investigated if metabolite concentrations and inhibitory performance differences occured in adult

participants with ASD compared to NCs. As we mentioned previously (chapter 1.4.2), most of the previous research in Glu and Glx metabolite concentrations in the ACC has focused on children and adolescents [247,358], and it is still unclear if metabolite abnormalities occur in adult participants with the disorder. Similarly, we investigated inhibitory resistance to distraction performance in adult participants with the disorder compared with NCs (chapter 1.7.3), which is also debated within the literature [27,358]. We concede that it would have been beneficial to include children in this study to assess cross-sectional variation across the lifespan of the disorder and future studies with larger cohort sizes will hopefully investigate this further.

During participant recruitment, we included a wide cross-section of age ranges to allow some analysis of how metabolite concentrations might vary from early to later adulthood in individuals with ASD compared to NCs. Nevertheless, the inclusion of such a large age range could also be considered a limitation of this study because it increased the variability in our participant sample. This limited the power of our analyses because we had to control for the impact of age in many group comparisons.

Individuals with ASD were invited to participate if they had a clinical diagnosis of ASD from a multi-disciplinary assessment service for ASD in South East Scotland and were not known to have a learning disability. We recruited 25 adult male participants between the ages of 23 and 53 with a diagnosis of high-functioning ASD. Before the final analysis, a further six participants with ASD were excluded because their total communication and social ADOS

(ADOS-G) scores were below seven, a criterion used to confirm a diagnosis of ASD. Following exclusion, we included a total of 19 participants with ASD in our statistical analysis.

The NCs were contacts, associates and employees of the Psychiatry Department at the University of Edinburgh. In addition to previously outlined study exclusion criteria to those with ASD, NCs were als excluded if they had a personal history of ASD or a first-degree relative with a diagnosis of the disorder. We initially recruited 21 NCs between the ages of 24 and 58, but one NC withdrew consent from the study for personal reasons (NC = 20).

The same participant population and recruitment procedure were used in all parts of this thesis, although some additional participants were excluded from analysis in subsequent chapters for various reasons (see chapter 3.2.1, 4.2.1 and 5.2.1 for full details of participant exclusions for metabolite concentrations, ANT and resting-state functional connectivity analyses, respectively). For greater clarity and future reference, we present a chart below with the recruitment numbers for each sub-chapter within this thesis (table 2.1).

Table 2.1 Exclusions and Final Participant Numbers For Each Thesis Chapter

	Exclusion Reason	Exclusion n		Final n		
		ASD	NC	ASD	NC	Total
Total Recruitment Numbers				**25**	**21**	**46**
Chapter 2: Participants Included in Full Analysis	ADOS-G < 7	6				
	Withdrew Consent to Participant in Study		1	**19**	**20**	**39**
Chapter 3: Metabolite Concentrations	Wrong 1H-MRS sequence applied		1			
	Did not complete 1H-MRS Scan		1			
	Poor water suppression	1		**18**	**18**	**36**
Chapter 4: Attentional Network Test	Do not complete Attentional Network Test		2			
	Accuracy < 60 %	2	2	**17**	**16**	**33**
Chapter 5: Resting-state Functional Connectivity	Did not participate in resting-state MRI		2			
	Scan lost		1			
	Movement artefact > 20%	4		**15**	**17**	**32**

The same recruitment procedure and participant sample were used throughout this thesis. In total, we obtained informed consent and collected data from 21 NCs and 25 individuals with ASD. At various parts of thesis analysis, participants were excluded for various reasons. We outline the reason for exclusion and final numbers for each analysis chapter within this thesis. For full detail of exclusions refer to chapter 2.6.1, 3.2.1, 4.2.1 and 5.2.1.
ADOS-G, Combined social and communication score for the Autism Diagnostic Observation Schedule-Generic Module 4, ASD, autism spectrum disorder; IQ, intelligence quotient as measured by the Wechsler Abbreviated Scale of Intelligence; MRI, magnetic resonance imaging; NC, neurotypical controls

2.6.2   Ethical Consent

All participants in this study received written information regarding this study and gave written consent to participate. This study was approved by the Multi-Centre Research Ethics Committee for Scotland.

2.6.3 Assessment Procedure

Participants completed a battery of clinical and neuropsychological assessments including a background clinical and demographic assessment, the Wechsler Abbreviated Scale of Intelligence version III (WASI) and the ANT. A research health nurse or a doctoral student in the division of psychiatry administered psychometric assessments. A clinician or psychologist qualified in ADOS administration gave this assessment to all participants with ASD. Most of the participants completed all clinical and neuropsychological assessments on the same day. Assessment took between four and eight hours, depending on the speed with which the participant completed each assessment and took breaks. Participants were permitted to take as many breaks from the assessments as needed. Most participants completed a series of MRI imaging scans on a separate day to the psychometric assessments. Nevertheless, due to time constraints, one NC and one participant with ASD completed their psychometric assessments and MRI scan on the same day. All individuals with ASD were high-functioning and able to attend the assessments independently without medical support or assistance from a guardian.

2.6.4 Background Clinical and Demographic Information

Each participant answered questions about their general demographic and clinical background. Background questions included employment, education, psychiatric and medical history as well as current medication.

2.6.5 Clinical Assessment

All individuals with ASD were given the Autistic Diagnostic Observation Schedule-Generic Module 4 (ADOS) to assess clinical symptoms of ASD as this module was designed for adults with this disorder. The ADOS is a semi-structured assessment. The assessment measures observable symptoms of ASD made evident through conversation, practical tasks and questions by the interviewer [516,517]. Following the assessment, the individual will receive two primary scores. Firstly, a communication score quantifies evidence of ASD related behaviours including language abnormalities or the use of gestures. Secondly, the social interaction score quantifies traits such as abnormal eye contact, facial expression, social reciprocity and empathy. The social and communication scores are added and known as the ADOS-G score. A score of seven or greater on the ADOS-G is the criterion for confirmation of ASD. Higher scores indicate more severe symptoms. The clinician will also give an imagination/creativity and stereotyped or repetitive behaviours scores when observed. The test takes around an hour to complete and allows direct observation of autistic behaviours in association with consistent semi-structured observation [517,518].

The ADOS was designed to mirror a clinical diagnosis of ASD as defined by measures such as the DSM-IV [517], but the assessment is meant to be used in accordance with a clinical diagnosis. The ADOS diagnosis is solely based on observable behaviours at the time of assessment. Unlike the DSM-IV criteria, the ADOS does not consider developmental history. Therefore, the ADOS

must be supplemented with a clinical diagnosis of ASD taking into account information such as such as the age of onset [517,519].

The combination of ADOS scores in supplement to a clinical diagnosis of ASD allows greater confidence that our participant group included individuals with ASD. The addition of the ADOS also permitted comparison to other previously published studies because the ADOS is a commonly presented metric in ASD cohorts.

2.6.6 Neuropsychiatric Assessments

The psychometric assessments applied were the WASI [520] (chapter 2.6.6.1) and ANT (chapter 2.6.6.2).

2.6.6.1 Wechsler Abbreviated Scale of Intelligence

The WASI is a standardised and quick measurement of IQ taking between 30 and 90 minutes to compete. This assessment provides total, verbal and performance IQ scores which are modified based on the individual's age [521,522]. The performance score is a nonverbal IQ measure [523].

2.6.6.2 Attentional Network Test

Apparatus

The adult version of the ANT was downloaded from Jin Fan's research webpage at www.sacklassays_and_tools/ant/jin.fan/erinstitute.org/cornell/ and saved to a Dell Inspiron laptop. The test was written in Java and run in a Windows environment. The ANT was completed on a laptop computer with a 14-inch screen. The participant sat approximately 65 centimetres from the screen during the assessment.

Conditions

There were three main conditions of interest during the ANT: the alerting, orienting and conflict effect. The alerting effect quantified the performance deficit associated with a lack of external cue (no cue - double cue conditions). The orienting effect quantified the performance deficit associated with reorienting attention from non-target to target location (centre cue - spatial cue conditions). The conflict effect was a measure of the performance deficit associated with increased non-target conflict (incongruent flanker – congruent flanker conditions). Cue and flanker conditions are explained in detail in the next section.

Stimuli

Throughout the ANT, the goal was to indicate which direction the centre arrow was facing (left or right) by pressing the left or right arrow key.

All stimuli were black and appeared against a grey background. The total time per trial was 4000 ms and included five consecutive events: central fixation cross, cue, short fixation period, target and post-target events (figure 2.2). During the central fixation cross event, the fixation cross first appeared on a blank screen for between 400 and 1600 ms (labelled D1 in figure 2.2). The fixation continued to appear in the centre of the screen throughout the experiment, except for the centre cue condition in which the fixation cross was temporarily replaced by the cue.
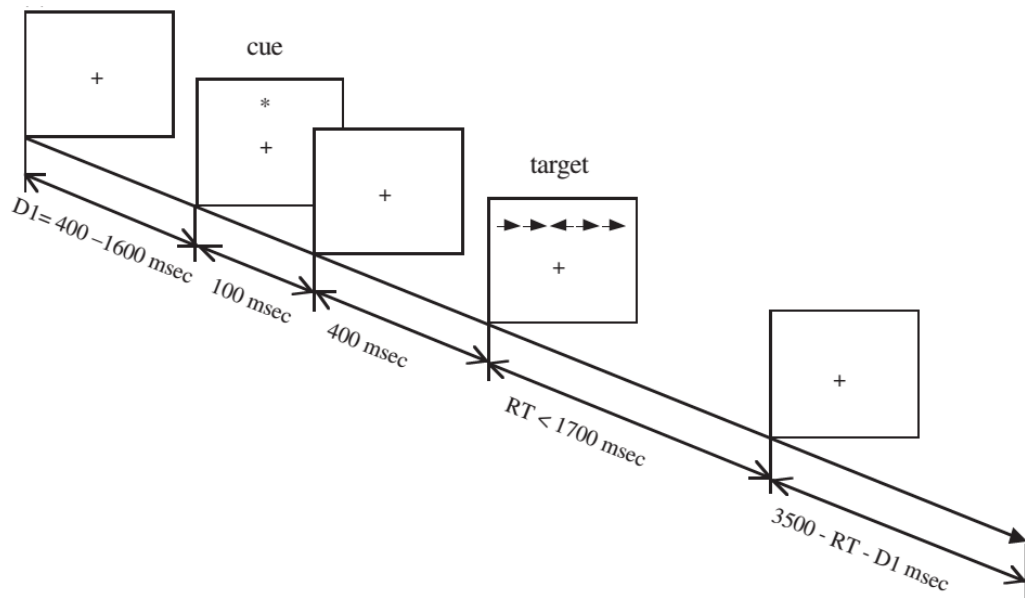
Figure 2.2 Graphical Representation of Time Course of Attentional Network Test (adapted from Fan et al. (2002)).

Visual time course of each trial in ANT. The visual time course moves left to right sequentially. D1 (first box on the left) is the central fixation cross condition which was followed by a cue, short fixation period, target and post-target events. The total time per trial was 4000 ms.

Next, the cue event lasted 100 ms. During this event, one of the four cue conditions appeared: centre cue, no cue, double cue or spatial cue (figure 2.3). The cue was always an asterisk. During the centre cue condition, an asterisk appeared over the fixation arrow. During the no cue condition, only the fixation cross remained on the screen. During the double cue condition, two arrows appeared above and below the fixation cross. During the spatial cue, an asterisk appeared above or below the fixation cross and always appeared in the same location as the upcoming target. Next, a short fixation event lasting 400 ms followed the cue event. This fixation period consisted of a fixation cross on a blank screen (figure 2.2).

86
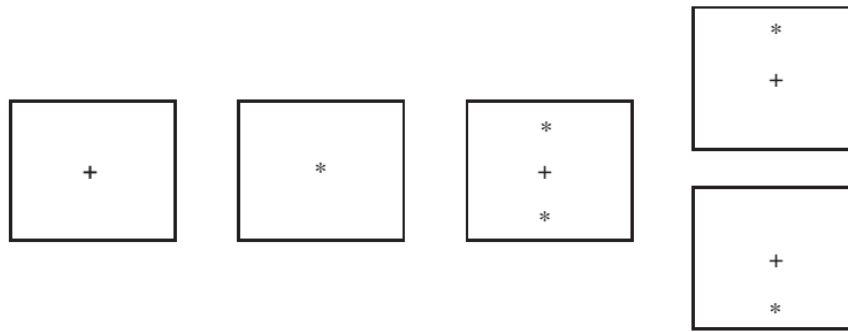
Figure 2.3 Graphical Representations of Cue Conditions for the Attentional Network Test (adapted from Fan et al. (2002)).

Four equally presented cue conditions include (left to right) no cue, centre cue, double cue and spatial cue which were presented during the ANT. Spatial cues always appeared at the same location as the target arrow.

During the target event, a series of arrows appeared on the screen. The target arrow could appear either above or below the fixation cross and was always the centre arrow. There were three flanker conditions: neutral, congruent and incongruent. During the neutral condition, a single arrow appeared without any flankers. During the congruent condition, two flankers appeared on either side of the target arrow and faced the same direction as the target arrow. During the incongruent condition, two incongruent flankers appeared on each side of the target arrow and pointed in the opposite direction of the target arrow (figure 2.4). Finally, there was a variable post-target event which lasted 3500 ms minus the fixation and participant RT. Again, it consisted of a fixation cross on a blank screen. If the participant did not respond by the end of the trial, then the next trial would begin, and the participant's response was coded as incorrect.

←   ← ← ← ← ←   → → ← → →

→   → → → → →   ← ← → ← ←
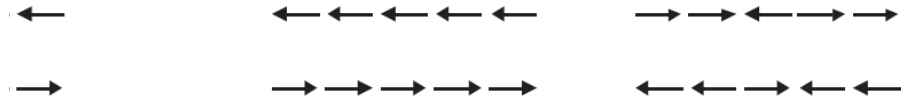
Figure 2.4 Graphical Representations of Flanker Conditions for the Attentional Network Test (adapted from Fan et al. (2002)).

Three equally presented flanker conditions which include (left to right) neutral flanker, congruent flanker and incongruent flanker.

Test Instructions, Practice and Assessment Blocks

At the start of the ANT, a participant was given an opportunity to read the written ANT instructions (figure 2.5). Each participant was instructed to indicate, with the left and the right arrow key, which direction the centre flanker was facing. Each participant received both verbal and written instructions to respond as quickly and precisely as possible.
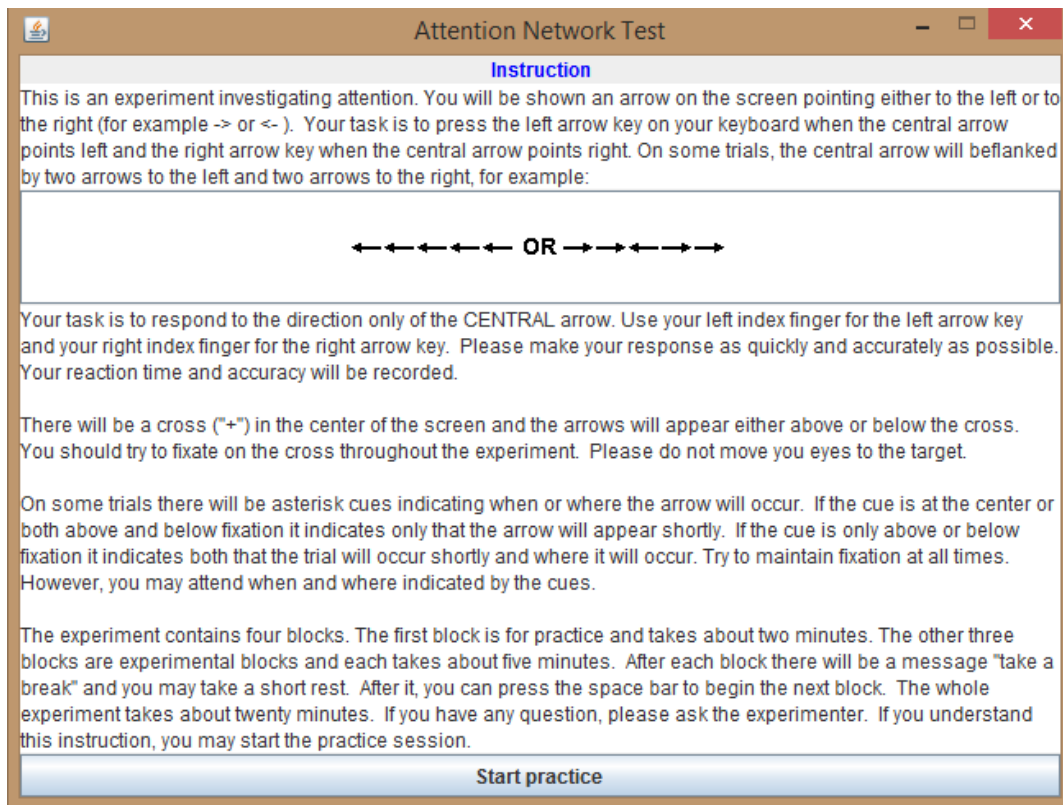
Figure 2.5 Test Instructions for the Attentional Network Test.

The written instructions for the ANT appeared on the computer screen before the practice block. Comprehension of ANT written instructions required reading aptitude. Nevertheless, researchers confirmed that each participant understood the test requirements regardless of reading ability. Before the start of the practice test, ANT test administrators verbally reiterated the test instructions and answered any participant questions. Investigators also checked the accuracy of performance during the practice block.

After reading the test instructions, a participant selected "Start practice" on the instruction screen with a laptop touchpad and then completed a block of 24 practice trials. During the practice block, the experimenter supervised participant accuracy and assisted with any questions. Following each stimulus trial, either a black "NO RESPONSE", black "CORRECT" or red "INCORRECT" appeared on screen, as applicable with each participant response. This provided feedback about the success of each trial. Except for

accuracy feedback for each response and a reduced trial number, the practice block was exactly the same as the test blocks.

Following completion of the practice block, the participant started the assessment blocks by pushing the enter key on the keypad. At the start of the ANT test block, the experimenter moved away and did not disturb the participant unless the participant indicated that there was a problem. During the experiment, there were three experimental blocks which each consisted of 96 trials. During each experimental block, two trials of each cue condition, target location, target direction and flanker condition were presented in random order. Each block took approximately five minutes to complete. Participants were encouraged to rest between each practice and assessment block.

Performance Calculations

We calculated the M and SD for both RT and ERs for seven conditions of the ANT (four cue conditions plus three flanker conditions) for each individual. The RT calculation only included trials with correct responses because incorrect data points were likely associated with different cognitive processes. Any RTs greater than or equal to two standard deviations (SD) from the individual's mean in each of the seven conditions were excluded from the condition means. This step was done to remove RTs that were not typical of the participant's performance abilities. Including these trials might have skewed the results of the assessment. Error rates were the total

number of incorrect responses for each condition divided by the total number of trials for that condition multiplied by 100.

We calculated the global RT by adding the RT for all seven conditions and dividing by seven. We calculated the global ER percentage by adding the total ER for each condition and dividing by 7.

Conditions were considered low cognitive demand because they had lower RT and ERs compared to the higher cognitive demand conditions in NCs [26,304,363]. We subtracted the RT mean and ER percentage of the low cognitively demanding conditions from the high cognitively demanding condition to obtain the alerting (no cue - double cue), orienting (centre cue - spatial cue) and conflict effect (incongruent flanker – congruent flanker) RT and ER. The conflict effect calculation did not include neutral target conditions.

The formulas used to calculate ANT results in Fan et al. (2002) [363] varied slightly from those applied within this thesis . Firstly, Fan et al. (2002) did not report removing extreme scores from each of the seven. Secondly, they did not report global RTs or ERs. Finally, Fan and colleagues included a slightly altered neutral flanker condition in which the arrows lines appeared next to the centre arrow without an arrowhead [363].

In this analysis, we also compare the results for individuals with ASD between the current study and Fan and colleagues (2012). Fan and colleagues (2012) did not include a centre cue condition but instead included

a valid and non-valid cue condition. During the valid condition, the cue appeared in the same place as the upcoming target. During the non-valid cue, the cue appears in the opposite position (either above or below the fixation) to the upcoming target. Differences in cue types slightly altered the calculation of the orienting effect. Nevertheless, the methodology for calculating the conflict effect has not changed between studies [26,363].

2.6.7 *Magnetic Resonance Imaging Acquisition*

Participants underwent all MRI scans at the Clinical Research Imaging Centre (CRIC) at the Queen's Medical Research Institute (Edinburgh, Scotland, United Kingdom) on a Siemens 3 T whole-body MRI Verio scanner (Siemens Medical Systems, Erlangen, Germany) using the matrix head coil with 12 elements.

Participants were not sedated or permitted to listen to music during the scanning sequence. Given the heightened anxiety often associated with being in a scanner, three participants with ASD underwent a practice MRI in a mock scanner before the actual MRI scan. As we previously mentioned, participants were asked to stop intake of nicotine, caffeine, alcohol or other non-legal drugs at least three hours before the MRI scan.

During the entire scanning sequence, participants wore MR-compatible goggles. Participants wore headphones and earplugs to reduce scanner noise and minimise subject discomfort. During the anatomical MP-RAGE, resting-state EPI and ^{1}H-MRS sequences participants looked at a blank screen. During all scans, participants were asked to attend to their breath or

the sound of the MRI scanner. During the resting-state fMRI scan, participants were instructed both before and immediately preceding the EPI acquisition to close their eyes. None of the participants included in the analysis had gross brain abnormalities.

2.6.8 Magnetic Resonance Imaging Parameters

2.6.8.1 Anatomical Three-Dimension Magnetization-Prepared Rapid Gradient-Echo (MP-RAGE) Sequence

A localising scan identified the interhemispheric angle and the anterior commissure-posterior commissure (AC-PC) line. Next, a volumetric scan sequence applied a T1-weighted, MP-RAGE sequence to acquire 160 slices with a slice thickness of 1 mm (FOV = 256 x 256 mm², TR = 2300 ms, TE = 2.98, T1 = 900 ms, flip angle = 9⁰). The full sequence took 5 min and 34 seconds.

2.6.8.2 Resting-State Echo Planar Sequence

The resting-state fMRI data were obtained from a single-shot gradient EPI sequence (TR=1560 ms, TE=26 ms, TA=7.42 minutes, flip angle - 66 degrees, 26 axial slices, voxel size = 3.4 x 3.4 x 4.0 mm, acquired with interleaved slice ordering, FoV = 220 X 220 mm) with 293 volumes acquired for each participant. The full scanning sequence took 7 minutes and 42 seconds.

2.6.8.3 Proton 1-Hydrogen Single Voxel Magnetic Resonance Spectroscopy Sequence

Proton 1-Hydrogen Single Voxel Magnetic Resonance Spectra (PRESS – Point Resolved Spectroscopy; TR = 3000 ms, TE = 80 ms, 128 water un-

suppressed averages, 16 water suppressed averages, 2048 data points, spectral width 2500 Hz., phase cycling set to Siemens 16 EXOR-cycle mode) were acquired in the dACC and were selected to optimise the measurement of Glu concentrations separate to Gln. The voxel was shimmed using Siemens advanced mode. These scanning parameters were optimal for the measurement of Glu concentrations [482–484]. The dACC voxel measurements were 30 x 20 x 15 mm (9 cm³). The full sequence took 7 min and 36 seconds.

Protocol for Selection of the Voxel of Interest

The centre voxel was located at 3 (± 5), 18, 33 in MNI coordinates (figure 2.6) and was equivalent to BA 32, although the voxel did have some overlap with BA 24 and 8. As part of a standard operating procedure, the coronal plane of the voxel was first set at 15 mm posterior to the genu of the corpus callosum. Next, the axial plane was assigned to the interhemispheric fissure. The sagittal slice was then defined as the anterior edge of the corpus callosum and centred on GM. Finally, the horizontal plane of the VOI was manually adjusted to follow the contour of the corpus callosum and based on individual differences so that the final voxel contained mostly GM and avoided overlapping with the corpus callosum.
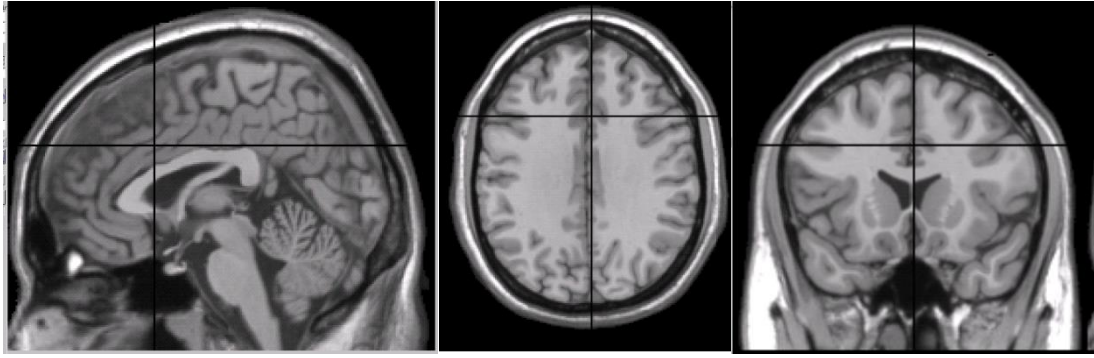
Figure 2.6 Centre Voxel Placement for Proton Magnetic Resonance Spectroscopy Sequence.

The crosshairs represent the centre of our dACC voxel for the ^{1}H-MRS sequence in the sagittal (left), axial (centre) and coronal plane (right), located at 3 (± 5), 18, 33 in MNI coordinates. The final voxel was manually positioned to following to contour of the corpus callosum in the transverse plane. The voxel size was 15 x 30 x 20 mm (9 cm³).

2.7 DEMOGRAPHIC CHARECTORISTICS

We present some the basic demographic details and compare individuals with ASD to NCs below on age (chapter 2.7.1), IQ (chapter 2.7.2), education (chapter 2.7.3) and employment status (chapter 2.7.4). We also present the ADOS diagnostic scores for participants with ASD (chapter 2.7.5). During age and IQ group comparisons, if the data complied with the assumptions of a parametric test, we applied an independent samples t-test to compare these demographic variables for each group. If the data violated the assumptions of normality and we were unable to transform the data, we then applied the appropriate non-parametric test to compare groups. The data for education and employment status were categorical, and we, therefore, applied a Fisher's exact test and chi-square test to compare groups, respectively.

2.7.1 Age

We compared NCs (*M* = 37.85, *SD* = 11.14, range = 24-58) and individuals

with ASD (*M* = 37.68, *SD* = 9.26, range = 23 - 53) to determine if there were

differences in age between groups. The age data did not comply with the

assumptions of an independent samples *t*-test as the standardised residuals

for age in the NC group were positively skewed and were not normally

distributed according to the Shapiro-Wilk's test (*p* = .015).

Transformation failed to correct for non-normality, and therefore, a non-

parametric Mann Whitney *U* test was used to determine if there were

differences in ages between groups. The distributions of age appeared

slightly dissimilar. Nevertheless, age for NCs (mean rank = 19.92) and

individuals with ASD (Mean rank = 20.08) were not significantly different (*U* =

188.50, *z* = -.04, *p* = .967) using an exact sampling distribution for *U* (table

2.1)*.*

2.7.2 Intelligence

All participants in this study had a total IQ above 80 (NC: *M* = 120.33, *SD* =

12.00, range = 93 - 139; ASD: *M* = 115.95, *SD* = 12.90, range = 87 – 136).

One participant did not complete the WASI IQ test and we substituted the

mean IQ for all NCs for this individual.

Performance (NC: *M* = 120.31, *SD* = 11.43, range = 97 - 134; ASD: *M* =

115.21, *SD* = 16.04, range = 76 - 138) and verbal IQ (NC: *M* = 115.95, *SD* =

12.14, range = 86 - 135; ASD: *M* = 113.21, *SD* = 10.20, range = 89 - 129)

were also compared separately between groups. There were no significant

differences between groups for total IQ (t(37) = 1.10, p = .279) and verbal IQ (t(37) = .76, p = .451) (table 2.1).

For performance IQ, standardised residuals for the full model (p = .018) and the NC group (p = .030) were not normally distributed according to Shapiro-Wilk's test. Therefore, we performed a reflect and square root transformation to correct for moderate negative skewing in performance scores which has the effect of reversing the scores and reducing their distribution. There were no significant differences between groups on the transformed performance IQ scores (t(37) = -.89, p = .378) (table 2.1).

2.7.3 Education

Participants were divided into tertiary, which was defined as those that had any attendance at university (NC = 17, ASD = 12) and high school, which was defined as those that attended high school only (NC = 3, ASD = 7). Cells sizes for NCs only attending high school were less than five. Therefore, we were unable to run a chi-square test. Instead, a Fisher's exact test compared education level between groups. There was no statistically significant association between groups and education (p = .155) (table 2.1).

2.7.4 Employment Status

A chi-square test assessed group differences in employment rates (percentage of sample employed: NC = 90.00%; ASD = 42.11%). A chi-square test for association was conducted between group and employment status. All cell frequencies were greater than five. NCs were significantly more likely to be associated with employment than participants with ASD

$(\chi^2(1) = 7.64$, $p = .006)$ (table 2.2). Other studies support reduced employment and education rates in participants with ASD [4,524]. Reduced participation may be related to symptoms of the disorder. For example, participants with ASD were less likely to be hired for a job due to communication problems made evident during the interview [525,526]. Our sample size was not large enough to explore these relationships further.

Table 2.2 Demographic Group Comparisons Between Neurotypical Controls and Individuals with Autism Spectrum Disorder

	NC Mean (SD)	ASD Mean (SD)	statistic	p
	$n = 20$	$n = 19$		
Mean Age in Years	37.85 (11.14)	37.68 (9.26)	$U = 188.50$, $z = -.04$	.967
Percentage Attended Tertiary Education [1]	85.00 %	63.16 %	NA	.155
Percentage Employed [2]	90.00 %	42.11%	$\chi^2(1) = 7.64$	**.006**
Total IQ	120.33 (12.00)	115.95 (12.90)	$t(37) = 1.10$	0.279
Performance IQ	120.31 (11.43)	115.21 (16.04)	$t(37) = -.89$	378
Verbal IQ	115.95 (12.14)	113.21 (10.20)	$t(37) = .76$	.451

Participant numbers (n), mean and standard deviation (SD) and group comparisons of demographic information for NCs and individuals with ASD. Unless otherwise noted there were 20 NCs and 19 individuals with ASD included in the group comparisons. There was no significant difference between groups for age or IQ. Furthermore, there was no significant difference in the number of participants that had attended tertiary education between groups. Compared to individuals with ASD, NCs were more likely to be employed as compared to being a student or unemployed. Significant results are bolded. Significance reported at $p < .05$ level.

[1] Group comparisons included NC = 17, ASD = 12

[2] Group comparisons included NC = 18, ASD = 8

ASD, autism spectrum disorder; IQ, intelligence quotient as measured by the Wechsler Abbreviated Scale of Intelligence; NA, not applicable; NC, neurotypical controls.

2.7.5 Autism Diagnostic Observation Schedule

All individuals with ASD including in this analysis had an ADOS-G score greater than or equal to seven (ADOS-G: $M = 9.58$, $SD = 3.2$, range = 7 – 18; communication: $M = 3.32$, $SD = 1.22$, range = 2 – 16; social: $M = 6.16$, $SD =$

2.41, range = 3 – 12). Individuals with ASD in this study scored low on imagination (M = .84, SD = .77, range = 0 – 2) and stereotyped behaviours (M = .84, SD = .96, range = 0 – 3) (table 2.3).

Table 2.3 Autism Diagnostic Observation Schedule Scores for Individuals with Autism Spectrum Disorder (n=19)

	Mean (SD)	Range
ADOS-G	9.58 (3.2)	7 - 18
Communication	3.32 (1.22)	2 - 6
Social	6.16 (2.41)	3 -12
Imagination	.84 (.77)	0 -2
Stereotyped Behaviours	.84 (.96)	0 -3

Mean, standard deviation (SD) and range of scores for ADOS scores for participants with ASD.
ADOS, Autism Diagnostic Observation Schedule; ADOS-G, combined social and communication scores for ADOS; ASD; autism spectrum disorder

2.8 CONCLUSION

In this chapter, we reviewed the various demographic, clinical, psychometric and neuroimaging measures which were investigated in association with Glu or Glx concentrations. The objective of this chapter was to highlight technical and theoretical considerations of the applied methodology as well as clearly detail study methodology in relation to participant recruitment and data collection. In the next chapter, we will present our measurement of Glu and Glx concentrations in individuals with ASD compared to NCs.

3 METABOLITE CONCENTRATIONS

3.1 INTRODUCTION

The ACC has been one of the most investigated brain regions for Glu or Glx concentrations in individuals with ASD. Nevertheless, this research has been contradictory (chapter 1.4.2). We utilised ^{1}H-MRS applied at a single voxel in the dACC to quantify both Glu and Glx concentrations to compare metabolite concentrations in a group of high functioning adults with ASD to NCs. We hypothesised that we would report altered (increased or decreased) Glu concentrations in individuals with ASD based on previous evidence of altered ACC Glu and Glx concentrations in adults with ASD [237]. We also explored the relationships between demographics and core symptoms of the disorder to add further context to previously contradictory Glu and Glx studies in individuals with ASD compared to NCs.

We also report NAA + NAAG, Cre, Cho and mI concentrations, which were secondary to our focus. Briefly, research suggests that NAA concentrations are associated with neural integrity and vitality [527–532]. We reported NAA + NAAG because these metabolites have closely overlapping signal peaks [441,501]. Previous research regarding NAA has also been contradictory with several studies reporting reduced [237,533] or increased [225,512] or no difference [233,242,474,475] in the ACC of adult participants with ASD compared to NCs.

There has been less evidence of group differences in Cre, Cho and mI concentrations in the ACC of individuals with ASD (chapter 2.5). Therefore, we did not expect to find group differences in these metabolite concentrations but reported them to provide further reference and comparison to other

studies. Briefly, Cre is considered a stable marker of energy metabolism [247] and Cho is thought to quantify membrane density and function of all cells in the brain [470]. Finally, mI is thought to be a marker of glial density [503].

Within this chapter we also included post-hoc investigations which assessed group differences in metabolite concentrations when excluding individuals taking psychotropic medications. We excluded these participants because there has been evidence that psychotropic medication moderated Glu and Glx concentrations in the human and rodent brains [534–542]. For example, one research group reported that the administration of Fluvoxamine, a serotonin reuptake inhibitor, increased Glu release in depressed mice [543]. The administration of psychotropic medications might lessen clear group differences in Glu or Glx concentrations. Ideally, it might have been beneficial to fully exclude participants taking psychotropic medications. Nevertheless, prior to participant recruitment, we felt it would be too difficult to exclude participants because of the wide use of these psychotropic medications in individuals with ASD.

The dACC is integral to many cognitive processes [303], has a high density of glutamatergic receptors [544–546] and has altered function in participants with ASD compared to NCs [26,30,400,408,547–551]. To our knowledge, this is the first study to investigate Glu concentrations specifically in the dACC for adult participants with ASD. This chapter will lay the foundations for further investigation into the relationship between Glu and Glx concentrations and both behaviour and brain function.

3.2 METHODS

3.2.1 Participants

The recruitment procedure was previously reported in chapter 2.6.1 and 2.6.2. There were 20 NCs and 19 individuals with ASD included in the statistical analysis for this thesis. For the ^{1}H-MRS analysis, a further three participants were excluded. The wrong single voxel spectroscopy sequence was applied to one NC during their scanning session, while another NC did not participate in an MRI scan. Furthermore, investigators excluded one individual with ASD due to evidence of poor water suppression which called into question the validity of this individual's results. Following these exclusions, there were 36 total participants included in single voxel spectroscopy analysis (NC = 18, ASD = 18) for all NAA, Cre and Cho metabolite concentrations.

From individuals with ASD, five participants were taking psychotropic medications, three were taking antidepressants only, and one was taking anticonvulsants only and one taking antidepressants and anticonvulsants. None of the participants had a reported history of seizure in the previous 12 months. No NCs reported taking psychotropic medications. Therefore, there were 31 participants not taking psychotropic medication at the time of scanning (18 = NC, ASD = 13). Some participants also reported taking other medications including statins (NC = 1, ASD = 1), antibiotics (ASD = 1), diabetic medications (NC = 1, ASD = 1) and hypertension medications (NC = 1).

Additionally, metabolite concentrations were excluded from this analysis if they had a CRLB value greater than or equal to 20%, which was a reliability guideline suggested for LCModel output [445,451]. Therefore, investigators excluded participants from Glu (ASD = 2), Glx (ASD = 3) and mI (ASD = 1) concentrations analysis. Additionally, one NC was excluded from both Glu and Glx analysis because these metabolite concentrations were greater than three SDs from the mean. Following these exclusions, there was 33 participants included in the Glu (17 = NC, 16 = ASD), 32 in the Glx analysis (17 = NC, 15 = ASD) and 35 in the mI analyses (18 = NC, 17 = ASD).

3.2.2 Demographic, Clinical and Psychometric Data Collection

The assessment procedure for background, demographic, clinical and neuropsychiatric assessment procedure were presented in chapter 2.6.3. Briefly, investigators collected age and current medications from all participants in this study. All participants completed the WASI from which full-scale IQ was obtained and presented in chapter 2.6.6.1. The background, clinical and demographic information were outlined in chapter 2.6.4. Finally, all participants with ASD completed the ADOS and scores were obtained as presented in chapter 2.6.5.

3.2.3 Magnetic Resonance Imaging Data Collection

The protocol for data acquisition of the anatomic MP-RAGE and single voxel 1H-MRS sequences were reported in chapter 2.6.7. Acquisition parameters for the MP-RAGE and ^{1}H-MRS were previously reported in chapter 2.6.8.1 and 2.6.8.3, respectively.

3.2.4 Neuroimaging Data Processing

3.2.4.1 Voxel Based Morphometry

We segmented whole brain T1-weighted volumetric images into GM, WM and CSF maps in SPM8 (Statistical Parametric Mapping: The Wellcome Department of Cognitive Neurology, Institute of Neurology, London, UK, http://www.filion.ucl.ac.uk/spm/software/spm8) for the matrix laboratory (MATLAB version 2015b, the Mathworks Inc., Natick, MA, 2015).

The processing steps for MP-RAGE images included: (1) inspection of scanner artefacts and gross anatomical abnormalities in volumetric scans (2) resetting the image origin to the anterior commissure (3) segmenting rigid body aligned GM, WM and CSF for each subject using the "New Segment" procedure in SPM8.

3.2.4.2 Metabolite Quantification

We fed raw proton spectra into the LCModel graphical user interface which automatically analyses proton spectra based on a standard basis set of ^{1}H-MRS metabolite peaks. The hydrogen proton spectra were also processed using both eddy current correction and internal water scaling. Water scaling contrasts the unsuppressed water signal intensity in the basis set and the sample with assumed tissue water concentrations [451]. The LCModel analysis output metabolite concentrations and CRLB scores for NAA+ NAAG, Cho, Cre, Glu, Glx and mI. An example of the spectra output from this experiment is shown in figure 3.1

3.2.4.3 Calculation of Grey Matter, White Matter and Cerebral Spinal Fluid Concentrations in Reconstructed Single Voxel Spectroscopy Voxel

We firstly reconstructed the single voxel spectroscopy voxel. The location of the original voxel acquired during the hydrogen proton single voxel spectroscopy sequence was reported in chapter 2.6.8.3. The centre of the single voxel spectroscopy voxel was identified through visual comparison of the three tag ^{1}H-MRS files, which indicated the centre of the voxel, and the previously bias corrected, aligned T1 image. We drew a rectangular VOI around the centre voxel in the MarsBar toolbox [552]. Each side of the VOI was dilated slightly by 1 mm to account for selection error (3.2 x 2.2 x 1.7 cm or 11.96 cm³). The reconstructed voxel was then tilted in sagittal view in ImageJ version 1.48 [553] to follow the contour of the corpus callosum as was done with the original voxel. The newly tilted voxel was then imported back into Marsbar and visually checked to confirm the correct location of the voxel with no overlap with the corpus callosum. Finally, GM, WM and CSF maps obtained during the "New Segment" procedure in SPM8 were applied to the reconstructed voxel to calculate the percentage GM, WM and CSF volume.

3.2.4.4 Partial Volume Correction

All metabolite values were further corrected for CSF content using the following formula:

$$C = C_0 * (1 / 1 - F_{CSF})$$

C = Partial volume correction

C_0 = uncorrected metabolite concentration

F = fractional content of CSF in the ROI

3.2.5 Statistical Analysis

Investigators conducted all statistical analyses on SPSS 22.0 (SPSS, Chicago, Il, U.S.A.). During correlational analysis, we applied a Pearson's correlation when the data complied with the assumptions of this parametric test. In all other cases, we applied a non-parametric Spearman's rank-order correlation. During group comparisons, if the data complied with the assumptions of a parametric test, we applied the appropriate parametric test. If the data violated these assumptions, we attempted appropriate transformations so that the data complied with the assumptions of a statistical test and then re-ran the parametric test on the transformed data. When a transformation failed to correct for violations of the assumptions of a parametric test, we substituted the group comparison with the appropriate non-parametric test. Unless otherwise noted, significance was reported at uncorrected $p < .05$.

3.2.5.1 Basic Demographic Group Comparisons

Firstly, investigators compared participant groups on age and total IQ with independent samples *t*-tests. A more detailed explanation of participant demographics for all participants and clinical analysis for individuals with ASD compared to NCs is available in chapter 2.7.

3.2.5.2 Correlations between Metabolite Concentrations and Autism Diagnostic Observation Schedule Scores

To investigate the relationship between metabolite concentrations and symptoms of the disorder, we also reported the correlation between Glu, Glx and NAA + NAAG concentrations and ADOS social and communication scores. We did not examine the relationship between imagination and stereotyped behaviour ADOS scores because most participants in our sample scored 0 on these sub-sections (chapter 2.7.5). Also, only individuals with ASD completed the ADOS and therefore, correlations between metabolites and ADOS scores were only possible for individuals with ASD.

3.2.5.3 *Cramér-Rao Lower Bounds Standard Deviation Scores Group Comparisons*

Next, we compared the CRLB SD scores for each metabolite between groups using the appropriate independent samples *t*-test or a non-parametric Mann Whitney *U* test.

3.2.5.4 *Group Comparisons in Grey Matter, White Matter, Cerebral Spinal Fluid Percentages and Metabolite Concentrations*

As a first step, investigators assessed if age or IQ correlated with tissue volume (GM, WM or CSF percentage) or metabolite concentrations (Glu, Glx, NAA + NAAG, Cho, mI and Cre). The purpose of this analysis was to identify potential confounding variables which also influenced metabolite concentrations. We wished to include these covariates even if it was weakly associated with metabolite concentration. Therefore, we did not correct for multiple comparisons and set the significance level at uncorrected $p < .05$. If there was a significant or trend correlation, age or IQ were included as covariates in group tissue volume or metabolite concentration comparisons

between groups through an analysis of covariance (ANCOVA) or non-parametric Quade's rank analysis of Covariance.

When inclusion of a covariate was justified, we firstly checked for an interaction between covariate and group. If the interaction was not significant, the interaction was not included as a predictor in group comparisons. When a covariate was not justified, we compared tissue and metabolite concentrations between groups with independent samples t-tests.

3.2.5.5 Post-Hoc Correlations between Metabolite Concentrations by Group

The data for Glu, Glx and NAA + NAAG concentrations appeared to be moving in similar directions with age. Therefore, we also investigated the correlations between the primary metabolites of interest, NAA + NAAG and both Glu and Glx concentrations in each group.

3.2.5.6 Post-Hoc Group Comparisons in Metabolite Group Comparisons Excluding Participants Taking Psychotropic Medications

To check that group differences were not confounded by psychotropic medication, we compared Glu, Glx and NAA + NAAG, concentrations between groups excluding participants taking antidepressant and anticonvulsant medication. These individuals were referred to as "psychotropic medication free" or PMF.

3.2.5.7 Corrections for multiple comparisons

For group metabolite concentrations comparisons and further post-hoc analysis, we also considered if results remained significant when correcting for multiple comparisons with Bonferroni correction. In total, there were 16

group comparisons which should meet a corrected *p*-value < .003 to remain

significant when correcting for multiple comparisons.

3.3 RESULTS

3.3.1 Example of Spectra Output

We present LCModel spectra from two participants in this study in figure 3.1.

NAA chemical shift is located at 2.0 ppm and Glu at 2.3 ppm on the

spectrum.
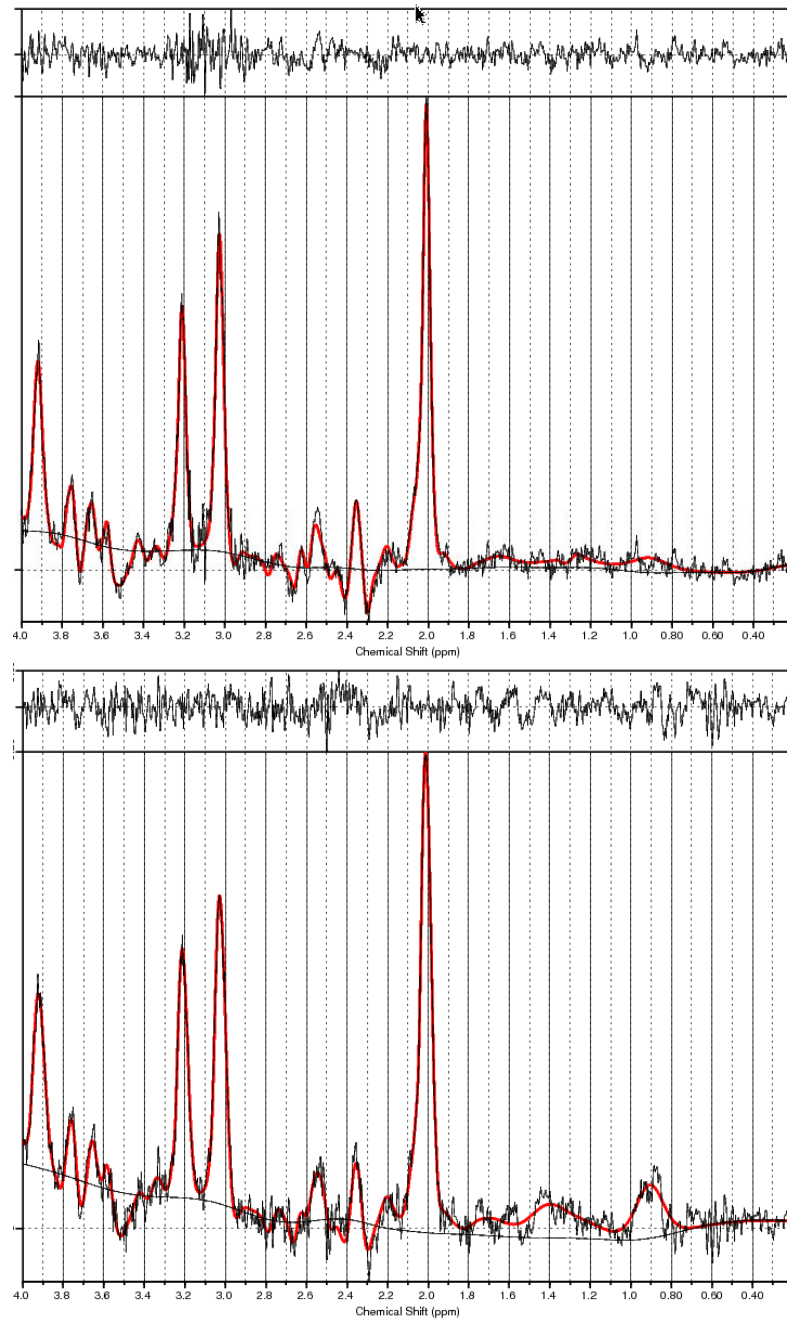
Figure 3.1 Proton Magnetic Resonance Spectra Output from the LCModel for Anonymous Neurotypical Control and Individual with Autism Spectrum Disorder

Proton magnetic resonance spectroscopy at 3 T as fit by the LCModel [445,451] from anonymous NC (top) and individual with ASD in this study (bottom). The three major peak metabolite landmarks are located at 3.22 for Cho, 3.03 for Cre and 2.0 for NAA. Glu is located at 2.3 ppm.

3.3.2 Basic Demographic Group Comparisons

The age range for individuals included in the metabolite concentrations analysis were similar (NC: M = 37.67, SD = 11.08, range in years = 24 – 58; ASD: M = 37.28, SD = 9.35, range = 23 - 53). The standardised residuals for age in NCs were non-normally distributed and positively skewed (Shapiro-Wilk's test, p = .023), and we applied a logarithmic transformation to allow the data to comply with the assumptions of normality. Following transformation, there were no significant differences between groups in age (t (34) = .05, p = .962).

We compared groups on total IQ with independent samples t-test (NC: M = 121.58, SD = 11.98, range= 93-139; ASD M = 115.78, SD = 13.26, range = 87 – 136). There were no significant difference between groups on total IQ scores (t (34) = 1.38, p = .177).

3.3.3 Correlation Between Metabolite Concentrations and Autism Diagnostic Observation Schedule

We did not report any significant association between Glu concentrations and total (r_p(16) = .24, p = .381), social (r_p(16) = .33, p = .211) or communication (r_p(16) = -.03, p = .906) ADOS scores. We did not report any significant association between Glx concentrations and total (r_p(15) = .21, p = .443), social (r_p (15) = .30, p = .274) or communication (r_p(15) = -.04, p = .886) ADOS scores. NAA + NAAG concentrations were non-normally distributed for individuals with ASD (Shapiro-Wilk p = .028) and, therefore, we applied a Spearman's rank order correlation for all ADOS correlations with this metabolite. There were no significant correlations between NAA + NAAG and

112

total (r_s(18) = .37, p = .135), social (r_s(18) = .20, p = .417) or communication (r_s(15) = .26, p = .297) ADOS scores.

3.3.4 Group Comparisons of Cramér-Rao Lower Bounds Standard Deviation Values

When comparing CRLB values for Glu concentrations and Glx concentrations between groups, the standardized residuals for the full participants group for Glu (Sharpo-Wilk = .045) and Glx (Sharpo-Wilk = .027) were non-normally distributed. A logarithmic transformation was applied to correct for positive skewing of Glu CRLB scores. Following transformation, there were no significant differences between groups for Glu CRLB scores (NC: M = 9.23, SD = 2.51, range= 6 - 15; ASD M = 10.25, SD = 3.04, range = 6 – 18; t(31)= -1.06, p = .299). Researchers applied a square root transformation to correct for moderate positive skewing in the Glx CRLB values and following transformation there were no significant differences between groups (NC: M = 9.94, SD = 2.80, range= 6 - 15; ASD M = 10.93, SD = 3.17, range = 6 – 17; t(30)= -.94, p = .355).

When comparing CRLB values by group, we were unable to correct non-normality of standardized residuals by transforming the data for the full sample for NAA+NAAG (Sharpo-Wilk = .000), Cho (Sharpo-Wilk = .000) and Cre concentrations (Sharpo-Wilk = .000). Therefore we applied a Mann-Whitney U non-parametric test to determine if there were differences in median CRLB scores between individuals with ASD and NCs. The CRLB percentage distributions for NAA+NAAG concentrations were similar and the median engagement scores were not significantly different between groups

(NC: M = 2.16, SD = .38, range=2 -3, Median = 2.0; ASD M = 2.44, SD = 1.25, range = 2 – 7, Median = 2.0; U = 165, z = .146, p = .938). The distributions of CRLB scores for Cho concentrations were similar and the median scores were not significantly different between groups (NC: M = 3.61, SD = .61, range= 3 – 5, Median = 4.0; ASD M = 3.94, SD = 1.86, range = 3 – 11, Median = 3.5; U = 159, z = -.106, p = .938). The distributions of Cre concentrations CRLB scores were similar and the median scores were not significantly different between groups (NC: M = 2.83, SD = .51, range= 2 - 4, Median = 3.0; ASD M = 3.39, SD = 1.33, range = 6 -19, Median = 3.0; U = 131.50, z = .128, p = .901).

Finally, there were no significant differences between groups for CRLB values between groups for ml (NC: M = 8.27, SD = 1.53, range= 6 - 11; ASD M = 8.76; SD = 1.63, range = 5 - 11; t(31)= -1.13, p = .269). The CRLB mean, SD, range and group comparisons for each metabolite are also presented in table 3.1.

Table 3.1 Cramér-Rao Lower Bounds Standard Deviation Percentages for Neurotypical Controls and Individuals with Autism Spectrum Disorder

Metabolite	NC			ASD			statistic	p
	n	Mean % (SD)	Range %	n	Mean % (SD)	Range		
Glu [2]	17	9.23 (2.51)	6 - 15	16	10.25 (3.04)	6 -18	$t(31) = -1.06$	.299
Glx [2]	17	9.94 (2.80)	6 -15	15	10.93 (3.17)	6 - 17	$t(30)=-.94$	.355
NAA + NAAG [1]	18	2.16 (.38)	2 -3	18	2.44 (1.25)	2 -7	$U = 165$, $z = .146$	.938
Cho [1]	18	3.61 (.61)	3 - 5	18	3.94 (1.86)	3 -11	$U = 159$, $z = -.106$	.938
Cre [1]	18	2.83 (.51)	2 - 4	18	3.39 (1.33)	6 -19	$U = 131.50$, $z = .128$	.901
ml	18	8.27 (1.53)	6 - 11	17	8.76 (1.63)	5 - 11	$t(31) = -1.13$	.269

Participant numbers, mean, standard deviation (*SD)* and range CRLB percentages for non-transformed metabolite concentrations for NCs and participants with ASD. All CRLB values greater than or equal to 20 were excluded from this analysis. Significance reported at uncorrected *p* < .05 level.

[1] Non-parametric Mann-Whitney *U* non-parametric test applied as data did not comply with assumptions of a parametric test.

[2] Data transformation applied to comply with assumptions of independent samples *t*-test.

ASD, autism spectrum disorder; Cho, choline containing compounds; Cre, creatine plus phosphocreatine; Glu, glutamate; Glx, glutamate and glutamine; ml, myo-inositol; NAA + NAAG, N-acetyl-aspartate and N-acetyl-aspartyl-glutamate; NC, neurotypical controls.

3.3.5 Group Comparisons In Grey Matter, White Matter and Cerebral Spinal Fluid Percentages in Reconstructed Voxel

There was a significant correlation between age and GM ($r_p(36) = -.39$, $p = .019$) and CSF ($r_p(36) = .52$, $p = .001$) percentages in reconstructed dACC voxel. As age increased, GM decreased and CSF increased. There were no other significant associations between age or IQ and tissue percentages. Therefore, when comparing groups for tissue volume percentages, we included age as a covariate for GM and CSF percentages.

Next, we compared tissue volume percentages in the reconstructed dACC voxel between groups. After adjustment for age, there were no significant differences between groups for GM tissue percentage (NC: *M* = 61.75%, *SD*

= 4.79%, range= 52.36 − 68.52%; ASD M = 62.26%, SD = 3.94%, range = 55.57 − 68.10 %; $F(1,33)$ = .10, p = .750). Age was a significant predictor of GM tissue percentage ($F(1,33)$ = 5.90, p = .021). There were no significant differences in WM (NC: M = 21.87%, SD = 4.05%, range= 14.17 − 29.40%; ASD M = 22.21%, SD = 4.74%, range = 15.60 − 30.57 %; t (34) = .23, p = .817) between groups.

Finally, when controlling for age, the standardized residuals for CSF percentages for the full group (Shapiro-Wilk p = .021) and NCs (Shapiro-Wilk p = .008) were positively skewed and non-normally distributed. We applied a logarithmic transformation to CSF percentages to correct for non-normality. Following transformation of CSF percentages, there were no significant differences between groups for CSF percentages (NC: M = 16.38%, SD = 4.26%, range= 10.03 − 23.66%; ASD M = 15.53%, SD = 3.74%, range = 9.36 − 30.57 %; $F(1,33)$ = .35, p = .561). Age was a significant predictor of CSF concentrations ($F(1,33)$ = .11.77, p = .002). The mean, SD, range and group comparisons for GM, WM and CSF percentages are presented in table 3.2.

Table 3.2 Grey Matter, White Matter and Cerebral Spinal Fluid Percentages in Reconstructed Dorsal Anterior Cingulate Voxel for Neurotypical Controls (*n* = 18) and Participants with Autism Spectrum Disorder (*n* = 18)

	NC Mean % (SD)	NC Range %	ASD Mean % (SD)	ASD Range %	statistic	*p*
Grey Matter	61.75 (4.79)	52.36 – 68.52	62.26 (3.94)	55.57 – 68.10	$F_{(1,33)} = .10$	.750
White Matter	21.87 (4.05)	14.17 – 29.40	22.21 (4.74)	15.60 – 30.57	$t_{(34)} = .23, p = .817$	.817
Cerebral Spinal Fluid [1]	16.38 (4.26)	10.03 – 23.66	15.53 (3.74)	9.36 – 30.57	$F_{(1,33)} = .35$ [1]	.561

The GM, WM and CSF non-transformed tissue percentages, SD and range for NCs and individuals with ASD. There were no significant differences in tissue concentrations in the reconstructed voxel in the dACC . Significance was reported at *p* < .05 level. Group comparisons for GM and CSF were corrected for age.
[1]A logarithmic transformation was applied to CSF percentage in single voxel spectroscopy voxel to correct for non-normality in data for group comparisons.
ASD, autism spectrum disorder; NC, neurotypical controls.

3.3.6 Correlation Between Metabolite Concentrations and Age and Intelligence

Next, we applied the Pearson's product-moment correlation to investigate if age and IQ correlated with metabolite concentrations across all participants when the data were normally distributed. For the full sample, the data for NAA+NAAG (Sharpo-Wilk *p* < .001) and IQ (Sharpo-Wilk *p* = .029) were non-normally distributed, and a non-parametric Spearman's rank order correlation was used in substitute of the Pearson's product-moment correlation for comparisons involving these variables.

There was no significant correlation between IQ and any metabolite concentration (*p* > .05). Across all participants, age was negatively correlated with several metabolite concentrations including NAA + NAAG (r_s = -.46, *p* = .005) and Glu (r_p= -.40, *p* = .022). There were also weak trend correlations between age and Glx (r_p = -.30, *p* = .098) and Cho (r_p= -29, *p* = .092). The

correlations between age, IQ and metabolite concentrations are also

presented in table 3.3.

Table 3.3 Correlation between Metabolite Concentrations and Both Age and Intelligence Quotient for All Participants

		Age		IQ	
	n	*r*	*p =*	*r*	*p =*
Glu	33	**-.40** [1]	**.022** [1]	.17	.357
Glx	32	-.30 [1]	.098 [1]	.27	.139
NAA + NAAG	36	**-.46**	**.005**	.04	.830
Cho	36	-.29 [1]	.092 [1]	.07	.705
Cre	36	-.25 [1]	.145 [1]	.02	.919
ml	35	.14	.421 [1]	-.01	.974

Correlation between age, IQ and metabolite concentrations. Investigators applied the Spearman's rank-order correlation unless otherwise noted. The IQ score was obtained from the Wechsler Abbreviated Scale of Intelligence. Significance reported at uncorrected $p < .05$ level.

[1] Pearson's correlation applied

Cho, choline containing compounds; Cre, creatine plus phosphocreatine; Glu, glutamate; Glx, glutamate and glutamine; IQ, intelligence quotient; ml, ml-Inositol; NAA + NAAG, N-acetyl-aspartate and N-acetyl-aspartyl-glutamate.

Age was included as a covariate in group comparisons for Glu, Glx, NAA +

NAAG and Cho concentrations given a significant or trend correlation.

3.3.7 Group Comparisons in Metabolite Concentrations

When comparing Glu concentrations between groups (table 3.4), the

assumption of homogeneity of variances was violated, as assessed by

Levene's test for equality of variance ($p = .033$). We were unable to transform

the data in a way that corrected for this heterogeneity. Therefore, we applied

a non-parametric Quade's rank analysis of covariance [554] to investigate if the

distribution of rank for Glu concentrations differed between groups when accounting for age. We found no significant group differences (NC: $M = 8.87$, $SD = .81$, range= 7.49 -10.37; ASD $M = 8.31$, $SD = 1.58$, range = 5.61 – 10.84; $F(1,31) = .90$, $p = .349$). A scatterplot of the relationship between Glu concentrations and age by is presented in figure 3.2.
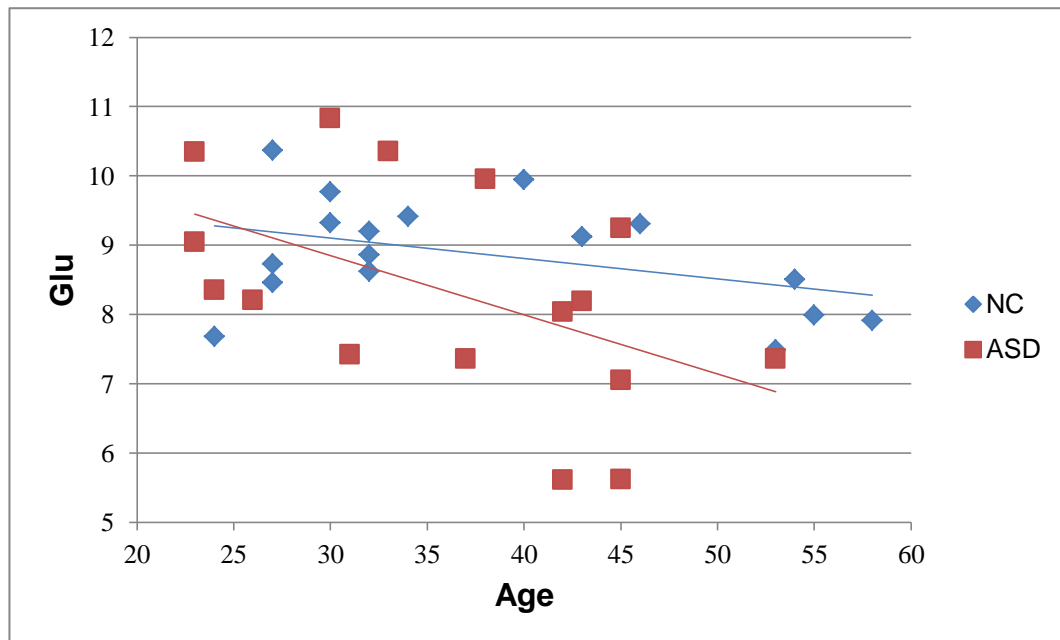
Figure 3.2 Glutamate Concentrations by Age for Neurotypical Controls ($n = 17$) and Participants with ASD ($n = 16$)

Scatterplot of the relationship between age and Glu concentrations for NCs and individuals with ASD.

Individuals with ASD had a trend reductions in Glx concentrations (NC: $M = 10.42$, $SD = .79$, range= 9.20 – 11.80; ASD $M = 9.55$, $SD = 1.79$, range = 5.83 – 12.50; $F(1,29)=4.06$, $p=.053$) compared to NCs. Age also was a trend predictor of Glx concentrations ($F(1,29)=3.71$, $p=.064$). There was no significant interaction between age and group for Glx concentrations. A

119

scatterplot of the relationship between Glx concentrations and age by group

is presented in figure 3.3.
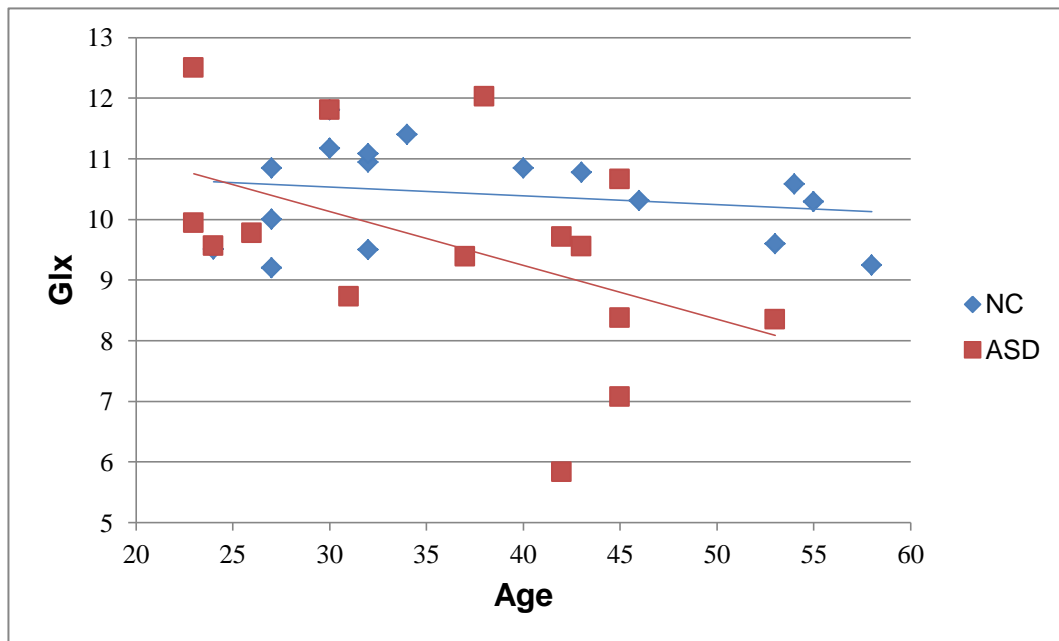
**Figure 3.3 Glutamate and Glutamine Concentrations by Age for Neurotypical Controls
(n = 17) and Participants with ASD (n = 15)**

The association between age and Glx concentrations in both individuals with ASD and NCs
is presented in the above scatterplot. Age was only a trend predictor of Glx concentrations.

Next, a reflect and square root transformation was applied to NAA + NAAG

concentrations to correct for moderate negative skewing and non-normally

distributed residuals for participants with ASD (Sharpo Wilk p =.005). For

NAA + NAAG, age was a significant predictor (F(1,33) = 10.33, p =.003)

while there was a trend difference between groups (NC: M = 11.95, SD =

1.04, range= 9.91 -13.89; ASD M = 11.07, SD = 1.89, range = 6.24 -12.80;

F(1,33) = 4.08, p =.052). We present a scatterplot of the relationship between

NAA + NAAG concentrations and age by group in figure 3.4.
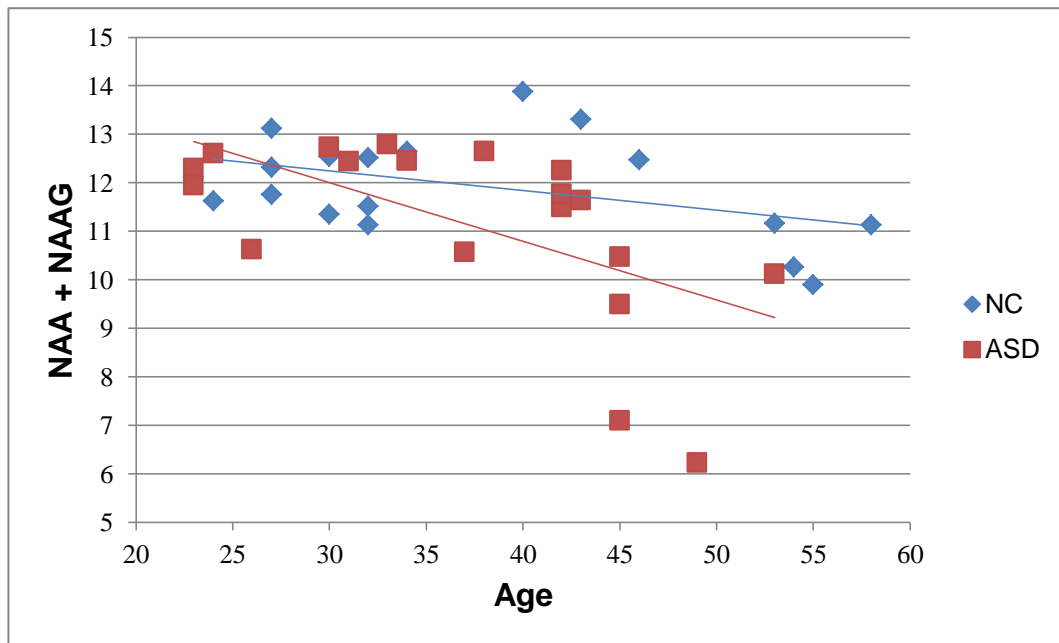
**Figure 3.4 N-Acetyl-Aspartate and N-Acetyl-Aspartyl-Glutamate Concentrations by Age for Neurotypical Controls (*n* = 18*)* and Participants with ASD (*n* = 18*)*

The relationship between age and NAA + NAAG is presented in the scatterplot for NCs and individuals with ASD. Age was significantly associated with reduced NAA + NAAG concentrations in both individuals with ASD and NCs.

There were no significant differences in Cho concentrations between groups (NC: *M* = 1.89, *SD* = .25, range= 1.43 – 2.34; ASD *M* = 2.00, *SD* = .34, range = 1.49 – 2.53; F(1,33)=1.17, *p*=.286). Age was also not a significant predictor of Cho concentrations (*F*(1,33)=2.95, *p*=.095). There were no significant differences in Cre between groups (NC: *M* = 7.54, *SD* = .56, range= 6.74 – 8.35; ASD *M* = 7.47, *SD* = .91, range = 5.29 – 8.87; *t* (34) = .09, *p*=.770).

For mI concentrations, a reflect and square root transformation was applied to correct for moderate negative skewing and non-normally distributed residuals for the entire group (Sharpiro-Wilk *p* =.034) and individuals with ASD (Sharpiro-Wilk *p* =.034). For the transformed mI concentrations, there were no significant differences between groups for mI (NC: *M* = 6.84, *SD* =

1.12, range= 4.21 – 8.62; ASD M = 6.63, SD = 1.52, range = 3.83 – 8.28;

t(1,33) = .11, p=.743).

In conclusion, there were no significant differences between groups at uncorrected $(p < .05)$ for metabolite concentrations or the more conservative Bonferroni-corrections for multiple comparisons $(p < .003)$.

Table 3.4 Mean Metabolite Concentrations for Neurotypical Controls and Participants with Autism Spectrum Disorder

Metabolite	NC			ASD			statistic	p
	n	Mean (SD)	Range	n	Mean (SD)	Range		
Glu [1]	17	8.87 (.81)	7.49 – 10.37	16	8.31 (1.58)	5.61 – 10.84	F(1,31) = .90	.349
Glx	17	10.42 (.79)	9.20 – 11.80	15	9.55 (1.79)	5.83 – 12.50	F(1,29)=4.06	.053
NAA + NAAG [2]	18	11.95 (1.04)	9.91 – 13.89	18	11.07 (1.89)	6.24 – 12.80	F(1,33) = 4.08	.052
Cho	18	1.89 (.25)	1.43 – 2.34	18	2.00 (.34)	1.49 – 2.53	F(1,33)=1.17	.286
Cr	18	7.54 (.56)	6.74 – 8.35	18	7.47 (.91)	5.29 – 8.87	t(34) = .09	.770
ml [2]	18	6.84 (1.12)	4.21 – 8.62	17	6.63 (1.52)	3.83 – 8.28	t(33) = .11	.743

Non-transformed means and standard deviations for metabolite concentrations in NCs and individuals with ASD. We report all metabolite values less than 20 CRLB. Significance reported at uncorrected $p < .05$ level.
[1] Non-parametric Quade's rank analysis of Covariance applied as data did not comply with assumptions of a parametric test.
[2] Data transformed to comply with assumptions of a parametric test.

ASD, autism spectrum disorder; Cho, choline containing compounds; Cre, creatine plus phosphocreatine; Glu, glutamate; Glx, glutamate and glutamine; ml, myo-inositol; NAA + NAAG, N-acetyl-aspartate and N-acetyl-aspartyl-glutamate; NC, neurotypical controls.

3.3.8 Post-Hoc Correlations Between Metabolite Concentrations by Group

We also investigated the relationship correlation between NAA + NAAG concentrations and both Glu and Glx in each group (table 3.5). The data for NAA + NAAG concentrations was non-normal. Therefore, non-parametric Spearman's rank correlations were used. For NCs, there was a positive

significant relationship between NAA + NAAG and Glu concentrations (r_s(17) = .58, p= .014). There was no significant relationship between NAA + NAAG and Glx concentrations (r_s(17) = .12, p= .639).

For individuals with ASD, there was also a significant positive relationship between NAA + NAAG concentrations and Glu concentrations (r_s(16) = .70, p = .002) and also Glx (r_s(15) = .55, p= .032).

Bonferroni adjusted alpha levels of $p < .003$ were also considered. Following this adjustment, only the correlation between NAA + NAAG and Glu concentrations in individuals with ASD survived this correction for multiple comparisons.

Table 3.5 Correlation Between Metabolites for Neurotypical Controls and Participants with Autism Spectrum Disorder

Metabolite x Metabolite	NC	ASD
NAA + NAAG x Glu	r_s(17) = .58, p = .014	r_s(16) = .70, p = .002
NAA + NAAG x Glx	r_s(17) = .12, p = .639	r_s(15) = .55, p = .032

Spearman correlations between Glu, Glx and NAA + NAAG concentrations by group Individuals with ASD had a significant correlation between NAA + NAAG concentrations and both Glu and Glx. In contrast, NCs only had a significant relationship between NAA + NAAG and Glut. Unadjusted significance values are reported at $p < .05$. Bonferroni adjusted p-values are significant at $p < .003$.
ASD, autism spectrum disorder; Glu, Glutamate; Glx, glutamate and glutamine; NAA + NAAG, N-acetyl-aspartate and N-acetyl-aspartyl-glutamate; NC, neurotypical controls.

3.3.9 Post-Hoc Group Comparisons in Metabolite Concentrations In Psychotropic Medication Free Participants Only

For PMF participants, age was a significant predictor of Glu concentrations, (F(1,26) = 7.99, p =.009) while group was not (NC: M = 8.87, SD = .81, range= 7.49 – 10.37; ASD M = 8.41, SD = 1.53, range = 5.62 10.84; F(1,26)

= 2.48, *p* = .127). For Glx concentrations, there was a significant interaction between age and group (NC: *M* = 10.42, *SD* = .80, range= 9.20 – 11.80; ASD *M* = 9.58, *SD* = 1.54, range = 7.08 – 12.50; *F*(1,24) = 4.58, *p* = .043).

For NAA + NAAG concentrations, a reflected and square root transformation was applied to correct for heterogeneity of variance (Levene's test *p* = .045). Following transformation, both group (NC: *M* = 11.95, *SD* = 1.04, range= 9.91 – 13.89; ASD *M* = 10.90, *SD* = 2.14, range = 6.24 – 12.80; F(1,28) = 5.19, *p* = .031,) and age (F(1,28) = 10.20, *p* = .003) were significant predictors of NAA+NAAG concentrations. None of the group comparisons survived Bonferroni correction for multiple comparisons (*p* < .003). The mean, SD and range of these metabolite concentrations for PMF participants are presented in table 3.6.

Table 3.6 Metabolite Concentrations for Neurotypical Controls and Individuals with ASD Free of Psychotropic Medications

Effect	NC *n*	NC Mean (SD)	Range	ASD *n*	ASD Mean (SD)	Range
Glu	17	8.87 (.81)	7.49 – 10.37	12	8.41 (1.53)	5.62 – 10.84
Glx	17	10.42 (.80)	9.20 – 11.80	11	9.58 (1.54)	7.08 – 12.50
NAA + NAAG	18	11.95 (1.04)	9.91 – 13.89	13	10.90 (2.14)	6.24 – 12.80

Metabolite concentrations for non-transformed means, standard deviations (SD) and range for NCs and participants with ASD not currently taking psychotropic medications. We report all metabolite values with a CRLB less than 20%. Significance reported at uncorrected *p* < .05 level.
ASD, autism spectrum disorder; Glu, glutamate, Glx, glutamate and glutamine; NAA + NAAG, N-acetyl-aspartate and N-acetyl-asparty-glutamate; NC, neurotypical controls.

3.4 DISCUSSION

Our primary goal in this chapter was to investigate group differences in Glu and Glx concentrations in the dACC between groups. We also investigated the relationship between metabolite concentrations and the core symptoms of ASD. We review the results for Glu (chapter 3.4.1), Glx (3.4.2) and NAA + NAAG concentrations (3.4.3).

We discuss results which did not survive correction for multiple comparisons and it is important not to overemphasize these findings. We made many group comparisons in a small cohort of inividuals. We cannot rule out the the possiblity that uncorrected significant group differences were false positive findings (type I error) and due to chance. Therefore, these results are a good starting point but our findings require further replication in a larger cohort of individuals with ASD.

3.4.1 Glutamate

Increased or decreased Glu concentrations did not differentiate individuals with high functioning ASD from NCs in both the full group and reduced PMF group. Moreover, ADOS scores did not have a significant correlation with metabolite concentrations (Glu, Glx or NAA + NAAG) in individuals with ASD, suggesting that metabolite concentrations were not altered in association with the disorder.

In contrast to these results, Tebartz van Elst and colleagues reported reduced Glu concentrations in the pACC in adults with ASD compared to NCs [237]. The scan acquisition, methodology and participant characteristics

125

were similar between the Tebartz van Elst study and this investigation. For example, both studies used a 3 T MRI scanner to investigate Glu concentrations. They also investigated a group of high functioning individuals with ASD with an average age around 35 (Tebartz Van Elst Mean age: NC: $M = 35.79$, $SD = 8.5$; ASD: $M = 35.31$, $SD =$ 9.1). Given the similarities between studies, one possible explanation for contradictory results was that Glu concentrations were altered in the pACC but not the dACC in individuals with ASD.

Nevertheless, we did report that age significantly correlated with Glu concentrations in both groups. As a participant aged, there was a reduction in Glu concentration in the dACC. In agreement, other studies have reported reductions with age in Glu concentrations in other brain regions, such as the motor cortex in NC participants [555].

Tebartz van Elst and colleagues matched groups on age, but they did not control for age during group comparisons. Investigators also had slightly increased statistical power with an increased sample size (Tebartz Van Elst Group size: NC = 29, ASD = 29). In our study, a scatterplot of the relationship between age and Glu concentrations suggested a sharper reduction with age in individuals with ASD compared to NCs (figure 3.2), but the statistical analysis did not support such a conclusion. Nevertheless, given contradictory results between studies, further investigation of how age is associated with Glu concentrations in individuals with ASD compared to NCs is warranted.

3.4.2 Glutamate and Glutamine Concentrations

In the full participant group, we reported no significant difference in Glx concentrations between groups. Nevertheless, in the PMF participants, researchers reported an interaction between age and group for Glx concentrations. Again, this result did not survive correction for multiple comparisons but weakly suggests that individuals with ASD and PMF have greater reductions in Glx concentrations with age.

It may be that Gln concentrations are atypical rather than Glu concentrations in individuals with ASD. Cochran and colleagues reported significantly increased Gln concentrations but not Glu concentrations in the pACC of adolescents with ASD compared to NCS [241].In ACC post-mortem tissue, investigators reported a reduction in kidney-type glutaminase, which has been associated with converting Glu to Gln [454]. Given this evidence, it may be useful to investigate Gln in more detail.

Interestingly, we also reported an uncorrected correlation between NAA + NAAG and Glx concentrations only in individuals with ASD. Our analysis cannot determine if one of these metabolites might be driving the other. Reductions in neural integrity or density, as measured by NAA + NAAG, were associated with reduced quantities of neurones which lead to reductions in Glx concentrations. Of course, cross sectional differences in metabolite concentrations with age could also be associated with differences in therapeutic interventions between generations rather than loss of neural

function over time. Replication of this result is required both in a larger cohort but also in a longitudinal study.

Two previous studies have reported no differences in Glx concentrations in both the dACC [556] and pACC [239]. Libero et al. (2015) (age NC: $M = 24.9$, $SD = 1.13$; ASD: $M = 26.8$, $SD = 1.35$) and Aoki et al. (2012) (age NC: $M = 29.5$, $SD = 6.2$; ASD $M = 29.5$, $SD = 6.9$) included younger participants than those in this investigation. In comparison, Tebartz van Elst et al. (2014) reported reductions in Glx concentrations in older participants [237]. Given that we report an interaction between Glx concentrations and age in PMF participants, this may partially explain the differences between these studies.

It is unclear why we did not find an interaction between age and group for Glx concentrations in the full sample of participants. One possibility was that psychotropic medications might have moderated Glu or Glx concentrations in the brain, as some studies have suggested [534–536,557]. Therefore, psychotropic medications resulted in a less clear relationship between age and group. As we mentioned earlier in this discussion, we had a small sample size, and these associations would be more clearly investigated with a larger sample of participants.

3.4.3 N-Acetyl-Aspartate and N-Acetyl-Aspartyl-Glutamate

The results for NAA + NAAG were not our primary focus, but we discuss these results here briefly. In both the full group and PMF group, age was a significant predictor of NAA+NAAG concentrations. One cross-sectional

study reported NAA age-related reductions of around 12% in the medial frontal lobe between 20 to 70 years of age in NCs [558]. Therefore, age-related reductions in NAA concentrations might be evident in broad age ranges of NCs and individuals with ASD.

Tebartz and colleagues reported a reduction in NAA concentrations in a group of participants in an older age range in the pACC [237]. We reported no significant group differences in the full sample, but a significant reduction in PMF individuals with ASD for NAA + NAAG concentrations compared to NCs when controlling for the impact of age.

Unlike Glx, our investigation did not report a significant interaction between age and NAA + NAAG concentrations between groups. Nevertheless, these relationships require more investigation. Cross-sectional studies have also suggested some variation in the trajectory of NAA concentrations in the amygdala-hippocampal region [559] and in the pACC [252] with age in individuals with ASD compared to NCs.

3.5 CONCLUSION

Contrary to our original hypothesis, our data did not support altered Glu concentrations in individuals with ASD. Instead, in PMF participants, there was weak evidence of greater reductions in Glx concentrations in adult participants with age compared to NCs. The data weakly suggest disease-specific variation in Glx metabolites with age and a more detailed understanding of these relationships will be useful in designing treatment interventions throughout the lifespan of individuals with this disorder.

Unfortunately, the strength of our conclusions were limited by a small sample size and these associations must be replicated in a larger study. None of our group metabolite comparisons survived correction for multiple comparisons.

Nevertheless, age-related reductions in metabolite concentrations in this study stress the importance of investigating older participants with ASD. To date, ASD studies have mostly focused on early development and prevention in children and adolescents with this disorder [560]. Older participants have differing and potentially more significant needs than younger participants with ASD [560,561]. Furthermore, longitudinal research in older participants might draw attention to long-term behaviours or treatments which impact the brain.

4   ATTENTIONAL NETWORK TEST

4.1 INTRODUCTION

In this chapter, we focus on the conflict effect task, which is thought to measure the speed and accuracy of inhibiting interference from distracting stimuli not relevant to a task goal [26,338,361,363]. Our primary motivation for using the conflict effect task was the close functional association to the dACC, a focus of this thesis. Greater incongruency and visual dominance of incongruent flanker arrows surrounding a target arrow have been associated with an increased BOLD response in the dACC in NCs [26,304,328].

Although the conflict effect has also been associated with other brain regions such as the supplementary motor area, DLPFC and VLPFC in NCs [26,304], researchers have specifically reported hypoactivation of the dACC in association with the conflict effect task in individuals with ASD. This evidence suggests that the conflict effect task might be a simple behavioural measure of altered function in the dACC in individuals with ASD compared to NCs. Researchers also reported that conflict effect accuracy was associated with impairments in language and communication scores [26] as defined by the Autism Diagnostic Interview-Revised [218]. This association suggested that performance on this task might be associated with core behaviours of the disorder.

Although there has been considerable evidence of altered Glu and Glx concentrations in the dACC [237,247]. There has been little understanding of how altered metabolite concentrations might be associated with behaviour. Investigators have reported that Glu concentrations in the dACC have a

direct correlation to behavioural measures of impulsivity in NCs [257,258]. In this analysis, we explore if Glu and Glx metabolite concentrations in the dACC might be associated with inhibition to distraction as quantified by the conflict effect.

The conflict effect is part of the ANT (chapter 2.2), an assessment of various forms of attentional processes. Although not a primary focus, the ANT also measures the alerting and orienting effect. The alerting effect is thought to measure internal vigilance [26,363,417,420,421]. The orienting effect quantifies an individual's ability to disengage attention from a cue location and reengaging attention at the target arrow location [26,363,417,420,421]. As a first step, we expected to replicate evidence of the alerting, orienting and conflict effect performance deficit across participants in this study. In contrast to Fan and colleagues [26], this experiment was completed outside of an MRI scanner to determine if participants with ASD continued to exhibit consistent conflict effect performance deficit when in a quiet laboratory environment.

Researchers have also reported a relationship between age and performance on the conflict effect task [562,563] and have suggested that older individuals were more susceptible to interference from non-target flankers [562,564]. In contrast, although other executive control tasks, such as working memory tasks have been associated with IQ, there is less evidence that inhibition tasks are related to IQ in NCs [565]. Nevertheless, lower IQ in individuals with ASD compared to NCs might contribute to executive control

133

differences between these groups [566,567]. Therefore, this investigation assessed the relationship between ANT performance and both age and IQ.

In conclusion, the primary objective was to investigate group performance differences on the conflict effect task and the relationship to metabolite concentrations. We hypothesised that conflict effect performance might index altered dACC brain function in individuals with ASD.

4.2 METHODS

4.2.1 Study Populations

The recruitment procedure (chapter 2.6.1) and ethical consent (chapter 2.6.2) have previously been reported in chapter 2. We report the additional participant exclusions all ANT (4.2.1.1) and metabolite concentrations (4.2.1.2) analyses within this research chapter.

4.2.1.1 Attentional Network Test

There were some additional exclusions for the ANT assessment. Two NCs did not complete the ANT when we administered the other neurocognitive assessments. We were unable to obtain these assessments at a later date. We also excluded four participants from the ANT analysis because of an accuracy rate below 60% for incongruent flanker stimuli conditions (NC = 2, ASD = 2). In this case, participant exclusion was done to confirm that included participant had understood and actively participated in the ANT. In the end, there were 33 participants (NC = 16, ASD = 17) included in the final analysis. In the final participant group, one participant had a block of five or more consecutive errors which were related to technical issues during the

assessment. Therefore, we removed seven trials from the start of this participants test data set.

4.2.1.2 Metabolite Concentrations

For the correlations between the ANT and metabolite concentrations, we excluded further participants. One NC did not complete a ^{1}H-MRS scan. Also, we excluded one individual with ASD from metabolite analysis due to evidence of poor water suppression.

We also excluded metabolite concentrations from the analysis if they had a CRLB value greater than or equal to 20. Therefore, we excluded further participants from Glu (ASD = 2) and Glx (ASD = 3) analyses. One further NC was excluded from both Glu and Glx analyses because metabolite concentrations were greater than three SDs from the mean. Following these exclusions, there were a total of 28 participants included in the Glu (14 = NC, 14 = ASD) and 27 in the Glx analyses (14 = NC, 13 = ASD).

4.2.2 Demographic, Clinical and Psychometric Data Collection

Participants in this study provided background clinical and demographic information (chapter 2.6.4) and also completed the WASI, ADOS and ANT as previously summarised in clinical (2.6.5) and psychometric data (chapter 2.6.6) collection procedures.

4.2.3 Attentional Network Test

The ANT apparatus, testing stimuli, assessment protocol and method for calculating the results were reported in chapter 2.6.6.2. Briefly, the goal on all sub-sections of the ANT was to indicate the direction that the target arrow

was pointing. Manipulation of pre-target cues and non-target flanker arrow directions test three separate sub-conditions which include the alerting, orienting and flanker conflict effect. Researchers measure performance by increases in RT and ERs [363].

4.2.4 Magnetic Resonance Imaging Acquisition

The protocol for data collection of the anatomic MP-RAGE and ^{1}H-MRS sequence was reported in chapter 2.6.7. Sequence parameters for the MP-RAGE and ^{1}H-MRS were reported in chapter 2.6.8.1 and 2.6.8.3, respectively.

4.2.5 Neuroimaging Data Processing

The methodology for metabolite quantification, calculation of CSF in the voxel and partial volume correction were reported in chapter 3.2.4.

4.2.6 Statistical Analysis

Investigators conducted all statistical analyses on SPSS 22.0 (SPSS, Chicago, Il, U.S.A.). During correlational analysis, researchers applied a Pearson's correlation when the data complied with the assumption of this parametric test. In all other cases, investigators applied a non-parametric Spearman's rank-order correlation. During group comparisons, if the data complied with the assumptions of a parametric test, we applied the appropriate parametric test. If the data violated these assumptions, we attempted appropriate transformations and then re-ran the parametric test on the transformed data. Unless noted, when a transformation failed to correct

136

for violations of the assumptions of a parametric test, we substituted the appropriate non-parametric test. All RT values are presented in ms.

4.2.6.1 Basic Demographic Group Comparisons

Firstly, we compared age and total IQ between groups. A more detailed analysis of participant demographics for all participants and clinical analysis for individuals with ASD are available in chapter 2.7.

4.2.6.2 Attentional Network Analysis Full Participant Group

We present the full details for how we calculate the ANT in the chapter 2.6.6.2. Briefly, we compared the RT and ER for the easier (low cognitive demand) and more difficult (high cognitive demand) condition for the alerting, orienting and conflict RT in all participants with paired samples signed tests with continuity correction because the data did not comply with the assumptions of a parametric test. We did not investigate RTs or ERs for the neutral flanker condition because this condition was not used to calculate alerting, orienting or conflict effect results.

Next, we determined if there was a correlation between age or IQ and ANT measures (alerting, orienting, conflict effect and global RT and ERs) measures for the entire group. The purpose of this analysis was to identify variables which might also contribute to and confound group comparisons of ANT performance. As it was reasonable that age or IQ might influence ANT performance, we wished to include a covariate even if it was only weakly associated. Therefore, we did not correct for multiple comparisons and set the significance level at uncorrected $p < .05$. If there was a significant

association, age or IQ was used as a covariate in future group comparisons for the appropriate ANT performance measure.

4.2.6.3 Attention Network Test Group Comparisons

We compared alerting, orienting, conflict and global RT and ER between groups. As mentioned above, when age or IQ correlated with an ANT performance measure (RT or ER), it was included as a covariate in an ANCOVA between groups. When a covariate was not justified, researchers compared group performance (RT or ER) with independent samples *t*-tests. When the data and the transformed data did not comply with the assumptions of a parametric test, we instead applied the appropriate non-parametric test. The significance level was set at uncorrected $p < .05$. When there was evidence of group differences at an uncorrected alpha level, we further considered if results remained significant when correcting for multiple comparisons with Bonferroni correction. In total, there were 6 group comparisons which would result in a corrected p-value $< .008$.

4.2.6.4 Attention Network Test and Correlation with Autism Diagnostic Observation Schedule for Participants with ASD

We investigated if there were any significant correlations between the ADOS and ANT measures (RT and ER) in individuals with ASD only. This correlational analysis could not be made across the full group because NCs did not complete the ADOS.

138

4.2.6.5 *Attention Network Test and Correlation with Metabolite Concentrations*

We investigated if there was a correlation between metabolite concentrations (Glu, Glx and NAA + NAAG) and RT on the ANT (global, alerting, orienting or conflict) in all participants, NCs and individuals with ASD. We did not investigate the relationship between metabolite concentrations and ANT accuracy because participants were highly accurate. When there was evidence of a significant correlation between ANT performance and either ADOS scores (chapter 4.2.6.4) or metabolite concentrations at an uncorrected $p < .05$, we further considered if results remained significant when correcting for multiple comparisons with Bonferroni correction. In total, there were 48 correlational analyses which would result in a corrected p-value $< .001$.

4.2.6.6 *Compare Participant Characteristics and Attentional Network Test Results of Current Study to Fan et al. (2012)*

We also present basic participant characteristics (age, IQ, ADOS-G Scores) and ANT performance outcomes (Alerting, Orienting, Conflict and Global RT/accuracy) between the current study and Fan et al. (2012) for comparison purposes within the discussion.

4.3 RESULTS

4.3.1 *Basic Demographic Group Comparisons*

We compared NCs (M = 36.88, SD = 11.00, range = 24 − 58) and participants with ASD (M = 38.12, SD = 8.91, range = 23 - 53) on age. The standardised residuals for age in NCs were non-normally distributed and

moderately positively skewed (Shapiro-Wilk's test, $p = .040$), and therefore we applied a logarithmic transformation to allow the data to comply with the assumptions of normality. Following transformation, there were no significant differences between groups in age (t (31) = -.47, $p = .644$).

Independent samples t-tests were used to compare groups for total IQ (NC: $M = 122.25$, $SD = 12.19$, range=93-139; ASD $M = 117.35$, $SD = 11.95$, range = 87 − 136). The data standardized residuals for the full sample (Shapiro-Wilk = .015) were non-normally distributed. A reflect and square root transformation corrected for minor negative skewing in the full sample. Following transformation, there were no significant differences between groups for the transformed total IQ (t(31) = -1.35, $p = .187$).

4.3.2 Attentional Network Test

4.3.2.1 Main Effects for Response Times and Error Rates

Standardized residuals were non-normal for all sub-conditions (no cue, centre cue, double cue and spatial cue, congruent flanker, incongruent flanker) of RT and ER effects across the entire group (Shapiro-Wilk $p < .05$). Data transformation failed to correct for non-normal distributions and therefore non-parametric paired samples signed tests with continuity correction were used to investigate group differences in the median difference between median high cognitively demand and median low cognitive demand trials. As part of this parametric test, when the overall differences between the low and high cognitive demand condition were equal

to zero that individual's data set was considered a tie and excluded for the non-parametric analysis. Therefore, we report the number of participant ties.

For the full participant group (16 NC: 17 ASD), there was a significant difference in RTs between the high and low cognitive demand condition for alerting (*M* = 25.76, *SD* = 20.37, range = -15.61 – 78.33), orienting (*M* = 37.04, *SD* = 23.65, range = -15.16 – 89.63) and conflict effect (*M* = 127.53, *SD* = 45.18, range = 55.05 – 276.92). All participants had a positive conflict effect RT. Four participants had a negative alerting effect and two had a negative orienting effect. No participants were considered ties and excluded from RT comparisons (table 4.1)

Table 4.1 Non-Parametric Paired Signed Test with Continuity Correction Comparing Median Response Time Between Low and High Cognitive Demand Condition for Full Participant Sample (*n* = 33)

Median Low CD	Median High CD	Median Effect	*z*	*p*
Double Cue	No Cue	Alerting		
594.88	613.05	25.93	**4.18**	**< .001**
Spatial Cue	Centre Cue	Orienting		
553.54	594.88	36.06	**4.87**	**< .001**
Congruent	Incongruent	Conflict		
502.57	681.89	110.70	**5.57**	**< .001**

Median RTs for high CD, low CD and overall effect (alerting, orienting and conflict). Total is the overall mean for all conditions. Significance reported at p < .05 level. There were no ties.

CD, cognitive demand.

Participants were highly accurate on the ANT (overall global accuracy rate: *M* = 99.23%, SD = 1.05%, range = 95.00% - 100.00%). Exact sign tests found no significant difference in ER between high and low cognitively demanding conditions of the alerting (*M* = -.29%, *SD* = 1.25%, range = -4.17 – 1.57%) and orienting (*M* = -.32%, *SD* = 1.42%, range = -4.17 – 4.48%) conditions.

Incongruent target conditions elicited a significantly greater ER across participants compared to congruent conditions in the conflict effect ER ($M =$ 1.55%, $SD =$ 2.12%, range = -1.04 – 7.50%). However, this result should be taken with caution as 13 participants had difference scores of 0 and were excluded from the exact sign test (table 4.2).

Table 4.2 Non-Parametric Paired Signed Test with Continuity Correction Comparing Median Error Rates Between Low and High Cognitive Demand Condition for Full Participant Sample (n = 33)

Median Low CD	Median High CD	Median Effect	p	Tie
Double Cue	No Cue	Alerting		
0.00%	0.00%	0.00%	0.45	17
Spatial Cue	Centre Cue	Orienting		
0.00%	0.00%	0.00%	0.15	21
Congruent	Incongruent	Conflict		
0.00%	0.00%	1.04%	**< 0.001**	13

Median ERs for low CD, high CD and overall effect (alerting, orienting and conflict). Initially, there were 33 participants included in this statistical analysis. Tie is the number of participants with a 0 difference effect. We excluded these participants from the analysis. Significance reported at p < .05 level.
CD, cognitive demand, ER, error rates

4.3.2.2 Correlation between Age and Full Wechsler Abbreviated Scale of Intelligence Score with Attentional Network Test Performance

We applied the Pearson's product-moment correlation to investigate if age and IQ correlated with performance on the ANT across all participants (table 4.3). The full data for the conflict effect RT (Shapiro-Wilk = .005), global RT (Shapiro-Wilk = .001), alerting error (Shapiro-Wilk < .001), orienting error (Shapiro-Wilk < .001), conflict error (Shapiro-Wilk < .001) and total accuracy (Shapiro-Wilk < .001) were non-normal, and therefore, Spearman rank order correlations were run for these analyses.

The Spearman's rank order correlation revealed a significant association between conflict effect RT and age ($n = 33$, $r_s = .35$, $p = .043$) (figure 4.1). There was also a significant correlation between age and total RT ($n = 33$, $r_s = .61$, $p < .001$). There were no other significant correlations (table 4.3).

Table 4.3 Correlation for Age and Full Wechsler Abbreviated Scale of Intelligence Score with Mean Response Times Accuracy (n =33)

		Age		IQ	
		r	*p*	*r*	*p*
Mean RT	**Alerting**	-.16	= .369	.15	= .395
	Orienting	.12	= .518	.03	= .854
	Conflict [1]	**.35**	**= .043**	-.22	= .224
	Global [1]	**.61**	**< .001**	-.17	= .349
Mean Accuracy	**Alerting** [1]	.34	= .054	-.08	= .677
	Orienting [1]	-.15	= .416	.04	= .819
	Conflict [1]	-.04	= .840	.09	= .605
	Global [1]	.06	= .724	-.17	= .344

Incorrectly answered RTs were excluded from mean RTs. There was a significant correlation between conflict and global RT with age. Pearson Correlation was run for each correlation unless noted otherwise. Significant correlations are reported at uncorrected $p < .05$ level. Global is defined as the overall mean for all conditions.
[1] Spearman's rank-order correlation was run as data was not normal. Shapiro-Wilk's test ($p < .05$).
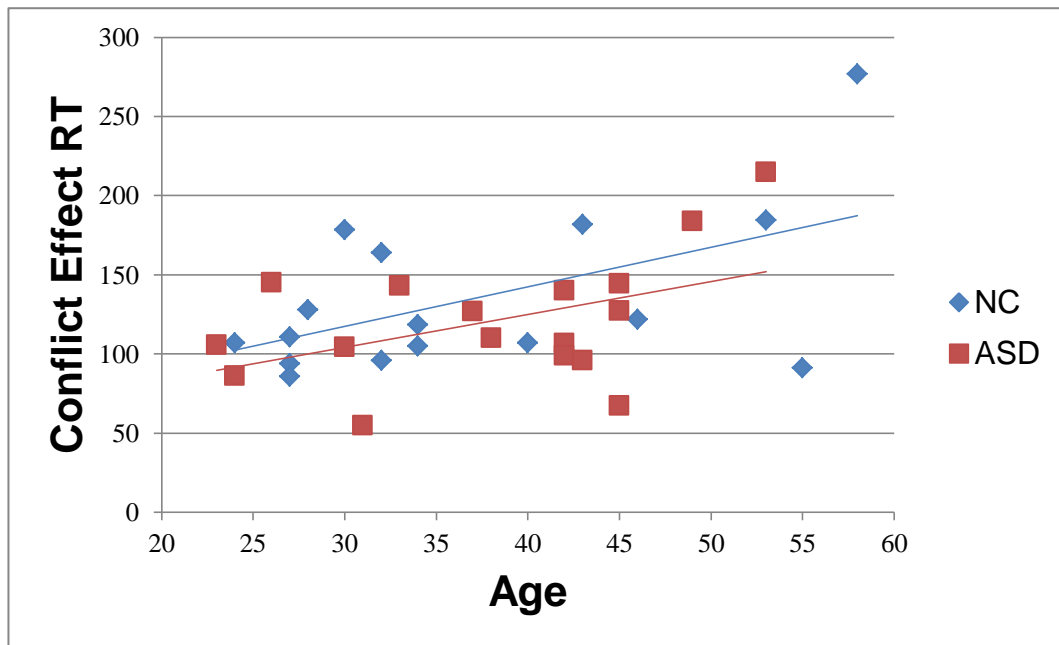
Figure 4.1 Relationship between Conflict Effect and Age (*NC = 17, ASD = 16*)

There was a significant correlation between age and flanker conflict effect RT for all participants ($r = .35$, $p = .043$). As age increased, there was also an increase in the conflict effect RT. The direction and slope of the association appear similar between groups. Conflict effect RT presented in ms.

4.3.2.3 Group Response Time Comparisons

We then investigated group differences in ANT performance (table 4.4). The mean global RT for correctly answered trials for NCs was 627.94 ms (SD = 112.80, range = 477.82 – 897.79 ms) and 654.51 ms (SD =153.16, range = 498.32 – 1073.69 ms) for participants with ASD. As mentioned above, age was correlated with global RT and was included as covariates in an analysis of covariance (ANCOVA) comparing overall RT to correctly answered trials between NC and participants with ASD. Data for global RT was non-normally distributed (Shapiro-Wilk's test, $p = .027$) and this was largely driven by four participants with large RT concentrations over 800 ms. Transformation of mean RT did not improve normality. The four large data points were not

considered outliers as no cases had standardised residuals greater than ± 3 SDs. Nevertheless, when these values were removed from the data set, the data complied with the assumptions of normality. As an ANCOVA is fairly robust to deviations from normality, we elected to run an ANCOVA with (NC = 16, ASD = 17) and without these participants (NC =15, ASD=14) and then compared results. There were no significant differences between groups in RT for the full (F(1,30) = .19, p =.668) or reduced sample (F(1,26) = 1.19, p = .285). Age for full sample (F(1,30) = 12.28, p =.001) and reduced sample (F(1,26) = 16.13, p =.000) significantly predicted RT during correctly answered trials.

Alerting (NC: M = 26.34 , SD = 18.85, range = -15.61 – 62.69 ms; ASD: M = 25.22 , SD = 22.27, range = -11.14 – 78.33 ms) and orienting RT (NC: M = 37.44, SD = 24.25, range = -11.68 – 89.63 ms; ASD: M = 36.66, SD = 23.81, range = -15.16 – 87.85 msec) were compared between groups. There was no significant difference between groups for alerting effect (t(31) = .16, p = .877) and orienting effect (t(31) = .09, p = .926)

Next we compared conflict effect RT by group (NC: M = 134.47, SD = 50.75, range = 85.82 – 276.92 msec; ASD: M = 120.99, SD = 39.68, range = 55.05 – 214.83 ms). Age was included as a covariate in this group comparison. There was no significant difference for conflict effect RT between groups (F(1,30)=1.39, p=.285), but age was a significant predictor of conflict effect RT (F(1,30) = 10.57, p=.003). None of the data was significant at uncorrected

p < .05 and therefore would also have not survived the more stringent corrected *p* < .008 level (table 4.4).

Table 4.4 Group Comparisons for Alerting, Orienting, Conflict and Global Response Times

Effect	NC Mean (SD)	ASD Mean (SD)	statistic	*p*
Alerting	26.34 (18.85)	25.22 (22.27)	*t*(31) = .16	0.877
Orienting	37.44 (24.25)	36.66 (23.81)	*t*(31) = .09	0.926
Conflict [1][2]	134.47 (50.75)	120.99 (39.68)	F(1,30)=1.39	0.246
Global [1]	627.94 (112.80)	654.51 (153.16)	*F*(1,26) = 1.19	.285

There were no significant differences in RT between groups. The alerting effect = mean no cue RT - mean double cue RT. The orienting effect = mean spatial cue RT - mean centre cue RT. The conflict effect = mean incongruent flanker RT - mean congruent flanker RT. Significance reported at uncorrected *p* < .05 level.

[1] Age included as a covariate in group comparison.

[2] Results reported for a reduced sample.

ASD, autism spectrum disorder; NC, neurotypical controls; SD, standard deviation

4.3.2.4 Group Error Rate Comparisons

Error rates for alerting (NC: *M* = .01%, *SD* = 1.53%, range = -1.43 – 1.43%; ASD *M* = -.48%, *SD* = 1.48%, range = - 4.17 – 1.57%) and orienting effect (NC: *M* = -.52%, *SD* = 1.23%, range = - 4.17 – 1.39%; ASD *M* = -.15%, *SD* = 1.60%, range = -2.78 – 4.48%) percentage error were low for both NC and participants with ASD. There were no in group differences in accuracy for alerting (*t*(31) = .90, *p* = .926) and orienting ERs (*t*(31) = -.75, *p* = .457).

We also investigated group differences in conflict ER (NC: *M* = 1.37%, Median =1.04% *SD* = 1.85%, range = -1.04 – 5.21%; ASD *M* = 1.73%, Median = 1.72%, *SD* = 2.39%, range = 0 – 7.5%). Standardized residuals were non-normally distributed for conflict ER as assessed by the Shapiro-Wilk's test for the full model (*p* = .000), NCs (*p* = .007) and individuals with

ASD (p = .000). Data transformation did not correct for non-normality and therefore, a non-parametric Kruskal-Wallis test was run. Distributions of scores for both groups were similar as assessed by inspection of a boxplot for each group. Median scores for conflict ER were not statistically different between groups (X^2(1) = .09, p = .765).

Finally, we compared groups on global ER between groups (NC: M = .67 Median = .52 %, SD = .74 %, range = 0 - 2 %; ASD M = .87 %, Median = .69 %, SD = 1.28 %, range = 0 – 5%). Data were non-normally distributed for global ER as assessed by the Shapiro-Wilk's test for the full model (p = .000), NCs (p = .007) and individuals with ASD (p = .000). Data transformation did correct for non-normality and therefore, a non-parametric Kruskal-Wallis test was run. Distributions of scores for both groups were similar as assessed by inspection of a boxplot for each group. Median scores for global ER were not statistically different between groups (X^2(1) = .02, p = .896). None of the data was significant at uncorrected p < .05 and therefore would also have not survived the more stringent corrected p < .008 level. These results are also displayed in table 4.5.

Table 4.5 Group Percentages for Alerting, Orienting and Conflict and Global Error Rates

Effect	NC Mean% (SD)	ASD Mean% (SD)	statistic	p
Alerting	.01 (1.53)	-.48 (1.48)	$t(31) = .90$,	.926
Orienting	-.52 (1.23)	-.15 (1.60)	$t(31) = -.75$	.457
Conflict [1]	1.37 (1.85)	1.73 (2.39)	$X^2(1) = .09$	.765
Global [1]	.67 (.74)	.87 (1.28)	$X^2(1) = .02$	.896

There were no significant differences in ER between groups. The alerting effect = percentage no cue ER - percentage double cue ER. The orienting effect = percentage spatial cue ER - percentage centre cue ER. The conflict effect = percentage incongruent flanker ER - percentage congruent flanker ER. Global ER was the total number wrong minus the total number of trials multiplied by 100. Significance reported at uncorrected $p < .05$ level. Unless otherwise noted, groups were compared with independent samples t-tests.
[1] Non-parametric Kruskal-Wallis test run as data were non-normally distributed

ASD, autism spectrum disorder; NC, neurotypical controls; SD, standard deviation

4.3.2.5 The Relationship between ANT Effect Scores and Autism Diagnostic Observation Schedule for Participants with ASD

ADOS scores were non-normally distributed, and therefore, a Spearman rank order correlation was run to compare ADOS and ANT sub-scores. For participants with ASD, conflict RT had a strong negative correlation with ADOS communication scores (r_s = -.73, p = .001) and overall ADOS total score (r_s = -.58, p = .015). Increased communication symptoms were associated with a reduced conflict effect in participants with ASD (figure 4.2). Nevertheless, neither of these relationships survived correction for multiple comparisons (p < .001). There were no other significant relationships between ADOS scores and ANT performance (p > .05).
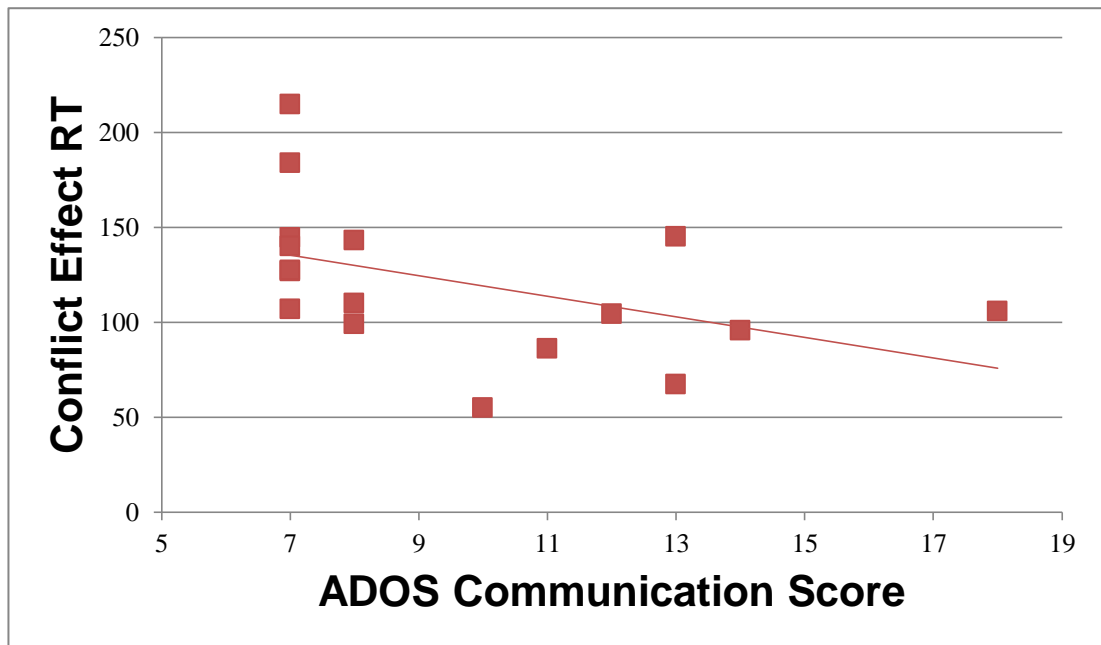
Figure 4.2 Relationship Between Conflict Effect Response Time and Autism Diagnostic Observations Schedule (ADOS) Communication Score for Participants with Autism Spectrum Disorder (*n* = 17).

For participants with ASD, increased communication scores, as measured by the ADOS, were associated with reduced conflict effect RT. Conflict RT is presented in ms.

4.3.2.6 *The Relationship between Attentional Network Test Scores and Metabolite Concentrations*

The data for global RT (Shapiro-Wilk = .001) and conflict RT (Shapiro-Wilk = .005) were non-normally distributed for the full sample. For consistency, we ran non-parametric Spearman's rank order correlation for these correlations for the full, NC and ASD analyses. The Pearson's correlation was used for all other correlations.

There were no significant correlations between the alerting, orienting, conflict and global RT and metabolite concentrations (Glu, Glx and NAA + NAAG) for the full participant sample (table 4.6), NCs (table 4.7) or individuals with ASD (table 4.8) (uncorrected $p > .05$). We did not further investigate corrections

149

for multiple comparisons as there were no significant correlations at uncorrected $p < .05$.

Table 4.6 Correlation Between Metabolite Concentrations and Mean Response Times, for All Study Participants

		Glu ($n = 28$)		Glx ($n = 27$)		NAA + NAAG ($n = 31$)	
		r	*p*	*r*	*p*	*r*	*p*
Mean RT	**Alerting**	.05	.809	.11	.594	-.09	.651
	Orienting	.08	.674	-.05	.793	-.15	.417
	Conflict [1]	.11	.585	.11	.590	-.12	.524
	Global [1]	-.22	.265	.29	.143	-.15	.431

There were no significant correlations between Glu, Glx or NAA + NAAG and ANT RT. Pearson correlations were run unless noted otherwise. Significant correlations are reported at uncorrected $p < .05$ level. Global is defined as the overall mean for all conditions.
[1] Spearman's rank-order correlation was run as data was not normal. Shapiro-Wilk's test ($p < .05$).

Table 4.7 Correlation Between Metabolite Concentrations and Mean Response Times for NCs

		Glu ($n = 1$)		Glx ($n = 13$)		NAA + NAAG ($n = 15$)	
		r	*p*	*r*	*p*	*r*	*p*
Mean RT	**Alerting**	.15	.601	-.07	.823	.01	.967
	Orienting	-.29	.307	-.28	.326	-.52	.05
	Conflict [1]	-.14	.637	-.04	.887	.1	.732
	Global [1]	-.39	.164	-.37	.197	-.16	.567

There were no significant correlations between Glu, Glx or NAA + NAAG and ANT RT. Pearson correlations were run unless noted otherwise. Significant correlations are reported at uncorrected $p < .05$ level. Global was defined as the overall mean for all conditions.
[1] Spearman's rank-order correlation was run as data was not normal. Shapiro-Wilk's test ($p < .05$).

Table 4.8 Correlation Between Metabolite Concentrations and Mean Response Times, for Individuals with ASD

		Glu (n = 14)		Glx (n = 13)		NAA + NAAG (n = 16)	
		r	*p*	*r*	*p*	*r*	*p*
Mean RT	**Alerting**	-.03	.932	.14	.660	-.14	.594
	Orienting	.34	.231	.20	.509	.07	.594
	Conflict [1]	.25	.392	.28	.354	-.35	.180
	Global [1]	-.18	.533	-.43	.138	-.21	.431

There were no significant correlations between Glu, Glx or NAA + NAAG and ANT. Pearson correlations were run unless noted otherwise. Significant correlations are reported at uncorrected $p < .05$ level. Global was defined as the overall mean for all conditions.
[1] Spearman's rank-order correlation was run as data was not normal. Shapiro-Wilk's test ($p < .05$).

4.3.2.7 Study Comparisons of Attentional Network Test Data for Participants with Autism Spectrum Disorder

We present a comparison table of the participant numbers, mean age, IQ and ANT scores for participants with ASD compared to Fan and colleagues 2012[26]. In the current study, individuals with ASD were slightly older but had similar IQ scores compared to Fan et al. (2012). Comparing studies, our investigation had slightly reduced global RT, conflict EP and increased accuracy rates (Table 4.9).

Table 4.9 Participant Characteristics and Results from Fan et al. (2012) Compared to Current Trial for Individuals with Autism Spectrum Disorder

	Fan et al. (2012) (*n = 12*)	Current Study (*n = 17*)
	Mean (SD)	Mean (SD)
Age	30 (6)	38 (9)
IQ	115 (14)	117 (12)
ADOS-G	12.2 (4.1)	9.65 (3.3)
Alerting RT	NR	25 (22)
Orienting RT	NR	37 (24)
Conflict RT	151 (72)	121 (40)
Global RT	878 (164)	654 (153)
Alerting EP	NR	0 (1)%
Orienting EP	NR	0 (2)%
Conflict EP	18 (15)%	2 (2) %
Global Accuracy Rate	79 (12)%	99 (1)%

Demographic, ADOS-G and ANT performance results for Fan et al. (2012) and the current study. Participants in Fan et al. (2012) completed the ANT inside an MRI scanner

ADOS-G, total communication and social ADOS scores, ASD, Participants with autism spectrum disorder; EP, error percentage; IQ, intelligence; NR, not reported; SD, standard deviation; RT, response time.

4.4 DISCUSSION

We investigated conflict effect performance in association with individuals with ASD relative to NCs and in association with core symptoms of the disorder. We also explored the relationship between conflict effect performance and metabolite concentrations.

We will firstly discuss our replication of the main effects of the ANT in all participants (chapter 4.4.1) and the ANT's relationship with age but not IQ (chapter 4.4.2). We then discuss the lack of significant performance differences between groups and suggest some possible reasons why our

study did not replicate the previous investigation of the ANT in adults with ASD [26] (chapter 4.4.2). Finally, we did not find any relationship between metabolites and ANT performance (chapter 4.4.5). In individuals with ASD, we did report a relationship between conflict effect performance and communication deficit (chapter 4.4.4), but this correlation did not survive correction for multiple comparisons.

4.4.1 Main Effects Attentional Network Test

Across participants, RTs were higher during the more cognitively demanding conditions for the alerting, orienting and CEs , as has been shown previously [26,304,363,417,568]. In contrast, participants were highly accurate, and there was no support for an alerting or orienting error effect across participants. There was some support for greater error during the high conflict incongruent flanker conditions compared to congruent flanker conditions across participants. Nevertheless, almost 40% of participants were excluded from the conflict error analysis because they had equal accuracy rates for incongruent and congruent flanker conditions, and therefore, this final statistical conclusion requires caution. Taken as a whole, RT was a better measure of variation in performance between groups than error.

In our ANT analysis, we did not investigate evidence of fatigue (see chapter 2.2.2) because we had few observable errors. Our inability to measure the impact of fatigue because of ER ceiling effects is a limitation of this study and hopefully future studies will assess the impact of fatigue on performance with a more difficult inhibition to distraction task.

4.4.2   Basic Demographic Characteristics and the Attentional Network Test

On the ANT, there was a positive correlation between age and both global accuracy and conflict RTs (figure 4.5). These associations have been supported by other studies [562–564,569], suggesting that, as both NCs and individuals with ASD age, their performance on the ANT declines. We did not report a relationship between IQ and ANT performance, which has also been previously shown [565]. Nevertheless, these results require further replication as our sample only included a small cross-sectional analysis of men with average to above average intelligence. Further studies would benefit from investigating a larger, more diverse longitudinal sample of participants.

4.4.3   Group Differences on the Attentional Network Test

There were no significant performance differences between groups on global, alerting, orienting or conflict effects (table 4.4 and 4.5). In comparison to our investigation, Fan et al. (2012) reported group differences in conflict effect performance for individuals with ASD compared to NCs [26] in participants with similar characteristics to our study. For example, both studies investigated similar participant sizes of high functioning adults with ASD (table 4.9).

Nevertheless, there was some variation in participant characteristics between studies, which might contribute to contradictory results and, therefore, deserve mention. Firstly, participants in this study were slightly older than those in Fan et al. (2012) (table 4.9). Nevertheless, both our own and previous analysis suggests that increased age was associated with increased conflict effect RT [562,563]. Instead, compared to Fan and colleagues, our

investigation reported lower mean conflict effect RT and ER with an older mean participant age.

Individuals in the previous study also reported higher mean ADOS scores than the participants in this study, which may have contributed to greater performance differences in individuals with ASD in Fan et al. (2012) (table 4.9). Fan and colleagues also included five female participants (NC = 2, ASD = 3), which may have contributed both to increased ADOS scores or varied the characteristics of the ASD group. One study investigated symptoms of ASD in over two thousand individuals with ASD between females and males. Investigators reported more severe symptoms in females with the disorder including greater communication, cognitive and adaptive deficits [570].

Furthermore, in contrast to our study, participants in Fan et al. (2012) completed the assessment inside an MRI scanner. We hypothesise that this difference might have increased the stress and complexity of the ANT. This hypothesis is supported by increased mean global and conflict effect RT performance for individuals with ASD when inside a scanner [26] which suggests increased cognitive effort (table 4.9). Researchers have reported that executive control tasks elicit a widening gap in performance differences between NCs and individuals with ASD when the cognitive complexity increased [571–576]. For example, one research group reported significant performance differences in mean RT and ER only when presentation speed increased during a response inhibition task in individuals with ASD compared to NCs [574].

Therefore, we suggest that performance deficit previously reported by Fan and colleagues [26] might have been more evident due to the increased complexity of completing the task inside an MRI scanner [571]. Altered function of the dACC in individuals with ASD compared to NCs does not always translate into inhibitory performance differences [53,408]. With age, adult participants with ASD may learn adaptive strategies to mask altered behaviours and brain function [109], which may only become apparent during more complex, real-world, multidimensional cognitively demanding situations.

Relatedly, conducting the ANT in a laboratory might have preferentially benefited individuals with ASD. The goal of conducting the ANT in a laboratory was to reduce external social and other stressful confounds. Nevertheless, this task was not an ecological valid representation of an inhibitory behaviour. Participants with ASD benefit from laboratory environments [425,577] and perform well under highly structured conditions with defined behavioural requirements and little irregularity [578,579]. Unfortunately, these situations are not typical of the real world and might explain the reported disconnect between carer rated and laboratory assessments of executive control in participants with ASD [580,581].

Alternatively, hypoactivation of the dACC as previously reported during the ANT assessment [26] might have been associated with reduced motivation or compliance. As we mentioned previously, researchers have linked the dACC with task motivation. For example, individuals with epilepsy have reported feelings of increased task preservation with electrical stimulation of the dACC

[360]. Therefore, reduced activation of the dACC during previous studies might suggest reduced motivation in the task leading to performance deficits in individuals with ASD [26].

In conclusion, our data suggest that when in a laboratory environment, individuals with ASD did not exhibit any conflict effect performance differences compared to NCs. We suggest that differences in autistic severity, task complexity or motivation might lead to differences between this study and Fan and colleagues, 2012 [26].

4.4.4 Correlation between Conflict Effect and Communication Score in Participants with Autism Spectrum Disorder

We report that higher ADOS communication scores were associated with reduced conflict effect scores. In other words, increased communication deficits were associated with reduced RT differences between incongruent flankers compared to congruent flankers in participants with ASD (figure 4.2). This result was unexpected especially as the previous study reported that greater communication deficit was also associated with increased conflict effect ER in individuals with ASD [26]. It may be that more severe communication deficit in individuals with ASD were associated with a similar cognitive response for both congruent and incongruent stimuli associated with decreased conflict effect RTs in our study but increased ER when task difficulty increased when completing the ANT within an MRI scanner [26]. Nevertheless, the relationship between ADOS communication scores and conflict effect RTs did not survive correction for multiple comparisons, and we

157

cannot rule out the possibility of a type I error within our study. Therefore, these relationships warrant further investigation and replication.

4.4.5 *Correlation between Conflict Effect and Metabolite Concentrations*

We were also interested in the relationship between metabolites and the CE, but did not report any significant relationship. In future experiments, a more difficult and regionally specific task might allow greater inference into the relationship between Glu or Glx concentrations and behaviour.

4.5 CONCLUSION

There was no evidence of reduced performance on the conflict effect task in individuals with ASD compared to NCs. Furthermore, there was no evidence of an association between performance on an inhibition to distraction task and dACC metabolite concentrations. Our data suggest that individuals with ASD with more severe communication deficits performed better on the conflict effect task, although this association did not survive correction for multiple comparisons. Future research must investigate the association between ASD severity and performance on the conflict effect task as well as assess the impact that environment has on inhibitory task performance in individuals with ASD.

5 RESTING-STATE FUNCTIONAL CONNECTIVITY

5.1 INTRODUCTION

We previously presented the salience network (chapter 1.7.5.1), with the dACC and anterior insular cortex as core salience network brain regions [302,306]. One study reported that increased resting-state functional connectivity between these core salience network regions (the anterior insula and dACC) was associated with an increase in self-reported prescan anxiety in NCs [302]. This suggests that functional connectivity between salience network regions were associated with a conscious response to one's environment.

Other fMRI studies have reported that the dACC is functionally associated with various tasks requiring increased executive control [26,254,334,334,394–397,582,583] including inhibition to distraction tasks, such as the ANT [26,304] . Additionally, one group reported that when NCs completed the ANT in an MRI scanner, left dACC to DLPFC functional connectivity was associated with conflict effect performance [387]. Further resting-state functional connectivity analysis suggests that the dACC is temporally correlated with cognitive brain regions such so the DLPFC even in the absence of a cognitive task [302,306,381]. Researchers have hypothesized that the dACC might moderate both incoming sensory information from paralimbic and subcortical brain regions and, in turn, influence the outgoing behavioural and cognitive response to that sensory information [302].

Throughout this research chapter, we implemented a seed-to-voxel functional connectivity analysis of the dACC because we were interested in mapping

the functional connectivity of only this region in relation to the rest of the brain.

As a first step in our functional connectivity analysis, we investigated dACC functional connectivity within each group. Based on previous studies [302,306,381], we hypothesized that the dACC would be functionally connected with cognitive brain regions such as the DLPFC and other salience network regions, such as the insular cortex. We investigated if there were group differences in dACC functional connectivity and if there was a relationship between dACC seed-based functional connectivity and autistic severity as quantified by the ADOS in individuals with ASD.

We wished to investigate brain function without having to interpret the varied group response to a defined experimental paradigm, such as the ANT [584]. Therefore, we also investigated how dACC resting-state functional connectivity was associated with conflict effect performance in both NCs and individuals with ASD. Additionally, we investigated if there were any group differences in these associations.

Finally, there has been evidence that Glu concentrations have a relationship to functional connectivity (chapter 1.6). For example, researchers have reported that dACC Glu concentrations were associated with inhibitory behaviours by moderating the functional connectivity between the dACC and other midbrain regions [258]. Therefore, our primary objective in this chapter was to explore the relationships between Glu and Glx concentrations and dACC seed-to-voxel functional connectivity in individuals with ASD compared

to NCs. To our knowledge, we are the first group to investigate such a relationship in individuals with ASD, and this analysis was mostly exploratory. Given evidence of an imbalance in Glu signalling and concentrations in individuals with ASD compared to NCs [194,207,247], we hypothesised that there might be an altered relationship between dACC Glu or Glx and seed-to-voxel resting-state functional connectivity for individuals with ASD compared to NCs.

5.2 METHODS

5.2.1 Study Populations

The full study population, ethical consent and assessment procedure resulting in a final 20 NCs and 19 individuals with ASD were reported in chapter 2.6.1, 2.6.2 and 2.6.3 respectively.

5.2.1.1 Resting- State Functional Connectivity

For our seed-to-voxel analysis, we further excluded two NCs because they did not complete a resting-state EPI sequence. One additional NC resting-state EPI scan was lost due to technological issues. Four participants with ASD were also excluded because they had greater than 20% of their fMRI scans labelled for movement artefact during the preprocessing steps. Our final functional connectivity analysis included 17 NCs and 15 adults with high functioning ASD.

5.2.1.2 Resting-State Functional Connectivity Association to Attentional Network

Two participants did not complete the ANT (NC = 1, ASD = 1) resulting in a total of 16 NCs and 14 individuals with ASD included in the final ANT

participant numbers. There were an additional four participants (NC =2, ASD =2) with low accuracy rates for the incongruent conditions of the conflict effect task (below 60%). Therefore, these participants were excluded from the conflict effect performance with a final 14 NCs and 12 individuals with ASD included in the analysis.

5.2.1.3 Resting-State Functional Connectivity Association to Metabolite Concentrations Study Population

From the total participant numbers for the functional connectivity analysis (20=NC, 19=ASD), one further NC was excluded from all metabolite analyses because the incorrect scanning sequence was applied and the ^{1}H-MRS sequence was not usable.

Metabolite concentrations were only included in the analysis if the CRLB percentage score was less than 20% [445]. We excluded a further three participants from the Glu (NC = 1; ASD = 2) and four participants from the Glx analysis (NC = 1; ASD =3) because CRLB scores were greater than 20%, There were 15 NCs and 13 individuals with ASD included in the Glu analysis and 15 NCs and 12 individuals with ASD for the Glx analysis.

5.2.2 Demographic, Clinical and Psychometric Data Acquisition

We included age, IQ, ADOS and conflict effect RT scores in this analysis. The assessment procedure for the obtaining this data was reported in chapter 2.6.3. Briefly, all of these assessments were completed in a quiet laboratory environment outside of an MRI scanner.

5.2.3 Demographic, Clinical and Psychometric Data

All participants provided basic demographic information, which included age as specified in chapter 2.6.4. Participants also completed the WASI which is fully detailed in chapter 2.6.6.1. All participants with ASD completed the ADOS to confirm ASD diagnosis as explained in chapter 2.6.5. The conflict effect RT was defined as the increase in RT associated with the addition of incongruent non-target stimuli when compared to conditions only including congruent non-target stimuli. The ANT assessment was reported in chapter 2.6.6.2.

5.2.4 Magnetic Resonance Imaging Acquisition

The acquisition procedure for the anatomical MP-RAGE, ^{1}H-MRS and resting-state EPI sequences were reported in chapter 2.6.7. Briefly, participants were asked to close their eyes and attend to their breathing or the external scanner noise when participating in the resting-state EPI scan. The EPI scan lasted 7 minutes and 42 seconds. During all of the other scans, participants were asked to relax and try to stay as still as possible.

5.2.5 Magnetic Resonance Imaging Parameters

The scanning parameters for the anatomical MP-RAGE, resting-state EPI and ^{1}H-MRS sequences were reported in chapter 2.6.8.1, 2.6.8.2 and 2.6.8.3, respectively.

5.2.6 Imaging Preprocessing

All functional connectivity preprocessing, first and second level analyses were performed in CONN-fMRI functional connectivity toolbox v16.b [585]

(http://www.nitrc.org/projects/conn) an SPM12 (Statistical Parametric Mapping: The Wellcome Department of Cognitive Neurology, Institute of Neurology, London, UK, http://www.filion.ucl.ac.uk/spm/software/spm12) toolbox for the matrix laboratory (MATLAB version 2015b, the Mathworks Inc., Natick, MA, 2015). This software program was selected because it is well validated, powerful and simple use in seed-to-voxel analysis.

The anatomical MP-RAGE and EPI image origins were first manually re-centred to the anterior commissure. Anatomical images were then skull-stripped, normalised to MNI space and segmented into GM, WM and CSF brain masks. Structural WM and CSF masks were later utilised to extract principal components (5 each) from WM and CSF functional time series and then added as confounds during the first level analysis to correct for the non-neural artefact as part of the Component Based Noise Correction method (aCompCor) method [586].

Global signal regression has been a common preprocessing step to remove non-neural artefact in resting-state fMRI. It takes the average signal over all the voxels of the brain at each time point and regresses out this average from the data. The technique assumes that global signal changes are non-neural artefact and of no interest to the analysis [587]. Research has shown that global signal regression removes motion confounds [277] and even improves tissue specificity [588]. Nevertheless, global signal regression also overvalues connectivity outcomes, alters the sight of significant associations and creates spurious negative correlations [589–591].

165

One alternative to GSR is the aCompCor method [586]. Unlike global signal regression, aCompCor allows for variation in nuisance signals across the brain, as is typical of non-neural artefact. Furthermore, aCompCor makes no predictions about the relationship between noise and signal change further allowing nonlinear correction. Studies have compared these two methods and support aCompCor as an improved strategy for removing noise [592]. Given evidence that the aCompCor is a better method, we applied it within this study.

Before preprocessing of the functional EPI images, we removed the four images to reduce magnetisation equilibrium effects. During the preprocessing steps, functional images were unwrapped and realigned to the first volume using a six-parameter rigid body transformation. The six parameters of rigid body head motion were later applied as regressors during the first level analysis. Next, images were normalised to MNI template brain using non-linear registration.

We further applied signal and motion correction through the Artefact Detection Toolbox (ART) [593,594]. We applied motion artefact scrubbing parameters to reduced motion artefact (global z-value threshold > 3, subject motion threshold of .5 mm in translational or rotational directions). All time points marked above this threshold were later included as covariates in the first-level analysis and regressed out of the analysis. All functional images were smoothed with an 8 mm³ isotropic Gaussian kernel.

Lastly, linear detrending was applied to reduce scanner drift and low band-pass filtering. It reduced the frequency range of interest to 0.008 – 0.9 Hz a range typically representative of resting-state neuronal variance investigating low-frequency oscillations [595–597].

5.2.7 Modified Whole Brain Mask

The field of view for our EPI functional images was not optimised to include the cerebellum, and therefore, we removed the cerebellum from the default CONN brain volume mask (mask.volume.brainmask.nii). This brain mask sets the voxels which are correlated with the seed region in a seed-based functional connectivity analysis.

The CONN analysis toolbox included a default GM atlas which was defined by a combination of cortical and subcortical regions from the FSL Harvard-Oxford maximum likelihood cortical atlas and the cerebellar regions from the Automated Anatomical Labelling Atlas [598]. We subtracted the cerebellar GM defined region in the default GM atlas from the default CONN brain volume mask. This step provided a clear outline of the cerebellum. Next, the new mask image was manually altered in Brain Suite (Version 16a1; http://brainsuite.org/) to remove any remaining mask regions posterior and ventral to the cerebellum. Also, WM in the cerebellum was removed manually from the new mask because the default GM atlas did not remove WM from the original mask. This updated mask was then imported into CONN and utilised as our analysis mask. Only voxels in this mask were correlated with the seed region.

5.2.8 Seed Regions

We conducted a seed-to-voxel analysis using two 5 mm diameter sphere region of interest corresponding with our initial centre voxel for the dACC spectroscopy analysis (3 (±5), 18, 33 MNI). We shifted the centre voxel of our single voxel spectroscopy laterally to create separate non-overlapping right and left ROIs. Our final seed ROIs were 5 mm sphere seeds located on the right (5, 18, 33 MNI) and left (-5, 18, 33 MNI) dACC. Seed regions were created in the MarsBar (version 44) [552] toolbox for SPM12 and imported into the CONN for the seed-to-voxel functional connectivity analysis.

5.2.9 Statistical Analysis

5.2.9.1 Demographic, Neuropsychological and Artefacts Group Comparisons

Age, IQ and total number of identified movement outlier scans group comparisons were assessed in SPSS (SPSS Inc., Released 2013. IBM SPSS Statistics for Windows, Version 22, Armonk, NY: IBM Corp). We compared age, total IQ and total number of flagged outlier scans between groups with independent samples t-tests. Again, outlier scans were flagged during the motion artefact scrubbing preprocessing step. When the data did not comply with the assumptions of the appropriate parametric test, we applied the appropriate transformation and then reapplied a parametric test. A more detailed demographic analysis was presented for the full participant sample in chapter 2.7. We also previously reported conflict effect RT within NCs and individuals with ASD, as well as compared group performance in chapter 4.3.2

5.2.9.2 First Level Seed-to-Voxel Functional Connectivity Analysis

For each individual participant functional connectivity map, we calculated the Pearson correlation coefficients between the average BOLD time series of all voxels in each seed region and the time series of each voxel lying in GM in our adapted study mask. Correlation coefficients indexed the strength of the linear relationship between the seed region and each voxel. Correlation coefficients from subject-specific maps were then converted to normally distributed scores through the application of Fisher's *r* to *z* transformation for the second-level general linear model analysis.

5.2.9.3 Second-Level Analysis of Seed-to-Voxel Functional Connectivity

Throughout the second level analysis, we only reported clusters with a voxel-wise height threshold of $p < 0.001$, greater than 50 voxels and with a false discovery rate (FDR) correction for multiple comparisons at the cluster-level $p < .05$.

Using the Conn toolbox, one sample *t*-tests were applied to seed-based functional connectivity *z*-maps to investigate within-group (NC and ASD separately) average functional connectivity in association with both the left and right dACC seed regions. We compared group (NC vs ASD) seed-to-voxel connectivity maps with independent samples *t*-tests.

Within each group, bivariate linear regression analyses were utilised to evaluate the association between dACC seed-based functional connectivity and the metabolite concentrations (Glu and Glx). Another bivariate linear regression analysis was utilised to evaluate the association between seed-

based functional connectivity and the conflict RT within each group. For individuals with ASD, we applied bivariate linear regression models to investigate the association between seed-based functional connectivity and autistic severity (as quantified by ADOS scores). We only investigated the relationship to ADOS social and communication scores because most individuals with ASD scored zero on imagination and stereotyped behaviours (see chapter 2.7.5). Finally, multiple linear regression analysis was used to investigate between group differences in the relationship between functional connectivity and both metabolite concentrations (Glu and Glx) and conflict effect RT.

All significant cortical and subcortical voxels reported were labelled according to the Harvard-Oxford Cortical and Subcortical Atlas [599–602] (http://www.cma.mgh.harvard.edu/fsl_atlas.html). For greater clarity, we also reported the closest GM regions within 5 mm of the peak voxel coordinate according to the Tailarach Daemon atlas in WFU-pickatlas software [603,604]. Most GM regions were defined by BA [378] unless they were sub-cortical structures without a BA label.

5.3 RESULTS

The results of the resting-state seed-to-voxel analysis are presented below. To start, basic demographic information demonstrated that individuals with ASD were well matched to NCs on age and IQ (chapter 5.3.1). There were no significant differences between the numbers of identified outlier scans by group (chapter 5.3.2). Next, the seed-to-voxel analysis group maps for the

left and right dACC seed regions within (chapter 5.3.3) and between groups (chapter 5.3.4) are presented. Then we present the results of the association between dACC functional connectivity and symptoms of the disorder (chapter 5.3.5.1), executive control RT performance (chapter 5.3.5.2), Glu (chapter 5.3.5.3) and Glx (chapter 5.3.5.4).

5.3.1 Age and Intelligence

We firstly compared NCs (n = 17, M = 39.42, SD = 11.37, range = 24 - 58) and individuals with ASD (n = 15, M = 35.93, SD = 9.70, range = 23 - 53) on age. The overall standardized residuals for the full model were positively skewed (Sharpo-Wilk = .041). Following transformation to correct for non-normality in the data, there were no significant differences between groups on the square root transformation of age (t(30) = .90, p = .376).

We then compared the total IQ (NC: n = 17, M = 120.09, SD = 12.64, range= 93 - 139; ASD: n = 15, M = 116.40, SD = 11.16, range = 90 – 129) between groups. The standardized residuals for individuals with ASD were moderately negatively skewed (Sharpo-Wilk = .038) and we therefore applied a reflect and square root transformation to total IQ. Following transformation, there were no significant differences between groups on the transformed total IQ (t(30) = -1.13, p = .268).

5.3.2 Group Comparison Movement Outlier Scans

The number of movement outlier scans were compared between groups (NC: n = 17, M = 15.29, SD = 0, range 0 – 40; ASD: n = 15, M = 16.71, SD =, range 0 - 54). In each group standardized residuals were both positively

skewed and non-normally distributed (NC: Sharpo-Wilk = .028; ASD: Sharpo-Wilk = .020). Following transformation, there were no significant difference in the number of transformed outlier scans between groups (t(30) = .73, *p* = .472).

5.3.3 *Functional Connectivity Within Groups*

For NCs, there were four clusters significantly correlated with the right dACC seed region ($t(1,16) \geq$ 3.69, k $\geq$ 537). The first cluster overlapped with the bilateral insular cortex, opercular cortex, frontal orbital cortex, pre and postcentral gyrus, inferior frontal gyrus (pars triangularis and pars opercularis), supramarginal gyrus, temporal pole, superior temporal gyrus (including the planum polare, planum temporale and Heschl's gyrus), putamen, pallidum, thalamus, brain-stem (cluster *t*-score = 12.39; p-cluster FDR < .001; MNI peak coordinates (36, 14, -04); cluster voxel size = 16,398; nearest (±5) GM peak voxel = BA 13). The second cluster overlapped with the cingulate cortex (anterior and posterior), bilateral paracingulate, frontal medial cortex, juxtapositional lobule cortex (also known as the supplementary motor cortex), pre-central gyrus, post-central gyrus, superior parietal lobule (including the precuneus), and right superior and middle frontal gyrus (cluster *t*-score = 16.47; p-cluster FDR < .001; MNI peak coordinates (06, 16, 34); cluster voxel size = 9,573; nearest (±5) GM peak voxel = BA 32). The third cluster overlapped with the right frontal pole and middle frontal gyrus (cluster *t*-score = 7.43; p-cluster FDR < .001; MNI peak coordinates (28, 40, 24); cluster voxel size = 603; nearest (±5) GM peak voxel = BA 10). The final

cluster overlapped with the left frontal pole and middle frontal gyrus (cluster *t*-score = 6.48; p-cluster FDR < .001; MNI peak coordinates (-34, 36, 30); cluster voxel size = 537; nearest (±5) GM peak voxel = BA 9).

In NCs, there were five clusters associated with the left dACC seed ($t(1,16) \geq$ 3.69, k ≥ 86). The first cluster overlapped with bilateral cingulate gyrus (anterior and posterior division), paracingulate gyrus, medial, superior and middle frontal cortex, precuneous cortex, juxtapositional lobule cortex (also known as the supplementary motor cortex), pre-central gyrus and right frontal pole (cluster t-score = 15.73; p-cluster FDR < .001; MNI peak coordinates (-06, 18, 34); cluster voxel size = 10,387; nearest (±5) GM peak voxel = BA 32). The second cluster overlapped with right insular cortex, opercular cortex, frontal orbital cortex, frontal pole, inferior frontal gyrus (pars opercularis and triangularis), pre and postcentral gyrus, supramarginal gyrus, (anterior and posterior division), temporal pole, superior temporal gyrus (including the planum polare, planum temporale and Heschl's gyrus), middle temporal gyrus, pallidum, putamen, thalamus, accumbens (cluster *t*-score = 11.44; p-cluster FDR < .001; MNI peak coordinates (38, 16, -02); cluster voxel size = 8,037; nearest (±5) GM peak voxel = BA 13). The third cluster overlapped with the left insular cortex, opercular cortex, frontal orbital cortex, inferior frontal gyrus (including pars opercularis and triangularis), pre and postcentral gyrus, supramarginal gyrus, temporal pole, superior temporal gyrus (including the planum polare, planum temporale and Heschl's gyrus), putamen, amygdala, accumbens, caudate, pallidum (cluster *t*-score = 13.43;

cluster FDR < .001; MNI peak coordinates (-42, 14, 00); cluster voxel size = 6,933; nearest (±5) GM peak voxel = BA 13). The forth cluster overlapped with the left frontal pole and middle frontal gyrus (cluster *t*-score = 9.95; p-cluster FDR < .001; MNI peak coordinates (-32, 46, 30); cluster voxel size = 1,230; nearest (±5) GM peak voxel = BA 10). The final cluster overlapped with the right precentral gyrus (cluster T-score = 6.29; p-cluster FDR = .047; MNI peak coordinates (60, 08, 34); cluster voxel size = 86; nearest (±5) GM peak voxel = BA 9) (table 5.1, figure 5.1 and 5.2).

Table 5.1 Seed-to-Voxel Analysis for Neurotypical Controls (*n* = 17)

Brain Region	Hemisphere	MNI coordinates			GM	k$_E$	T-score	*p*-value
		x	*y*	*z*				
RDACC Seed								
Insula	B	36	14	-04	BA 13	16,398	12.39	< .001
Anterior Cingulate	B	06	16	34	BA 32	9,573	16.47	< .001
Frontal Pole	R	28	40	24	BA 10	603	7.43	< .001
Frontal Pole	L	-34	36	30	BA 9	537	6.48	< .001
Left DACC Seed								
Anterior Cingulate	B	-06	18	34	BA 32	10,387	15.73	< .001
Insula	R	38	16	-02	BA 13	8,037	11.44	< .001
Insula	L	-42	14	00	BA 13	6,933	13.43	< .001
Frontal Pole	L	-32	46	30	BA 10	1,230	9.95	< .001
Precentral gyrus	R	60	08	34	BA 9	86	6.29	= .047

Clusters positively correlated with the right and left dACC in NCs (voxel-wise uncorrected *p* < 0.001 and FDR cluster corrected *p* < .05). Brain region and hemisphere represent brain region overlapping with the largest number of voxels in the cluster. MNI coordinates represent peak effect in a cluster. GM represent closest GM defined area (within 5 mm) to peak voxel coordinate according to the Talairach Daemon atlas in WFU-pickatlas software [603,604]. Cluster size, k$_E$, represents the spatial extent or the number of voxels in a cluster. T-score and p-value are at the cluster level.

Amg, amygdala; bilateral; dACC, dorsal anterior cingulate cortex, BA; Brodmann area; FDR, false discovery rate; Hemi, hemisphere; Hip, Hippocampus; L, left; MNI, Montreal Neurological Institute; R, right

For individuals with ASD, there were nine clusters positively correlated between the right dACC seed (*t*(1,14) ≥ 3.79, k ≥ 151). The first and largest cluster overlapped with the bilateral cingulate gyrus (anterior and posterior), paracingulate gyrus, juxtapositional lobule cortex (also known as the supplementary motor cortex), pre-central gyrus, post-central gyrus, superior frontal gyrus and superior parietal lobule. The cluster also including the right insula cortex, operculum cortex, frontal orbital cortex, frontal pole, middle

frontal gyrus, inferior frontal gyrus (including pars opercularis and pars triangularis), precuneous, supramarginal gyrus, superior temporal gyrus (including the planum polare, planum temporale and Heschl's gyrus), putamen, pallidum and thalamus (cluster t-score = 12.06; p-cluster FDR < .001; MNI peak coordinates (06, 18, 32); cluster voxel size = 19,624; nearest (±5) GM peak voxel = BA 32). The second cluster overlapped with the left insular cortex, operculum cortex, frontal orbital cortex, inferior frontal gyrus (including pars opercularis), supramarginal gyrus (anterior division), pre and postcentral gyrus, superior temporal gyrus (including the planum polare, planum temporale, Heschl's gyrus and temporal pole), putamen, (cluster t-score = 9.04; p-cluster FDR < .001; MNI peak coordinates (-50, 06, 04); cluster voxel size = 6945; nearest (±5) GM peak voxel = BA 22). The third cluster overlapped with the right frontal pole and middle frontal gyrus (cluster t-score = 7.14; p-cluster FDR < .001; MNI peak coordinates (28, 42, 30); cluster voxel size = 605; nearest (±5) GM peak voxel = BA 10). The forth cluster overlapped with the left lateral occipital cortex and middle temporal gyrus (cluster t-score = 7.68; p-cluster FDR < .001; MNI peak coordinates (-42, -72, -06); cluster voxel size = 511; nearest (±5) GM peak voxel = BA 19). The fifth cluster overlapped with the left temporal/ occipital fusiform cortex, inferior temporal gyrus and lingual gyrus (cluster t-score = 6.23; p-cluster FDR < .001; MNI peak coordinates (-30, -58, -20); cluster voxel size = 416; nearest (±5) GM peak voxel = BA 19). The sixth cluster included the left frontal pole and middle frontal gyrus (cluster t-score = 6.17; p-cluster FDR < .001; MNI peak coordinates (-30, 36, 26); cluster voxel size = 404; nearest

(±5) GM peak voxel = BA 10). The seventh cluster included the right lateral occipital cortex, middle temporal gyrus and temporal/ occipital fusiform cortex (*p*-cluster FDR < .001; MNI peak coordinates (cluster *t*-score = 7.28; 48, -64, 0; cluster voxel size = 290; nearest (±5) GM peak voxel = BA 9). The eighth cluster overlapped with the right precuneus (cluster *t*-score = 5.38; *p*-cluster FDR = .003; MNI peak coordinates (16, -60, 42); cluster voxel size = 177; nearest (±5) GM peak voxel = BA 7). The final cluster overlapped with the left precuneus and lateral occipital cortex (cluster *t*-score = 5.79; *p*-cluster FDR = .006; MNI peak coordinates (-14, -74, 36); cluster voxel size = 151; nearest (±5) GM peak voxel = BA 7).

For individuals with ASD, the left dACC seed region overlapped with seven clusters. The first cluster included the bilateral cingulate gyrus, paracingulate gyrus, superior frontal gyrus, juxtapositional lobule cortex (also known as the supplementary motor cortex), pre-central gyrus, post-central gyrus, precuneus, superior parietal lobule (cluster *t*-score = 14.62; *p*-cluster FDR < .001; MNI peak coordinates (-08, 16, 34); cluster voxel size = 10,029; nearest (±5) GM peak voxel = BA 32). The second cluster included the right insular cortex, opercular cortex (frontal, central and parietal), frontal orbital cortex, frontal pole, inferior frontal gyrus (including pars triangularis and opercularis), supramarginal gyrus, pre and post-central gyrus, superior temporal gyrus (including the planum polare, planum temporale and Heschl's gyrus), middle temporal gyrus (posterior division), temporal pole, putamen, pallidum, thalamus (cluster *t*-score = 8.71; *p*-cluster FDR < .001; MNI peak coordinates

(46, 12, 00); cluster voxel size = 8,444; nearest (±5) GM peak voxel = BA 13). The third cluster overlapped with the left insular cortex, opercular cortex, frontal orbital cortex, inferior frontal gyrus (including pars triangularis and opercularis), supramarginal gyrus, pre and post-central gyrus, superior temporal gyrus (including the planum polare, planum temporale, Heschl's gyrus and temporal pole), putamen, pallidum, thalamus, accumbens and amygdala (cluster *t*-score = 8.94; *p*-cluster FDR < .001; MNI peak coordinates (-42, 08, 04); cluster voxel size = 7,259; nearest (±5) GM peak voxel = BA 13). The forth cluster encompassed the left frontal pole and middle frontal gyrus (cluster *t*-score = 9.63; *p*-cluster FDR < .001; MNI peak coordinates (-32, 44, 26); cluster voxel size = 917; nearest (±5) GM peak voxel = BA 10). The firth cluster overlapped with the right frontal pole and middle frontal gyrus (cluster *t*-score = 6.66; *p*-cluster FDR < .001; MNI peak coordinates (28, 44, 30); cluster voxel size = 524; nearest (±5) GM peak voxel = BA 10). The sixth cluster comprised of the left lateral occipital cortex and occipital fusiform gyrus (cluster *t*-score = 7.31; *p*-cluster FDR < .001; MNI peak coordinates (-46, -76, -08); cluster voxel size = 471; nearest (±5) GM peak voxel = BA 19). The seventh cluster overlapped with the brainstem and hippocampus (cluster *t*-score = 6.20; *p*-cluster FDR = .015; MNI peak coordinates (-10, -16, -14); cluster voxel size = 139; nearest (±5) GM peak voxel = substantia nigra) (table 5.2, figure 5.1 and 5.2).

Table 5.2 Seed-to-Voxel Analysis For Individuals with Autism Spectrum Disorder (*n* = 15)

Brain Region	Hemisphere	MNI coordinates			GM	k_E	t-score	p-value
		x	*y*	*z*				
RDACC Seed								
Anterior Cingulate	B	06	18	32	BA 32	19,624	12.06	< .001
Insula	L	-50	06	04	BA 22	6,945	9.04	< .001
Frontal Pole	R	28	42	30	BA 10	605	7.14	< .001
Lateral Occipital Cortex	L	-42	-72	-06	BA 19	511	7.68	< .001
Temporal Occipital Fusiform Cortex	L	-30	-58	-20	BA 19	416	6.23	< .001
Frontal Pole	L	-30	36	26	BA 10	404	6.17	< .001
Lateral Occipital Cortex	R	48	-64	00	BA 9	290	7.28	< .001
Precuneous	L	16	-60	42	BA 7	177	5.38	= .003
Precuneus	R	-14	-74	36	BA 7	151	5.79	=.006
Left DACC Seed								
Anterior Cingulate	B	-08	16	34	BA 32	10,029	14.62	< .001
Insula	R	46	12	00	BA 13	8,444	8.71	< .001
Insula	L	-42	08	04	BA 13	7,259	8.94	< .001
Frontal Pole	L	-32	44	26	BA 10	917	9.63	< .001
Frontal Pole	R	28	44	30	BA 10	524	6.66	< .001
Lateral Occipital Cortex	L	-46	-76	-08	BA 19	471	7.31	< .001
Brain Stem/ Hippocampus	L	-10	-16	-14	Sub N	139	6.20	.015

Clusters significantly associated with the right and left dACC in individuals with ASD (voxel-wise uncorrected $p < 0.001$ and FDR cluster corrected $p < .05$). Brain region and Hemisphere represent brain region overlapping with the largest number of voxels in the cluster. MNI coordinates represent peak effect in a cluster. GM represent closest GM defined area (within 5 mm) to peak voxel coordinate according to the Talairach Daemon atlas in WFU-pickatlas software [603,604]. Cluster size, K_E, represents the spatial extent or the number of voxels in a cluster. *T*-score and p-value are at the cluster level.

B, bilateral; dACC, dorsal anterior cingulate cortex, BA; Brodmann area; FDR, false discovery rate; Hemi, hemisphere; L, left; MNI, Montreal Neurological Institute; R, right; Sub N, Substantia Nigra
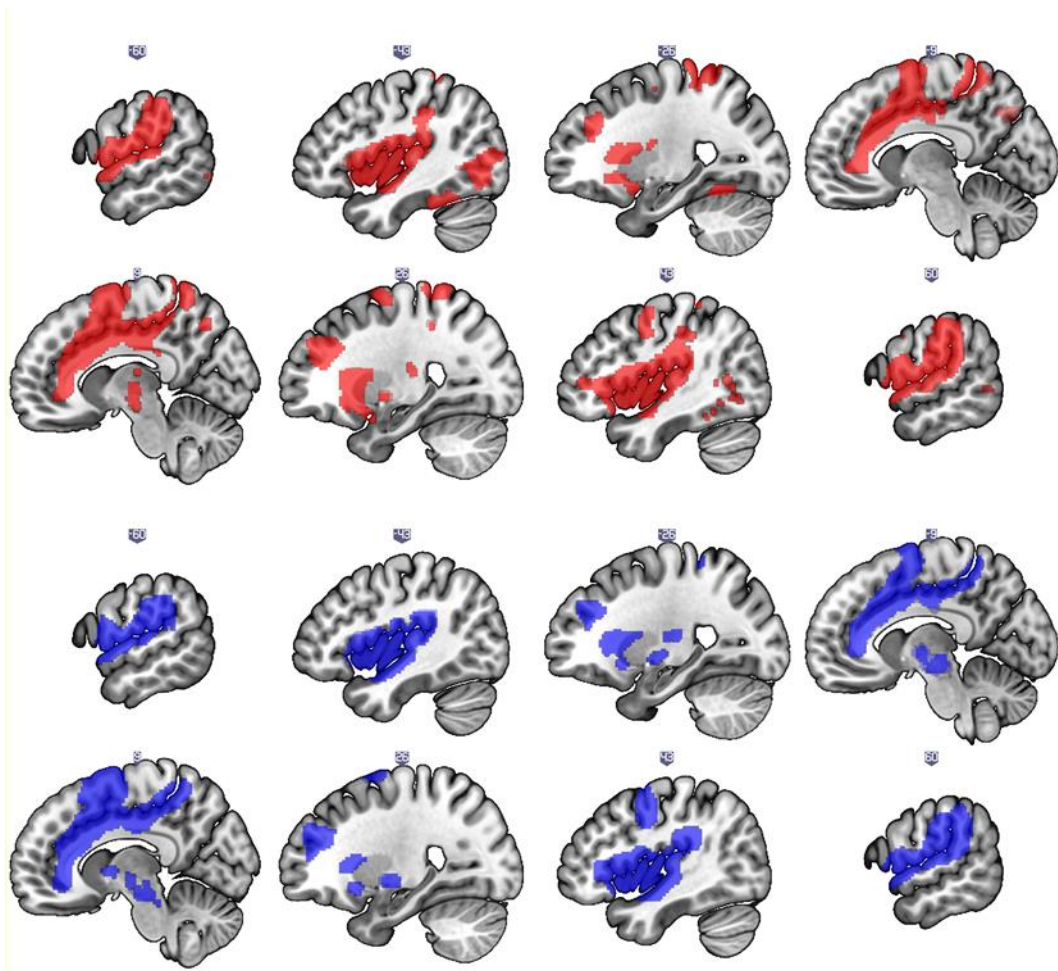
Figure 5.1 Right Dorsal Anterior Cingulate Resting-State Functional Connectivity Maps for Each Group

Regions of the brain which were functionally correlated with the right dACC for individuals with ASD in red ($t(1,14) \geq 3.79$, $k \geq 151$) and NCs in blue ($t(1,16) \geq 3.69$, $k \geq 537$). Results were voxel-wise uncorrected $p < .001$ and FDR cluster corrected $p < .05$.
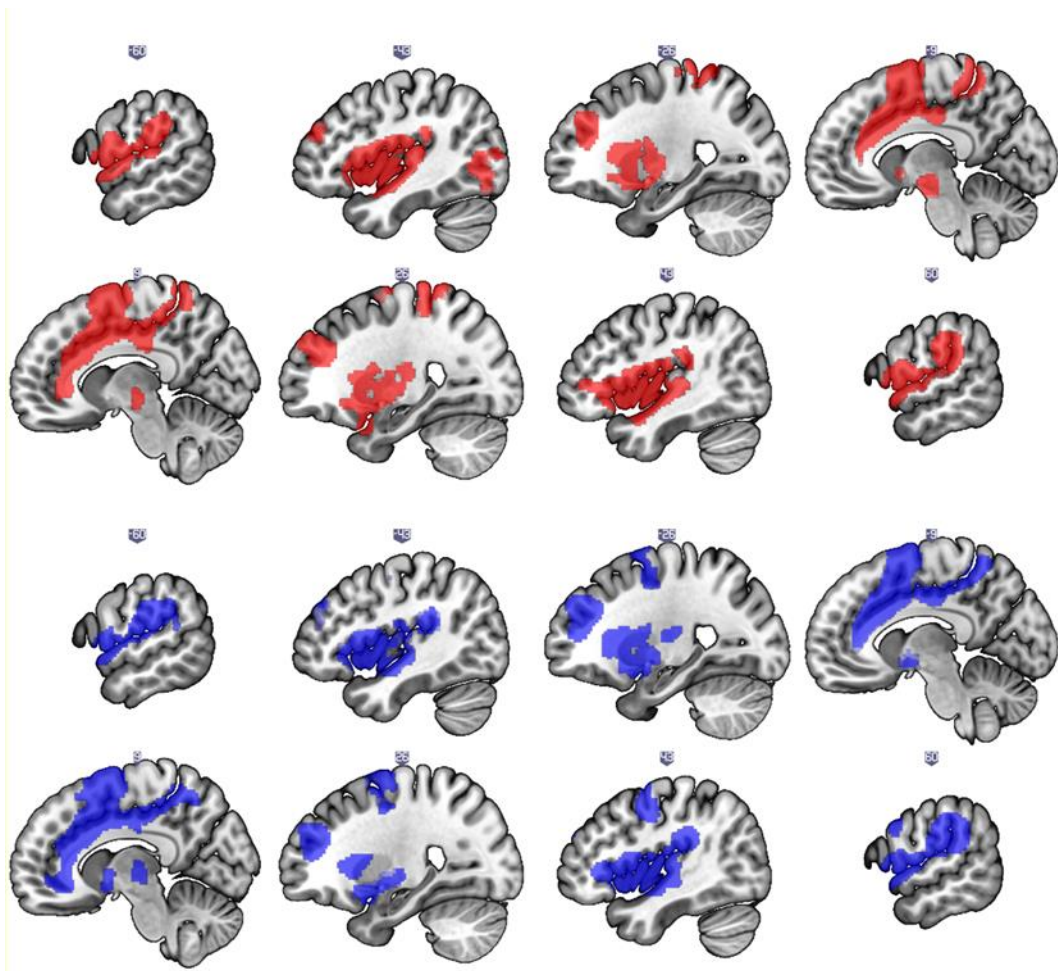
Figure 5.2 Left Dorsal Anterior Cingulate Resting-State Functional Connectivity Maps for Each Group

Regions of the brain which were functionally correlated with the left dACC for individuals with ASD (n =15) in red (t(1,14) ≥ 3.79, k ≥ 139) and NCs (n= 17) in blue (t(1,16) ≥ 3.69, k ≥ 86). Results were voxel-wise uncorrected $p < .001$ and FDR cluster corrected $p < .05$.

5.3.4 Functional Connectivity Between Groups

There were no significant differences between groups in dACC functional connectivity for either seed region at voxel-wise uncorrected $p < 0.001$ and FDR cluster corrected $p < .05$.

5.3.5 Functional Connectivity and Associations

5.3.5.1 Autism Diagnostic Observation Scores

For individuals with ASD, there were no significant associations between dACC functional connectivity and ADOS scores (total, communication or social) at voxel-wise uncorrected $p < 0.001$ and FDR cluster corrected $p < .05$.

5.3.5.2 Conflict Effect Response Time

For individuals with ASD, the connectivity between the left dACC to right superior lateral occipital cortex (LOC) was significantly and negatively associated with conflict RT (cluster *t*-score = -6.15, *p*-cluster FDR = .028; MNI peak coordinates (30, -60, 56); cluster voxel size = 133; nearest (±5) GM peak voxel = BA 7). In other words, RTs for incongruent flanker conditions were closer to congruent flanker RTs (considered improved conflict effect performance) when there was closer coupling between the left dACC and the LOC in individuals with ASD. There were no other significant relationships or group interactions between functional connectivity for the dACC and conflict RT (figure 5.3).
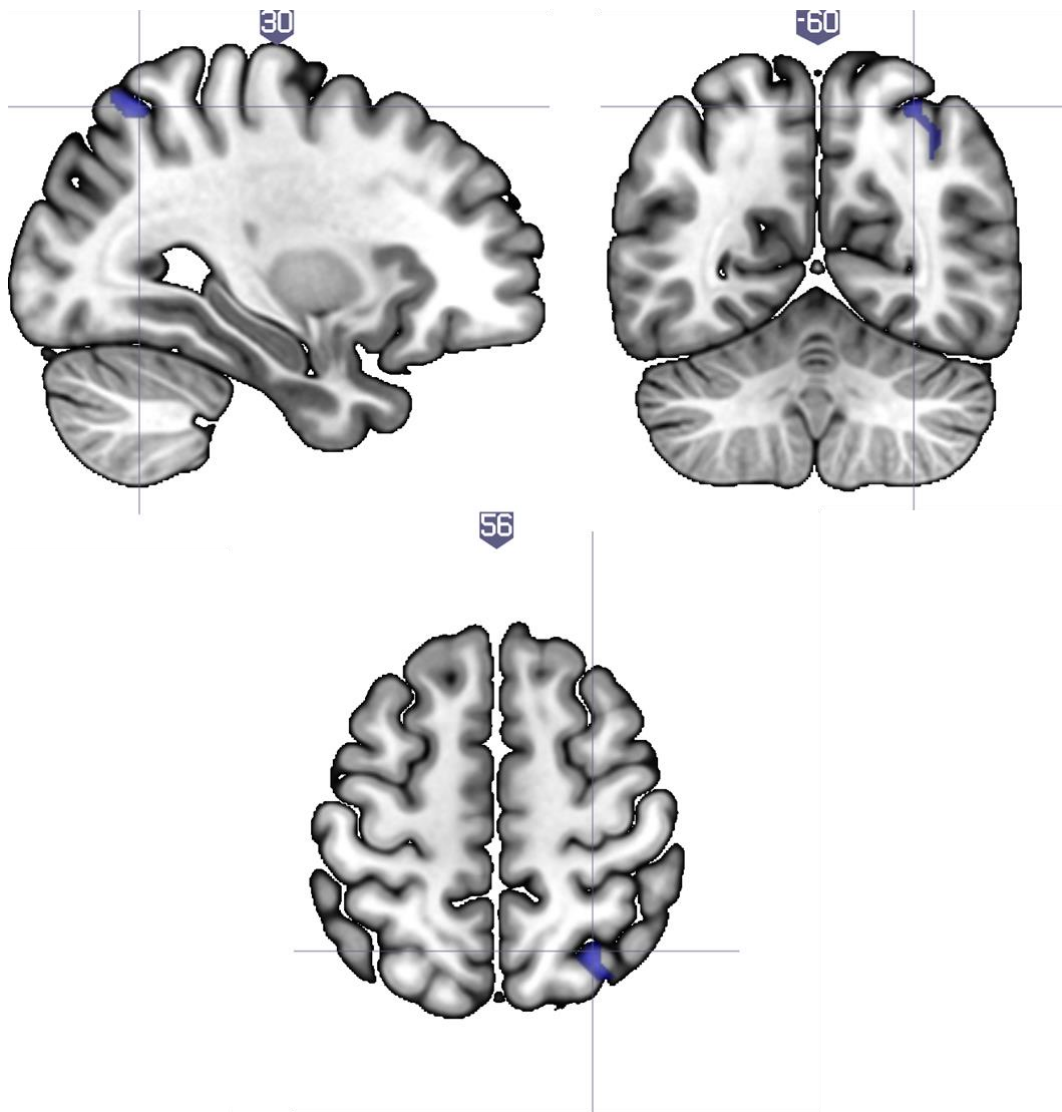
Figure 5.3 Left Dorsal Anterior Cingulate Seed-to-voxel Cluster Correlated with Conflict Response Time in Individuals with Autism Spectrum Disorder ($n = 12$)

Individuals with ASD had improved performance during tasks requiring increased cognitive control in association with increased functional connectivity between the left dACC and the right occipital cortex cluster (cluster t-score = -6.15,.p-cluster FDR = .028; MNI peak coordinates (30, -60, 56); cluster voxel size = 133; nearest (±5) GM peak voxel = BA 7). The cluster is shown in blue.

For further clarification of this association in NCs and individuals with ASD, we ran a ROI-to-ROI analysis of functional connectivity between the left dACC and previously identified right superior LOC cluster for all participants.

Then we visually investigated the association between connectivity and conflict RT via a scatterplot. Individuals with ASD have a clear relationship between the left dACC and right LOC functional connectivity. This relationship was less evident in NCs (figure 5.4).
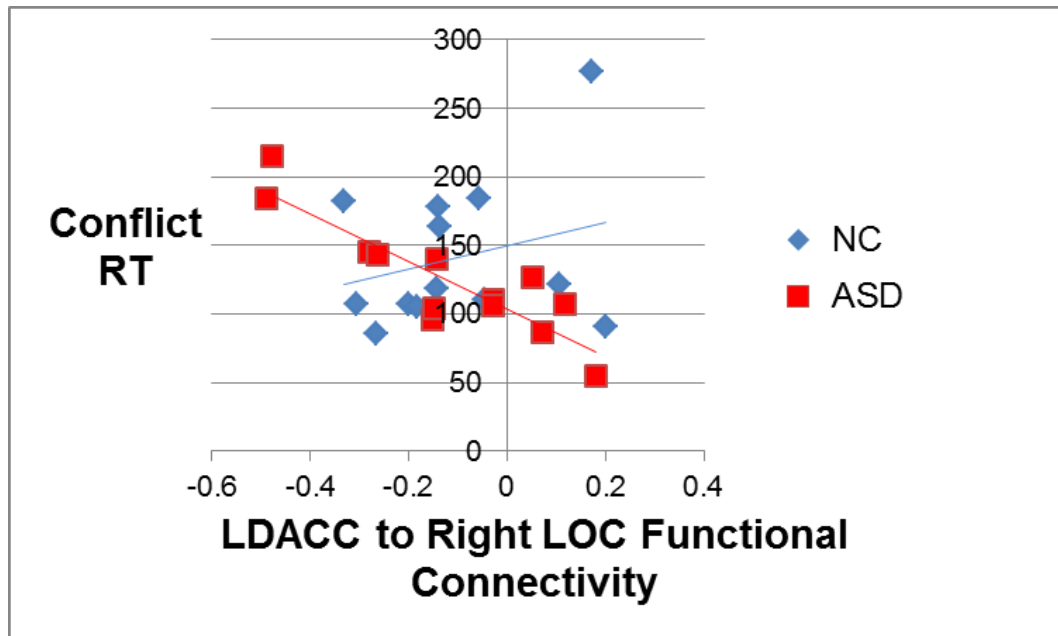
Figure 5.4 Conflict Response Time and Left Dorsal Anterior Cingulate Functional Connectivity to the Right Lateral Occipital Cortex

In individuals with ASD (n = 12), conflict RT scores were negatively associated with functional connectivity between the left dACC and the Right LOC. This relationship was not shown in NCs (n = 14).

5.3.5.3 Glutamate

In NCs, there was no significant relationship between resting-state functional connectivity and Glu concentrations for the left or right dACC seed region.

For individuals with ASD, connectivity between the right dACC and a cluster overlapping with the left anterior temporal fusiform cortex, temporal pole, frontal orbital cortex and parahippocampal gyrus were significantly and negatively associated with dACC Glu concentrations (cluster t-score = -8.49;

184

p-cluster FDR < .001; MNI peak coordinates (-34, 02, -26); cluster voxel size = 326; nearest (±5) GM peak voxel = BA = 28) (figure 5.5).

Furthermore, in individuals with ASD, connectivity between the left dACC and the left anterior temporal fusiform cortex, parahippocampal gyrus and temporal pole was significantly and negatively associated with dACC Glu concentrations (figure 5.6) (cluster *t*-score = -7.19, *p*-cluster FDR = .015; MNI peak coordinates (-32, -02, -36); cluster voxel size = 158; nearest (±5) GM peak voxel = BA 28). There was no significant group interaction between Glu and FC.
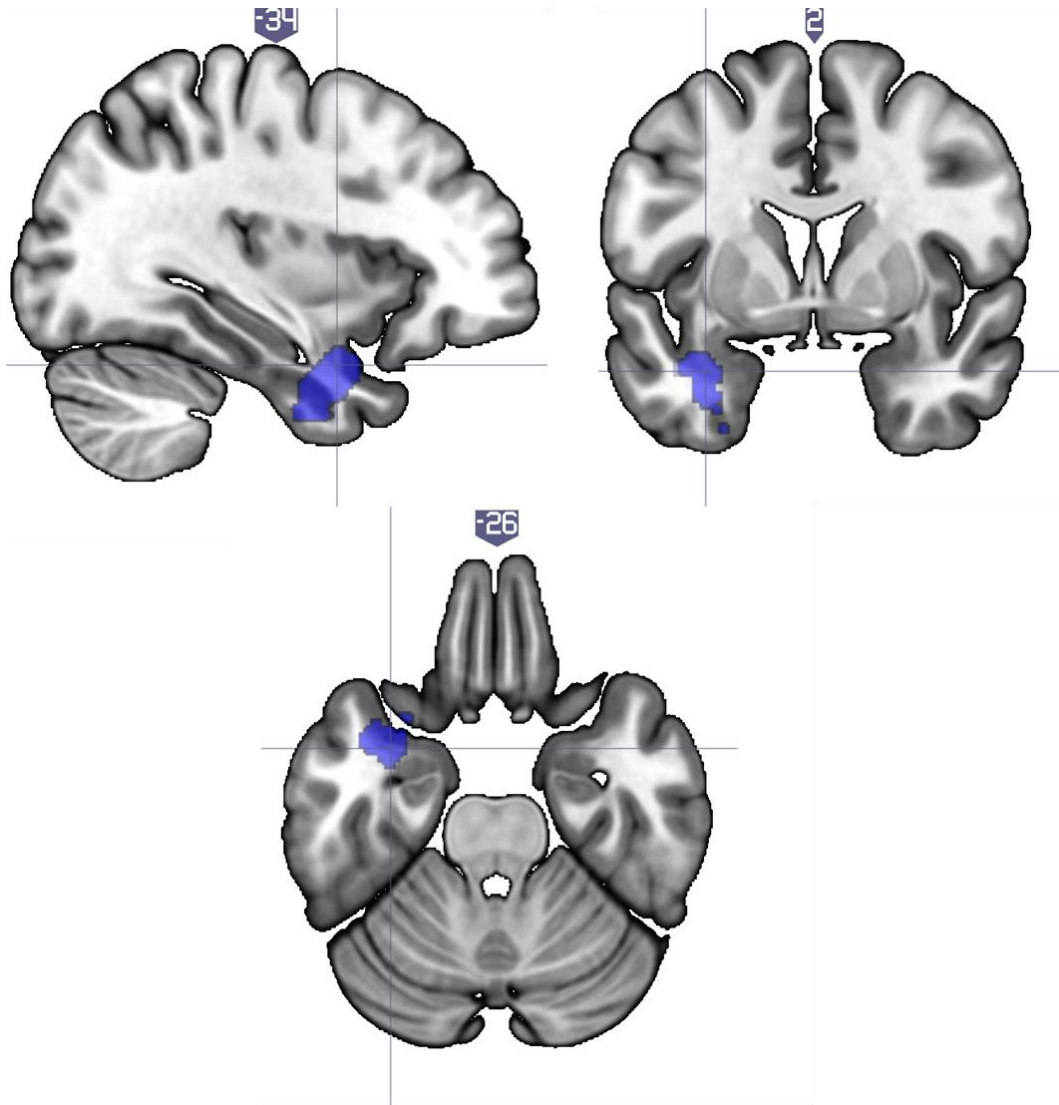
Figure 5.5 Glutamate Concentrations Associated with Right Cingulate to Left Medial Temporal Lobe Functional Connectivity in Individuals with Autism Spectrum Disorder (*n* = 13)

Glu concentrations in individuals with ASD were positively associated with right dACC connectivity and a cluster primarily located in the left medial temporal lobe (cluster *t*-score = -8.49; *p*-cluster FDR < .001; MNI peak coordinates (-34, 02, -26); cluster voxel size = 326; nearest (±5) GM peak voxel = BA 28). The significant cluster is displayed in blue.
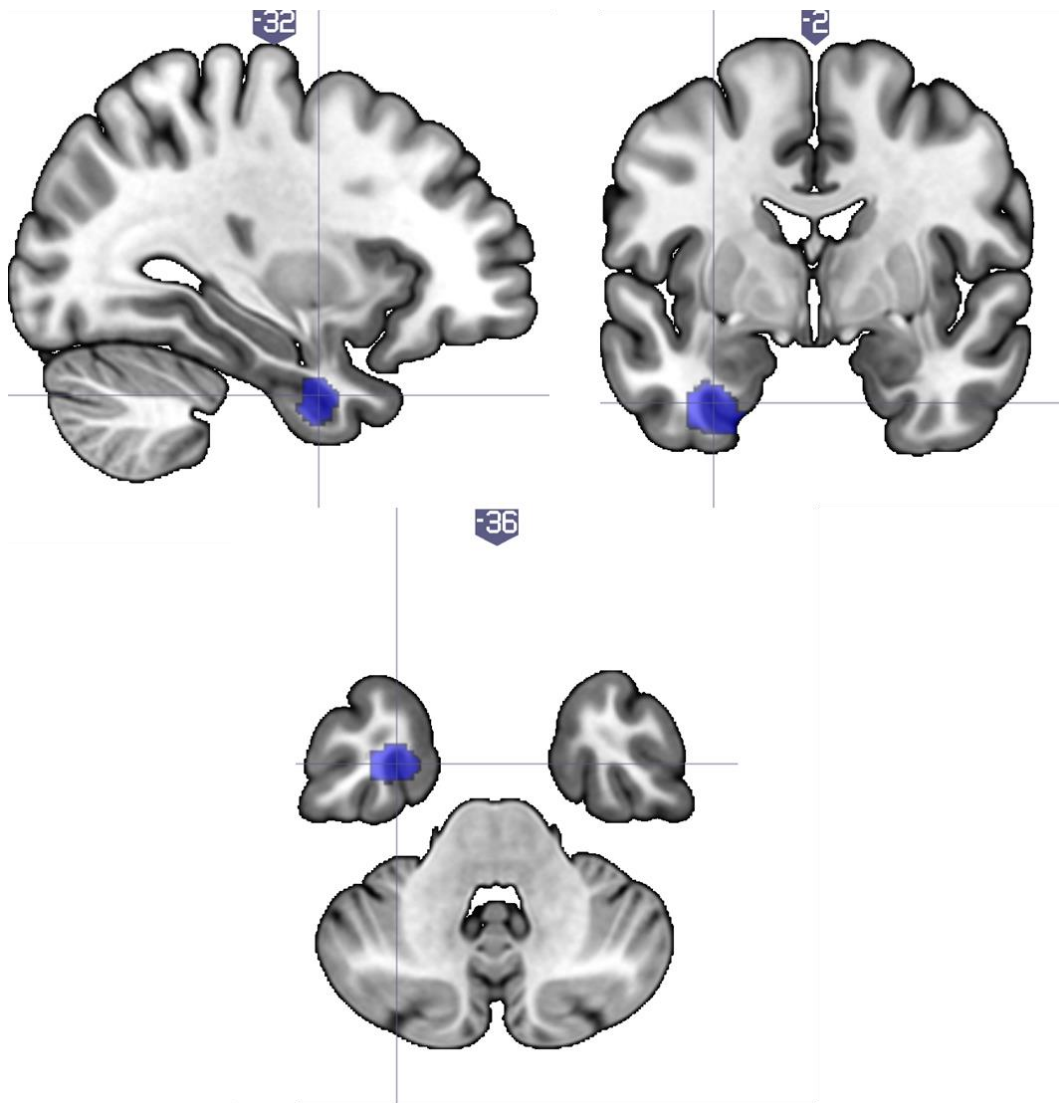
Figure 5.6 Glutamate Concentrations Associated with Left Cingulate to Left Medial Temporal Lobe Cluster Functionally Connectivity in Individuals with Autism Spectrum Disorder (*n* = 13)

Glutamate concentrations in individuals with ASD were positively associated with left dACC connectivity and a cluster in the left temporal lobe (cluster *t*-score = -7.19; *p*-cluster FDR = .015; MNI peak coordinates (-32, -02, -36); cluster voxel size = 158; nearest (±5) GM peak voxel = BA 28). The significant cluster is displayed in blue.

5.3.5.4 Glutamate and Glutamine Concentrations

For NCs, connectivity between the left dACC functional connectivity in a cluster overlapping with the right insular and central opercular cortex was

significantly and positively associated with dACC Glx concentrations and (cluster *t*-score = 7.21; *p*-cluster FDR < .001; MNI peak coordinates (36, -10, 20); cluster voxel size = 162; nearest (±5) GM peak voxel = BA 13). Additionally for NCs, the connectivity pattern between the left dACC in a cluster overlapping with the right supramarginal gyrus was significantly and negatively associated with dACC Glx concentrations (cluster *t*-score = -7.41, *p*-cluster FDR = .004; MNI peak coordinates (56, -36, 52); cluster voxel size = 197; nearest (±5) GM peak voxel = BA 40). There were no further relationships in NCs (figure 5.7).
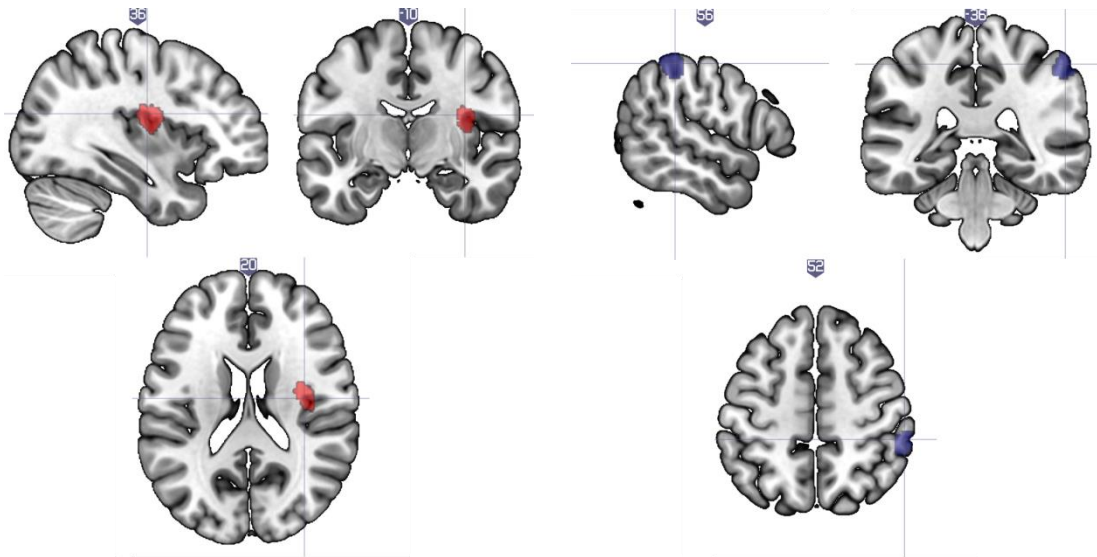
Figure 5.7 Left Dorsal Anterior Cingulate Cortex Functional Connectivity in Two Clusters Associated with Glutamate and Glutamine Concentrations in Neurotypical Controls (*n* = 15)

The associations between left dACC Glx concentrations and functional connectivity in NCs. (Left) Glx concentrations in NCs were positively associated with resting-state functional connectivity between the left dACC and a cluster including the insular cortex and central operculum cortex (cluster *t*-score = 7.21; *p*-cluster FDR < .001; MNI peak coordinates (36, -10, 20); cluster voxel size = 162; nearest (±5) GM peak voxel = BA 13). (Right) Glx concentrations were also negatively associated with functional connectivity between the left dACC and the right supramarginal gyrus (cluster *t*-score = -7.41; *p*-cluster FDR = .004; MNI peak coordinates (56, -36, 52); cluster voxel size = 197; nearest (±5) GM peak voxel = 40).

For individuals with ASD, Glx concentrations for the dACC were significantly and negatively associated with right dACC functional connectivity between five clusters. The first cluster overlapped with the left temporal pole, temporal fusiform cortex, amygdala, hippocampus, frontal orbital cortex and parahippocampal gyrus (cluster *t*-score =-11.43; *p*-cluster FDR < .001; MNI peak coordinates (-32, 02, -26); cluster voxel size = 429; nearest (±5) GM peak voxel = BA 28). The second cluster overlapped with the right superior temporal gyrus (including the planum polare, planum temporale and Heschl's gyrus), insular cortex, central and parietal operculum cortex (cluster *t*-score =

189

-9.40; *p*-cluster FDR < .001; MNI peak coordinates (42, -16, -06); cluster voxel size = 349; nearest (±5) GM peak voxel =BA 13). The third cluster overlapped with the right temporal pole, anterior parahippocampal gyrus, hippocampus, amygdala and temporal fusiform cortex (cluster *t*-score = -8.86; *p*-cluster FDR < .001; MNI peak coordinates (28, -06, -30); cluster voxel size = 319; nearest (±5) GM peak voxel =BA 28). The fourth cluster overlapped with the left superior temporal gyrus (including the planum polare, planum temporale and Heschl's gyrus) (cluster *t*-score = -10.24; *p*-cluster FDR = .027; MNI peak coordinates (-38, -28, 02); cluster voxel size = 105; nearest (±5) GM peak voxel = BA 13). The final cluster overlapped with the brain stem (cluster *t*-score = -8.39; *p*-cluster FDR = .046; MNI peak coordinates (-04, -20, -26); cluster voxel size = 86; nearest (±5) GM peak voxel = Pons) (table 5.3).

For individuals with ASD, increased Glx concentrations for the dACC were associated with decreased left dACC functional connectivity between two clusters. The first cluster overlapped with the right superior temporal gyrus (including the planum temporale and Heschl's gyrus) and central and parietal operculum (cluster *t*-score = -8.90; *p*-cluster FDR = .001; MNI peak coordinates (54 -24 10); cluster voxel size = 244; nearest (±5) GM peak voxel = BA 41). The second cluster overlapped with the left temporal fusiform cortex, anterior parahippocampal gyrus and inferior temporal (cluster *t*-score = -9.23; *p*-cluster FDR = .001; MNI peak coordinates (-36 -08 -32); cluster voxel size = 255; nearest (±5) GM peak voxel = BA 20) (table 5.3). For

individuals with ASD, there were no clusters with a positive association with

Glx and functional connectivity for the left or right dACC.

Table 5.3 Glutamate and Glutamine Concentrations Association with Seed-to-Voxel Resting-State Functional Connectivity in Individuals with Autism Spectrum Disorder (*n*=12)

Brain Region	Hemi	MNI coordinates			GM	k_E	*t*-score	*p*-value
		x	*y*	*z*				
RDACC Seed								
Superior Temporal Gyrus (Temporal Pole)	L	-32	02	-26	BA 28	429	-11.43	<.001
Superior Temporal Gyrus/ Insula	R	42	-16	-06	BA 13	349	-9.40	<.001
Temporal Pole	R	28	-06	-30	BA 28	319	-8.86	<.001
Superior Temporal Gyrus	L	-38	-28	02	BA 13	105	-10.24	= .027
Brain Stem	B	-04	-20	-26	Pons	140	-8.39	= .006
Left DACC Seed								
Superior Temporal Gyrus	R	54	-24	10	BA 41	244	-8.90	= .001
Temporal Fusiform Cortex	L	-36	-08	-32	BA 20	225	-9.23	= .001

Association between Glx concentrations and seed-to-voxel resting-state functional connectivity (right and left dACC) in individuals with ASD (voxel-wise uncorrected $p < 0.001$ and FDR cluster corrected $p < .05$). Increased Glx concentrations were associated with decreased functional connectivity in the above clusters. There were no significant positive associations between Glx and resting-state seed-to-voxel functional connectivity for individuals with ASD.
Brain region and Hemi represent brain region overlapping with the largest number of voxels in the cluster. MNI coordinates represent peak effect in a cluster. GM represent closest GM defined area (within 5 mm) to peak voxel coordinate according to the Talairach Daemon atlas in WFU-pickatlas software [603,604]. Cluster size, k_E, represents the spatial extent or the number of voxels in a cluster. p-value is reported at the cluster level.
Amg, amygdala; bilateral; dACC, dorsal anterior cingulate cortex, BA; Brodmann area; FDR, false discovery rate; Hemi, hemisphere; Hip, Hippocampus; L, left; MNI, Montreal Neurological Institute; NA, Not applicable; R, right;

For the right dACC, there was a significant interaction between group and

Glx concentration in two clusters. The first cluster overlapped with the right

insular cortex, superior temporal cortex (Heschl's gyrus) and central and

parietal operculum (cluster *t*-score = 5.49; *p*-cluster FDR = .003; MNI peak

coordinates (38, -14, 18); cluster voxel size = 271; nearest (±5) GM peak

voxel = BA 13). The second cluster overlapped with the left thalamus, hippocampus, parahippocampal gyus, precuneous, posterior cingulate cortex and lingual gyrus (cluster *t*-score = 6.78; *p*-cluster FDR = .003; MNI peak coordinates (-14, -36, 04); cluster voxel size = 251; nearest (±5) GM peak voxel = thalamus) (figure 5.8 and 5.9).
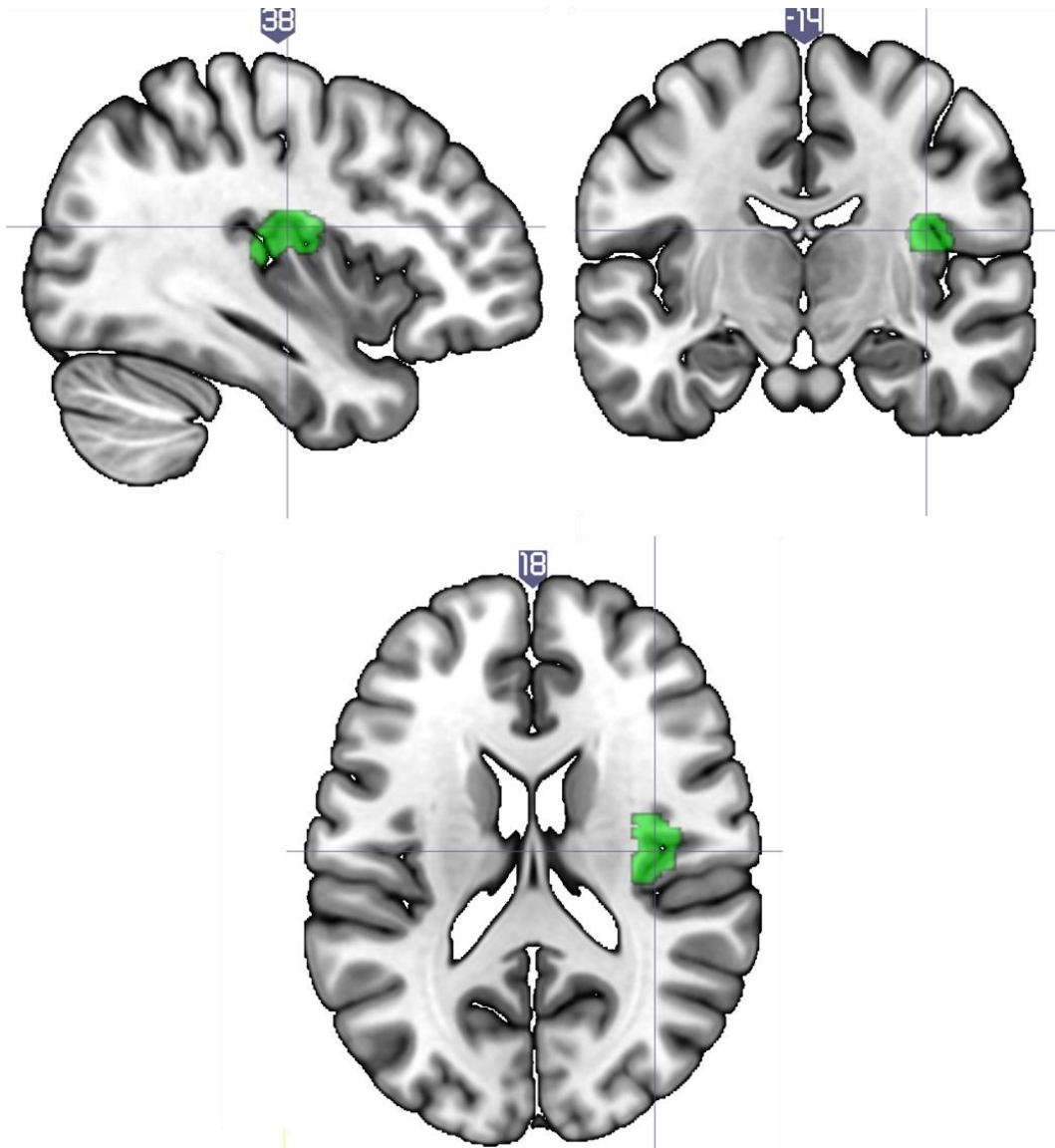
Figure 5.8 Cluster 1: Brain Region with Group Interaction in Association Between Right Dorsal Anterior Cingulate Seed Functional Connectivity and Glutamate and Glutamine Concentrations

There was a significant interaction between groups in the relationship between Glx concentrations and functional connectivity between the right dACC and cluster overlapping with the right insular cortex, operculum and superior temporal cortex (cluster t-score = 5.49; p-cluster FDR = .003; MNI peak coordinates (38 -14 18); cluster voxel size = 271; nearest (±5) GM peak voxel = BA 13). The cluster is displayed in green.
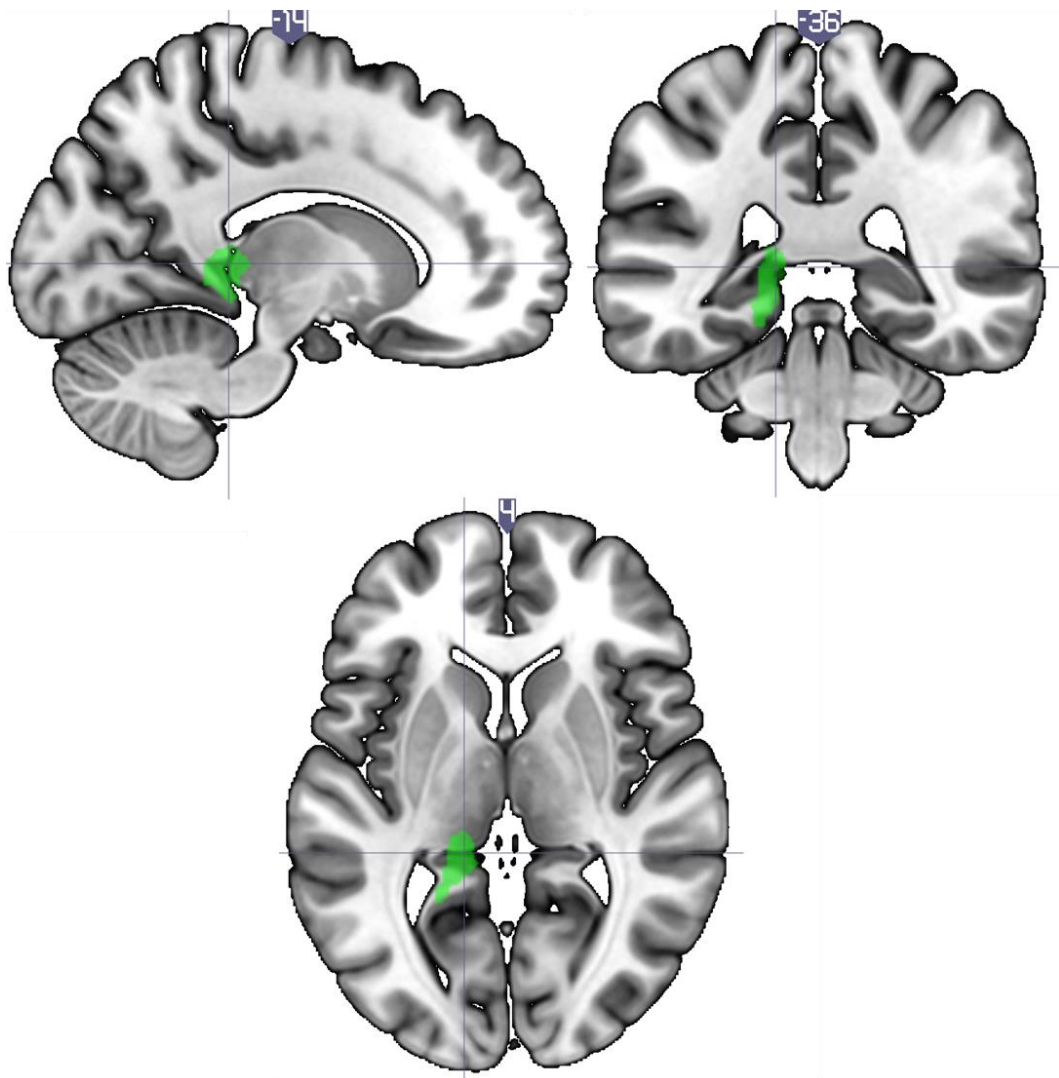
Figure 5.9 Cluster 2: Brain Region with Group Interaction in Association Between Right Dorsal Anterior Cingulate Seed Functional Connectivity and Glutamate and Glutamine Concentrations

There was a significant interaction between groups in the relationship between Glx concentrations and functional connectivity between the right dACC and cluster overlapping with the subcortical structures such as the left thalamus, hippocampus and parahippocampal gyrus (cluster t-score = 6.78; p-cluster FDR = .003; MNI peak coordinates (-14, -36, 04); cluster voxel size = 251; nearest (±5) GM peak voxel = thalamus). The cluster is highlighted in green above.
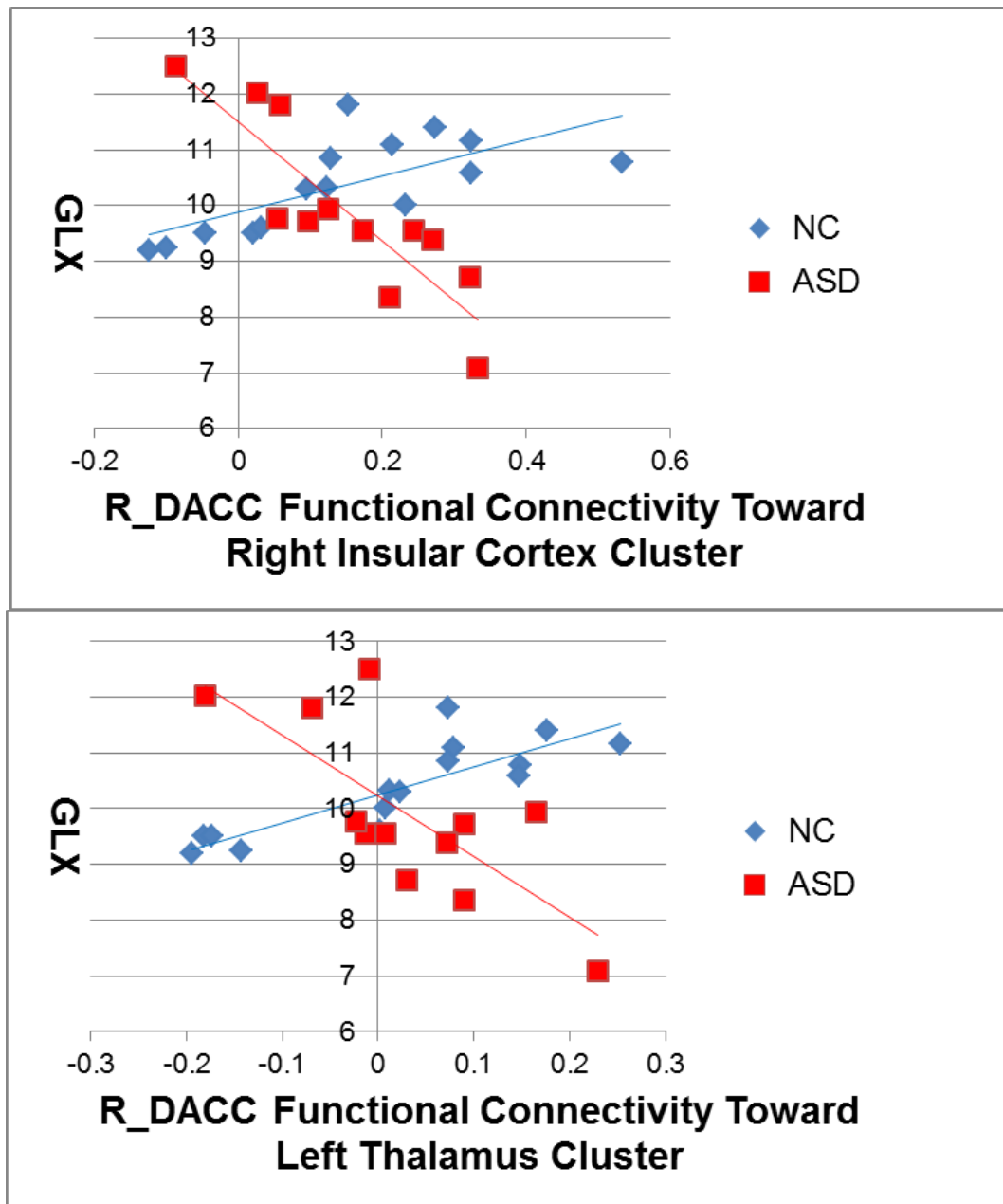
Figure 5.10 Contrasting Group Relationships between Glutamate and Glutamine Concentrations and Right Dorsal Anterior Cingulate Functional Connectivity

(Top) The relationship between Glx concentrations and right dACC functional connectivity with a cluster overlapping with the right insular cortex, superior temporal cortex and opercular cortex by group. (Bottom) The relationship between Glx concentrations and right dACC functional connectivity with a cluster overlapping with the left thalamus, hippocampus, parahippocampal gyrus, precuneus, posterior cingulate cortex and lingual gyrus by group. In NCs, as Glx concentrations increased there was a definite increase in FC. In contrast, for individuals with ASD, the relationship between Glx and functional connectivity had a negative association.

For the left dACC, there was a significant interaction between group and Glx concentrations in a cluster overlapping with the right insular cortex, superior temporal cortex (Heschl's gyrus) and central and parietal operculum (cluster t-score = 6.33; p-cluster FDR < .001; MNI peak coordinates (32, -04, 18); cluster voxel size = 420; nearest (±5) GM peak voxel = BA 13) (figures 5.8, 5.11 and 5.12).
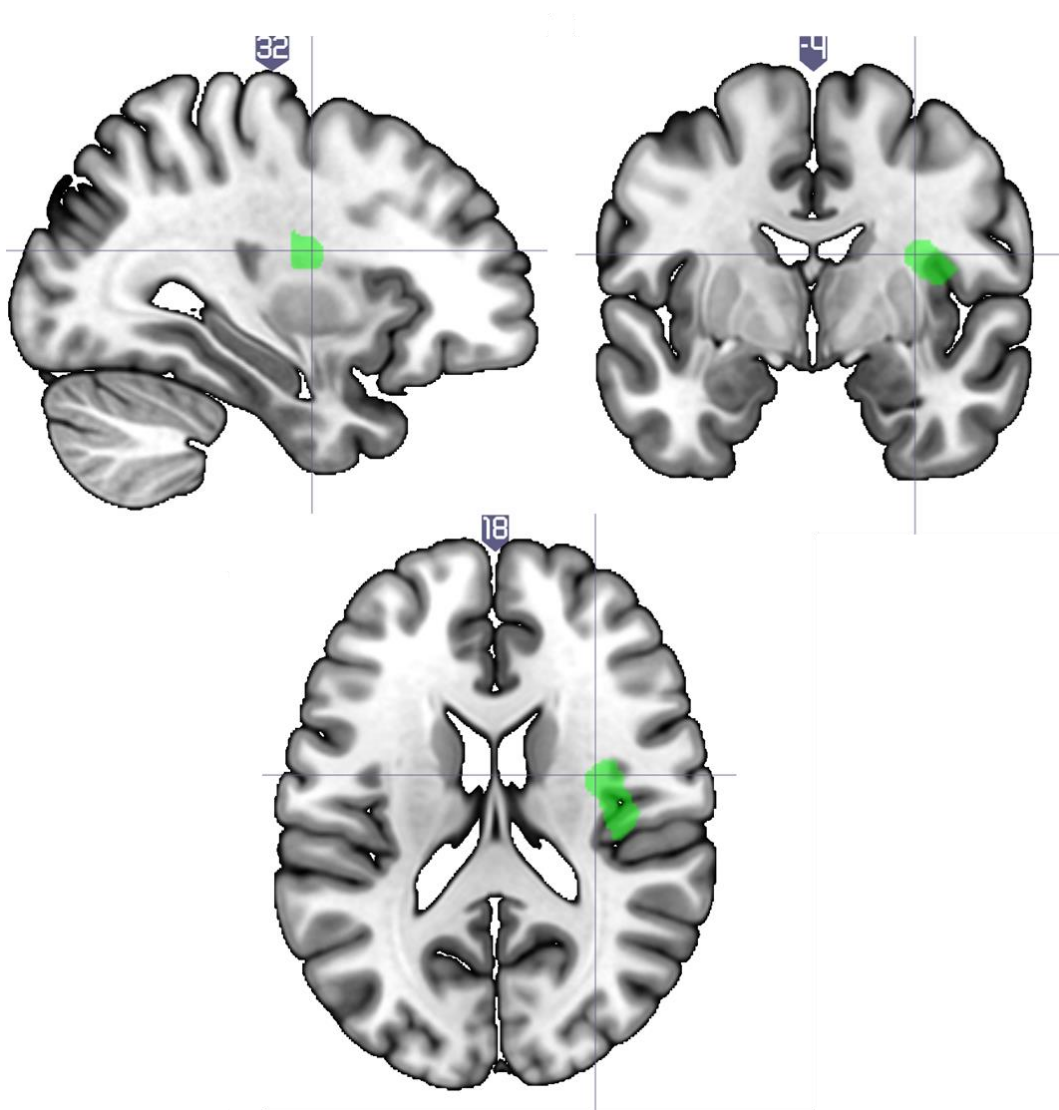
Figure 5.11 Brain Regions with Group Interaction in Association between Left Dorsal Anterior Cingulate Seed Functional Connectivity and Glutamate and Glutamine Concentrations

There was a significant interaction between groups in the relationship between Glx concentrations and functional connectivity between the right dACC and cluster overlapping with the right insular cortex, operculum and superior temporal cortex (cluster t-score = 6.33; p-cluster FDR < .001; MNI peak coordinates (; 32, -04, 18); cluster voxel size = 420; nearest (±5) GM peak voxel = BA 13). Significant clusters are displayed in green.
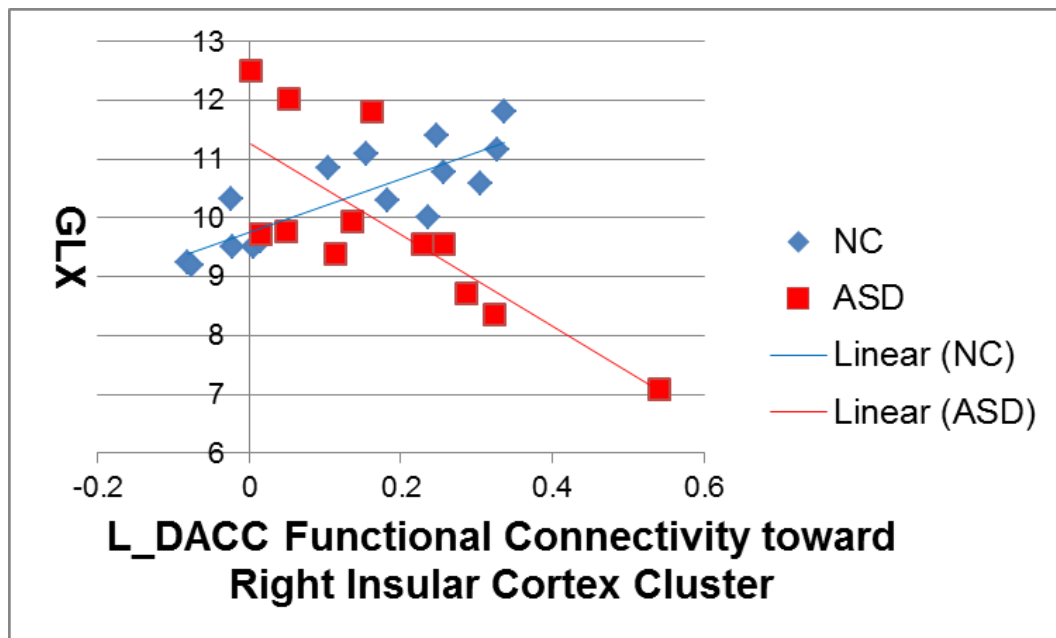
Figure 5.12 Contrasting Group Relationships between Glutamate and Glutamine Concentrations and Left Dorsal Anterior Cingulate Functional Connectivity

The relationship between Glx concentrations and right dACC functional connectivity with a cluster overlapping with the insular cortex, superior temporal cortex (Heschl's gyrus) and opercular cortex. In NCs, as Glx concentrations increased there was a definite increase in functional connectivity. In contrast, for individuals with ASD, the relationship between Glx and functional connectivity is less defined but appears to show a negative relationship.

5.4 DISCUSSION

We investigated the relationship between Glu and Glx concentrations and functional connectivity to add further context into how altered metabolite concentrations might contribute to ASD pathology. Our analysis suggests that Glx concentrations have an altered relationship to dACC seed-to-voxel resting-state functional connectivity within salience network brain regions in individuals with ASD compared to NCs (chapter 5.3.5.3). To our knowledge, we are the first group to report this relationship, and therefore, more research is required. Nevertheless, our analysis suggests an incongruence between local metabolites and long-distance function in individuals with ASD.

Although not our primary focus, we also reported that increased dACC resting-state functional connectivity to the occipital lobe correlated with improved conflict effect RT only in participants with ASD (chapter 5.3.5.2). We did not report any group difference in functional connectivity (chapter 5.3.4) nor did we report any association between dACC functional connectivity and core ASD symptoms (as measured by the ADOS) in individuals with ASD (chapter 5.3.5.1). We discuss these results in more detail below.

5.4.1 Functional Connectivity Within and Between Groups

Overall, the data further support evidence that the dACC is functionally connected to neocortical, motor, paralimbic and subcortical brain regions in both NCs and individuals with ASD. Resting-state functional connectivity analyses have linked the dACC with frontal cognitive brains regions such as the DLPFC and VLPFC [380,381]. In agreement with these studies, our dACC seed regions were positively correlated with seed regions in the superior, middle and inferior frontal gyrus in NCs. In agreement with Cao and colleagues [381], we also reported that the dACC was positively correlated with other parietal regions such as the precuneus and the supramarginal gyrus [302]. Again, like previous analyses [302,380,381], we also reported that the dACC was positively correlated with the motor areas including the pre, post-central gyrus and supplementary motor cortex. Our results also replicate previous functional connectivity studies reporting an association between the dACC and paralimbic, limbic and subcortical regions [302,380,381]. The dACC was

functionally connected with the insular cortex, operculum, frontal orbital cortex and temporal pole. We also reported that the dACC was correlated with the thalamus, striatum, pallidum and nucleus accumbens.

In agreement with Zhou et al. (2016), we did not report group differences in dACC seed-to-voxel functional connectivity in individuals with ASD compared to NCs. Furthermore, there were no significant associations between dACC functional connectivity and ADOS scores in participants with ASD, suggesting that the functional connectivity between the dACC and the brain had little relationship to a diagnosis of ASD or the core symptoms of the disorder. This may also reflect heterogeneity in our sample of individuals with ASD. Furthermore, we were limited by small sample sizes, and it is unclear if our lack of group differences in functional connectivity might be related to false negative results or type II error.

Unfortunately, we were unable to investigate the relationship between ADOS scores for both imagination and stereotyped behaviours and dACC functional connectivity because most participants in our study had a score of zero on this section of the ADOS. Previous studies have reported an association between resting-state functional connectivity between the caudal ACC and insular cortex and repetitive and stereotypical movement scores in individuals with ASD [605]. In the future, a more sensitive measure for various ASD behaviours and symptoms might provide more meaningful associations with dACC functional connectivity.

As an aside, functional connectivity clusters in participants with ASD were smaller and more numerous suggesting greater fracture in brain networks associated with the dACC. In individuals with ASD, we reported two or three large brain clusters overlapping with salience network and neocortical regions, which were similar to those which we reported in NCs. On the other hand, we also reported small clusters of brain regions in individuals with ASD. For example, for the right dACC region, we reported several clusters separately in left and right precuneus, frontal pole/middle frontal gyrus, and lateral occipital cortex/middle temporal gyrus.

There has been evidence of network fracture during executive control tasks in individuals with ASD compared to NCs. Just and colleagues (2007) investigated the functional connectivity of individuals with ASD compared to NCs during the Tower of London task. As a first step in the analysis, investigators reported little difference in the BOLD response between low executive control compared to high executive control conditions between groups. Nevertheless, investigators reported evidence of less synchronization between frontal and parietal brain regions in individuals with ASD compared to NCs. Firstly, participants with ASD had reduced mean functional connectivity between regions in the frontal cortex (DLPFC and inferior frontal gyrus) and parietal cortex (precuneus and intraparietal sulcus). Secondly, researchers also applied an exploratory factor analysis to thirteen predefined ROIs including the frontal and parietal brain regions. Individuals with ASD had two independent factors separating parietal and frontal brain

regions while these brain regions were incorporated into one factor for NCs [606].

Nevertheless, our result of greater network fracture was only speculation. We discuss this point to suggest useful future analysis. For example, an independent components analysis might better define separate networks of brain regions and offer a clearer picture of network fracture in individuals with ASD compared to NCs.

5.4.2 Functional Connectivity Association with Metabolite Concentrations

In NCs, it is unclear why we did not find a relationship between Glu concentrations and functional connectiity. We cannot entirely exclude the possibility that our methodology imprecisely quantified Glu concentrations. Nevertheless, we argue this was unlikely because our methodology was taken from and supported by evidence that Glu concentrations can be reliably obtained at 3 T [484]. Furthermore, all CRLB scores included in this analysis for Glu and Glx concentrations had good validity being below 18%.

Alternatively, Glu has many other functions besides neurotransmission and is stored in large pools in neurons. One of the limitations of ^{1}H-MRS is that it cannot differentiate the location of a metabolite in the voxel and the many functions of Glu. Following neurotransmission, Glu is rapidly converted to Gln. Therefore, Glx concentrations, which includes the Gln signal, might be more closely associated with the GGC between neurones and astrocytes and, therefore, more closely index excitatory signalling [490,607–609]. In NCs, the

lack of relationship between Glu and functional connectivity weakly support this conclusion.

In individuals with ASD, increased Glu and Glx concentrations were correlated with decreased dACC functional connectivity to temporal, paralimbic and subcortical regions (table 5.4; figure 5.5 and 5.6). In contrast, for NCs, increased Glx concentrations correlated with increased functional connectivity with the insular and opercular cortex (figure 5.7).

We also reported an interaction between groups in the association between Glx and functional connectivity in the salience network. In participants with ASD, increased Glx concentrations were associated with reduced functional connectivity between the right dACC and a cluster overlapping with the right insular cortex, superior temporal lobe and opercular cortex while NCs exhibited the opposite relationship. Similarly, increased Glx concentrations in individuals with ASD were associated with reduced functional connectivity between the left dACC and a cluster overlapping the right insular cortex, operculum and superior temporal lobe (figure 5.9 and 5.10), while NCs again had the opposite relationship. Finally, increased Glx concentrations were associated with reduced functional connectivity between the right dACC and a cluster primarily overlapping with the thalamus in individuals with ASD, while again NCs have the opposite relationship (figure 5.9).

The thalamus is a relay station between bottom-up sensory information and both the neocortex and the paralimbic cortex [610]. Researchers have reported

altered volume [611,612], neural integrity [242], glucose metabolism [613], and WM integrity near the thalamus of individuals with ASD compared to NCs [614].

The superior temporal lobe has been associated with social-emotional neurocognitive function and multisensory integration [615–617] and also auditory processing and language development [618]. Several studies have suggested an altered functional response in individuals with ASD in this region [619–622].

Finally, the insular cortex is structural and functionally interconnected with the frontal cortex and limbic/subcortical brain regions [302,379,623]. The insular cortex and dACC are central regions in the salience network [302,306] and closely functionally connected in NCs [310]. Functional connectivity between the dACC and insular cortex have been associated with the integration of emotional and body perceptions to guide behaviour [302,383,384,386]. Studies have reported an altered functional response in the insular cortex [120,620,622,624–627] and altered functional connectivity to salience network brain regions in individuals with ASD [404,408,628–631]. Altered functional connectivity and function in the salience network, particularly in association with the insular cortex, could be associated with altered sensory and social symptoms associated with ASD [632,633].

Nevertheless, or analysis did not provide any clues to indicate if increased functional connectivity in the salience network was a benefit or deficit to behaviour in individuals with ASD. Based on previous evidence, increased functional connectivity in the salience network regions was associated with reduced symptom severity in individuals with ASD. Greater resting-state

functional connectivity between the salience network, centred on the dACC and insular cortex, has been associated with greater long-term improvement in adaptive behaviours in children with a diagnosis of ASD [634] and reduced stereotyped behaviours and restricted interests in adults with ASD compared to NCs [605]. Evidence also suggests that increased functional connectivity in the salience network was associated with increased attention to emotion and internal experience in NCs [302].

Several investigators have proposed the theory of local overconnectivity in association with reduced long-range functional connectivity in participants with ASD [635–637]. The reason for this disconnect is unclear. Some hypotheses include increased excitatory to inhibitory signalling which favour local function over long-distance function [637]. Alternatively, alterations in cortical development such as altered apoptosis, neuronal migration or neurogenesis might also lead to incongruency between local and distant brain function [97,638]. Although much more research is required to fully confirm evidence of local over-connectivity [639], our data appear to support a general disconnect between local Glx and long-distance functional connectivity in individuals with ASD compared to NCs.

In the ACC, there has been evidence of reduced inhibitory influence and future studies might wish to further investigate GABA in more detail. A post-mortem autoradiography study reported a reduction in $GABA_B$ receptors in both the ACC/MPFC and fusiform gyrus of individuals with ASD compared to NCs [640]. Although one group did not report a baseline difference in Glu to

GABA, they did report that pharmacologically manipulating the proportion of GABA concentrations relative to both Glu and GABA concentrations in individuals with ASD lead to a more neurotypical functional connectivity in association with the dACC [641]. If Glx concentrations are not properly balanced by inhibition in ASD, extreme Glx might be associated with local hyper or hypo excitation in resting-state functional networks leading to extreme (increased or decreased) local function and altered long-distance functional connectivity [637].

Interestingly, in NCs, greater Glx concentrations in the dACC were also associated with reduced functional connectivity between the left dACC and the right supramarginal gyrus located in inferior parietal cortex. This evidence likely reflects anticorrelations between the salience network and the default mode network [597,642], a network of brain regions having an increased BOLD response in association with spontaneous internal thought [643,644]. The right supramarginal gyrus has been associated with tasks involving proprioception [645] and empathy in NCs [646]. Researchers have demonstrated that the default mode network includes the inferior parietal cortex along with the posterior cingulate cortex and retrosplenial cortex [268,647,648].

Kapogiannis and colleagues (2013) reported that in NCs Glu/Cre concentrations in the posterior medial cortex, a region associated with the default mode network, were positively associated with functional connectivity, as measured by independent component analysis, with only other default mode network regions. Researchers concluded that Glu/Cre predicted within

network functional connectivity but was not associated with functional connectivity within other brain networks [291]. Our analysis suggests a slightly different interpretation in the case of the dACC. In NCs, our data also suggest that dACC Glx concentrations were negatively associated with brain regions in the default mode network [597,642]. Nevertheless, this result requires further investigation as other studies have reported that the BOLD activity in the dACC was positively correlated with the supramarginal gyrus [381].

5.4.3 Functional Connectivity Association with Conflict Effect Performance

Contrary to previous evidence [387], we did not report any association between dACC functional connectivity and conflict effect RT in NCs. We assessed resting-state functional connectivity in relation to performance of the ANT when completed in a laboratory environment at a different time. Therefore, functional connectivity between these regions may impact performance while an individual completes the ANT, but it does not appear to predict future performance in NCs.

In individuals with ASD, shorter conflict effect RTs were associated with increased functional connectivity between the left dACC and the right superior LOC. A metanalysis of brain research suggests that LOC is functionally associated with sensory visual object recognition tasks in NCs [649]. Much more research is required to investigate this relationship, but this result may reflect altered brain function in individual with ASD as the LOC was not associated with the conflict effect task in NCs [24,26]

In further support of altered function in the LOC in individuals with this disorder, one fMRI investigation assessed the BOLD response to an oddball task in individuals with ASD and NCs. During the task, circles changed to novel shapes, ovals pointed in a deviant direction or ovals pointe in a standard direction. Researchers reported an increased BOLD response in both the bilateral LOC and dACC in individuals with ASD to both novel and deviant shapes compared to NCs. Investigators also applied a psychophysiological interaction analysis, which models how a seed region (in this study the dACC) influences other regions of the brain in association with various experimental conditions [650]. Investigators reported that during the introduction of deviant shapes the dACC time series correlated with cognitive brain regions such as the superior parietal lobule, frontal-pole and middle frontal gyrus in NCs while individuals with ASD had increased connectivity to sensory regions such as the LOC.

There were some limitations to our analysis. In addition to a small sample size which we previously discussed, we were unable to independently quantify extracellular and intracellular Glu concentrations or establish the specific function of Glu in a voxel with ^{1}H-MRS [651]. Given that Glu has various functions in the brain, it is impossible to determine the exact role of Glu or Glx concentrations [652]. Therefore, it was unclear if metabolite concentrations had the same role in each group.

Furthermore, although we attempted to correct for non-neural artefacts, the issue of head motion has been shown to exacerbate group differences in

functional connectivity analyses [273]. Therefore, as with ^{1}H-MRS, the results of our resting-state functional connectivity analysis require follow up and confirmation with more direct investigation [264].

Even with these disadvantages, 1H-MRS is an imaging method which allows an investigator to measure metabolite concentrations in human participants within the brain both non-invasively and *in-vivo*. In comparison, other methods of measuring Glu concentrations typically rely on post-mortem dissection or require invasive contrast agents, as applied in PET imaging. Furthermore, a ^{1}H-MRS dataset can be easily acquired during the same scanning session because it utilises conventional MRI technology. Therefore, it is a good starting point to investigate the relationship between altered Glu or Glx concentrations and functional connectivity.

5.5 CONCLUSION

Our analysis suggested that Glx concentrations in the dACC, rather than Glu, predicted resting-state functional connectivity to other functionally associated brain regions in NCs. Most strikingly, Glx concentrations in the dACC were incongruent with functional connectivity in individuals with ASD but congruent in NCs. Researchers have suggested that variations in local excitatory or inhibitory signalling mechanisms might be implicated in cortical alterations that cause altered long-distance functional connectivity typical of participants with ASD [637,653]. We support this hypothesis with our data, although we can

only speculate about the cause of group interactions. More research is required to both replicate and understand the mechanism behind our results.

Additionally, we were unable to provide further behavioural context to this group interaction. We did not report any relationship between salience network functional connectivity and symptoms of the disorder in individuals with ASD. Previous evidence has suggested that increased salience network functional connectivity is beneficial for individuals with ASD [605,634]. Therefore we speculate that increased Glx concentrations might be maladaptive in individuals with ASD. In the future, a more thorough analysis must clarify how and if altered Glx mediates behaviour by impacting functional connectivity in individuals with ASD.

6 GENERAL DISCUSSION

6.1 INTRODUCTION

Glutamate is the primary excitatory neurotransmitter in the brain and essential for cortical development, neural communication and plasticity. Altered Glu concentrations in the brain will likely have far-reaching consequences regarding cerebral health, development and function [132]. Previous ^{1}H-MRS studies have reported altered Glu and Glx concentrations in the brains of individuals with ASD compared to NCs [217,225–234,236–238] while other studies reported no differences [240–246].

This investigation applied a multimodal imaging sequence to investigate dACC Glu and Glx concentrations, brain anatomy and resting-state functional connectivity in NCs and individuals with ASD. We also investigated the relationships between metabolite concentrations and core autistic symptoms, demographic characteristics and conflict effect performance. The conflict effect task was an inhibition to distraction task which was selected because of its functional association with the dACC in NCs. There has also been evidence of hypoactivation of the dACC during the conflict effect task in individuals with ASD compared to NCs [26]. Finally, given evidence that Glu and Glx concentrations were associated with functional connectivity to other brain regions in NCs [258,290], we also investigated the relationship between Glu and Glx concentrations in the dACC and resting-state seed-to-voxel functional connectivity.

The purpose of investigating these relationship was to provide further context of Glu and Glx alteration in the brains of individuals with ASD. To our

212

knowledge, we are the first group to investigate Glu concentrations in the dACC of adult participants with ASD, although other groups have investigated Glx concentrations in the same brain region [245]. We are also the first group to explore the relationship between Glu or Glx concentrations and functional connectivity in participants with ASD.

The first objective of this chapter is to summarise the primary results (chapter 6.2). Next, we explain the implications (chapter 6.3), strengths (chapter 6.4) and limitations (chapter 6.5) of this research. In conclusion, a discussion of worthwhile avenues for future research following on from our analysis is presented (chapter 6.6).

6.2 SUMMARY OF MAIN FINDINGS

We reported no significant difference in Glu concentrations in individuals with ASD compared to NCs both in the full group and when excluding participants taking anticonvulsant and antidepressant medications. Age was a significant predictor of Glu concentrations for both study groups. We also reported no significant differences in both Glx and NAA + NAAG concentrations for individuals with ASD compared to NCs.

Nevertheless, when excluding individuals not taking psychotropic medications, there was an interaction between age and group for Glx concentrations for individuals. This evidence weakly suggests that individuals with ASD had a greater decrease in Glx concentrations with age than NCs. Also, Glx concentrations were significantly correlated with NAA + NAAG concentrations in individuals with ASD but not NCs. Nevertheless, none of

these results survived correction for multiple comparisons. Given our small sample size, replication of these uncorrected results is warranted to rule out type I error.

During our second experiment, we reported that the conflict effect inhibition task had no relationship to metabolite concentrations in the dACC. Furthermore, in contrast to Fan and colleagues 2012 [26], our analysis was unable to replicate performance deficits on the ANT in individuals with ASD compared to NCs. We did report that when participants with ASD had decreased conflict effect RT, they also had increased communication deficit as measured by the ADOS. Again, this later correlation did not survive correction for multiple comparisons and requires replication.

In NCs, Glx and not Glu concentrations predicted functional connectivity to salience network brain regions. We reported that increased Glx concentrations in the dACC in individuals with ASD were associated with reduced functional connectivity to salience network brain regions, such as the insular cortex, while NCs had the opposite relationship. This later result suggests incongruency between local compared to long-distance function in individuals with ASD. Nevertheless, we did not report group differences in functional connectivity or any relationship to functional connectivity and core symptoms of the disorder.

6.3 IMPLICATIONS OF PRESENT RESEARCH

One of the main findings of this study was a lack of support for altered Glu concentrations in individuals with ASD compared to NCs. At least for adult

male participants with normal IQ, our data suggest no consistent increase or decrease in Glu concentrations in the dACC of individuals with ASD compared to NCs. Therefore, evidence of increased Glu concentrations in children and adolescents with ASD compared to NCs [217,225,230,231] might only occur during development.

We measured Glx concentrations primarily for comparison to Glu measurements in this thesis and other research studies. Our ^{1}H-MRS protocol was not optimised for the collection Glx concentrations, but we obtained robust Glx measurements with CRLB scores below 17%. For the full cohort, we did not report significant differences in Glx concentrations between groups.

We did report greater age-related changes in Glx concentrations in individuals with ASD compared to NCs, which may partially explain contradictory results in previous studies in adult participants with ASD. Single voxel spectroscopy studies of the ACC in younger adults reported no difference in Glx concentrations [239,556] while one study in older adults reported reductions in both Glu and Glx concentrations [556]. Our investigation highlights the importance of considering age when interpreting group differences in relation to metabolite concentrations in individuals with ASD. The neurobiology of the disorder might change with increased age in individuals with ASD.

In addition, our research was not designed to investigate the causal relationship between Glx and NAA + NAAG concentrations, but the

correlation between these variables suggest that reduced neural integrity as indexed by NAA + NAAG concentrations may lead to reductions in Glx in individuals with ASD with increased age.

Local dACC Glx concentrations but not Glu concentrations predicted resting-state functional connectivity to other brain regions in NCs. This result suggests that Glx concentrations might be more closely associated with local excitation or the GGC. With greater investigation, the relationship between Glx and functional connectivity might be a useful marker of altered brain function in individuals with ASD compared to NCs.

Also, increased Glx concentrations in individuals with ASD were associated with reduced long-distance functional connectivity in salience network brain regions such as the insular cortex while NCs had the opposite relationship. We suggest that this result might be associated with atypical cortical development [97,638] or a local imbalance between excitation and inhibition [637]. Much more research is required to understand and confirm this result, but this evidence suggests incongruency between local metabolites and long-distance function in individuals with ASD. Increased Glx concentrations may have a different relationship with long-distance brain function in individuals with ASD.

Unfortunately, we were unable to determine if increased Glx concentrations had some benefit to ASD symptoms or behaviours. Based on previous evidence that increased salience network functional connectivity was associated with reduced symptom severity in individuals with ASD [605,634], we

interpreted this relationship to suggest that, unlike NCs, increased Glx concentrations were disadvantageous in individuals with ASD. Nevertheless, we did not report any association between clinical symptoms and dACC functional connectivity. Therefore, these results require further investigation in relation to behaviour and disease severity.

In contrast to Fan et al. (2012) [26], we did not report reduced performance on the conflict effect task in individuals with ASD compared to NCs. In fact, individuals with increased ASD communication deficits had improved conflict effect RTs. We suggest that differences in environment, participant motivations or ASD severity between Fan et al. (2012) [26] and the current study may have contributed to conflicting performance outcomes.

6.4 STRENGTHS

There were several strengths within these experiments. Firstly, the ^{1}H-MRS sequence applied in this study was designed and optimised to measure Glu concentrations, allowing investigators to make conclusions about Glu concentrations rather than having to infer about Glu based on Glx. Furthermore, the application of a multimodal imaging sequence was a major strength of this study permitting greater exploration of how Glu and Glx might be associated with the ASD. Finally, we were able to investigate these relationships both non-invasively and *in vivo* rather than having to rely only on post-mortem or animal models of the disorder.

6.5 LIMITATIONS

The primary limitation of this study was a small sample size which limited the power of the statistical analysis. For example, we reported trend reductions at uncorrected alpha levels in Glx and NAA + NAAG concentrations for individuals with ASD compared to NCs. A larger cohort would have likely resulted in a more conclusive finding. Our sample size also limited a more detailed exploration of the data. For example, our small cohort did not score highly on stereotypical and repetitive movements and we could not investigate this symptom in relationship to dACC functional connectivity. Nevertheless, the purpose of this study was to explore how Glu or Glx concentrations might be associated with behaviour and brain function in ASD. Future studies with larger and more diverse cohorts will hopefully build on our preliminary findings.

Additionally, although we could measure metabolite concentrations, we were unable to make any conclusions regarding the function of a particular metabolite. Glutamate has many functions in the brain, and the grouping of intercellular and extracellular Glu concentrations by MRS might not be a sensitive enough measure to detect abnormalities in Glu function in individuals with ASD compared to NCs (chapter 1.3) [651]. Given our current technological constraints, more direct investigation of Glu function would be beneficial but would require more invasive methods.

Finally, the decision to investigate the conflict effect task outside of an fMRI scanner limited the conclusions that we could make regarding dACC

function. We were only able to infer about dACC function based on previous BOLD fMRI investigations. Compared to a behavioural performance task, neuroimaging is typically a more fine-tuned measure of brain function to an external task. In fact, other groups have reported hypofunction of the dACC in the absence of behavioural performance differences [407,408]. Future multimodal studies may wish to incorporate task-based fMRI and ^{1}H-MRS in addition to behavioural analysis [407,408].

6.6 SUGGESTIONS FOR FUTURE STUDIES

The most exciting outcome of this thesis has been the many additional research questions it has raised. Fundamentally, our results require replication in other brain regions and in larger, more diverse samples of individuals with ASD. It would also be interesting to investigate and compare metabolite concentrations and functional connectivity in brain regions associated with emotion and social behaviour, such as the pACC [404]. Given the region-specific nature of the disorder, we anticipate that the results might vary between brain regions.

Furthermore, a longitudinal investigation of metabolites concentrations would also be useful in understanding the trajectory of these metabolites across the lifespan of individuals with ASD. Our cross-sectional study suggested that individuals with ASD have sharper reductions in Glx concentrations with age than NCs. As we mentioned previously, this result might also be associated with improved interventions for younger generations of individuals with the disorder. A longitudinal investigation of these relationships will permit a

clearer understanding of the cause of altered metabolites concentrations over time. Nevertheless, it is unclear how long participants would need to be followed to identify significant reductions with age. A cross-sectional study suggested only a 12% reduction in NAA concentrations between the ages of 20 and 70 years of age in NCs [558].

Future research might also clarify if altered Glx concentrations are associated with behaviour and symptoms of the disorder in individuals with ASD compared to NCs. It was unclear if decreased Glx concentrations with age in individuals with ASD were adaptive or related to some degenerative progression of the disorder.

Additionally, both NCs and individuals with ASD had excellent performance rates on the inhibition to distraction task employed in this study and a more difficult task might better index variation in dACC function. Previous evidence suggests reduced dACC function and increased ER during this task in individuals with ASD compared to NCs [26]. Nevertheless, researchers have also reported that many other brain regions are also associated with this task, such as the DLPFC [26,304]. Therefore, future behavioural measures or task-based fMRI studies more clearly and singularly associated with dACC function might more closely correlate with metabolite concentrations.

Furthermore, it would be interesting to further investigate Glu, Glx and Gln separately in individuals with ASD. One method for doing this might be the use of carbon-13 magnetic resonance spectroscopy (^{13}C-MRS) which allows for clear differentiation between these metabolites without the requirement for

higher magnetic field strengths [132]. Nevertheless, this method is not without other complications. Carbon-13 exists in low concentrations in the brain and requires editing techniques to increase sensitivity during data collection [654].

Also, it would be useful to further investigate the relationship between local excitatory to inhibitory concentrations in association with functional connectivity in participants with ASD. Investigators have hypothesised that an altered proportion of inhibition to excitation at the local level in individuals with ASD compared to NCs might be associated with altered long-distance functional connectivity [637,653]. These relationships might be more evident when also investigating GABA, the primary inhibitory neurotransmitter in the brain [655] in relation to Glx, Glu and Gln.

Finally, our study reliably measured Glu and Glx concentrations in individuals with ASD. As improved technology and methodological research for measuring metabolite concentrations become more readily available, subsequent ^{1}H-MRS studies might benefit from techniques which further increase the precision of Glu and Glx measurement. For example, future studies may wish to apply increased magnetic field strengths [459,460].

6.7 CONCLUSION

In conclusion, this research has prompted many more questions and provided opportunities for future studies to better understand the role of Glu and Glx in the brain of individuals with ASD. We did not report evidence of altered Glu concentrations in adults with ASD compared to NCs. Although we did report weak evidence that Glx had greater reductions with age in adults

with ASD compared to NCs, this result requires further replication as it did not survive correction for multiple comparisons. We reported an altered relationship between Glx and long-distance functional connectivity in association with salience network regions in individuals with ASD compared to NCs. Further replication of these relationships might provide a useful marker of altered brain function in individuals with ASD. Our research suggests that a more detailed multimodal investigation of Glu and Glx concentrations in the brain might prove useful in understanding heterogeneity in ASD.

7   BIBLIOGRAPHY

1. Association, A. P. *DSM-IV: Diagnostic and Statistical Manual of Mental Disorders*. (American Psychiatric Association, 1994).

2. Buescher, A. V. S., Cidav, Z., Knapp, M. & Mandell, D. S. Costs of Autism Spectrum Disorders in the United Kingdom and the United States. *JAMA Pediatr* **168,** 721–728 (2014).

3. Cadman, T. *et al.* Caregiver burden as people with autism spectrum disorder and attention-deficit/hyperactivity disorder transition into adolescence and adulthood in the United Kingdom. *J Am Acad Child Adolesc Psychiatry* **51,** 879–888 (2012).

4. Howlin, P., Goode, S., Hutton, J. & Rutter, M. Adult outcome for children with autism. *J Child Psychol Psychiatry* **45,** 212–229 (2004).

5. Murphy, C. M. *et al.* Autism spectrum disorder in adults: diagnosis, management, and health services development. *Neuropsychiatric Disease and Treatment* (2016).

6. Association, A. P. *Diagnostic and Statistical Manual of Mental Disorders, 5th Edition: DSM-5*. (American Psychiatric Publishing, 2013).

7. Diamond, A. Executive Functions. *Annu Rev Psychol* **64,** 135–168 (2013).

8. Botvinick, M. M., Braver, T. S., Barch, D. M., Carter, C. S. & Cohen, J. D. Conflict monitoring and cognitive control. *Psychol Rev* **108,** 624–652 (2001).

9. Hill, E. L. Evaluating the theory of executive dysfunction in autism. *Developmental Review* **24,** 189–233 (2004).

10. Shallice, T. & Burgess, P. W. Deficits in Strategy Application Following Frontal Lobe Damage in Man. *Brain* **114,** 727–741 (1991).

11. Snyder, H. R., Banich, M. T. & Munakata, Y. Choosing our words: retrieval and selection processes recruit shared neural substrates in left ventrolateral prefrontal cortex. *J Cogn Neurosci* **23,** 3470–3482 (2011).

12. Welsh, M. C. & Pennington, B. F. Assessing frontal lobe functioning in children: Views from developmental psychology. *Developmental Neuropsychology* **4,** 199–230 (1988).

13. Bunge, S. A., Dudukovic, N. M., Thomason, M. E., Vaidya, C. J. & Gabrieli, J. D. E. Immature frontal lobe contributions to cognitive control in children: evidence from fMRI. *Neuron* **33,** 301–311 (2002).

14. Blair, C. School readiness. Integrating cognition and emotion in a neurobiological conceptualization of children's functioning at school entry. *Am Psychol* **57,** 111–127 (2002).

15. Borella, E., Carretti, B. & Pelegrina, S. The specific role of inhibition in reading comprehension in good and poor comprehenders. *J Learn Disabil* **43,** 541–552 (2010).

16. Crescioni, A. W. *et al.* High trait self-control predicts positive health behaviors and success in weight loss. *J Health Psychol* **16,** 750–759 (2011).

17. Miller, H. V., Barnes, J. C. & Beaver, K. M. Self-control and health outcomes in a nationally representative sample. *Am J Health Behav* **35,** 15–27 (2011).

18. Riggs, N. R., Spruijt-Metz, D., Sakuma, K.-L., Chou, C.-P. & Pentz, M. A. Executive cognitive function and food intake in children. *J Nutr Educ Behav* **42,** 398–403 (2010).

19. Davis, J. C., Marra, C. A., Najafzadeh, M. & Liu-Ambrose, T. The independent contribution of executive functions to health related quality of life in older women. *BMC Geriatr* **10,** 16 (2010).

20. Moffitt, T. E. *et al.* A gradient of childhood self-control predicts health, wealth, and public safety. *Proc. Natl. Acad. Sci. U.S.A.* **108,** 2693–2698 (2011).

21. Bennetto, L., Pennington, B. F. & Rogers, S. J. Intact and Impaired Memory Functions in Autism. *Child Development* **67,** 1816–1835 (1996).

22. Ozonoff, S. *et al.* Performance on Cambridge Neuropsychological Test Automated Battery subtests sensitive to frontal lobe function in people with autistic disorder: evidence from the Collaborative Programs of Excellence in Autism network. *J Autism Dev Disord* **34,** 139–150 (2004).

23. Pennington, B. F. *et al.* Validity tests of the executive dysfunction hypothesis of autism. in *Autism as an executive disorder* 143–178 (Oxford University Press, 1997).

24. Solomon, M. *et al.* The neural substrates of cognitive control deficits in autism spectrum disorders. *Neuropsychologia* **47,** 2515–2526 (2009).

25. Solomon, M., Ozonoff, S. J., Cummings, N. & Carter, C. S. Cognitive control in autism spectrum disorders. *Int. J. Dev. Neurosci.* **26,** 239–247 (2008).

26. Fan, J. *et al.* Functional deficits of the attentional networks in autism. *Brain Behav* **2,** 647–660 (2012).

27. Christ, S. E., Holt, D. D., White, D. A. & Green, L. Inhibitory control in children with autism spectrum disorder. *J Autism Dev Disord* **37,** 1155–1165 (2007).

28. Sinzig, J., Morsch, D., Bruning, N., Schmidt, M. H. & Lehmkuhl, G. Inhibition, flexibility, working memory and planning in autism spectrum disorders with and without comorbid ADHD-symptoms. *Child Adol Psych Ment Health* **2,** 1–12 (2008).

29. Luna, B., Doll, S. K., Hegedus, S. J., Minshew, N. J. & Sweeney, J. A. Maturation of executive function in autism. *Biol. Psychiatry* **61,** 474–481 (2007).

30. Thakkar, K. N. *et al.* Response monitoring, repetitive behaviour and anterior cingulate abnormalities in autism spectrum disorders (ASD). *Brain* **131,** 2464–2478 (2008).

31. Hughes, C., Russell, J. & Robbins, T. W. Evidence for executive dysfunction in autism. *Neuropsychologia* **32,** 477–492 (1994).

32. Minshew, N. J., Luna, B. & Sweeney, J. A. Oculomotor evidence for neocortical systems but not cerebellar dysfunction in autism. *Neurology* **52,** 917–922 (1999).

33. Turner, M. A. Generating novel ideas: fluency performance in high-functioning and learning disabled individuals with autism. *J Child Psychol Psychiatry* **40,** 189–201 (1999).

34. Ozonoff, S. & McEvoy, R. E. A longitudinal study of executive function and theory of mind development in autism. *Development and Psychopathology* **6,** 415–431 (1994).

35. Dichter, G. S., Felder, J. N. & Bodfish, J. W. Autism is characterized by dorsal anterior cingulate hyperactivation during social target detection. *Soc Cogn Affect Neurosci* **4,** 215–226 (2009).

36. Ozonoff, S., Pennington, B. F. & Rogers, S. J. Executive function deficits in high-functioning autistic individuals: relationship to theory of mind. *J Child Psychol Psychiatry* **32,** 1081–1105 (1991).

37. Szatmari, P., Tuff, L., Finlayson, M. A. J. & Bartolucci, G. Asperger's syndrome and autism: Neurocognitive aspects. *Journal of the American Academy of Child and Adolescent Psychiatry* **29,** 130–136 (1990).

38. Hughes, C. & Russell, J. Autistic Children's Difficulty With Mental Disengagement From an Object: Its Implications for Theories of Autism. *Developmental Psychology* **29,** 498–510 (1993).

39. Russell, J., Hala, S. & Hill, E. The automated windows task: The performance of preschool children, children with autism, and children with moderate learning difficulties. *Cognitive Development* **18,** 111–137 (2003).

40. Kenworthy, L., Black, D. O., Harrison, B., Della Rosa, A. & Wallace, G. L. Are executive control functions related to autism symptoms in high-functioning children? *Child Neuropsychol* **15,** 425–440 (2009).

41. Lopez, B. R., Lincoln, A. J., Ozonoff, S. & Lai, Z. Examining the relationship between executive functions and restricted, repetitive symptoms of Autistic Disorder. *J Autism Dev Disord* **35,** 445–460 (2005).

42. Yerys, B. E. *et al.* Set-shifting in children with autism spectrum disorders: reversal shifting deficits on the Intradimensional/Extradimensional Shift Test correlate with repetitive behaviors. *Autism* **13,** 523–538 (2009).

43. Hume, K., Loftin, R. & Lantz, J. Increasing independence in autism spectrum disorders: a review of three focused interventions. *J Autism Dev Disord* **39,** 1329–1338 (2009).

44. Pennington, B. F. & Ozonoff, S. Executive Functions and Developmental Psychopathology. *Journal of Child Psychology and Psychiatry* **37,** 51–87 (1996).

45. Bishop, D. V. M. Annotation: Autism, Executive Functions and Theory of Mind: A Neuropsychological Perspective. *Journal of Child Psychology and Psychiatry* **34,** 279–293 (1993).

46. Hill, E. L. & Bird, C. M. Executive processes in Asperger syndrome: patterns of performance in a multiple case series. *Neuropsychologia* **44,** 2822–2835 (2006).

47. Schmitz, N. *et al.* Neural correlates of executive function in autistic spectrum disorders. *Biol. Psychiatry* **59,** 7–16 (2006).

48. Eskes, G. A., Bryson, S. E. & McCormick, T. A. Comprehension of concrete and abstract words in autistic children. *J Autism Dev Disord* **20,** 61–73 (1990).

49. Ozonoff, S. & Jensen, J. Brief report: specific executive function profiles in three neurodevelopmental disorders. *J Autism Dev Disord* **29,** 171–177 (1999).

50. Christ, S. E., Kester, L. E., Bodner, K. E. & Miles, J. H. Evidence for selective inhibitory impairment in individuals with autism spectrum disorder. *Neuropsychology* **25,** 690–701 (2011).

51. South, M., Larson, M. J., Krauskopf, E. & Clawson, A. Error processing in high-functioning Autism Spectrum Disorders. *Biol Psychol* **85,** 242–251 (2010).

52. Adams, N. C. & Jarrold, C. Inhibition in autism: children with autism have difficulty inhibiting irrelevant distractors but not prepotent responses. *J Autism Dev Disord* **42,** 1052–1063 (2012).

53. Dichter, G. S. & Belger, A. Social stimuli interfere with cognitive control in autism. *NeuroImage* **35,** 1219–1230 (2007).

54. Henderson, H. *et al.* Response monitoring, the error-related negativity, and differences in social behavior in autism. *Brain Cogn* **61,** 96–109 (2006).

55. Vaidya, C. J. *et al.* Controlling attention to gaze and arrows in childhood: an fMRI study of typical development and Autism Spectrum Disorders. *Dev Sci* **14,** 911–924 (2011).

56. Friedman, N. P. & Miyake, A. The relations among inhibition and interference control functions: a latent-variable analysis. *J Exp Psychol Gen* **133,** 101–135 (2004).

57. Lotter, V. Epidemiology of autistic conditions in young children. *Soc Psychiatry* **1,** 124–135 (1966).

58. Baio J. Centers for Disease Control and Prevention (CDC). Prevalence of Autism Spectrum Disorders — Autism and Developmental Disabilities Monitoring Network, 14 Sites, United States, 2008. *Surveillance Summaries* **61,** 1–19 (2012).

59. Chakrabarti, S. & Fombonne, E. Pervasive developmental disorders in preschool children. *JAMA* **285,** 3093–3099 (2001).

60. Fombonne, E. The epidemiology of autism: a review. *Psychol Med* **29,** 769–786 (1999).

61. Fombonne, E. Epidemiology of Pervasive Developmental Disorders. *Pediatr Res* **65,** 591–598 (2009).

62. Parner, E. T., Schendel, D. E. & Thorsen, P. Autism prevalence trends over time in Denmark: changes in prevalence and age at diagnosis. *Arch Pediatr Adolesc Med* **162,** 1150–1156 (2008).

63. Rutter, M. Incidence of autism spectrum disorders: changes over time and their meaning. *Acta Paediatr.* **94,** 2–15 (2005).

64. Brugha, T *et al. Estimating the prevalence of autism spectrum conditions in adults: extending the 2007 adult psychiatric morbidity survey*. (The NHS Information Centre for Health and Social care by the University of Leicester, the Leicestershire Partnership NHS Trust, the National Centre for Social Research and the University of Glasgow, 2012).

65. Baron-Cohen, S. *et al.* Prevalence of autism-spectrum conditions: UK school-based population study. *Br J Psychiatry* **194,** 500–509 (2009).

66. Kogan, M. D. *et al.* Prevalence of parent-reported diagnosis of autism spectrum disorder among children in the US, 2007. *Pediatrics* **124,** 1395–1403 (2009).

67. Miles, J. H. & Hillman, R. E. Value of a clinical morphology examination in autism. *Am. J. Med. Genet.* **91,** 245–253 (2000).

68. Fombonne, E. Epidemiological trends in rates of autism. *Mol. Psychiatry* **7 Suppl 2,** S4-6 (2002).

69. Shao, Y. *et al.* Genomic screen and follow-up analysis for autistic disorder. *Am. J. Med. Genet.* **114,** 99–105 (2002).

70. Liu, J. *et al.* A Genomewide Screen for Autism Susceptibility Loci. *The American Journal of Human Genetics* **69,** 327–340 (2001).

71. Baron-Cohen, S. *et al.* Why are autism spectrum conditions more prevalent in males? *PLoS Biol.* **9,** e1001081 (2011).

72. Newschaffer, C. J. *et al.* The epidemiology of autism spectrum disorders. *Annu Rev Public Health* **28,** 235–258 (2007).

73. Folstein, S. & Rutter, M. Infantile Autism: A Genetic Study of 21 Twin Pairs. *Journal of Child Psychology and Psychiatry* **18,** 297–321 (1977).

74. Bailey, A. *et al.* Autism as a strongly genetic disorder: evidence from a British twin study. *Psychological Medicine* **25,** 63–77 (1995).

75. Lichtenstein, P., Carlström, E., Råstam, M., Gillberg, C. & Anckarsäter, H. The genetics of autism spectrum disorders and related neuropsychiatric disorders in childhood. *Am J Psychiatry* **167,** 1357–1363 (2010).

76. Hallmayer, J. *et al.* Genetic heritability and shared environmental factors among twin pairs with autism. *Arch. Gen. Psychiatry* **68,** 1095–1102 (2011).

77. Abrahams, B. S. & Geschwind, D. H. Advances in autism genetics: on the threshold of a new neurobiology. *Nat. Rev. Genet.* **9,** 341–355 (2008).

78. Verkerk, A. J. *et al.* Identification of a gene (FMR-1) containing a CGG repeat coincident with a breakpoint cluster region exhibiting length variation in fragile X syndrome. *Cell* **65,** 905–914 (1991).

79. Pieretti, M. *et al.* Absence of expression of the FMR-1 gene in fragile X syndrome. *Cell* **66,** 817–822 (1991).

80. Sutcliffe, J. S. *et al.* DNA methylation represses FMR-1 transcription in fragile X syndrome. *Hum. Mol. Genet.* **1,** 397–400 (1992).

81. Pop, A. S., Gomez-Mancilla, B., Neri, G., Willemsen, R. & Gasparini, F. Fragile X syndrome: a preclinical review on metabotropic glutamate receptor 5 (mGluR5) antagonists and drug development. *Psychopharmacology* **231,** 1217–1226 (2014).

82. Rojas, D. C. The role of glutamate and its receptors in autism and the use of glutamate receptor antagonists in treatment. *J Neural Transm* **121,** 891–905 (2014).

83. Tranfaglia, M. R. The psychiatric presentation of fragile x: evolution of the diagnosis and treatment of the psychiatric comorbidities of fragile X syndrome. *Dev. Neurosci.* **33,** 337–348 (2011).

84. Berry-Kravis, E. Epilepsy in fragile X syndrome. *Dev Med Child Neurol* **44,** 724–728 (2002).

85. Incorpora, G., Sorge, G., Sorge, A. & Pavone, L. Epilepsy in fragile X syndrome. *Brain Dev.* **24,** 766–769 (2002).

86. Rogers, S. J., Wehner, D. E. & Hagerman, R. The behavioral phenotype in fragile X: symptoms of autism in very young children with fragile X syndrome, idiopathic autism, and other developmental disorders. *J Dev Behav Pediatr* **22,** 409–417 (2001).

87. Harris, S. W. *et al.* Autism profiles of males with fragile X syndrome. *Am J Ment Retard* **113,** 427–438 (2008).

88. Ziats, M. N. & Rennert, O. M. The Evolving Diagnostic and Genetic Landscapes of Autism Spectrum Disorder. *Front. Genet.* **7,** (2016).

89. He, X. *et al.* Integrated model of de novo and inherited genetic variants yields greater power to identify risk genes. *PLoS Genet.* **9,** e1003671 (2013).

90. Iossifov, I. *et al.* De novo gene disruptions in children on the autistic spectrum. *Neuron* **74,** 285–299 (2012).

91. Ronemus, M., Iossifov, I., Levy, D. & Wigler, M. The role of de novo mutations in the genetics of autism spectrum disorders. *Nat. Rev. Genet.* **15,** 133–141 (2014).

92. Jorde, L. B. *et al.* Complex segregation analysis of autism. *Am. J. Hum. Genet.* **49,** 932–938 (1991).

93. Risch, N. *et al.* A genomic screen of autism: evidence for a multilocus etiology. *Am. J. Hum. Genet.* **65,** 493–507 (1999).

94. Chaste, P. & Leboyer, M. Autism risk factors: genes, environment, and gene-environment interactions. *Dialogues Clin Neurosci* **14,** 281–292 (2012).

95. Choudhury, P. R., Lahiri, S. & Rajamma, U. Glutamate mediated signaling in the pathophysiology of autism spectrum disorders. *Pharmacology Biochemistry and Behavior* **100,** 841–849 (2012).

96. D'Amelio, M. *et al.* Paraoxonase gene variants are associated with autism in North America, but not in Italy: possible regional specificity in gene-environment interactions. *Mol. Psychiatry* **10,** 1006–1016 (2005).

97. Geschwind, D. H. & Levitt, P. Autism spectrum disorders: developmental disconnection syndromes. *Curr. Opin. Neurobiol.* **17,** 103–111 (2007).

98. Kim, Y. S. & Leventhal, B. L. Genetic epidemiology and insights into interactive genetic and environmental effects in autism spectrum disorders. *Biol. Psychiatry* **77,** 66–74 (2015).

99. Krishnan, A. *et al.* Genome-wide prediction and functional characterization of the genetic basis of autism spectrum disorder. *Nat. Neurosci.* **19,** 1454–1462 (2016).

100. Park, H. R. *et al.* A Short Review on the Current Understanding of Autism Spectrum Disorders. *Exp Neurobiol* **25,** 1–13 (2016).

101. Chiocchetti, A. G., Bour, H. S. & Freitag, C. M. Glutamatergic candidate genes in autism spectrum disorder: an overview. *J Neural Transm* **121,** 1081–1106 (2014).

102. Gardener, H., Spiegelman, D. & Buka, S. L. Perinatal and neonatal risk factors for autism: a comprehensive meta-analysis. *Pediatrics* **128,** 344–355 (2011).

103. Atladóttir, H. O. *et al.* Maternal infection requiring hospitalization during pregnancy and autism spectrum disorders. *J Autism Dev Disord* **40,** 1423–1430 (2010).

104. Malkova, N. V., Yu, C. Z., Hsiao, E. Y., Moore, M. J. & Patterson, P. H. Maternal immune activation yields offspring displaying mouse versions of the three core symptoms of autism. *Brain Behav. Immun.* **26,** 607–616 (2012).

105. Rasalam, A. D. *et al.* Characteristics of fetal anticonvulsant syndrome associated autistic disorder. *Dev Med Child Neurol* **47,** 551–555 (2005).

106. Guinchat, V. *et al.* Pre-, peri- and neonatal risk factors for autism. *Acta Obstet Gynecol Scand* **91,** 287–300 (2012).

107. Kolevzon, A., Gross, R. & Reichenberg, A. Prenatal and perinatal risk factors for autism: a review and integration of findings. *Arch Pediatr Adolesc Med* **161,** 326–333 (2007).

108. Minshew, N. J. & Keller, T. A. The nature of brain dysfunction in autism: functional brain imaging studies. *Curr. Opin. Neurol.* **23,** 124–130 (2010).

109. Frith, U. Why we need cognitive explanations of autism. *Q J Exp Psychol (Hove)* **65,** 2073–2092 (2012).

110. Courchesne, E. *et al.* Unusual brain growth patterns in early life in patients with autistic disorder: an MRI study. *Neurology* **57,** 245–254 (2001).

111. Courchesne, E., Carper, R. & Akshoomoff, N. Evidence of brain overgrowth in the first year of life in autism. *JAMA* **290,** 337–344 (2003).

112. Stanfield, A. C. *et al.* Towards a neuroanatomy of autism: a systematic review and meta-analysis of structural magnetic resonance imaging studies. *Eur. Psychiatry* **23,** 289–299 (2008).

113. Bandettini, P. A., Wong, E. C., Hinks, R. S., Tikofsky, R. S. & Hyde, J. S. Time course EPI of human brain function during task activation. *Magn Reson Med* **25,** 390–397 (1992).

114. Kwong, K. K. *et al.* Dynamic magnetic resonance imaging of human brain activity during primary sensory stimulation. *Proc. Natl. Acad. Sci. U.S.A.* **89,** 5675–5679 (1992).

115. Ogawa, S. *et al.* Intrinsic signal changes accompanying sensory stimulation: functional brain mapping with magnetic resonance imaging. *Proc Natl Acad Sci U S A* **89,** 5951–5955 (1992).

116. Biswal, B., Zerrin, Y., Haughton, V. M. & Hyde, J. S. Functional connectivity in the motor cortex of resting human brain using echo-planar mri. *Magnetic Resonance in Medicine* **34,** 537–541 (1995).

117. Kana, R. K., Uddin, L. Q., Kenet, T., Chugani, D. & Müller, R.-A. Brain connectivity in autism. *Front Hum Neurosci* **8,** (2014).

118. Maximo, J. O., Cadena, E. J. & Kana, R. K. The implications of brain connectivity in the neuropsychology of autism. *Neuropsychol Rev* **24,** 16–31 (2014).

119. Raichle, M. E. Two views of brain function. *Trends Cogn. Sci. (Regul. Ed.)* **14,** 180–190 (2010).

120. Di Martino, A. *et al.* Relationship Between Cingulo-Insular Functional Connectivity and Autistic Traits in Neurotypical Adults. *AJP* **166,** 891–899 (2009).

121. Mundy, P. Annotation: the neural basis of social impairments in autism: the role of the dorsal medial-frontal cortex and anterior cingulate system. *J Child Psychol Psychiatry* **44,** 793–809 (2003).

122. Simms, M. L., Kemper, T. L., Timbie, C. M., Bauman, M. L. & Blatt, G. J. The anterior cingulate cortex in autism: heterogeneity of qualitative and quantitative cytoarchitectonic features suggests possible subgroups. *Acta Neuropathol* **118,** 673–684 (2009).

123. Masi, A., DeMayo, M. M., Glozier, N. & Guastella, A. J. An Overview of Autism Spectrum Disorder, Heterogeneity and Treatment Options. *Neurosci. Bull.* **33,** 183–193 (2017).

124. Siegel, M. & Beaulieu, A. A. Psychotropic medications in children with autism spectrum disorders: a systematic review and synthesis for evidence-based practice. *J Autism Dev Disord* **42,** 1592–1605 (2012).

125. Yatawara, C. J., Einfeld, S. L., Hickie, I. B., Davenport, T. A. & Guastella, A. J. The effect of oxytocin nasal spray on social interaction

deficits observed in young children with autism: a randomized clinical crossover trial. *Mol. Psychiatry* **21,** 1225–1231 (2016).

126. Eldevik, S. *et al.* Meta-analysis of Early Intensive Behavioral Intervention for children with autism. *J Clin Child Adolesc Psychol* **38,** 439–450 (2009).

127. Marcus, R. N. *et al.* A placebo-controlled, fixed-dose study of aripiprazole in children and adolescents with irritability associated with autistic disorder. *J Am Acad Child Adolesc Psychiatry* **48,** 1110–1119 (2009).

128. McCracken, J. T. *et al.* Risperidone in children with autism and serious behavioral problems. *N. Engl. J. Med.* **347,** 314–321 (2002).

129. Oswald, D. P. & Sonenklar, N. A. Medication use among children with autism spectrum disorders. *J Child Adolesc Psychopharmacol* **17,** 348–355 (2007).

130. Owen, R. *et al.* Aripiprazole in the treatment of irritability in children and adolescents with autistic disorder. *Pediatrics* **124,** 1533–1540 (2009).

131. Erecińska, M. & Silver, I. A. Metabolism and role of glutamate in mammalian brain. *Progress in Neurobiology* **35,** 245–296 (1990).

132. Shen, J. Glutamate. in *Magnetic Resonance Spectroscopy* (eds. Stagg, C. & Rothman, D.) 111–121 (Academic Press, 2014).

133. Johnston, M. V. Neurotransmitters and vulnerability of the developing brain. *Brain and Development* **17,** 301–306 (1995).

134. Dingledine, R., Borges, K., Bowie, D. & Traynelis, S. F. The glutamate receptor ion channels. *Pharmacol. Rev.* **51,** 7–61 (1999).

135. Dingledine, R. & McBain, C. J. Three Classes of Ionotropic Glutamate Receptor. (1999).

136. Berg, C. J. V. D. & Garfinkel, D. A simulation study of brain compartments. Metabolism of glutamate and related substances in mouse brain. *Biochemical Journal* **123,** 211–218 (1971).

137. Contractor, A., Mulle, C. & Swanson, G. T. Kainate receptors coming of age: milestones of two decades of research. *Trends Neurosci.* **34,** 154–163 (2011).

138. Nicoll, R. A. & Roche, K. W. Long-term potentiation: peeling the onion. *Neuropharmacology* **74,** 18–22 (2013).

139. Nicoletti, F. *et al.* Coupling of inositol phospholipid metabolism with excitatory amino acid recognition sites in rat hippocampus. *J. Neurochem.* **46,** 40–46 (1986).

140. Nicoletti, F. *et al.* Metabotropic glutamate receptors: from the workbench to the bedside. *Neuropharmacology* **60,** 1017–1041 (2011).

141. Sladeczek, F., Pin, J. P., Récasens, M., Bockaert, J. & Weiss, S. Glutamate stimulates inositol phosphate formation in striatal neurones. *Nature* **317,** 717–719 (1985).

142. Bruno, V. *et al.* Metabotropic Glutamate Receptor Subtypes as Targets for Neuroprotective Drugs. *Journal of Cerebral Blood Flow & Metabolism* **21,** 1013–1033 (2001).

143. Nakanishi, S. Molecular diversity of glutamate receptors and implications for brain function. *Science* **258,** 597–603 (1992).

144. Doherty, J. & Dingledine, R. The roles of metabotropic glutamate receptors in seizures and epilepsy. *Curr Drug Targets CNS Neurol Disord* **1,** 251–260 (2002).

145. Nakanishi, S. *et al.* Glutamate receptors: brain function and signal transduction. *Brain Res. Brain Res. Rev.* **26,** 230–235 (1998).

146. Bear, M. F., Cooper, L. N. & Ebner, F. F. A physiological basis for a theory of synapse modification. *Science* **237,** 42–48 (1987).

147. Bliss, T. V. & Collingridge, G. L. A synaptic model of memory: long-term potentiation in the hippocampus. *Nature* **361,** 31–39 (1993).

148. Cooke, S. F. & Bliss, T. V. P. Plasticity in the human central nervous system. *Brain* **129,** 1659–1673 (2006).

149. Nadler, J. V. Plasticity of Glutamate Synaptic Mechanisms. in *Jasper's Basic Mechanisms of the Epilepsies* (eds. Noebels, J. L., Avoli, M., Rogawski, M. A., Olsen, R. W. & Delgado-Escueta, A. V.) (National Center for Biotechnology Information (US), 2012).

150. Bliss, T. V. P., Collingridge, G. L., Kaang, B.-K. & Zhuo, M. Synaptic plasticity in the anterior cingulate cortex in acute and chronic pain. *Nat Rev Neurosci* **17,** 485–496 (2016).

151. Koga, K. *et al.* Coexistence of two forms of LTP in ACC provides a synaptic mechanism for the interactions between anxiety and chronic pain. *Neuron* **85,** 377–389 (2015).

152. Shum, F. W. F. *et al.* Alteration of cingulate long-term plasticity and behavioral sensitization to inflammation by environmental enrichment. *Learn Mem* **14,** 304–312 (2007).

153. Lledo, P. M., Zhang, X., Südhof, T. C., Malenka, R. C. & Nicoll, R. A. Postsynaptic membrane fusion and long-term potentiation. *Science* **279,** 399–403 (1998).

154. Lüscher, C. *et al.* Role of AMPA Receptor Cycling in Synaptic Transmission and Plasticity. *Neuron* **24,** 649–658 (1999).

155. Malenka, R. C. & Bear, M. F. LTP and LTD: An Embarrassment of Riches. *Neuron* **44,** 5–21 (2004).

156. Sihra, T. S., Flores, G. & Rodríguez-Moreno, A. Kainate receptors: multiple roles in neuronal plasticity. *Neuroscientist* **20,** 29–43 (2014).

157. Lynch, M. A. Long-term potentiation and memory. *Physiol. Rev.* **84,** 87–136 (2004).

158. Kelleher, R. J., Govindarajan, A. & Tonegawa, S. Translational regulatory mechanisms in persistent forms of synaptic plasticity. *Neuron* **44,** 59–73 (2004).

159. Engert, F. & Bonhoeffer, T. Dendritic spine changes associated with hippocampal long-term synaptic plasticity. *Nature* **399,** 66–70 (1999).

160. Toni, N., Buchs, P. A., Nikonenko, I., Bron, C. R. & Muller, D. LTP promotes formation of multiple spine synapses between a single axon terminal and a dendrite. *Nature* **402,** 421–425 (1999).

161. Yuste, R. & Bonhoeffer, T. Morphological changes in dendritic spines associated with long-term synaptic plasticity. *Annu. Rev. Neurosci.* **24,** 1071–1089 (2001).

162. Daoudal, G. & Debanne, D. Long-Term Plasticity of Intrinsic Excitability: Learning Rules and Mechanisms. *Learn. Mem.* **10,** 456–465 (2003).

163. Collingridge, G. L., Peineau, S., Howland, J. G. & Wang, Y. T. Long-term depression in the CNS. *Nat. Rev. Neurosci.* **11,** 459–473 (2010).

164. Lüscher, C. & Malenka, R. C. NMDA Receptor-Dependent Long-Term Potentiation and Long-Term Depression (LTP/LTD). *Cold Spring Harb Perspect Biol* **4,** a005710 (2012).

165. Bashir, Z. I. *et al.* Induction of LTP in the hippocampus needs synaptic activation of glutamate metabotropic receptors. *Nature* **363,** 347–350 (1993).

166. Bortolotto, Z. A. & Collingridge, G. L. Characterisation of LTP induced by the activation of glutamate metabotropic receptors in area CA1 of the hippocampus. *Neuropharmacology* **32,** 1–9 (1993).

167. Huber, K. M., Kayser, M. S. & Bear, M. F. Role for rapid dendritic protein synthesis in hippocampal mGluR-dependent long-term depression. *Science* **288,** 1254–1257 (2000).

168. Huemmeke, M., Eysel, U. T. & Mittmann, T. Metabotropic glutamate receptors mediate expression of LTP in slices of rat visual cortex. *Eur. J. Neurosci.* **15,** 1641–1645 (2002).

169. Norenberg, M. D. & Martinez-Hernandez, A. Fine structural localization of glutamine synthetase in astrocytes of rat brain. *Brain Research* **161,** 303–310 (1979).

170. Bak, L. K., Schousboe, A. & Waagepetersen, H. S. The glutamate/GABA-glutamine cycle: aspects of transport, neurotransmitter homeostasis and ammonia transfer. *Journal of Neurochemistry* **98,** 641–653 (2006).

171. Daikhin, Y. & Yudkoff, M. Compartmentation of brain glutamate metabolism in neurons and glia. *J. Nutr.* **130,** 1026S–31S (2000).

172. Meldrum, B. S. Glutamate as a neurotransmitter in the brain: review of physiology and pathology. *J. Nutr.* **130,** 1007S–15S (2000).

173. Rodrigo, R. & Felipo, V. Control of brain glutamine synthesis by NMDA receptors. *Front. Biosci.* **12,** 883–890 (2007).

174. Bosoi, C. R. & Rose, C. F. Identifying the direct effects of ammonia on the brain. *Metab Brain Dis* **24,** 95–102 (2009).

175. Sibson, N. R. *et al.* Stoichiometric coupling of brain glucose metabolism and glutamatergic neuronal activity. *PNAS* **95,** 316–321 (1998).

176. Shulman, R. G., Rothman, D. L., Behar, K. L. & Hyder, F. Energetic basis of brain activity: implications for neuroimaging. *Trends Neurosci.* **27,** 489–495 (2004).

177. Komuro, H. & Rakic, P. Modulation of neuronal migration by NMDA receptors. *Science* **260,** 95–97 (1993).

178. Behar, T. N. *et al.* Glutamate acting at NMDA receptors stimulates embryonic cortical neuronal migration. *J. Neurosci.* **19,** 4449–4461 (1999).

179. Manent, J.-B. & Represa, A. Neurotransmitters and brain maturation: early paracrine actions of GABA and glutamate modulate neuronal migration. *Neuroscientist* **13,** 268–279 (2007).

180. Pearce, I. A., Cambray-Deakin, M. A. & Burgoyne, R. D. Glutamate acting on NMDA receptors stimulates neurite outgrowth from cerebellar granule cells. *FEBS Letters* **223,** 143–147 (1987).

181. Rajan, I. & Cline, H. T. Glutamate receptor activity is required for normal development of tectal cell dendrites in vivo. *J. Neurosci.* **18,** 7836–7846 (1998).

182. LoTurco, J. J., Owens, D. F., Heath, M. J., Davis, M. B. & Kriegstein, A. R. GABA and glutamate depolarize cortical progenitor cells and inhibit DNA synthesis. *Neuron* **15,** 1287–1298 (1995).

183. Ikonomidou, C. *et al.* Blockade of NMDA receptors and apoptotic neurodegeneration in the developing brain. *Science* **283,** 70–74 (1999).

184. Ikonomidou, C. *et al.* Ethanol-induced apoptotic neurodegeneration and fetal alcohol syndrome. *Science* **287,** 1056–1060 (2000).

185. Bonfoco, E., Krainc, D., Ankarcrona, M., Nicotera, P. & Lipton, S. A. Apoptosis and necrosis: two distinct events induced, respectively, by mild and intense insults with N-methyl-D-aspartate or nitric oxide/superoxide in cortical cell cultures. *Proc. Natl. Acad. Sci. U.S.A.* **92,** 7162–7166 (1995).

186. Shigeri, Y., Seal, R. P. & Shimamoto, K. Molecular pharmacology of glutamate transporters, EAATs and VGLUTs. *Brain Res. Brain Res. Rev.* **45,** 250–265 (2004).

187. Matsugami, T. R. *et al.* Indispensability of the glutamate transporters GLAST and GLT1 to brain development. *PNAS* **103,** 12161–12166 (2006).

188. Burnashev, N. *et al.* Control by asparagine residues of calcium permeability and magnesium blockade in the NMDA receptor. *Science* **257,** 1415–1419 (1992).

189. Kato, N. & Yoshimura, H. Reduced Mg2+ block of N-methyl-D-aspartate receptor-mediated synaptic potentials in developing visual cortex. *Proc Natl Acad Sci U S A* **90,** 7114–7118 (1993).

190. Morrisett, R. A., Mott, D. D., Lewis, D. V., Wilson, W. A. & Swartzwelder, H. S. Reduced sensitivity of the N-methyl-D-aspartate component of synaptic transmission to magnesium in hippocampal slices from immature rats. *Brain Res. Dev. Brain Res.* **56,** 257–262 (1990).

191. McDonald, J. W. & Johnston, M. V. Physiological and pathophysiological roles of excitatory amino acids during central nervous system development. *Brain Res. Brain Res. Rev.* **15,** 41–70 (1990).

192. Trescher, W. H., McDonald, J. W. & Johnston, M. V. Quinolinate-induced injury is enhanced in developing rat brain. *Brain Res. Dev. Brain Res.* **83,** 224–232 (1994).

193. Polleux, F. & Lauder, J. M. Toward a developmental neurobiology of autism. *Ment Retard Dev Disabil Res Rev* **10,** 303–317 (2004).

194. Carlsson, M. L. Hypothesis: is infantile autism a hypoglutamatergic disorder? Relevance of glutamate - serotonin interactions for pharmacotherapy. *J Neural Transm* **105,** 525–535 (1998).

195. Rodriguez-Rodriguez, P., Almeida, A. & Bolaños, J. P. Brain energy metabolism in glutamate-receptor activation and excitotoxicity: role for APC/C-Cdh1 in the balance glycolysis/pentose phosphate pathway. *Neurochem. Int.* **62,** 750–756 (2013).

196. Choi, D. W. Glutamate neurotoxicity in cortical cell culture is calcium dependent. *Neurosci. Lett.* **58,** 293–297 (1985).
246

197. During, M. J. & Spencer, D. D. Extracellular hippocampal glutamate and spontaneous seizure in the conscious human brain. *The Lancet* **341,** 1607–1610 (1993).

198. Greenamyre, J. T. The role of glutamate in neurotransmission and in neurologic disease. *Arch. Neurol.* **43,** 1058–1063 (1986).

199. Olney, J. W. Brain lesions, obesity, and other disturbances in mice treated with monosodium glutamate. *Science* **164,** 719–721 (1969).

200. Rothman, S. M. & Olney, J. W. Glutamate and the pathophysiology of hypoxic--ischemic brain damage. *Ann. Neurol.* **19,** 105–111 (1986).

201. Schousboe, A. Role of astrocytes in the maintenance and modulation of glutamatergic and GABAergic neurotransmission. *Neurochem. Res.* **28,** 347–352 (2003).

202. Schousboe, A. & Waagepetersen, H. S. Role of astrocytes in glutamate homeostasis: implications for excitotoxicity. *Neurotox Res* **8,** 221–225 (2005).

203. Lau, A. & Tymianski, M. Glutamate receptors, neurotoxicity and neurodegeneration. *Pflugers Arch - Eur J Physiol* **460,** 525–542 (2010).

204. Martin, L. J. Neuronal cell death in nervous system development, disease, and injury (Review). *Int. J. Mol. Med.* **7,** 455–478 (2001).

205. Stieg, P. E., Sathi, S., Warach, S., Le, D. A. & Lipton, S. A. Neuroprotection by the NMDA receptor-associated open-channel blocker memantine in a photothrombotic model of cerebral focal ischemia in neonatal rat. *Eur. J. Pharmacol.* **375,** 115–120 (1999).

206. Kingston, A. E. *et al.* Neuroprotective actions of novel and potent ligands of group I and group II metabotropic glutamate receptors. *Ann. N. Y. Acad. Sci.* **890,** 438–449 (1999).

207. Fatemi, S. H. The hyperglutamatergic hypothesis of autism. *Prog. Neuropsychopharmacol. Biol. Psychiatry* **32,** 911, author reply 912-913 (2008).

208. Shinohe, A. *et al.* Increased serum levels of glutamate in adult patients with autism. *Prog. Neuropsychopharmacol. Biol. Psychiatry* **30,** 1472–1477 (2006).

209. Abu Shmais, G. A., Al-Ayadhi, L. Y., Al-Dbass, A. M. & El-Ansary, A. K. Mechanism of nitrogen metabolism-related parameters and enzyme activities in the pathophysiology of autism. *J Neurodev Disord* **4,** 4 (2012).

210. Aldred, S., Moore, K. M., Fitzgerald, M. & Waring, R. H. Plasma amino acid levels in children with autism and their families. *J Autism Dev Disord* **33,** 93–97 (2003).

211. Zheng, Z., Zhu, T., Qu, Y. & Mu, D. Blood Glutamate Levels in Autism Spectrum Disorder: A Systematic Review and Meta-Analysis. *PLoS ONE* **11,** e0158688 (2016).

212. Cai, J., Ding, L., Zhang, J.-S., Xue, J. & Wang, L.-Z. Elevated plasma levels of glutamate in children with autism spectrum disorders. *Neuroreport* **27,** 272–276 (2016).

213. Moreno, H. *et al.* [Clinical heterogeneity of the autistic syndrome: a study of 60 families]. *Invest Clin* **33,** 13–31 (1992).

248

214. Moreno-Fuenmayor, H., Borjas, L., Arrieta, A., Valera, V. & Socorro-Candanoza, L. Plasma excitatory amino acids in autism. *Invest Clin* **37,** 113–128 (1996).

215. Tirouvanziam, R. *et al.* Distinct plasma profile of polar neutral amino acids, leucine, and glutamate in children with Autism Spectrum Disorders. *J Autism Dev Disord* **42,** 827–836 (2012).

216. Shimmura, C. *et al.* Alteration of plasma glutamate and glutamine levels in children with high-functioning autism. *PLoS ONE* **6,** e25340 (2011).

217. Hassan, T. H. *et al.* Blood and brain glutamate levels in children with autistic disorder. *Research in Autism Spectrum Disorders* **7,** 541–548 (2013).

218. Lord, C., Rutter, M. & Le Couteur, A. Autism Diagnostic Interview-Revised: a revised version of a diagnostic interview for caregivers of individuals with possible pervasive developmental disorders. *J Autism Dev Disord* **24,** 659–685 (1994).

219. Arnold, G. L., Hyman, S. L., Mooney, R. A. & Kirby, R. S. Plasma Amino Acids Profiles in Children with Autism: Potential Risk of Nutritional Deficiencies. *J Autism Dev Disord* **33,** 449–454 (2003).

220. ElBaz, F. M., Zaki, M. M., Youssef, A. M., ElDorry, G. F. & Elalfy, D. Y. Study of plasma amino acid levels in children with autism: An Egyptian sample. *Egyptian Journal of Medical Human Genetics* **15,** 181–186 (2014).

221. Hawkins, R. A. The blood-brain barrier and glutamate. *Am J Clin Nutr* **90,** 867S-874S (2009).

222. Hawkins, R. A. & Viña, J. R. How Glutamate Is Managed by the Blood–Brain Barrier. *Biology (Basel)* **5,** (2016).

223. McGale, E. H. F., Pye, I. F., Stonier, C., Hutchinson, E. C. & Aber, G. M. Studies of the Inter-Relationship Between Cerebrospinal Fluid and Plasma Amino Acid Concentrations in Normal Individuals. *Journal of Neurochemistry* **29,** 291–297 (1977).

224. Alfredsson, G., Wiesel, F.-A. & Tylec, A. Relationships between glutamate and monoamine metabolites in cerebrospinal fluid and serum in healthy volunteers. *Biological Psychiatry* **23,** 689–697 (1988).

225. Bejjani, A. *et al.* Elevated glutamatergic compounds in pregenual anterior cingulate in pediatric autism spectrum disorder demonstrated by 1H MRS and 1H MRSI. *PLoS ONE* **7,** e38786 (2012).

226. Brown, M. S., Singel, D., Hepburn, S. & Rojas, D. C. Increased Glutamate Concentration in the Auditory Cortex of Persons With Autism and First-Degree Relatives: A 1H-MRS Study. *Autism Research* **6,** 1–10 (2013).

227. Doyle-Thomas, K. A. R. *et al.* The effect of diagnosis, age, and symptom severity on cortical surface area in the cingulate cortex and insula in autism spectrum disorders. *J. Child Neurol.* **28,** 732–739 (2013).

228. Drenthen, G. S. *et al.* Altered neurotransmitter metabolism in adolescents with high-functioning autism. *Psychiatry Research: Neuroimaging* **256,** 44–49 (2016).

229. Ito, H. *et al.* A Proton Magnetic Resonance Spectroscopic Study in Autism Spectrum Disorder Using a 3-Tesla Clinical Magnetic Resonance

Imaging (MRI) System: The Anterior Cingulate Cortex and the Left Cerebellum. *J Child Neurol* **32,** 731–739 (2017).

230. Joshi, G. *et al.* Magnetic resonance spectroscopy study of the glutamatergic system in adolescent males with high-functioning autistic disorder: a pilot study at 4T. *Eur Arch Psychiatry Clin Neurosci* **263,** 379–384 (2013).

231. Naaijen, J., Lythgoe, D. J., Amiri, H., Buitelaar, J. K. & Glennon, J. C. Fronto-striatal glutamatergic compounds in compulsive and impulsive syndromes: a review of magnetic resonance spectroscopy studies. *Neurosci Biobehav Rev* **52,** 74–88 (2015).

232. Page, L. A. *et al.* In vivo 1H-magnetic resonance spectroscopy study of amygdala-hippocampal and parietal regions in autism. *Am J Psychiatry* **163,** 2189–2192 (2006).

233. Bernardi, S. *et al.* In vivo 1H-magnetic resonance spectroscopy study of the attentional networks in autism. *Brain Res.* **1380,** 198–205 (2011).

234. Corrigan, N. M. *et al.* Atypical developmental patterns of brain chemistry in children with autism spectrum disorder. *JAMA Psychiatry* **70,** 964–974 (2013).

235. DeVito, T. J. *et al.* Evidence for cortical dysfunction in autism: a proton magnetic resonance spectroscopic imaging study. *Biol. Psychiatry* **61,** 465–473 (2007).

236. Horder, J. *et al.* Reduced subcortical glutamate/glutamine in adults with autism spectrum disorders: a [1H]MRS study. *Transl Psychiatry* **3,** e279 (2013).

237. Tebartz van Elst, L. *et al.* Disturbed cingulate glutamate metabolism in adults with high-functioning autism spectrum disorder: evidence in support of the excitatory/inhibitory imbalance hypothesis. *Mol Psychiatry* **19,** 1314–1325 (2014).

238. Kubas, B. *et al.* Metabolite alterations in autistic children: a 1H MR spectroscopy study. *Adv Med Sci* **57,** 152–156 (2012).

239. Aoki, Y. *et al.* Absence of age-related prefrontal NAA change in adults with autism spectrum disorders. *Transl Psychiatry* **2,** e178 (2012).

240. Brix, M. K. *et al.* Brain MR spectroscopy in autism spectrum disorder—the GABA excitatory/inhibitory imbalance theory revisited. *Front Hum Neurosci* **9,** (2015).

241. Cochran, D. M. *et al.* Relationship among Glutamine, γ-Aminobutyric Acid, and Social Cognition in Autism Spectrum Disorders. *J Child Adolesc Psychopharmacol* **25,** 314–322 (2015).

242. Friedman, S. D. *et al.* Regional brain chemical alterations in young children with autism spectrum disorder. *Neurology* **60,** 100–107 (2003).

243. Harada, M. *et al.* Non-invasive evaluation of the GABAergic/glutamatergic system in autistic patients observed by MEGA-editing proton MR spectroscopy using a clinical 3 tesla instrument. *J Autism Dev Disord* **41,** 447–454 (2011).

244. Hardan, A. Y. *et al.* An MRI and proton spectroscopy study of the thalamus in children with autism. *Psychiatry Res* **163,** 97–105 (2008).

245. Libero, L. E., DeRamus, T. P., Lahti, A. C., Deshpande, G. & Kana, R. K. Multimodal neuroimaging based classification of autism spectrum

disorder using anatomical, neurochemical, and white matter correlates. *Cortex* **66,** 46–59 (2015).

246. Robertson, C. E., Ratai, E.-M. & Kanwisher, N. Reduced GABAergic Action in the Autistic Brain. *Current Biology* **26,** 80–85 (2016).

247. Ford, T. C. & Crewther, D. P. A Comprehensive Review of the 1H-MRS Metabolite Spectrum in Autism Spectrum Disorder. *Front Mol Neurosci* **9,** (2016).

248. Pouwels, P. J. & Frahm, J. Regional metabolite concentrations in human brain as determined by quantitative localized proton MRS. *Magn Reson Med* **39,** 53–60 (1998).

249. Ozawa, S., Kamiya, H. & Tsuzuki, K. Glutamate receptors in the mammalian central nervous system. *Prog. Neurobiol.* **54,** 581–618 (1998).

250. Purcell, A. E., Jeon, O. H., Zimmerman, A. W., Blue, M. E. & Pevsner, J. Postmortem brain abnormalities of the glutamate neurotransmitter system in autism. *Neurology* **57,** 1618–1628 (2001).

251. Blüml, S. Magnetic Resonance Spectroscopy: Basics. in *MR Spectroscopy of Pediatric Brain Disorders* (eds. Blüml, S. & Panigrahy, A.) 11–23 (Springer New York, 2013).

252. Aoki, Y., Kasai, K. & Yamasue, H. Age-related change in brain metabolite abnormalities in autism: a meta-analysis of proton magnetic resonance spectroscopy studies. *Transl Psychiatry* **2,** e69 (2012).

253. Baron-Cohen, S. & Wheelwright, S. The empathy quotient: an investigation of adults with Asperger syndrome or high functioning

autism, and normal sex differences. *J Autism Dev Disord* **34,** 163–175 (2004).

254. Bush, Luu & Posner. Cognitive and emotional influences in anterior cingulate cortex. *Trends Cogn. Sci.* **4,** 215–222 (2000).

255. Devinsky, O., Morrell, M. J. & Vogt, B. A. Contributions of anterior cingulate cortex to behaviour. *Brain* **118 (Pt 1),** 279–306 (1995).

256. Ritvo, R. A. *et al.* A scale to assist the diagnosis of autism and Asperger's disorder in adults (RAADS): a pilot study. *J Autism Dev Disord* **38,** 213–223 (2008).

257. Hoerst, M. *et al.* Correlation of glutamate levels in the anterior cingulate cortex with self-reported impulsivity in patients with borderline personality disorder and healthy controls. *Arch. Gen. Psychiatry* **67,** 946–954 (2010).

258. Schmaal, L., Goudriaan, A. E., van der Meer, J., van den Brink, W. & Veltman, D. J. The association between cingulate cortex glutamate concentration and delay discounting is mediated by resting state functional connectivity. *Brain Behav* **2,** 553–562 (2012).

259. Scholl, J. *et al.* Excitation and inhibition in anterior cingulate predict use of past experiences. *eLife Sciences* **6,** e20365 (2017).

260. Friston, K. J., Frith, C. D., Liddle, P. F. & Frackowiak, R. S. Functional connectivity: the principal-component analysis of large (PET) data sets. *J. Cereb. Blood Flow Metab.* **13,** 5–14 (1993).

261. Rogers, B. P., Morgan, V. L., Newton, A. T. & Gore, J. C. Assessing Functional Connectivity in the Human Brain by FMRI. *Magn Reson Imaging* **25,** 1347–1357 (2007).

262. Van den Heuvel, M. P. & Hulshoff Pol, H. E. Exploring the brain network: a review on resting-state fMRI functional connectivity. *Eur Neuropsychopharmacol* **20,** 519–534 (2010).

263. Wang, H. E. *et al.* A systematic framework for functional connectivity measures. *Front Neurosci* **8,** 405 (2014).

264. Buckner, R. L., Krienen, F. M. & Yeo, B. T. T. Opportunities and limitations of intrinsic functional connectivity MRI. *Nat Neurosci* **16,** 832–837 (2013).

265. Fox, M. D. & Raichle, M. E. Spontaneous fluctuations in brain activity observed with functional magnetic resonance imaging. *Nat. Rev. Neurosci.* **8,** 700–711 (2007).

266. Itahashi, T. *et al.* Altered network topologies and hub organization in adults with autism: a resting-state fMRI study. *PLoS ONE* **9,** e94115 (2014).

267. Di Martino, A. *et al.* The autism brain imaging data exchange: towards a large-scale evaluation of the intrinsic brain architecture in autism. *Mol Psychiatry* (2013).

268. Greicius, M. D., Krasnow, B., Reiss, A. L. & Menon, V. Functional connectivity in the resting brain: A network analysis of the default mode hypothesis. *Proc Natl Acad Sci U S A* **100,** 253–258 (2003).

269. Van Dijk, K. R. A. *et al.* Intrinsic functional connectivity as a tool for human connectomics: theory, properties, and optimization. *J. Neurophysiol.* **103,** 297–321 (2010).

270. Yan, C. *et al.* Spontaneous brain activity in the default mode network is sensitive to different resting-state conditions with limited cognitive load. *PLoS ONE* **4,** e5743 (2009).

271. Power, J. D., Barnes, K. A., Snyder, A. Z., Schlaggar, B. L. & Petersen, S. E. Spurious but systematic correlations in functional connectivity MRI networks arise from subject motion. *Neuroimage* **59,** 2142–2154 (2012).

272. Geurts, H. M., Luman, M. & van Meel, C. S. What's in a game: the effect of social motivation on interference control in boys with ADHD and autism spectrum disorders. *J Child Psychol Psychiatry* **49,** 848–857 (2008).

273. Jones, T. B. *et al.* Sources of group differences in functional connectivity: an investigation applied to autism spectrum disorder. *Neuroimage* **49,** 401–414 (2010).

274. Birn, R. M., Murphy, K. & Bandettini, P. A. The effect of respiration variations on independent component analysis results of resting state functional connectivity. *Hum Brain Mapp* **29,** 740–750 (2008).

275. Chang, C. & Glover, G. H. Relationship between respiration, end-tidal CO_2, and BOLD signals in resting-state fMRI. *Neuroimage* **47,** 1381–1393 (2009).

276. Havsteen, I. *et al.* Are Movement Artifacts in Magnetic Resonance Imaging a Real Problem?—A Narrative Review. *Front. Neurol.* **8,** (2017).

277. Satterthwaite, T. D. *et al.* An improved framework for confound regression and filtering for control of motion artifact in the preprocessing of resting-state functional connectivity data. *Neuroimage* **64,** 240–256 (2013).

278. Van Dijk, K. R. A., Sabuncu, M. R. & Buckner, R. L. The influence of head motion on intrinsic functional connectivity MRI. *Neuroimage* **59,** 431–438 (2012).

279. Biswal, B. B., Van Kylen, J. & Hyde, J. S. Simultaneous assessment of flow and BOLD signals in resting-state functional connectivity maps. *NMR Biomed* **10,** 165–170 (1997).

280. Jiang, T., He, Y., Zang, Y. & Weng, X. Modulation of functional connectivity during the resting state and the motor task. *Hum Brain Mapp* **22,** 63–71 (2004).

281. Li, K., Guo, L., Nie, J., Li, G. & Liu, T. Review of methods for functional brain connectivity detection using fMRI. *Comput Med Imaging Graph* **33,** 131–139 (2009).

282. Buckner, R. L. & Vincent, J. L. Unrest at rest: default activity and spontaneous network correlations. *Neuroimage* **37,** 1091–1096; discussion 1097-1099 (2007).

283. Beckmann, C. F., DeLuca, M., Devlin, J. T. & Smith, S. M. Investigations into resting-state connectivity using independent component analysis. *Philos Trans R Soc Lond B Biol Sci* **360,** 1001–1013 (2005).

284. Beckmann, C. F. & Smith, S. M. Probabilistic independent component analysis for functional magnetic resonance imaging. *IEEE Trans Med Imaging* **23,** 137–152 (2004).

285. De Luca, M., Beckmann, C. F., De Stefano, N., Matthews, P. M. & Smith, S. M. fMRI resting state networks define distinct modes of long-distance interactions in the human brain. *Neuroimage* **29,** 1359–1367 (2006).

286. Duncan, N. W. *et al.* Glutamate Concentration in the Medial Prefrontal Cortex Predicts Resting-State Cortical-Subcortical Functional Connectivity in Humans. *PLoS ONE* **8,** e60312 (2013).

287. Duncan, N. W., Enzi, B., Wiebking, C. & Northoff, G. Involvement of glutamate in rest-stimulus interaction between perigenual and supragenual anterior cingulate cortex: a combined fMRI-MRS study. *Hum Brain Mapp* **32,** 2172–2182 (2011).

288. Falkenberg, L. E., Westerhausen, R., Specht, K. & Hugdahl, K. Resting-state glutamate level in the anterior cingulate predicts blood-oxygen level-dependent response to cognitive control. *Proc. Natl. Acad. Sci. U.S.A.* **109,** 5069–5073 (2012).

289. Hu, Y., Chen, X., Gu, H. & Yang, Y. Resting-State Glutamate and GABA Concentrations Predict Task-Induced Deactivation in the Default Mode Network. *J. Neurosci.* **33,** 18566–18573 (2013).

290. Hunter, M. A. *et al.* Baseline effects of transcranial direct current stimulation on glutamatergic neurotransmission and large-scale network connectivity. *Brain Research* **1594,** 92–107 (2015).

291. Kapogiannis, D., Reiter, D. A., Willette, A. A. & Mattson, M. P. Posteromedial cortex glutamate and GABA predict intrinsic functional connectivity of the default mode network. *Neuroimage* **64,** 112–119 (2013).

292. Passow, S. *et al.* Default-mode network functional connectivity is closely related to metabolic activity. *Hum Brain Mapp* **36,** 2027–2038 (2015).

293. Wagner, G. *et al.* Resting state functional connectivity of the hippocampus along the anterior-posterior axis and its association with glutamatergic metabolism. *Cortex* **81,** 104–117 (2016).

294. Duncan, N. W., Wiebking, C. & Northoff, G. Associations of regional GABA and glutamate with intrinsic and extrinsic neural activity in humans—A review of multimodal imaging studies. *Neuroscience & Biobehavioral Reviews* **47,** 36–52 (2014).

295. Perez-Gomez, M., Junque, C., Mercader, J. M. & Berenguer, J. [Application of magnetic resonance spectroscopy in the study of brain disease]. *Rev Neurol* **30,** 155–60 (2000).

296. Sehm, B. *et al.* Dynamic modulation of intrinsic functional connectivity by transcranial direct current stimulation. *J. Neurophysiol.* **108,** 3253–3263 (2012).

297. Keeser, D. *et al.* Prefrontal transcranial direct current stimulation changes connectivity of resting-state networks during fMRI. *J. Neurosci.* **31,** 15284–15293 (2011).

298. Nitsche, M. A. & Paulus, W. Excitability changes induced in the human motor cortex by weak transcranial direct current stimulation. *J. Physiol. (Lond.)* **527 Pt 3,** 633–639 (2000).

299. Stagg, C. J. *et al.* Relationship between physiological measures of excitability and levels of glutamate and GABA in the human motor cortex. *J. Physiol. (Lond.)* **589,** 5845–5855 (2011).

300. Medeiros, L. F. *et al.* Neurobiological effects of transcranial direct current stimulation: a review. *Front Psychiatry* **3,** 110 (2012).

301. Clark, V. P., Coffman, B. A., Trumbo, M. C. & Gasparovic, C. Transcranial direct current stimulation (tDCS) produces localized and specific alterations in neurochemistry: A 1H magnetic resonance spectroscopy study. *Neuroscience Letters* **500,** 67–71 (2011).

302. Seeley, W. W. *et al.* Dissociable intrinsic connectivity networks for salience processing and executive control. *J. Neurosci* **27,** 2349–2356 (2007).

303. Sheth, S. A. *et al.* Human dorsal anterior cingulate cortex neurons mediate ongoing behavioural adaptation. *Nature* **488,** 218–221 (2012).

304. Fan, J., McCandliss, B. D., Fossella, J., Flombaum, J. I. & Posner, M. I. The activation of attentional networks. *Neuroimage* **26,** 471–479 (2005).

305. Barbas, H., Ghashghaei, H., Dombrowski, S. M. & Rempel-Clower, N. L. Medial prefrontal cortices are unified by common connections with superior temporal cortices and distinguished by input from memory-related areas in the rhesus monkey. *J. Comp. Neurol.* **410,** 343–367 (1999).

306. Dosenbach, N. U. F. *et al.* Distinct brain networks for adaptive and stable task control in humans. *PNAS* **104,** 11073–11078 (2007).

307. Menon, V. Large-scale brain networks and psychopathology: a unifying triple network model. *Trends Cogn. Sci. (Regul. Ed.)* **15,** 483–506 (2011).

308. Menon, V. & Uddin, L. Q. Saliency, switching, attention and control: a network model of insula function. *Brain Struct Funct* **214,** 655–667 (2010).

309. Passingham, R. *The Frontal Lobes and Voluntary Action.* (Oxford University Press, 1995).

310. Sridharan, D., Levitin, D. J. & Menon, V. A critical role for the right fronto-insular cortex in switching between central-executive and default-mode networks. *Proc. Natl. Acad. Sci. U.S.A.* **105,** 12569–12574 (2008).

311. Van den Heuvel, M. P. & Sporns, O. Rich-club organization of the human connectome. *J. Neurosci.* **31,** 15775–15786 (2011).

312. Zhao, Y. *et al.* Left Anterior Temporal Lobe and Bilateral Anterior Cingulate Cortex Are Semantic Hub Regions: Evidence from Behavior-Nodal Degree Mapping in Brain-Damaged Patients. *J. Neurosci.* **37,** 141–151 (2017).

313. Shenhav, A., Botvinick, M. M. & Cohen, J. D. The expected value of control: an integrative theory of anterior cingulate cortex function. *Neuron* **79,** 217–240 (2013).

314. Heilbronner, S. R. & Hayden, B. Y. Dorsal Anterior Cingulate Cortex: A Bottom-Up View. *Annu. Rev. Neurosci.* **39,** 149–170 (2016).

315. Vogt, B. A., Nimchinsky, E. A., Vogt, L. J. & Hof, P. R. Human cingulate cortex: Surface features, flat maps, and cytoarchitecture. *J. Comp. Neurol.* **359,** 490–506 (1995).

316. Yarkoni, T. *et al.* Sustained neural activity associated with cognitive control during temporally extended decision making. *Brain Res Cogn Brain Res* **23,** 71–84 (2005).

317. Vogt, B. A. *Cingulate neurobiology and disease / edited by Brent A. Vogt.* (Oxford ; New York : Oxford University Press, 2009).

318. Ridderinkhof, K. R., Ullsperger, M., Crone, E. A. & Nieuwenhuis, S. The Role of the Medial Frontal Cortex in Cognitive Control. *Science* **306,** 443–447 (2004).

319. Etkin, A., Egner, T., Peraza, D. M., Kandel, E. R. & Hirsch, J. Resolving emotional conflict: a role for the rostral anterior cingulate cortex in modulating activity in the amygdala. *Neuron* **51,** 871–882 (2006).

320. Floden, D. & Stuss, D. T. Inhibitory control is slowed in patients with right superior medial frontal damage. *J Cogn Neurosci* **18,** 1843–1849 (2006).

321. Kennerley, S. W., Dahmubed, A. F., Lara, A. H. & Wallis, J. D. Neurons in the Frontal Lobe Encode the Value of Multiple Decision Variables. *J Cogn Neurosci* **21,** 1162–1178 (2009).

322. Kennerley, S. W., Walton, M. E., Behrens, T. E. J., Buckley, M. J. & Rushworth, M. F. S. Optimal decision making and the anterior cingulate cortex. *Nat Neurosci* **9,** 940–947 (2006).

323. Shenhav, A., Cohen, J. D. & Botvinick, M. M. Dorsal anterior cingulate cortex and the value of control. *Nat Neurosci* **19,** 1286–1291 (2016).

324. Rushworth, M. F. S., Walton, M. E., Kennerley, S. W. & Bannerman, D. M. Action sets and decisions in the medial frontal cortex. *Trends Cogn. Sci. (Regul. Ed.)* **8,** 410–417 (2004).

325. Carter, C. S. *et al.* Anterior Cingulate Cortex, Error Detection, and the Online Monitoring of Performance. *Science* **280,** 747–749 (1998).

326. Cohen, J. D., Botvinick, M. & Carter, C. S. Anterior cingulate and prefrontal cortex: who's in control? *Nat Neurosci* **3,** 421–423 (2000).

327. Nee, D. E., Jonides, J. & Berman, M. G. Neural Mechanisms of Proactive Interference-Resolution. *Neuroimage* **38,** 740–751 (2007).

328. Botvinick, M., Nystrom, L. E., Fissell, K., Carter, C. S. & Cohen, J. D. Conflict monitoring versus selection-for-action in anterior cingulate cortex. *Nature* **402,** 179–181 (1999).

329. MacDonald, A. W., 3rd, Cohen, J. D., Stenger, V. A. & Carter, C. S. Dissociating the role of the dorsolateral prefrontal and anterior cingulate cortex in cognitive control. *Science* **288,** 1835–1838 (2000).

330. Barch, D. M., Braver, T. S., Sabb, F. W. & Noll, D. C. Anterior cingulate and the monitoriing of response conflict: evidence from an fMRI study of overt verb generation. *J Cogn Neurosci* **12,** 298–309 (2000).

331. Ebitz, R. B. & Platt, M. L. Neuronal activity in primate dorsal anterior cingulate cortex signals task conflict and predicts adjustments in pupil-linked arousal. *Neuron* **85,** 628–640 (2015).

332. Michelet, T. *et al.* Electrophysiological Correlates of a Versatile Executive Control System in the Monkey Anterior Cingulate Cortex. *Cereb. Cortex* bhv004 (2015).

333. Botvinick, M. M. Conflict monitoring and decision making: reconciling two perspectives on anterior cingulate function. *Cogn Affect Behav Neurosci* **7,** 356–366 (2007).

334. Kerns, J. G. Anterior cingulate and prefrontal cortex activity in an FMRI study of trial-to-trial adjustments on the Simon task. *Neuroimage* **33,** 399–405 (2006).

335. Matsumoto, K. & Tanaka, K. Conflict and Cognitive Control. *Science* **303,** 969–970 (2004).

336. Botvinick, M. M., Cohen, J. D. & Carter, C. S. Conflict monitoring and anterior cingulate cortex: an update. *Trends Cogn. Sci. (Regul. Ed.)* **8,** 539–546 (2004).

337. Egner, T. & Hirsch, J. Cognitive control mechanisms resolve conflict through cortical amplification of task-relevant information. *Nat Neurosci* **8,** 1784–1790 (2005).

338. Fan, J., Flombaum, J. I., McCandliss, B. D., Thomas, K. M. & Posner, M. I. Cognitive and brain consequences of conflict. *Neuroimage* **18,** 42–57 (2003).

339. Van Veen, V. & Carter, C. S. The anterior cingulate as a conflict monitor: fMRI and ERP studies. *Physiol. Behav.* **77,** 477–482 (2002).

340. Magno, E., Foxe, J. J., Molholm, S., Robertson, I. H. & Garavan, H. The Anterior Cingulate and Error Avoidance. *J. Neurosci.* **26,** 4769–4773 (2006).

341. O'Reilly, J. X. *et al.* Dissociable effects of surprise and model update in parietal and anterior cingulate cortex. *Proc. Natl. Acad. Sci. U.S.A.* **110,** E3660-3669 (2013).

342. Holroyd, C. B. & Coles, M. G. H. The neural basis of human error processing: reinforcement learning, dopamine, and the error-related negativity. *Psychol Rev* **109,** 679–709 (2002).

343. Brown, J. W. & Braver, T. S. Learned predictions of error likelihood in the anterior cingulate cortex. *Science* **307,** 1118–1121 (2005).

344. Ito, S., Stuphorn, V., Brown, J. W. & Schall, J. D. Performance monitoring by the anterior cingulate cortex during saccade countermanding. *Science* **302,** 120–122 (2003).

345. Narayanan, N. S., Cavanagh, J. F., Frank, M. J. & Laubach, M. Common medial frontal mechanisms of adaptive control in humans and rodents. *Nat. Neurosci.* **16,** 1888–1895 (2013).

346. Ullsperger, M. & von Cramon, D. Y. Subprocesses of performance monitoring: a dissociation of error processing and response competition revealed by event-related fMRI and ERPs. *Neuroimage* **14,** 1387–1401 (2001).

347. Shackman, A. J. *et al.* The integration of negative affect, pain and cognitive control in the cingulate cortex. *Nat. Rev. Neurosci.* **12,** 154–167 (2011).

348. Rainville, P., Duncan, G. H., Price, D. D., Carrier, B. & Bushnell, M. C. Pain affect encoded in human anterior cingulate but not somatosensory cortex. *Science* **277,** 968–971 (1997).

349. Kawamoto, T. *et al.* Is dorsal anterior cingulate cortex activation in response to social exclusion due to expectancy violation? An fMRI study. *Front Evol Neurosci* **4,** (2012).

350. Eisenberger, N. I. & Lieberman, M. D. Why rejection hurts: a common neural alarm system for physical and social pain. *Trends in Cognitive Sciences* **8,** 294–300 (2004).

351. Hayden, B. Y., Pearson, J. M. & Platt, M. L. Fictive reward signals in the anterior cingulate cortex. *Science* **324,** 948–950 (2009).

352. Luk, C.-H. & Wallis, J. D. Dynamic Encoding of Responses and Outcomes by Neurons in Medial Prefrontal Cortex. *J. Neurosci.* **29,** 7526–7539 (2009).

353. Kennerley, S. W., Behrens, T. E. J. & Wallis, J. D. Double dissociation of value computations in orbitofrontal and anterior cingulate neurons. *Nat Neurosci* **14,** 1581–1589 (2011).

354. Botvinick, M. M. & Cohen, J. D. The Computational and Neural Basis of Cognitive Control: Charted Territory and New Frontiers. *Cognitive Science* **38,** 1249–1285 (2014).

355. Posner, M. I. & Snyder, C. R. R. Attention and Cognitive Control. in *Information Processing and Cognition: The Loyola Symposium* (ed. Solso, R. L.) (Lawrence Erlbaum, 1975).

356. Botvinick, M. & Braver, T. Motivation and cognitive control: from behavior to neural mechanism. *Annu Rev Psychol* **66,** 83–113 (2015).

357. Dixon, M. L. & Christoff, K. The decision to engage cognitive control is driven by expected reward-value: neural and behavioral evidence. *PLoS ONE* **7,** e51637 (2012).

358. Geurts, H. M., van den Bergh, S. F. W. M. & Ruzzano, L. Prepotent response inhibition and interference control in autism spectrum disorders: two meta-analyses. *Autism Res* **7,** 407–420 (2014).

359. Hosking, J. G., Cocker, P. J. & Winstanley, C. A. Dissociable contributions of anterior cingulate cortex and basolateral amygdala on a rodent cost/benefit decision-making task of cognitive effort. *Neuropsychopharmacology* **39,** 1558–1567 (2014).

360. Parvizi, J., Rangarajan, V., Shirer, W. R., Desai, N. & Greicius, M. D. The will to persevere induced by electrical stimulation of the human cingulate gyrus. *Neuron* **80,** 1359–1367 (2013).

361. Eriksen, B. A. & Eriksen, C. W. Effects of noise letters upon the identification of a target letter in a nonsearch task. *Perception & Psychophysics* **16,** 143–149 (1974).

362. Fan, J., Flombaum, J. I., McCandliss, B. D., Thomas, K. M. & Posner, M. I. Cognitive and brain consequences of conflict. *Neuroimage* **18,** 42–57 (2003).

363. Fan, J., McCandliss, B. D., Sommer, T., Raz, A. & Posner, M. I. Testing the efficiency and independence of attentional networks. *J Cogn Neurosci* **14,** 340–347 (2002).

364. Coles, M. G. H., Gratton, G. & Donchin, E. Detecting early communication: Using measures of movement-related potentials to illuminate human information processing. *Biological Psychology* **26,** 69– 89 (1988).

365. Eriksen, C. W. & Schultz, D. W. Information processing in visual search: A continuous flow conception and experimental results. *Perception & Psychophysics* **25,** 249–263 (1979).

366. Happé, F. & Frith, U. The weak coherence account: detail-focused cognitive style in autism spectrum disorders. *J Autism Dev Disord* **36,** 5– 25 (2006).

367. Robertson, A. E. & Simmons, D. R. The relationship between sensory sensitivity and autistic traits in the general population. *J Autism Dev Disord* **43,** 775–784 (2013).

368. Koldewyn, K., Jiang, Y. V., Weigelt, S. & Kanwisher, N. Global/local processing in autism: not a disability, but a disinclination. *J Autism Dev Disord* **43,** 2329–2340 (2013).

369. Shah, A. & Frith, U. Why Do Autistic Individuals Show Superior Performance on the Block Design Task? *Journal of Child Psychology and Psychiatry* **34,** 1351–1364 (1993).

370. Jachim, S., Warren, P. A., McLoughlin, N. & Gowen, E. Collinear facilitation and contour integration in autism: evidence for atypical visual integration. *Front Hum Neurosci* **9,** (2015).

371. Keehn, B., Nair, A., Lincoln, A. J., Townsend, J. & Müller, R.-A. Under- reactive but easily distracted: An fMRI investigation of attentional

capture in autism spectrum disorder. *Dev Cogn Neurosci* **17,** 46–56 (2016).

372. Murphy, J. W., Foxe, J. J., Peters, J. B. & Molholm, S. Susceptibility to distraction in autism spectrum disorder: probing the integrity of oscillatory alpha-band suppression mechanisms. *Autism Res* **7,** 442–458 (2014).

373. Vaidya Chandan J. *et al.* Controlling attention to gaze and arrows in childhood: an fMRI study of typical development and Autism Spectrum Disorders. *Developmental Science* **14,** 911–924 (2011).

374. Larson, M. J., South, M., Clayson, P. E. & Clawson, A. Cognitive control and conflict adaptation in youth with high-functioning autism. *J Child Psychol Psychiatry* **53,** 440–448 (2012).

375. Corbett, B. A., Constantine, L. J., Hendren, R., Rocke, D. & Ozonoff, S. Examining executive functioning in children with autism spectrum disorder, attention deficit hyperactivity disorder and typical development. *Psychiatry Res* **166,** 210–222 (2009).

376. Craig, F. *et al.* A review of executive function deficits in autism spectrum disorder and attention-deficit/hyperactivity disorder. *Neuropsychiatr Dis Treat* **12,** 1191–1202 (2016).

377. Luna, B., Garver, K. E., Urban, T. A., Lazar, N. A. & Sweeney, J. A. Maturation of Cognitive Processes From Late Childhood to Adulthood. *Child Development* **75,** 1357–1372 (2004).

378. Brodmann, K. *Vergleichende Lokalisationslehre der Grosshirnrinde in ihren Prinzipien dargestellt auf Grund des Zellenbaues*. (Johann Ambrosius Barth, 1909).

379. Mesulam, M. M. & Mufson, E. J. Insula of the old world monkey. III: Efferent cortical output and comments on function. *J. Comp. Neurol.* **212,** 38–52 (1982).

380. Margulies, D. S. *et al.* Mapping the functional connectivity of anterior cingulate cortex. *NeuroImage* **37,** 579–588 (2007).

381. Cao, W. *et al.* Resting-state functional connectivity in anterior cingulate cortex in normal aging. *Front Aging Neurosci* **6,** (2014).

382. Augustine, J. R. Circuitry and functional aspects of the insular lobe in primates including humans. *Brain Res. Brain Res. Rev.* **22,** 229–244 (1996).

383. Critchley, H. D., Wiens, S., Rotshtein, P., Ohman, A. & Dolan, R. J. Neural systems supporting interoceptive awareness. *Nat. Neurosci.* **7,** 189–195 (2004).

384. Geng, H., Li, X., Chen, J., Li, X. & Gu, R. Decreased Intra- and Inter-Salience Network Functional Connectivity is Related to Trait Anxiety in Adolescents. *Front Behav Neurosci* **9,** (2016).

385. Tu, P.-C. *et al.* Structural and functional correlates of a quantitative autistic trait measured using the social responsive scale in neurotypical male adolescents. *Autism Res* **9,** 570–578 (2016).

386. Andrews-Hanna, J. R., Smallwood, J. & Spreng, R. N. The default network and self-generated thought: component processes, dynamic control, and clinical relevance. *Ann N Y Acad Sci* **1316,** 29–52 (2014).

387. Han, Y. *et al.* [Effects of functional connectivity between anterior cingulate cortex and dorsolateral prefrontal cortex on executive control of attention in healthy individuals]. *Zhonghua Yi Xue Za Zhi* **93,** 995–998 (2013).

388. Dum, R. P. & Strick, P. L. The origin of corticospinal projections from the premotor areas in the frontal lobe. *J. Neurosci.* **11,** 667–689 (1991).

389. Dum, R. P. & Strick, P. L. Motor areas in the frontal lobe of the primate. *Physiology & Behavior* **77,** 677–682 (2002).

390. Dum, R. P. & Strick, P. L. Medial wall motor areas and skeletomotor control. *Current Opinion in Neurobiology* **2,** 836–839 (1992).

391. Picard, N. & Strick, P. L. Motor Areas of the Medial Wall: A Review of Their Location and Functional Activation. *Cereb. Cortex* **6,** 342–353 (1996).

392. Asemi, A., Ramaseshan, K., Burgess, A., Diwadkar, V. A. & Bressler, S. L. Dorsal anterior cingulate cortex modulates supplementary motor area in coordinated unimanual motor behavior. *Front Hum Neurosci* **9,** (2015).

393. Thaler, D., Chen, Y. C., Nixon, P. D., Stern, C. E. & Passingham, R. E. The functions of the medial premotor cortex. I. Simple learned movements. *Exp Brain Res* **102,** 445–460 (1995).

394. Crone, E. A., Wendelken, C., Donohue, S. E. & Bunge, S. A. Neural evidence for dissociable components of task-switching. *Cereb. Cortex* **16,** 475–486 (2006).

395. Fan, J. *et al.* Response anticipation and response conflict: an event-related potential and functional magnetic resonance imaging study. *J. Neurosci.* **27,** 2272–2282 (2007).

396. Kerns, J. G. *et al.* Anterior Cingulate Conflict Monitoring and Adjustments in Control. *Science* **303,** 1023–1026 (2004).

397. Weissman, D. H., Gopalakrishnan, A., Hazlett, C. J. & Woldorff, M. G. Dorsal anterior cingulate cortex resolves conflict from distracting stimuli by boosting attention toward relevant events. *Cereb. Cortex* **15,** 229–237 (2005).

398. Ohnishi, T. *et al.* Abnormal regional cerebral blood flow in childhood autism. *Brain* **123,** 1838–1844 (2000).

399. Jann, K. *et al.* Altered resting perfusion and functional connectivity of default mode network in youth with autism spectrum disorder. *Brain Behav* **5,** e00358 (2015).

400. Haznedar, M. M. *et al.* Limbic circuitry in patients with autism spectrum disorders studied with positron emission tomography and magnetic resonance imaging. *Am J Psychiatry* **157,** 1994–2001 (2000).

401. Chatton, J.-Y., Pellerin, L. & Magistretti, P. J. GABA uptake into astrocytes is not associated with significant metabolic cost: Implications for brain imaging of inhibitory transmission. *Proc Natl Acad Sci U S A* **100,** 12456–12461 (2003).

402. Ercińska, M. & Silver, I. A. Energy relationships between ATP synthesis and K+ gradients in cultured glial-derived cell line. *Acta Biochim. Pol.* **34,** 195–203 (1987).

403. Monaghan, D. T., Bridges, R. J. & Cotman, C. W. The excitatory amino acid receptors: their classes, pharmacology, and distinct properties in the function of the central nervous system. *Annu. Rev. Pharmacol. Toxicol.* **29,** 365–402 (1989).

404. Di Martino, A. *et al.* Functional Brain Correlates of Social and Non-Social Processes in Autism Spectrum Disorders: an ALE Meta-Analysis. *Biol Psychiatry* **65,** 63–74 (2009).

405. Delmonte, S. *et al.* Social and monetary reward processing in autism spectrum disorders. *Mol Autism* **3,** 7 (2012).

406. Delmonte, S., Gallagher, L., O'Hanlon, E., McGrath, J. & Balsters, J. H. Functional and structural connectivity of frontostriatal circuitry in Autism Spectrum Disorder. *Front Hum Neurosci* **7,** 430 (2013).

407. Velasquez, F. *et al.* Neural correlates of emotional inhibitory control in autism spectrum disorders. *Res Dev Disabil* **64,** 64–77 (2017).

408. Kana, R. K., Keller, T. A., Minshew, N. J. & Just, M. A. Inhibitory control in high-functioning autism: decreased activation and underconnectivity in inhibition networks. *Biol. Psychiatry* **62,** 198–206 (2007).

409. Agam, Y., Joseph, R. M., Barton, J. J. S. & Manoach, D. S. Reduced cognitive control of response inhibition by the anterior cingulate cortex in autism spectrum disorders. *Neuroimage* **52,** 336–347 (2010).

410. Baruth, J. M., Wall, C. A., Patterson, M. C. & Port, J. D. Proton Magnetic Resonance Spectroscopy as a Probe into the Pathophysiology of Autism Spectrum Disorders (ASD): A Review. *Autism Research* **6,** 119–133 (2013).

411. Haznedar, M. M. *et al.* Anterior cingulate gyrus volume and glucose metabolism in autistic disorder. *Am J Psychiatry* **154,** 1047–1050 (1997).

412. Bustillo, J. R. Use of proton magnetic resonance spectroscopy in the treatment of psychiatric disorders: a critical update. *Dialogues Clin Neurosci* **15,** 329–337 (2013).

413. Astrakas, L. G. & Argyropoulou, M. I. Key concepts in MR spectroscopy and practical approaches to gaining biochemical information in children. *Pediatr Radiol* **46,** 941–951 (2016).

414. Govindaraju, V., Young, K. & Maudsley, A. A. Proton NMR chemical shifts and coupling constants for brain metabolites. *NMR Biomed* **13,** 129–153 (2000).

415. Dager, S., Oskin, N., Richards, T. & Posse, S. Research Applications of Magnetic Resonance Spectroscopy (MRS) to Investigate Psychiatric Disorders. *Top Magn Reson Imaging* **19,** 81–96 (2008).

416. Eriksen, C. W. The flankers task and response competition: A useful tool for investigating a variety of cognitive problems. *Visual Cognition* **2,** 101–118 (1995).

417. Fan, J. *et al.* Testing the behavioral interaction and integration of attentional networks. *Brain and Cognition* **70,** 209–220 (2009).

418. Sanderson, C. & Allen, M. L. The specificity of inhibitory impairments in autism and their relation to ADHD-type symptoms. *J Autism Dev Disord* **43,** 1065–1079 (2013).

419. Wager, T. D. & Smith, E. E. Neuroimaging studies of working memory: a meta-analysis. *Cogn Affect Behav Neurosci* **3,** 255–274 (2003).

420. Posner, M. I. Orienting of attention. *Q J Exp Psychol* **32,** 3–25 (1980).

421. Posner, M. I., Walker, J. A., Friedrich, F. J. & Rafal, R. D. Effects of parietal injury on covert orienting of attention. *J. Neurosci.* **4,** 1863–1874 (1984).

422. American Psychiatric Association, American Psychiatric Association & Task Force on DSM-IV. *Diagnostic and statistical manual of mental disorders: DSM-IV-TR.* (American Psychiatric Association, 2000).

423. Garretson, H. B., Fein, D. & Waterhouse, L. Sustained attention in children with autism. *J Autism Dev Disord* **20,** 101–114 (1990).

424. Ozonoff, S. Reliability and validity of the Wisconsin Card Sorting Test in studies of autism. *Neuropsychology* **9,** 491–500 (1995).

425. Kenworthy, L., Yerys, B. E., Anthony, L. G. & Wallace, G. L. Understanding executive control in autism spectrum disorders in the lab and in the real world. *Neuropsychol Rev* **18,** 320–338 (2008).

426. Hanson, L. G. *Introduction to Magnetic Resonance Imaging Techniques.* (2009).

427. Moser, E., Stadlbauer, A., Windischberger, C., Quick, H. H. & Ladd, M. E. Magnetic resonance imaging methodology. *Eur J Nucl Med Mol Imaging* **36,** 30 (2009).

428. Berger, A. Magnetic resonance imaging. *BMJ* **324,** 35 (2002).

429. Gore, J. C. Principles and practice of functional MRI of the human brain. *J Clin Invest* **112,** 4–9 (2003).

430. Symms, M., Jager, H., Schmierer, K. & Yousry, T. A review of structural magnetic resonance neuroimaging. *J Neurol Neurosurg Psychiatry* **75,** 1235–1244 (2004).

431. Damoiseaux, J. S. & Greicius, M. D. Greater than the sum of its parts: a review of studies combining structural connectivity and resting-state functional connectivity. *Brain Struct Funct* **213,** 525–533 (2009).

432. Murphy, K. J. & Brunberg, J. A. Adult claustrophobia, anxiety and sedation in MRI. *Magnetic Resonance Imaging* **15,** 51–54 (1997).

433. Sarji, S. A., Abdullah, B. J. J., Kumar, G., Tan, A. H. & Narayanan, P. Failed magnetic resonance imaging examinations due to claustrophobia. *Australasian Radiology* **42,** 293–295 (1998).

434. Grey, S. J., Price, G. & Mathews, A. Reduction of anxiety during MR imaging: a controlled trial. *Magnetic Resonance Imaging* **18,** 351–355 (2000).

435. Ogawa, S., Lee, T. M., Kay, A. R. & Tank, D. W. Brain magnetic resonance imaging with contrast dependent on blood oxygenation. *PNAS* **87,** 9868–9872 (1990).

436. Logothetis, N. K. MR imaging in the non-human primate: studies of function and of dynamic connectivity. *Curr. Opin. Neurobiol.* **13,** 630–642 (2003).

437. Pauling, L. & Coryell, C. D. The Magnetic Properties and Structure of Hemoglobin, Oxyhemoglobin and Carbonmonoxyhemoglobin. *Proc Natl Acad Sci U S A* **22,** 210–216 (1936).

438. Ogawa, S. *et al.* Functional brain mapping by blood oxygenation level-dependent contrast magnetic resonance imaging. A comparison of signal characteristics with a biophysical model. *Biophys. J.* **64,** 803–812 (1993).

439. Murphy, K., Bodurka, J. & Bandettini, P. A. How long to scan? The relationship between fMRI temporal signal to noise ratio and necessary scan duration. *NeuroImage* **34,** 565–574 (2007).

440. Belliveau, J. W. *et al.* Functional mapping of the human visual cortex by magnetic resonance imaging. *Science* **254,** 716–719 (1991).

441. Maddock, R. J. & Buonocore, M. H. MR spectroscopic studies of the brain in psychiatric disorders. *Curr Top Behav Neurosci* **11,** 199–251 (2012).

442. Ross, B. & Bluml, S. Magnetic resonance spectroscopy of the human brain. *Anat. Rec.* **265,** 54–84 (2001).

443. Friedman, S. D., Mathis, C. M., Hayes, C., Renshaw, P. & Dager, S. R. Brain pH response to hyperventilation in panic disorder: preliminary evidence for altered acid-base regulation. *Am J Psychiatry* **163,** 710–715 (2006).

444. Strózik-Kotlorz, D. Magnetic resonance spectroscopy of the human brain. *Phys. Part. Nuclei* **45,** 347–348 (2014).

445. Provencher, S. W. Estimation of metabolite concentrations from localized in vivo proton NMR spectra. *Magn Reson Med* **30,** 672–679 (1993).

446. Naressi, A. *et al.* Java-based graphical user interface for the MRUI quantitation package. *MAGMA* **12,** 141–152 (2001).

447. Govindaraju, V., Basus, V. J., Matson, G. B. & Maudsley, A. A. Measurement of chemical shifts and coupling constants for glutamate and glutamine. *Magn Reson Med* **39,** 1011–1013 (1998).

448. Zhu, H. & Barker, P. B. MR Spectroscopy and Spectroscopic Imaging of the Brain. *Methods Mol Biol* **711,** 203–226 (2011).

449. Balteau, E., Hutton, C. & Weiskopf, N. Improved shimming for fMRI specifically optimizing the local BOLD sensitivity. *Neuroimage* **49,** 327–336 (2010).

450. Tkác, I. *et al.* Highly resolved in vivo 1H NMR spectroscopy of the mouse brain at 9.4 T. *Magn Reson Med* **52,** 478–484 (2004).

451. Provencher, S. W. LCModel & LCMgui User's Manual. (2014).

452. Doyle-Thomas, K. A. R. *et al.* Metabolic mapping of deep brain structures and associations with symptomatology in autism spectrum disorders. *Research in Autism Spectrum Disorders* **8,** 44–51 (2014).

453. Ross, B. D. Biochemical considerations in 1H spectroscopy. Glutamate and glutamine; Myo-inositol and related metabolites. *NMR in Biomedicine* **4,** 59–63 (1991).

454. Shimmura, C. *et al.* Enzymes in the glutamate-glutamine cycle in the anterior cingulate cortex in postmortem brain of subjects with autism. *Molecular Autism* **4,** 6 (2013).

455. Bartha, R., Drost, D. J., Menon, R. S. & Williamson, P. C. Comparison of the quantification precision of human short echo time 1H spectroscopy at 1.5 and 4.0 Tesla. *Magn. Reson. Med.* **44,** 185–192 (2000).

456. Prost, R. W., Mark, L., Mewissen, M. & Li, S. J. Detection of glutamate/glutamine resonances by 1H magnetic resonance spectroscopy at 0.5 tesla. *Magn Reson Med* **37,** 615–618 (1997).

457. Stanley, J. A. In vivo magnetic resonance spectroscopy and its application to neuropsychiatric disorders. *Can J Psychiatry* **47,** 315–326 (2002).

458. Juchem, C. & de Graaf, R. A. B0 magnetic field homogeneity and shimming for in vivo magnetic resonance spectroscopy. *Analytical Biochemistry* **529,** 17–29 (2017).

459. Tkác, I. *et al.* In vivo 1H NMR spectroscopy of the human brain at 7 T. *Magn Reson Med* **46,** 451–456 (2001).

460. Tkáč, I. & Gruetter, R. Methodology of H NMR Spectroscopy of the Human Brain at Very High Magnetic Fields. *Appl Magn Reson* **29,** 139–157 (2005).

461. Michaelis, T., Merboldt, K. D., Bruhn, H., Hänicke, W. & Frahm, J. Absolute concentrations of metabolites in the adult human brain in vivo: quantification of localized proton MR spectra. *Radiology* **187,** 219–227 (1993).

462. Barker, P. B., Hearshen, D. O. & Boska, M. D. Single-voxel proton MRS of the human brain at 1.5T and 3.0T. *Magn Reson Med* **45,** 765–769 (2001).

463. Mullins, P. G. *et al.* Reproducibility of 1H-MRS measurements in schizophrenic patients. *Magn. Reson. Med.* **50,** 704–707 (2003).

464. Bottomley, P. A. Spatial localization in NMR spectroscopy in vivo. *Ann. N. Y. Acad. Sci.* **508,** 333–348 (1987).

465. Frahm, J., Merboldt, K.-D. & Hänicke, W. Localized proton spectroscopy using stimulated echoes. *Journal of Magnetic Resonance (1969)* **72,** 502–508 (1987).

466. Lin, F.-H. *et al.* Sensitivity-encoded (SENSE) proton echo-planar spectroscopic imaging (PEPSI) in the human brain. *Magn Reson Med* **57,** 249–257 (2007).

467. Moonen, C. T. *et al.* Comparison of single-shot localization methods (STEAM and PRESS) for in vivo proton NMR spectroscopy. *NMR Biomed* **2,** 201–208 (1989).

468. Yang, S., Hu, J., Kou, Z. & Yang, Y. Spectral simplification for resolved glutamate and glutamine measurement using a standard STEAM sequence with optimized timing parameters at 3, 4, 4.7, 7, and 9.4T. *Magn Reson Med* **59,** 236–244 (2008).

469. Amaro, E., Jr & Barker, G. J. Study design in fMRI: basic principles. *Brain Cogn* **60,** 220–232 (2006).

470. Kousi, E., Tsougos, I. & Eftychi, K. Proton Magnetic Resonance Spectroscopy of the Central Nervous System. in *Novel Frontiers of Advanced Neuroimaging* (ed. Fountas, K.) (InTech, 2013).

471. Sartorius, A. *et al.* Proton magnetic resonance spectroscopic creatine correlates with creatine transporter protein density in rat brain. *Journal of Neuroscience Methods* **172,** 215–219 (2008).

472. Li, B. S. Y., Babb, J. S., Soher, B. J., Maudsley, A. A. & Gonen, O. Reproducibility of 3D proton spectroscopy in the human brain. *Magn. Reson. Med.* **47,** 439–446 (2002).

473. Fujii, E. *et al.* Function of the frontal lobe in autistic individuals: a proton magnetic resonance spectroscopic study. *J. Med. Invest.* **57,** 35–44 (2010).

474. Levitt, J. G. *et al.* Proton magnetic resonance spectroscopic imaging of the brain in childhood autism. *Biol. Psychiatry* **54,** 1355–1366 (2003).

475. Vasconcelos, M. M. *et al.* Proton magnetic resonance spectroscopy in school-aged autistic children. *J Neuroimaging* **18,** 288–295 (2008).

476. Ipser, J. C. *et al.* 1H-MRS in autism spectrum disorders: a systematic meta-analysis. *Metab Brain Dis* **27,** 275–287 (2012).

477. Murphy DM, Critchley HD, Schmitz N & et al. Asperger syndrome: A proton magnetic resonance spectroscopy study of brain. *Arch Gen Psychiatry* **59,** 885–891 (2002).

478. Zhu, H. & Barker, P. B. MR Spectroscopy and Spectroscopic Imaging of the Brain. *Methods Mol Biol* **711,** 203–226 (2011).

479. Drost, D. J., Riddle, W. R., Clarke, G. D. & AAPM MR Task Group #9. Proton magnetic resonance spectroscopy in the brain: report of AAPM MR Task Group #9. *Med Phys* **29,** 2177–2197 (2002).

480. Stanley, J. A., Drost, D. J., Williamson, P. C. & Thompson, R. T. The use of a priori knowledge to quantify short echo in vivo 1H MR spectra. *Magn Reson Med* **34,** 17–24 (1995).

481. Zhong, K. & Ernst, T. Localized in vivo human 1H MRS at very short echo times. *Magn Reson Med* **52,** 898–901 (2004).

482. Hancu, I. Optimized glutamate detection at 3T. *J. Magn. Reson. Imaging* **30,** 1155–1162 (2009).

483. Yahya, A., Mädler, B. & Fallone, B. G. Exploiting the chemical shift displacement effect in the detection of glutamate and glutamine (Glx) with PRESS. *J. Magn. Reson.* **191,** 120–127 (2008).

484. Schubert, F., Gallinat, J., Seifert, F. & Rinneberg, H. Glutamate concentrations in human brain using single voxel proton magnetic resonance spectroscopy at 3 Tesla. *Neuroimage* **21,** 1762–1771 (2004).

485. Jang, D.-P. *et al.* Interindividual reproducibility of glutamate quantification using 1.5-T proton magnetic resonance spectroscopy. *Magn. Reson. Med.* **53,** 708–712 (2005).

486. Mullins, P. G., Chen, H., Xu, J., Caprihan, A. & Gasparovic, C. Comparative reliability of proton spectroscopy techniques designed to improve detection of J-coupled metabolites. *Magn Reson Med* **60,** 964–969 (2008).

487. Buggy, D. J., Nicol, B., Rowbotham, D. J. & Lambert, D. G. Effects of intravenous anesthetic agents on glutamate release: a role for GABAA receptor-mediated inhibition. *Anesthesiology* **92,** 1067–1073 (2000).

488. Zhang, H. *et al.* Effect of propofol on the levels of neurotransmitters in normal human brain: A magnetic resonance spectroscopy study. *Neuroscience Letters* **467,** 247–251 (2009).

489. Xin, L. & Tkáč, I. A practical guide to in vivo proton magnetic resonance spectroscopy at high magnetic fields. *Analytical Biochemistry* **529,** 30–39 (2017).

490. Ramadan, S., Lin, A. & Stanwell, P. Glutamate and Glutamine: A Review of In Vivo MRS in the Human Brain. *NMR Biomed* **26,** (2013).

491. Rae, C. D. A guide to the metabolic pathways and function of metabolites observed in human brain 1H magnetic resonance spectra. *Neurochem. Res.* **39,** 1–36 (2014).

492. Tallan, H. H. Studies on the distribution of N-acetyl-L-aspartic acid in brain. *J. Biol. Chem.* **224,** 41–45 (1957).

493. Tallan, H. H., Moore, S. & Stein, W. H. N-Acetyl-L-aspartic acid in brain. *J. Biol. Chem.* **219,** 257–264 (1956).

494. Koller, K. J., Zaczek, R. & Coyle, J. T. N-Acetyl-Aspartyl-Glutamate: Regional Levels in Rat Brain and the Effects of Brain Lesions as Determined by a New HPLC Method. *Journal of Neurochemistry* **43,** 1136–1142 (1984).

495. Simmons, M. L., Frondoza, C. G. & Coyle, J. T. Immunocytochemical localization of N-acetyl-aspartate with monoclonal antibodies. *Neuroscience* **45,** 37–45 (1991).

496. Urenjak, J., Williams, S. R., Gadian, D. G. & Noble, M. Specific expression of N-acetylaspartate in neurons, oligodendrocyte-type-2 astrocyte progenitors, and immature oligodendrocytes in vitro. *J. Neurochem.* **59,** 55–61 (1992).

497. Urenjak, J., Williams, S. R., Gadian, D. G. & Noble, M. Proton nuclear magnetic resonance spectroscopy unambiguously identifies different neural cell types. *J. Neurosci.* **13,** 981–989 (1993).

498. Tyson, R. L. & Sutherland, G. R. Labeling of N-acetylaspartate and N-acetylaspartylglutamate in rat neocortex, hippocampus and cerebellum from [1-13C]glucose. *Neuroscience Letters* **251,** 181–184 (1998).

499. Baslow, M. H. Functions of N-acetyl-L-aspartate and N-acetyl-L-aspartylglutamate in the vertebrate brain: role in glial cell-specific signaling. *J. Neurochem.* **75,** 453–459 (2000).

500. Passani, L., Elkabes, S. & Coyle, J. T. Evidence for the presence of N-acetylaspartylglutamate in cultured oligodendrocytes and LPS activated microglia. *Brain Research* **794,** 143–145 (1998).

501. Edden, R. A. E., Pomper, M. G. & Barker, P. B. In vivo differentiation of N-acetyl aspartyl glutamate from N-acetyl aspartate at 3 Tesla. *Magn Reson Med* **57,** 977–982 (2007).

502. Pouwels, P. J. & Frahm, J. Differential distribution of NAA and NAAG in human brain as determined by quantitative localized proton MRS. *NMR Biomed* **10,** 73–78 (1997).

503. Soares, D. P. & Law, M. Magnetic resonance spectroscopy of the brain: review of metabolites and clinical applications. *Clinical Radiology* **64,** 12–21 (2009).

504. Suzuki, K. *et al.* Metabolite alterations in the hippocampus of high-functioning adult subjects with autism. *Int. J. Neuropsychopharmacol.* **13,** 529–534 (2010).

505. Goji, A. *et al.* Assessment of Anterior Cingulate Cortex (ACC) and Left Cerebellar Metabolism in Asperger's Syndrome with Proton Magnetic Resonance Spectroscopy (MRS). *PLoS One* **12,** (2017).

506. Nelson, S. J. Multivoxel magnetic resonance spectroscopy of brain tumors. *Mol. Cancer Ther.* **2,** 497–507 (2003).

507. Bertholdo, D., Watcharakorn, A. & Castillo, M. Brain proton magnetic resonance spectroscopy: introduction and overview. *Neuroimaging Clin. N. Am.* **23,** 359–380 (2013).

508. Gabis, L. *et al.* 1H-Magnetic Resonance Spectroscopy Markers of Cognitive and Language Ability in Clinical Subtypes of Autism Spectrum Disorders. *J Child Neurol* **23,** 766–774 (2008).

509. McBride, D. Q. *et al.* Analysis of brain tumors using 1H magnetic resonance spectroscopy. *Surg Neurol* **44,** 137–144 (1995).

510. Chang, L. *et al.* Localized in vivo 1H magnetic resonance spectroscopy and in vitro analyses of heterogeneous brain tumors. *J Neuroimaging* **5,** 157–163 (1995).

511. Blüml, S., Seymour, K. J. & Ross, B. D. Developmental changes in choline- and ethanolamine-containing compounds measured with proton-decoupled (31)P MRS in in vivo human brain. *Magn Reson Med* **42,** 643–654 (1999).

512. Oner, O. *et al.* Proton MR spectroscopy: higher right anterior cingulate N-acetylaspartate/choline ratio in Asperger syndrome compared with healthy controls. *AJNR Am J Neuroradiol* **28,** 1494–1498 (2007).

513. Brand, A., Richter-Landsberg, C. & Leibfritz, D. Multinuclear NMR studies on the energy metabolism of glial and neuronal cells. *Dev. Neurosci.* **15,** 289–298 (1993).

514. Strange, K., Emma, F., Paredes, A. & Morrison, R. Osmoregulatory changes in myo-inositol content and Na+/myo-inositol cotransport in rat cortical astrocytes. *Glia* **12,** 35–43 (1994).

515. Lin, A., Ross, B. D., Harris, K. & Wong, W. Efficacy of Proton Magnetic Resonance Spectroscopy in Neurological Diagnosis and Neurotherapeutic Decision Making. *NeuroRx* **2,** 197–214 (2005).

516. Lord, C. *et al.* Autism diagnostic observation schedule: a standardized observation of communicative and social behavior. *J Autism Dev Disord* **19,** 185–212 (1989).

517. Lord, C. *et al.* The autism diagnostic observation schedule-generic: a standard measure of social and communication deficits associated with the spectrum of autism. *J Autism Dev Disord* **30,** 205–223 (2000).

518. Vllasaliu, L. *et al.* Diagnostic instruments for autism spectrum disorder (ASD). in *Cochrane Database of Systematic Reviews* (John Wiley & Sons, Ltd, 2016).

519. Molloy, C. A., Murray, D. S., Akers, R., Mitchell, T. & Manning-Courtney, P. Use of the Autism Diagnostic Observation Schedule (ADOS) in a clinical setting. *Autism* **15,** 143–162 (2011).

520. PsychCorp. *WASI Manual; Wechsler Abbreviated Scale of Intelligence Manual.* (Harcourt Assessment, Inc., 1999).

521. Wechsler, D. *Manual for the Wechsler Adult Intelligence Scale.* **vi,** (Psychological Corp., 1955).

522. McCrimmon, A. W. & Smith, A. D. Review of the Wechsler Abbreviated Scale of Intelligence, Second Edition (WASI-II). *Journal of Psychoeducational Assessment* **31,** 337–341 (2013).

523. Kaplan, R. M. & Saccuzzo, D. P. *Psychological Testing: Principles, Applications, and Issues.* (Wadsworth Publishing, 2017).

524. Taylor, J. L. & Seltzer, M. M. Employment and post-secondary educational activities for young adults with autism spectrum disorders during the transition to adulthood. *J Autism Dev Disord* **41,** 566–574 (2011).

525. Hillier, A. *et al.* Two-Year Evaluation of a Vocational Support Program for Adults on the Autism Spectrum. *Career Development for Exceptional Individuals* **30,** 35–47 (2007).

526. Hendricks, D. Employment and adults with autism spectrum disorders: Challenges and strategies for success. *Journal of Vocational Rehabilitation* **32,** 125–134 (2010).

527. De Stefano, N., Matthews, P. M. & Arnold, D. L. Reversible decreases in N-acetylaspartate after acute brain injury. *Magn Reson Med* **34,** 721–727 (1995).

528. Kalra, S., Cashman, N. R., Genge, A. & Arnold, D. L. Recovery of N-acetylaspartate in corticomotor neurons of patients with ALS after riluzole therapy. *Neuroreport* **9,** 1757–1761 (1998).

529. Salo, R. *et al.* Extended findings of brain metabolite normalization in MA-dependent subjects across sustained abstinence: a proton MRS study. *Drug Alcohol Depend* **113,** 133–138 (2011).

530. Narayanan, S. *et al.* Axonal metabolic recovery in multiple sclerosis patients treated with interferon beta-1b. *J. Neurol.* **248,** 979–986 (2001).

531. Yoon, S. J. *et al.* Neurochemical alterations in methamphetamine-dependent patients treated with cytidine-5'-diphosphate choline: a longitudinal proton magnetic resonance spectroscopy study. *Neuropsychopharmacology* **35,** 1165–1173 (2010).

532. Moffett, J. R., Ross, B., Arun, P., Madhavarao, C. N. & Namboodiri, M. A. A. N-Acetylaspartate in the CNS: From Neurodiagnostics to Neurobiology. *Prog Neurobiol* **81,** 89–131 (2007).

533. Fujii, E. *et al.* Function of the frontal lobe in autistic individuals: a proton magnetic resonance spectroscopic study. *The Journal of Medical Investigation* **57,** 35–44 (2010).

534. Musazzi, L. *et al.* Acute stress increases depolarization-evoked glutamate release in the rat prefrontal/frontal cortex: the dampening action of antidepressants. *PLoS ONE* **5,** e8566 (2010).

535. Tarazi, F. I., Baldessarini, R. J., Kula, N. S. & Zhang, K. Long-term effects of olanzapine, risperidone, and quetiapine on ionotropic glutamate receptor types: implications for antipsychotic drug treatment. *J. Pharmacol. Exp. Ther.* **306,** 1145–1151 (2003).

536. Gołembiowska, K. & Dziubina, A. Effect of acute and chronic administration of citalopram on glutamate and aspartate release in the rat prefrontal cortex. *Pol J Pharmacol* **52,** 441–448 (2000).

537. Yang, J. & Shen, J. In vivo evidence for reduced cortical glutamate–glutamine cycling in rats treated with the antidepressant/antipanic drug phenelzine. *Neuroscience* **135,** 927–937 (2005).

538. MOORE, C. M. *et al.* Glutamine and Glutamate Levels in Children and Adolescents With Bipolar Disorder: A 4.0-T Proton Magnetic Resonance Spectroscopy Study of the Anterior Cingulate Cortex. *J Am Acad Child Adolesc Psychiatry* **46,** 524–534 (2007).

539. Petroff, O. A., Rothman, D. L., Behar, K. L., Hyder, F. & Mattson, R. H. Effects of valproate and other antiepileptic drugs on brain glutamate, glutamine, and GABA in patients with refractory complex partial seizures. *Seizure* **8,** 120–127 (1999).

540. Rosenberg, D. R. *et al.* Decrease in Caudate Glutamatergic Concentrations in Pediatric Obsessive-Compulsive Disorder Patients Taking Paroxetine. *Journal of the American Academy of Child & Adolescent Psychiatry* **39,** 1096–1103 (2000).

541. Fu, Y. *et al.* Fluvoxamine increased glutamate release by activating both 5-HT3 and sigma-1 receptors in prelimbic cortex of chronic restraint stress C57BL/6 mice. *Biochimica et Biophysica Acta (BBA) - Molecular Cell Research* **1823,** 826–837 (2012).

542. Reznikov, L. R. *et al.* Acute stress-mediated increases in extracellular glutamate levels in the rat amygdala: differential effects of antidepressant treatment. *Eur. J. Neurosci.* **25,** 3109–3114 (2007).

543. Fu, C. H. Y. *et al.* Attenuation of the neural response to sad faces in major depression by antidepressant treatment: a prospective, event-related functional magnetic resonance imaging study. *Arch. Gen. Psychiatry* **61,** 877–889 (2004).

544. Ametamey, S. M. *et al.* Human PET studies of metabotropic glutamate receptor subtype 5 with 11C-ABP688. *J. Nucl. Med.* **48,** 247–252 (2007).

545. Bozkurt, A. *et al.* Distributions of transmitter receptors in the macaque cingulate cortex. *Neuroimage* **25,** 219–229 (2005).

546. Palomero-Gallagher, N., Vogt, B. A., Schleicher, A., Mayberg, H. S. & Zilles, K. Receptor architecture of human cingulate cortex: evaluation of the four-region neurobiological model. *Hum Brain Mapp* **30,** 2336–2355 (2009).

547. Allen, G. & Courchesne, E. Attention function and dysfunction in autism. *Front. Biosci.* **6,** D105-119 (2001).

548. Luna, B., Doll, S. K., Hegedus, S. J., Minshew, N. J. & Sweeney, J. A. Maturation of Executive Function in Autism. *Biological Psychiatry* **61,** 474–481 (2007).

549. Silk, T. J. *et al.* Visuospatial processing and the function of prefrontal-parietal networks in autism spectrum disorders: a functional MRI study. *Am J Psychiatry* **163,** 1440–1443 (2006).

550. Solomon, M., Ozonoff, S., Carter, C. & Caplan, R. Formal thought disorder and the autism spectrum: relationship with symptoms, executive control, and anxiety. *J Autism Dev Disord* **38,** 1474–1484 (2008).

551. Williams, K. D. & Jarvis, B. Cyberball: a program for use in research on interpersonal ostracism and acceptance. *Behav Res Methods* **38,** 174–180 (2006).

552. Brett, M., Anton, J., Valabregue, R. & Poline, J.-B. Region of interest analysis using an SPM toolbox. in (2002).

553. Schneider, C. A., Rasband, W. S. & Eliceiri, K. W. NIH Image to ImageJ: 25 years of image analysis. *Nat. Methods* **9,** 671–675 (2012).

554. Quade, D. Rank Analysis of Covariance. *Journal of the American Statistical Association* **62,** 1187–1200 (1967).

555. Kaiser, L. G., Schuff, N., Cashdollar, N. & Weiner, M. W. Age-related glutamate and glutamine concentration changes in normal human brain: 1H MR spectroscopy study at 4 T. *Neurobiol Aging* **26,** 665–672 (2005).

556. Libero, L. E. *et al.* Biochemistry of the cingulate cortex in autism: An MR spectroscopy study. *Autism Res* **9,** 643–657 (2016).

557. Goto, N. *et al.* Six-month treatment with atypical antipsychotic drugs decreased frontal-lobe levels of glutamate plus glutamine in early-stage first-episode schizophrenia. *Neuropsychiatr Dis Treat* **8,** 119–122 (2012).

558. Brooks, J. C. W. *et al.* A Proton Magnetic Resonance Spectroscopy Study of Age-related Changes in Frontal Lobe Metabolite Concentrations. *Cereb. Cortex* **11,** 598–605 (2001).

559. O'Brien, F. M. *et al.* Maturation of limbic regions in Asperger syndrome: a preliminary study using proton magnetic resonance spectroscopy and structural magnetic resonance imaging. *Psychiatry Res* **184,** 77–85 (2010).

560. Happé, F. & Charlton, R. A. Aging in autism spectrum disorders: a mini-review. *Gerontology* **58,** 70–78 (2012).

561. Kantrowitz, B. & PM, J. S. O. 11/26/06 at 7:00. Autism: What Happens When They Grow Up. *Newsweek* (2006).

562. Zeef, E. J., Sonke, C. J., Kok, A., Buiten, M. M. & Kenemans, J. L. Perceptual factors affecting age-related differences in focused attention: Performance and psychophysiological analyses. *Psychophysiology* **33,** 555–565 (1996).

563. Zeef, E. J. & Kok, A. Age-related differences in the timing of stimulus and response processes during visual selective attention: Performance

and psychophysiological analyses. *Psychophysiology* **30,** 138–151 (1993).

564. Machado, L., Devine, A. & Wyatt, N. Distractibility with advancing age and Parkinson's disease. *Neuropsychologia* **47,** 1756–1764 (2009).

565. Friedman, N. P. *et al.* Not All Executive Functions Are Related to Intelligence. *Psychological Science* **17,** 172–179 (2006).

566. Liss, M. *et al.* Executive Functioning in High-functioning Children with Autism. *Journal of Child Psychology and Psychiatry* **42,** 261–270 (2001).

567. Williams, D. L., Goldstein, G., Carpenter, P. A. & Minshew, N. J. Verbal and spatial working memory in autism. *J Autism Dev Disord* **35,** 747–756 (2005).

568. Fossella, J. *et al.* Assessing the molecular genetics of attention networks. *BMC Neuroscience* **3,** 14 (2002).

569. Earles, J. L. *et al.* Age differences in inhibition: Possible causes and consequences. *Aging, Neuropsychology, and Cognition* **4,** 45–57 (1997).

570. Frazier, T. W., Georgiades, S., Bishop, S. L. & Hardan, A. Y. Behavioral and Cognitive Characteristics of Females and Males With Autism in the Simons Simplex Collection. *J Am Acad Child Adolesc Psychiatry* **53,** 329-340.e3 (2014).

571. Minshew, N. J., Goldstein, G. & Siegel, D. J. Neuropsychologic functioning in autism: profile of a complex information processing disorder. *J Int Neuropsychol Soc* **3,** 303–316 (1997).

572. Ozonoff, S., Strayer, D. L., McMahon, W. M. & Filloux, F. Executive Function Abilities in Autism and Tourette Syndrome: An Information Processing Approach. *Journal of Child Psychology and Psychiatry* **35,** 1015–1032 (1994).

573. Prior, M. R. Conditional matching learning set performance in autistic children. *J Child Psychol Psychiatry* **18,** 183–189 (1977).

574. Raymaekers, R., van der Meere, J. & Roeyers, H. Event-rate manipulation and its effect on arousal modulation and response inhibition in adults with high functioning autism. *J Clin Exp Neuropsychol* **26,** 74–82 (2004).

575. Rinehart, N. J., Bradshaw, J. L., Moss, S. A., Brereton, A. V. & Tonge, B. J. A Deficit in Shifting Attention Present in High-Functioning Autism but not Asperger's Disorder. *Autism* **5,** 67–80 (2001).

576. Rinehart, N. J., Bradshaw, J. L., Tonge, B. J., Brereton, A. V. & Bellgrove, M. A. A neurobehavioral examination of individuals with high-functioning autism and Asperger's disorder using a fronto-striatal model of dysfunction. *Behav Cogn Neurosci Rev* **1,** 164–177 (2002).

577. Geurts, H. M., Corbett, B. & Solomon, M. The paradox of cognitive flexibility in autism. *Trends Cogn. Sci. (Regul. Ed.)* **13,** 74–82 (2009).

578. Bennett, K., Reichow, B. & Wolery, M. Effects of Structured Teaching on the Behavior of Young Children With Disabilities. *Focus Autism Other Dev Disabl* **26,** 143–152 (2011).

579. Schopler, E., Mesibov, G. B. & Hearsey, K. Structured Teaching in the TEACH System. in *Learning and Cognition in Autism* (eds. Schopler, E. & Mesibov, G. B.) 243–268 (Springer, 1995).

580. Chaytor, N., Schmitter-Edgecombe, M. & Burr, R. Improving the ecological validity of executive functioning assessment. *Archives of Clinical Neuropsychology* **21,** 217–227 (2006).

581. Teunisse, J. *et al.* Flexibility in children with autism spectrum disorders (ASD): Inconsistency between neuropsychological tests and parent-based rating scales. *Journal of Clinical and Experimental Neuropsychology* **34,** 714–723 (2012).

582. Cole, M. W. & Schneider, W. The cognitive control network: Integrated cortical regions with dissociable functions. *Neuroimage* **37,** 343–360 (2007).

583. Dosenbach, N. U. F. *et al.* A core system for the implementation of task sets. *Neuron* **50,** 799–812 (2006).

584. Daliri, M. R. & Behroozi, M. Advantages and Disadvantages of Resting State Functional Connectivity Magnetic Resonance Imaging for Clinical Applications. *OMICS Journal of Radiology* (2013).

585. Whitfield-Gabrieli, S. & Nieto-Castanon, A. Conn: a functional connectivity toolbox for correlated and anticorrelated brain networks. *Brain Connect* **2,** 125–141 (2012).

586. Behzadi, Y., Restom, K., Liau, J. & Liu, T. T. A Component Based Noise Correction Method (CompCor) for BOLD and Perfusion Based fMRI. *Neuroimage* **37,** 90–101 (2007).

587. Macey, P. M., Macey, K. E., Kumar, R. & Harper, R. M. A method for removal of global effects from fMRI time series. *Neuroimage* **22,** 360–366 (2004).

588. Fox, M. D., Zhang, D., Snyder, A. Z. & Raichle, M. E. The Global Signal and Observed Anticorrelated Resting State Brain Networks. *J Neurophysiol* **101,** 3270–3283 (2009).

589. Gotts, S. J. *et al.* The perils of global signal regression for group comparisons: a case study of Autism Spectrum Disorders. *Front Hum Neurosci* **7,** 356 (2013).

590. Murphy, K., Birn, R. M., Handwerker, D. A., Jones, T. B. & Bandettini, P. A. The impact of global signal regression on resting state correlations: Are anti-correlated networks introduced? *NeuroImage* **44,** 893–905 (2009).

591. Weissenbacher, A. *et al.* Correlations and anticorrelations in resting-state functional connectivity MRI: A quantitative comparison of preprocessing strategies. *Neuroimage* **47,** 1408–1416 (2009).

592. Muschelli, J. *et al.* Reduction of motion-related artifacts in resting state fMRI using aCompCor. *Neuroimage* **96,** 22–35 (2014).

593. Mazaika, P. K., Hoeft, F., Glover, G. H. & Reiss, A. L. Methods and Software for fMRI Analysis of Clinical Subjects. *NeuroImage* **47,** S58 (2009).

594. Mazaika, Paul, Whitfield, Susan & Cooper, Jeffrey. Detection and Repair of Transient Artifacts in fMRI Data. in (2005).

595. Alaerts, K. *et al.* Underconnectivity of the superior temporal sulcus predicts emotion recognition deficits in autism. *Soc Cogn Affect Neurosci* (2013).

596. Fischer, A. S., Whitfield-Gabrieli, S., Roth, R. M., Brunette, M. F. & Green, A. I. Impaired Functional Connectivity of Brain Reward Circuitry in Patients with Schizophrenia and Cannabis Use Disorder: Effects of Cannabis and THC. *Schizophr Res* **158,** 176–182 (2014).

597. Fox, M. D. *et al.* The human brain is intrinsically organized into dynamic, anticorrelated functional networks. *PNAS* **102,** 9673–9678 (2005).

598. Tzourio-Mazoyer, N. *et al.* Automated anatomical labeling of activations in SPM using a macroscopic anatomical parcellation of the MNI MRI single-subject brain. *Neuroimage* **15,** 273–289 (2002).

599. Desikan, R. S. *et al.* An automated labeling system for subdividing the human cerebral cortex on MRI scans into gyral based regions of interest. *Neuroimage* **31,** 968–980 (2006).

600. Frazier, J. A. *et al.* Structural Brain Magnetic Resonance Imaging of Limbic and Thalamic Volumes in Pediatric Bipolar Disorder. *AJP* **162,** 1256–1265 (2005).

601. Goldstein, J. M. *et al.* Hypothalamic abnormalities in schizophrenia: sex effects and genetic vulnerability. *Biol. Psychiatry* **61,** 935–945 (2007).

602. Makris, N. *et al.* Decreased volume of left and total anterior insular lobule in schizophrenia. *Schizophr. Res.* **83,** 155–171 (2006).

603. Lancaster, J. L. *et al.* Automated Talairach atlas labels for functional brain mapping. *Hum Brain Mapp* **10,** 120–131 (2000).

604. Maldjian, J. A., Laurienti, P. J., Kraft, R. A. & Burdette, J. H. An automated method for neuroanatomic and cytoarchitectonic atlas-based interrogation of fMRI data sets. *Neuroimage* **19,** 1233–1239 (2003).

605. Zhou, Y., Shi, L., Cui, X., Wang, S. & Luo, X. Functional Connectivity of the Caudal Anterior Cingulate Cortex Is Decreased in Autism. *PLoS One* **11,** (2016).

606. Just, M. A., Cherkassky, V. L., Keller, T. A., Kana, R. K. & Minshew, N. J. Functional and Anatomical Cortical Underconnectivity in Autism: Evidence from an fMRI Study of an Executive Function Task and Corpus Callosum Morphometry. *Cereb. Cortex* **17,** 951–961 (2007).

607. Hertz, L. Glutamate, a neurotransmitter--and so much more. A synopsis of Wierzba III. *Neurochem. Int.* **48,** 416–425 (2006).

608. Hertz, L. & Zielke, H. R. Astrocytic control of glutamatergic activity: astrocytes as stars of the show. *Trends Neurosci.* **27,** 735–743 (2004).

609. Rothman, D. L., Behar, K. L., Hyder, F. & Shulman, R. G. In vivo NMR studies of the glutamate neurotransmitter flux and neuroenergetics: implications for brain function. *Annu. Rev. Physiol.* **65,** 401–427 (2003).

610. Groh, A. *et al.* Convergence of Cortical and Sensory Driver Inputs on Single Thalamocortical Cells. *Cereb Cortex* **24,** 3167–3179 (2014).

611. Tamura, R., Kitamura, H., Endo, T., Hasegawa, N. & Someya, T. Reduced thalamic volume observed across different subgroups of autism spectrum disorders. *Psychiatry Res* **184,** 186–188 (2010).

612. Tsatsanis, K. D. *et al.* Reduced thalamic volume in high-functioning individuals with autism. *Biol. Psychiatry* **53,** 121–129 (2003).

613. Haznedar, M. M. *et al.* Volumetric Analysis and Three-Dimensional Glucose Metabolic Mapping of the Striatum and Thalamus in Patients With Autism Spectrum Disorders. *AJP* **163,** 1252–1263 (2006).

614. Failla, M. D. *et al.* Intrainsular connectivity and somatosensory responsiveness in young children with ASD. *Molecular Autism* **8,** 25 (2017).

615. Hein, G. & Knight, R. T. Superior temporal sulcus--It's my area: or is it? *J Cogn Neurosci* **20,** 2125–2136 (2008).

616. Lahnakoski, J. M. *et al.* Naturalistic fMRI Mapping Reveals Superior Temporal Sulcus as the Hub for the Distributed Brain Network for Social Perception. *Front Hum Neurosci* **6,** (2012).

617. Radua, J. *et al.* Neural response to specific components of fearful faces in healthy and schizophrenic adults. *Neuroimage* **49,** 939–946 (2010).

618. Bigler, E. D. *et al.* Superior temporal gyrus, language function, and autism. *Dev Neuropsychol* **31,** 217–238 (2007).

619. Kaiser, M. D. *et al.* Neural signatures of autism. *Proc. Natl. Acad. Sci. U.S.A.* **107,** 21223–21228 (2010).

620. Kaiser, M. D. *et al.* Brain Mechanisms for Processing Affective (and Nonaffective) Touch Are Atypical in Autism. *Cereb. Cortex* **26,** 2705–2714 (2016).

621. Kim, E. *et al.* Neural responses to affective and cognitive theory of mind in children and adolescents with autism spectrum disorder. *Neurosci. Lett.* **621,** 117–125 (2016).

622. Kim, S.-Y. *et al.* Abnormal activation of the social brain network in children with autism spectrum disorder: an FMRI study. *Psychiatry Investig* **12,** 37–45 (2015).

623. Simmons, W. K. *et al.* Keeping the body in mind: insula functional organization and functional connectivity integrate interoceptive, exteroceptive, and emotional awareness. *Hum Brain Mapp* **34,** 2944–2958 (2013).

624. Leung, R. C. *et al.* Early neural activation during facial affect processing in adolescents with Autism Spectrum Disorder. *Neuroimage Clin* **7,** 203–212 (2015).

625. Odriozola, P. *et al.* Insula response and connectivity during social and non-social attention in children with autism. *Soc Cogn Affect Neurosci* **11,** 433–444 (2016).

626. Rahko, J. S. *et al.* Attention and Working Memory in Adolescents with Autism Spectrum Disorder: A Functional MRI Study. *Child Psychiatry Hum Dev* **47,** 503–517 (2016).

627. Shafritz, K. M., Dichter, G. S., Baranek, G. T. & Belger, A. The Neural Circuitry Mediating Shifts in Behavioral Response and Cognitive Set in Autism. *Biological Psychiatry* **63,** 974–980 (2008).

628. Abbott, A. E. *et al.* Patterns of Atypical Functional Connectivity and Behavioral Links in Autism Differ Between Default, Salience, and Executive Networks. *Cereb. Cortex* (2015).

629. Barttfeld, P. *et al.* State-dependent changes of connectivity patterns and functional brain network topology in autism spectrum disorder. *Neuropsychologia* **50,** 3653–3662 (2012).

630. Ebisch, S. J. H. *et al.* Altered intrinsic functional connectivity of anterior and posterior insula regions in high-functioning participants with autism spectrum disorder. *Hum Brain Mapp* **32,** 1013–1028 (2011).

631. Paakki, J.-J. *et al.* Alterations in regional homogeneity of resting-state brain activity in autism spectrum disorders. *Brain Research* **1321,** 169–179 (2010).

632. Toyomaki, A. & Murohashi, H. "Salience network" dysfunction hypothesis in autism spectrum disorders. *Jpn Psychol Res* **55,** 175–185 (2013).

633. Uddin, L. Q., Supekar, K. & Menon, V. Reconceptualizing functional brain connectivity in autism from a developmental perspective. *Front Hum Neurosci* **7,** 458 (2013).

634. Plitt, M., Barnes, K. A., Wallace, G. L., Kenworthy, L. & Martin, A. Resting-state functional connectivity predicts longitudinal change in autistic traits and adaptive functioning in autism. *Proc. Natl. Acad. Sci. U.S.A.* **112,** E6699-6706 (2015).

635. Belmonte, M. K. *et al.* Autism and Abnormal Development of Brain Connectivity. *J. Neurosci.* **24,** 9228–9231 (2004).

636. Minshew, N. J. & Williams, D. L. The New Neurobiology of Autism: Cortex, Connectivity, and Neuronal Organization. *Arch Neurol* **64,** 945–950 (2007).

637. Rubenstein, J. L. R. & Merzenich, M. M. Model of autism: increased ratio of excitation/inhibition in key neural systems. *Genes Brain Behav.* **2,** 255–267 (2003).

638. Anagnostou, E. & Taylor, M. J. Review of neuroimaging in autism spectrum disorders: what have we learned and where we go from here. *Mol Autism* **2,** 4 (2011).

639. O'Reilly, C., Lewis, J. D. & Elsabbagh, M. Is functional brain connectivity atypical in autism? A systematic review of EEG and MEG studies. *PLOS ONE* **12,** e0175870 (2017).

640. Oblak, A. L., Rosene, D. L., Kemper, T. L., Bauman, M. L. & Blatt, G. J. Altered posterior cingulate cortical cyctoarchitecture, but normal density of neurons and interneurons in the posterior cingulate cortex and fusiform gyrus in autism. *Autism Res* **4,** 200–211 (2011).

641. Ajram, L. A. *et al.* Shifting brain inhibitory balance and connectivity of the prefrontal cortex of adults with autism spectrum disorder. *Transl Psychiatry* **7,** e1137 (2017).

642. Fox, M. D., Corbetta, M., Snyder, A. Z., Vincent, J. L. & Raichle, M. E. Spontaneous neuronal activity distinguishes human dorsal and ventral attention systems. *PNAS* **103,** 10046–10051 (2006).

643. Buckner, R. L., Andrews-Hanna, J. R. & Schacter, D. L. The brain's default network: anatomy, function, and relevance to disease. *Ann. N. Y. Acad. Sci.* **1124,** 1–38 (2008).

644. Gusnard, D. A., Akbudak, E., Shulman, G. L. & Raichle, M. E. Medial prefrontal cortex and self-referential mental activity: relation to a default

mode of brain function. *Proc. Natl. Acad. Sci. U.S.A.* **98,** 4259–4264 (2001).

645. Ben-Shabat, E., Matyas, T. A., Pell, G. S., Brodtmann, A. & Carey, L. M. The Right Supramarginal Gyrus Is Important for Proprioception in Healthy and Stroke-Affected Participants: A Functional MRI Study. *Front Neurol* **6,** (2015).

646. Silani, G. *et al.* Levels of emotional awareness and autism: an fMRI study. *Soc Neurosci* **3,** 97–112 (2008).

647. Greicius, M. D., Supekar, K., Menon, V. & Dougherty, R. F. Resting-State Functional Connectivity Reflects Structural Connectivity in the Default Mode Network. *Cereb Cortex* **19,** 72–78 (2009).

648. Raichle, M. E. *et al.* A default mode of brain function. *PNAS* **98,** 676–682 (2001).

649. Grill-Spector, K., Kourtzi, Z. & Kanwisher, N. The lateral occipital complex and its role in object recognition. *Vision Res.* **41,** 1409–1422 (2001).

650. Friston, K. J. *et al.* Psychophysiological and modulatory interactions in neuroimaging. *Neuroimage* **6,** 218–229 (1997).

651. Gruetter, R., Seaquist, E. R., Kim, S. & Ugurbil, K. Localized in vivo 13C-NMR of glutamate metabolism in the human brain: initial results at 4 tesla. *Dev. Neurosci.* **20,** 380–388 (1998).

652. Shen, J. *et al.* Determination of the rate of the glutamate/glutamine cycle in the human brain by in vivo 13C NMR. *Proc. Natl. Acad. Sci. U.S.A.* **96,** 8235–8240 (1999).

653. Renart, A. *et al.* The Asynchronous State in Cortical Circuits. *Science* **327,** 587–590 (2010).

654. Kurhanewicz, J., Bok, R., Nelson, S. J. & Vigneron, D. B. Current and Potential Applications of Clinical 13C MR Spectroscopy. *J Nucl Med* **49,** 341–344 (2008).

655. Watanabe, M., Maemura, K., Kanbara, K., Tamayama, T. & Hayasaki, H. GABA and GABA receptors in the central nervous system and other organs. *Int. Rev. Cytol.* **213,** 1–47 (2002).